

**THE ROLE PLAYED BY *ALKALINE PHOSPHATASE* IN LIPID  
DROPLET FORMATION IN DIFFERENT LIPID-STORING CELL  
TYPES**

**George Malipa Chirambo**

**A thesis submitted to the Faculty of Health Sciences, University of the  
Witwatersrand, Johannesburg, in fulfillment of the requirements for the  
degree of Doctor of Philosophy.**

**Johannesburg 2012**

## DECLARATION

I, George Chirambo, do hereby declare that this thesis, **The Role Played By Alkaline phosphatase In Lipid Droplet Formation In Different Lipid-storing Cell Types**, presented for the degree of Doctor of Philosophy, at the University of the Witwatersrand, Johannesburg, is my own work and has not been presented for a Degree at any other University.

Signed by:

A handwritten signature in black ink, appearing to read 'G. Chirambo', is placed on a light blue rectangular background.

On this the        day of        **2012**

## DEDICATION

To Ashads: asani mwengapu

*Kuti chenga chipusu cha!*

***We must learn our limits. We are all something, but none of us are  
everything.***

***B. Pascal (1879-1933)***

## CONFERENCE CONTRIBUTIONS

### *PathTech Congress, 2009 (Durban, RSA)*

1. Chirambo G, van Niekerk C and Crowther N. Peroxisome proliferator activated receptor gamma (*PPAR $\gamma$* ) gene expression and alkaline phosphatase activity during intra-cellular lipid accumulation in pre-adipocyte and hepatic cell lines (oral).
2. Chirambo G, van Niekerk C and Crowther N. Identifying single nucleotide polymorphisms in the promoter region of the human tissue non-specific alkaline phosphatase gene (poster).

### *Society of Endocrinology, Metabolism and Diabetes of South Africa, 2009 (Johannesburg, RSA)*

1. Chirambo G, van Niekerk C and Crowther N. The role played by alkaline phosphatase in the formation of lipid droplet in different lipid-storing cell types (oral).
2. Chirambo G, van Niekerk C and Crowther N. Identifying single nucleotide polymorphisms in the promoter region of the human tissue non-specific alkaline phosphatase gene (poster).

### *Society of Endocrinology, Metabolism and Diabetes of South Africa, 2010 (Durban, RSA)*

1. Chirambo G, van Niekerk C and Crowther N. Post-transcriptional silencing of the Tissue Non-Specific Alkaline phosphatase (TNSAP) gene blocks intracellular lipid accumulation in a murine preadipocyte cell line, 3T3-L1 and in a human hepatocarcinoma cell line, HepG2 (oral).

## ABSTRACT

Alkaline phosphatases (ALPs) are a group of membrane-bound glycoproteins that occur in many species of animals and have a wide tissue distribution. ALPs have been shown to play a role in cell differentiation and organogenesis. In humans, the physiological role of ALP in skeletal mineralization is well documented. In routine clinical practice, ALP measurement is frequently used in the differential diagnosis of liver and bone diseases.

Studies have shown the presence of tissue non-specific ALP (*TNSALP*) activity in rat adipocytes, human preadipocytes and in a murine preadipocytic cell line, 3T3-L1. ALP has also been shown to play a role in adipogenesis in 3T3-L1 cells and human preadipocytes. The purpose of the present study was to determine whether the ALP that is expressed in a human hepatocarcinoma cell line, HepG2 has a role in intracellular lipid accumulation.

Intracellular lipid droplet accumulation in HepG2 cells was induced by addition of oleic acid coupled to albumin (Sigma-Aldrich, UK) to culture medium (Earle's Minimum Essential Medium [EMEM]) and used at a final concentration of 400 $\mu$ M. Tissue non-specific ALP inhibitors (levamisole and histidine) inhibited ALP activity and intracellular lipid accumulation in both the 3T3-L1 and HepG2 cells. Post-transcriptional silencing of the tissue non-specific alkaline phosphatase (*TNSALP*) gene using siRNA oligos inhibited intracellular lipid accumulation in both 3T3-L1 and HepG2 cells.

In both cell lines, the ALP mRNA levels decreased in cells transfected with the anti-ALP siRNA compared to untransfected cells. This decrease in gene expression was mirrored by a corresponding fall in ALP activity in both cell lines.

Quantification of the expression levels of the peroxisome proliferator activated receptor gamma (*PPAR $\gamma$* ) gene (an important regulator of adipogenesis) using real-time quantitative polymerase chain reaction (real-time qPCR) showed an upward regulation of its expression four days after induction of intracellular lipid droplet accumulation in both cell types after which the levels declined. Neither levamisole nor histidine affected the expression of *PPAR $\gamma$* .

Immunostaining of HepG2 cells with monoclonal antibodies against adipophilin and staining for ALP using the ELF 97 kit (Molecular Probes, Holland) demonstrated that ALP activity was localized to the surface of the lipid droplet membrane.

A previous investigation has shown that ALP activity is higher in preadipocytes isolated from black compared to white females. Investigation of single nucleotide polymorphisms in the promoter region of the human *TNSALP* gene shows that genetic variation in the ALP promoter is not responsible for the ethnic differences in ALP activity observed in black and white South Africans.

In conclusion, the close association of ALP activity with the lipid droplet membrane in HepG2 and 3T3-L1 cells and the ability to block intracellular lipid accumulation using sequence specific oligonucleotides for ALP and pharmacological agents (histidine & levamisole) strongly indicates that ALP is involved in intracellular lipid accumulation in HepG2 cells and 3T3-L1 cells. This study also shows that *PPAR $\gamma$*

gene expression increases during lipid accumulation in HepG2 cells but that inhibition of ALP with histidine or levamisole does not affect the expression of this gene. Thus, ALP must act downstream of *PPAR $\gamma$*  during intra-cellular lipid accumulation.

## **ACKNOWLEDGEMENTS**

I would like to thank the following individuals and institutions for the support and contributions they made towards this study:

1. Prof. N Crowther (my supervisor) for their untiring guidance during the study.
2. College of Medicine (University of Malawi), the National Research Foundation (NRF), National Health Laboratory Service (NHLS) and the University of the Witwatersrand (Johannesburg) for their financial and material support.
3. Carol Crowther (Department of Molecular Medicine and Hematology, WITS University & NHLS) for assisting with the capturing of all the images that were done on the Carl Zeiss Confocal fluorescence microscope.
4. Staff in the routine Chemistry Laboratory (Johannesburg General Hospital) for the ALP assay.
5. Dr. Clem Penny (Department of Internal Medicine [Oncology Division], WITS University and NHLS) for his contribution in the immunocytochemistry work.
6. A special thank you to the Head of the Chemical Pathology Department (WITS Medical School) and all the staff in the Development laboratory for the help they rendered to me in various ways to make this study a reality.



## LIST OF ABBREVIATIONS

$\delta$	-	delta
$\alpha$	-	alpha
$\beta$	-	beta
$\gamma$	-	gamma
$\mu$ l	-	microliter
ACTH	-	adrenocorticosteroid hormone
ADD1	-	adipocyte determination and differentiation factor 1
ADRP	-	adipose differentiation related protein
ALP	-	alkaline phosphatase
Asp	-	aspartic acid
ATCC	-	American type cell collection
ATP	-	adenosine triphosphate
BSA	-	bovine serum albumin
BMI	-	body mass index
C/EBP	-	CCAAT –enhancer binding protein
cAMP	-	cyclic adenosine monophosphate
cDNA	-	complementary deoxyribonucleic acid
DAG	-	diacyl glyceride
DAPI	-	4'-6-Diamidino-2-phenylindole
DEX	-	dexamethasone
DMEM	-	Dulbecco's modified essential medium
DMSO	-	dimethyl sulphoxide
DNA	-	deoxyribonucleic acid
dNTPs	-	dinucleotide phosphates
EDTA	-	ethylenediaminetetraacetic acid
ELF 97	-	enzyme labelled fluorescence 97
EMEM	-	Earle's minimal essential medium
ENPP1	-	ectonucleotide pyrophosphatase/phosphodiesterase 1

EGFR	-	epidermal growth factor receptor
ER	-	endoplasmic reticululm
ETCC	-	European type cell collection
FFA	-	free fatty acid
Fig	-	Figure
FKHR	-	forkhead receptor
FRE	-	forkhead receptor elements
G-ALP	-	germ cell alkaline phosphatase
GH	-	growth hormone
HOP	-	phosphate
HPLC	-	high performance liquid chromatography
I-ALP	-	intestinal alkaline phosphatase
IBMX	-	isobutyl-1-methyl xanthine
ICES	-	international clinical enzyme scale
IEF	-	isoelectric focussing
IFCC	-	international federation of clinical chemists
IGF	-	insulin like growth factor
IL	-	interleukin
IU	-	international unit
KCl	-	potassium chloride
KH <sub>2</sub> PO <sub>4</sub>	-	potassium dihydrogen phosphate
L/B/K	-	liver/bone/kidney
LPL	-	lipoprotein lipase
LXR	-	liver x receptor
mg	-	milligram
MIX	-	methyl isobutyl xanthine
ml	-	milliliter
MMuLV	-	Moloney murine leukemia virus
MRI	-	magnetic resonance imaging
mRNA	-	messenger ribonucleic acid

MWM	-	molecular weight marker
Na <sub>2</sub> HPO <sub>4</sub>	-	disodium hydrogen phosphate
NASH	-	non-alcoholic steatohepatitis
nM	-	nanomolar
ox-LDL	-	oxidized low density lipoprotein
P-ALP	-	placental alkaline phosphatase
PAP	-	phosphatidic acid phosphatase
PBS	-	phosphate buffered saline
PCR	-	polymerase chain reaction
PEPCK	-	phosphoenol pyruvate carboxylase kinase
PGF	-	prostaglandin F
Pi	-	inorganic phosphate
PIG	-	phosphatidyl inositol glycan
PPi	-	pyrophosphate
pNPP	-	paranitrophenyl phosphate
PPAR	-	peroxisome proliferator activated receptor
PPi	-	pyrophosphate
qPCR	-	quantitative polymerase chain reaction
RAR	-	retinoic acid receptor
RARE	-	retinoic acid receptor elements
Redox	-	reduction oxidation
RISC	-	ribonucleic acid silencing complex
RNA	-	ribonucleic acid
RNAi	-	ribonucleic acid interfering
ROH	-	monophosphate ester
ROP	-	alcohol
RT-PCR	-	reverse transcriptase polymerase chain reaction
RXR	-	retinoid X receptor
SIP1	-	smad interacting protein 1
SEM	-	standard error of mean

SDS-PAGE	-	sodium dodecyl sulphate polyacrylamide gel electrophoresis
siRNA	-	short interfering ribonucleic acid
SNP	-	single nucleotide polymorphism
SP	-	specificity protein
SRE	-	sterol regulatory element
SREBP	-	sterol regulatory element binding protein
ST Gold	-	supertherm Gold
TAG	-	triacylglyceride
Taq	-	thermo aquaticus
TBE	-	Tris boric acid EDTA
TBP	-	TATA box binding protein
TNSALP	-	tissue non-specific alkaline phosphatase
TZD	-	thiazolidinediones
UTR	-	untranslated region
UPGM	-	Unweighted group method with arithmetic mean
Val	-	valine
VLDL	-	very low density lipoprotein
WHR	-	waist to hip circumference ratio

# LIST OF CONTENTS

DECLARATION .....	II
DEDICATION .....	III
CONFERENCE CONTRIBUTIONS .....	IV
ABSTRACT.....	V
ACKNOWLEDGEMENTS .....	VIII
LIST OF ABBREVIATIONS.....	IX
LIST OF CONTENTS.....	XIII
LIST OF FIGURES .....	XVIII
LIST OF TABLES .....	XXI
<b>1.1 INTRODUCTION.....</b>	<b>1</b>
<b>2.1 THE BIOCHEMISTRY OF ALPs .....</b>	<b>4</b>
<b>2.2 HUMAN ALP ISOENZYMES .....</b>	<b>5</b>
<b>2.3 PHYSIOLOGICAL ROLES OF ALP .....</b>	<b>7</b>
<b>2.4 ATTACHED AND SOLUBLE FORMS OF ALP.....</b>	<b>9</b>
<b>2.5 DISCRIMINATION AND QUANTIFICATION OF TOTAL SERUM ALP AND ITS ISOENZYMES .....</b>	<b>10</b>
<b>2.6 GENETICS OF ALP ISOENZYMES .....</b>	<b>11</b>
2.6.1 <i>Gene structures .....</i>	11
2.6.2 <i>Regulation of ALP gene expression.....</i>	13
<b>2.7 MUTATIONS IN THE TNSALP GENE .....</b>	<b>19</b>
<b>2.8 INTRACELLULAR LIPID ACCUMULATION .....</b>	<b>22</b>
2.8.1 <i>Lipid droplet formation.....</i>	23
2.8.2 <i>Tissues involved in lipid accumulation.....</i>	27
2.8.3 <i>Cell line models used in studying lipid metabolism .....</i>	35
2.8.3.1 <i>Preadipocyte cell lines.....</i>	36
2.8.3.2 <i>Other lipid accumulating cell lines.....</i>	38
<b>2.9 REGULATION OF LIPID ACCUMULATION IN SELECTED CELL TYPES.....</b>	<b>38</b>

2.9.1	<i>Adipocytes</i> .....	38
2.9.1.1	<i>Genes involved in adipocyte differentiation</i> .....	43
2.9.1.2	<i>Transcriptional regulation of adipogenesis</i> .....	46
2.9.1.3	<i>Hormonal regulation of adipogenesis</i> .....	53
2.9.2	<i>Hepatocytes</i> .....	54
<b>2.10</b>	<b>ALP AND ADIPOGENESIS</b> .....	<b>55</b>
<b>2.11</b>	<b>ALP GENE SILENCING BY RNA INTERFERENCE</b> .....	<b>56</b>
<b>2.12</b>	<b>AIMS OF THE STUDY</b> .....	<b>59</b>
<b>3.1</b>	<b>ALP ACTIVITY AND PROTEIN MEASUREMENTS IN HEPG2 AND 3T3-L1 CELLS WITH THE PROGRESSION OF LIPID DROPLET ACCUMULATION</b> .....	<b>60</b>
3.1.1	<i>3T3-L1 and HepG2 cell culture</i> .....	60
3.1.3	<i>Induction of adipogenesis in 3T3-L1 Cells</i> .....	62
3.1.4	<i>Induction of lipid droplet accumulation in HepG2 cells</i> .....	63
3.1.5	<i>Measurement of lipid droplet accumulation in 3T3-L1 and HepG2 cells - Oil Red O staining.</i> ..	64
3.1.6	<i>ALP and protein extraction of cultured cells</i> .....	66
3.1.7	<i>ALP activity measurement</i> .....	67
3.1.8	<i>Total protein measurement using the Bradford method</i> .....	68
<b>3.2</b>	<b>THE EFFECT OF ALP INHIBITORS ON THE PROGRESSION OF LIPID DROPLET ACCUMULATION AND ALP ACTIVITY IN HEPG2 &amp; 3T3-L1 CELLS</b> .....	<b>70</b>
3.2.1	<i>Cell culture</i> .....	70
<b>3.3</b>	<b>PEROXISOME PROLIFERATOR ACTIVATED RECEPTOR GAMMA (PPAR<math>\gamma</math>) GENE EXPRESSION STUDIES IN HEPG2 &amp; 3T3-L1 CELLS.</b> .....	<b>71</b>
3.3.1	<i>Isolation of total RNA using the Qiagen <sup>®</sup>RNeasy Mini Kit (Germany)</i> .....	71
3.3.2	<i>Reverse Transcriptase PCR (RT-PCR)</i> .....	73
3.3.3	<i>Amplification of PPAR<math>\gamma</math> and TBP genes and optimization of PCR conditions using a Biorad Thermocycler and the Rotor-Gene 6000 light cyclor</i> .....	76
3.3.4	<i>Gel electrophoresis</i> .....	80
3.3.5	<i>Quantitative real-time PCR (qPCR) in HepG2 cells</i> .....	81
3.3.6	<i>Quantitative real-time PCR (qPCR) in 3T3-L1 cells</i> .....	88
<b>3.4</b>	<b>RNAI STUDIES FOR THE TNSALP GENE IN HEPG2 AND 3T3-L1 CELLS</b> .....	<b>91</b>
3.4.1	<i>Optimized transfection conditions using the Fast-Forward protocol</i> .....	92

3.4.2	<i>Transfection efficiency</i> .....	93
3.4.3	<i>Gene knockdown efficiency</i> .....	93
3.4.4	<i>Post-transcriptional silencing of the TNSALP gene in 3T3-L1 and HepG2 cells using the long-term transfection protocol</i> .....	95
<b>3.5</b>	<b>SUBCELLULAR LOCALIZATION OF ALP IN HEPG2 CELLS</b> .....	<b>98</b>
3.5.1	<i>Cell culture</i> .....	98
3.5.2	<i>Preparation of reagents</i> .....	98
3.5.3	<i>Specificity of the immunocytochemical methods</i> .....	101
3.5.3.1	<i>Negative controls</i> .....	101
3.5.4	<i>Indirect immunolabeling of perilipin and ELF 97 staining of ALP in differentiated 3T3-L1 cells.</i> 101	
3.5.5	<i>Indirect immunolabeling of ADRP and ELF 97 staining of ALP in HepG2 cells</i> .....	104
<b>3.6</b>	<b>ANALYSIS OF SINGLE NUCLEOTIDE POLYMORPHISMS (SNPs) IN THE PROMOTER REGION OF THE HUMAN TNSALP GENE</b> .....	<b>104</b>
3.6.1	<i>Primer design and synthesis</i> .....	105
3.6.2	<i>DNA extraction</i> .....	107
3.6.3	<i>Optimization of the PCR conditions for the promoter region of the human TNSALP gene</i> ....	107
3.6.4	<i>Gel electrophoresis of PCR products for the promoter region of the human TNSALP gene</i> ..	109
3.6.5	<i>DNA sequencing</i> .....	110
<b>3.7</b>	<b>STATISTICAL ANALYSIS</b> .....	<b>111</b>
<b>4.1</b>	<b>ALP ACTIVITY AND INTRACELLULAR LIPID DROPLET ACCUMULATION IN HEPG2 &amp; 3T3-L1 CELLS</b> ....	<b>112</b>
4.1.1	<i>Intracellular lipid accumulation</i> .....	113
4.1.2	<i>ALP activity in HepG2 and 3T3-L1 cells</i> .....	115
<b>4.2</b>	<b>EFFECT OF ALP INHIBITORS (LEVAMISOLE &amp; HISTIDINE) ON INTRACELLULAR LIPID ACCUMULATION IN HEPG2 AND 3T3-L1 CELLS.</b> .....	<b>117</b>
4.2.1	<i>Lipid accumulation</i> .....	118
4.2.2	<i>ALP activity in the presence and absence of histidine and levamisole.</i> .....	124
<b>4.3</b>	<b>THE EXPRESSION OF THE PPAR<math>\gamma</math> GENE IN THE ABSENCE AND PRESENCE OF HISTIDINE AND LEVAMISOLE</b> .....	<b>126</b>
4.3.1	<i>Conventional PCR</i> .....	127
4.3.2	<i>Optimized conditions for quantitative real-time PCR on Rotor-Gene 6000</i> .....	129

4.3.3	<i>PPAR<math>\gamma</math> gene expression in HepG2 and 3T3-L1 cells.....</i>	132
4.3.4	<i>PPAR<math>\gamma</math> gene expression in the presence of histidine and levamisole in HepG2 and 3T3-L1 cells. 134</i>	
<b>4.4</b>	<b>RNAI STUDIES FOR THE TNSALP GENE IN HEPG2 AND 3T3-L1 CELLS .....</b>	<b>138</b>
4.4.1	<i>Transfection efficiency of siRNA oligos in 3T3-L1 and HepG2 cells using the RNAi human/mouse/rat starter kit.....</i>	138
4.4.2	<i>MAPK1 gene knockdown efficiency.....</i>	142
4.4.2.1	<i>Optimized qPCR conditions on the Rotor-Gene 6000 .....</i>	142
4.4.2.2	<i>MAPK1 gene knockdown efficiency.....</i>	145
4.4.3	<i>Knockdown efficiency of the TNSALP gene in 3T3-L1 and HepG2 cells transfected with siRNA directed against TNSALP mRNA .....</i>	148
4.4.4	<i>ALP activity in 3T3-L1 &amp; HepG2 cells transfected with siRNA directed against TNSALP mRNA 163</i>	
4.4.5	<i>Intracellular lipid droplet accumulation in 3T3-L1 &amp; HepG2 cells transfected with siRNA directed against TNSALP mRNA .....</i>	167
<b>4.5</b>	<b>SUBCELLULAR LOCALIZATION OF ALP IN HEPG2 &amp; 3T3-L1 CELLS .....</b>	<b>173</b>
4.5.1	<i>Immunolabelling of perilipin and staining of ALP in 3T3-L1 cells.....</i>	173
4.5.2	<i>Immunolabelling of Adipose differentiation-related protein (ADRP) and staining of ALP in HepG2 cells.....</i>	179
<b>4.6</b>	<b>SINGLE NUCLEOTIDE POLYMORPHISMS IN THE PROMOTER REGION OF THE HUMAN TNSALP GENE. 185</b>	
4.6.1	<i>Optimized PCR conditions and gel electrophoresis of PCR products .....</i>	186
4.6.2	<i>Sequencing of PCR products.....</i>	187
<b>5.0</b>	<b>INTRODUCTION.....</b>	<b>189</b>
<b>5.1</b>	<b>ALP ACTIVITY AND INTRACELLULAR LIPID DROPLET ACCUMULATION IN 3T3-L1 AND HEPG2 CELLS 190</b>	
<b>5.2</b>	<b>PHARMACOLOGICAL INHIBITION OF ALP ACTIVITY BLOCKS INTRACELLULAR LIPID ACCUMULATION IN HEPG2 CELLS AND ADIPOGENESIS IN 3T3-L1 CELLS. ....</b>	<b>193</b>
<b>5.3</b>	<b>THE RNA INTERFERENCE PATHWAY AND THE KNOCKDOWN OF SPECIFIC MRNA TRANSCRIPTS .....</b>	<b>197</b>
5.3.1	<i>Effect of siRNA transfection on ALP activity and intracellular lipid accumulation. ....</i>	198
5.3.2	<i>Effect of siRNA transfection on TNSALP gene expression .....</i>	199
<b>5.4</b>	<b>SUBCELLULAR LOCALIZATION OF ALP IN HEPG2 CELLS .....</b>	<b>201</b>
5.4.1	<i>Proposed mechanisms of TNSALP mediated intracellular lipid accumulation. ....</i>	203



5.4.1.1	<i>ALP in neutral lipid synthesis.....</i>	204
5.4.1.2	<i>Interaction with lipid droplet associated proteins.....</i>	206
<b>5.5</b>	<b><i>PPAR<math>\gamma</math> GENE EXPRESSION IN 3T3-L1 AND HEPG2 CELLS .....</i></b>	<b>208</b>
5.5.1	<i>Levamisole and histidine do not alter the expression pattern of the PPAR<math>\gamma</math> gene in 3T3-L1 and HepG2 cells.....</i>	210
<b>5.6</b>	<b><i>ETHNIC DIFFERENCES IN ALP ACTIVITY AND THE ROLE OF SNPs IN THE PROMOTER REGION OF THE HUMAN TNSALP GENE.....</i></b>	<b>211</b>
5.6.1	<i>Polymorphisms in TNSALP and ENPP1 genes and its association with biochemical features of obesity .....</i>	213
<b>5.7</b>	<b><i>CONCLUSIONS .....</i></b>	<b>216</b>
<b>5.8</b>	<b><i>STRATEGIES FOR FUTURE WORK.....</i></b>	<b>217</b>
	<b>APPENDIX I.....</b>	<b>218</b>
	<b>APPENDIX II.....</b>	<b>241</b>
	<b>BIBLIOGRAPHY .....</b>	<b>251</b>

## LIST OF FIGURES

FIGURE 2. 1	HUMAN ALP ISOENZYMES. ....	6
FIGURE 2. 2	ROLES OF ALP IN DIFFERENT TISSUES IN THE HUMAN BODY. ....	8
FIGURE 2. 3	THE 5'-END OF THE <i>TNSALP</i> GENE.....	14
FIGURE 2. 4	LIPID DROPLET FORMATION AND MOTILITY. ....	24
FIGURE 2. 5	LIPID DROPLET-ORGANELLE ASSOCIATIONS. ....	25
FIGURE 2. 6	DEVELOPMENT OF MESENCHYMAL/MESODERMAL DERIVATIVES. ....	40
FIGURE 2. 7	PROGRESSION OF 3T3-L1 PREADIPOCYTE DIFFERENTIATION.....	44
FIGURE 2. 8	BASIC MECHANISM OF ACTION OF NUCLEAR HORMONE RECEPTORS.....	48
FIGURE 2. 9	ACTIONS OF PPARs AT THE CELLULAR LEVEL.....	49
FIGURE 2. 10	THE RNAI PATHWAY. ....	58
FIGURE 4. 1	PHOTOGRAPHS OF 3T3-L1 & HEPG2 CELLS (STAINED WITH OIL RED O).....	114
FIGURE 4. 2	ALP ACTIVITY AND LIPID ACCUMULATION IN 3T3-L1 CELLS. ....	116
FIGURE 4. 3	ALP ACTIVITY AND LIPID ACCUMULATION IN HEPG2 CELLS.....	117
FIGURE 4. 4	OIL RED O STAIN PHOTOGRAPHS OF HEPG2 CELLS.....	119
FIGURE 4. 5	OIL RED O STAIN PHOTOGRAPHS OF 3T3-L1 CELLS. ....	120
FIGURE 4. 6	THE EFFECT OF HISTIDINE AND LEVAMISOLE TREATMENT ON INTRACELLULAR LIPID ACCUMULATION IN HEPG2 CELLS.....	122
FIGURE 4. 7	THE EFFECT OF HISTIDINE AND LEVAMISOLE TREATMENT ON INTRACELLULAR LIPID ACCUMULATION IN 3T3-L1 CELLS. ....	123
FIGURE 4. 8	EFFECT OF HISTIDINE AND LEVAMISOLE TREATMENT ON ALP ACTIVITY IN HEPG2 CELLS. ....	125
FIGURE 4. 9	EFFECT OF HISTIDINE AND LEVAMISOLE TREATMENT ON ALP ACTIVITY IN 3T3-L1 CELLS. ....	126
FIGURE 4. 10	AGAROSE GEL IMAGE OF PCR PRODUCTS FROM HEPG2 CELLS. ....	128
FIGURE 4. 11	AGAROSE GEL IMAGE OF PCR PRODUCTS FROM 3T3-L1 CELLS. ....	128
FIGURE 4. 12	REAL TIME AMPLIFICATION PLOT (TOP) AND MELTING CURVE OF PCR PRODUCTS FOR HEPG2 CELLS.	130
FIGURE 4. 13	REAL TIME AMPLIFICATION PLOT (TOP) AND MELTING CURVE OF PCR PRODUCTS FOR 3T3-L1 CELLS. ....	131
FIGURE 4. 14	<i>PPAR<math>\gamma</math></i> GENE EXPRESSION IN HEPG2 CELLS. ....	133
FIGURE 4. 15	<i>PPAR<math>\gamma</math></i> GENE EXPRESSION IN 3T3-L1 CELLS.....	134
FIGURE 4. 16	<i>PPAR<math>\gamma</math></i> GENE EXPRESSION IN HEPG2 CELLS GROWN IN THE PRESENCE OF LEVAMISOLE AND HISTIDINE. ....	136

FIGURE 4. 17	<i>PPAR<math>\gamma</math></i> GENE EXPRESSION IN 3T3-L1 CELLS GROWN IN THE PRESENCE OF LEVAMISOLE AND HISTIDINE. .....	137
FIGURE 4. 18	CONFOCAL FLUORESCENCE PICTURE OF HEPG2 CELLS. ....	140
FIGURE 4. 19	CONFOCAL FLUORESCENCE PICTURE OF 3T3-L1 CELLS.....	141
FIGURE 4. 20	REAL TIME PCR AMPLIFICATION PLOT (TOP) AND MELTING CURVE OF PCR PRODUCTS ( <i>MAPK1</i> GENE) FOR HEPG2 CELLS.....	143
FIGURE 4. 21	REAL TIME PCR AMPLIFICATION PLOT (TOP) AND MELTING CURVE OF PCR PRODUCTS ( <i>MAPK1</i> GENE) FOR 3T3-L1 CELLS. ....	144
FIGURE 4. 22	<i>MAPK1</i> GENE EXPRESSION IN 3T3-L1 CELLS 72 HOURS POST-TRANSFECTION.....	146
FIGURE 4. 23	<i>MAPK1</i> GENE EXPRESSION IN HEPG2 CELLS 72 HOURS POST-TRANSFECTION.....	147
FIGURE 4. 24	REAL TIME PCR AMPLIFICATION (TOP) AND MELTING CURVES FOR THE <i>TNSALP</i> GENE IN 3T3-L1 CELLS. .....	149
FIGURE 4. 25	REAL TIME PCR AMPLIFICATION (TOP) AND MELTING CURVES FOR THE <i>TNSALP</i> & <i>TBP</i> GENES IN HEPG2 CELLS.....	150
FIGURE 4. 26	<i>TNSALP</i> GENE EXPRESSION IN TRANSFECTED 3T3-L1 CELLS 7 DAYS POST-TRANSFECTION.....	153
FIGURE 4. 27	<i>TNSALP</i> GENE EXPRESSION IN TRANSFECTED 3T3-L1 CELLS 11 DAYS POST-TRANSFECTION. ....	154
FIGURE 4. 28	<i>TBP</i> GENE EXPRESSION IN TRANSFECTED 3T3-L1 CELLS 7 DAYS POST-TRANSFECTION.....	155
FIGURE 4. 29	<i>TBP</i> GENE EXPRESSION IN TRANSFECTED 3T3-L1 CELLS 11 DAYS POST-TRANSFECTION.....	156
FIGURE 4. 30	<i>TNSALP</i> GENE EXPRESSION IN TRANSFECTED HEPG2 CELLS 4 DAYS POST-TRANSFECTION.....	158
FIGURE 4. 31	<i>TNSALP</i> GENE EXPRESSION IN TRANSFECTED HEPG2 CELLS 7 DAYS POST-TRANSFECTION.....	159
FIGURE 4. 32	<i>TNSALP</i> GENE EXPRESSION IN TRANSFECTED HEPG2 CELLS 11 DAYS POST-TRANSFECTION.....	160
FIGURE 4. 33	<i>TBP</i> GENE EXPRESSION IN TRANSFECTED HEPG2 CELLS 4 DAYS POST-TRANSFECTION. ....	161
FIGURE 4. 34	<i>TBP</i> GENE EXPRESSION IN TRANSFECTED HEPG2 CELLS 7 DAYS POST-TRANSFECTION. ....	162
FIGURE 4. 35	<i>TBP</i> GENE EXPRESSION IN TRANSFECTED HEPG2 CELLS 11 DAYS POST-TRANSFECTION. ....	163
FIGURE 4. 36	ALP ACTIVITY IN 3T3-L1 CELLS TRANSFECTED WITH SIRNA.....	165
FIGURE 4. 37	ALP ACTIVITY IN HEPG2 CELLS TRANSFECTED WITH SIRNA. ....	166
FIGURE 4. 38	INTRACELLULAR LIPID ACCUMULATION IN 3T3-L1 CELLS TRANSFECTED WITH ANTI- <i>TNSALP</i> SIRNA OLIGOS.....	169
FIGURE 4. 39	INTRACELLULAR LIPID ACCUMULATION IN HEPG2 CELLS TRANSFECTED WITH SIRNA FOR <i>TNSALP</i> GENE. .....	170
FIGURE 4. 40	OIL RED O STAIN PICTURES OF TRANSFECTED 3T3-L1 CELLS. ....	171
FIGURE 4. 41	OIL RED O STAIN PICTURES OF TRANSFECTED HEPG2 CELLS.....	172

FIGURE 4. 42	IMMUNOLABELLING OF PERILIPIN IN 3T3-L1 CELLS.....	174
FIGURE 4. 43	PRIMARY ANTIBODY CONTROL IN IMMUOSTAINING OF PERILIPIN IN 3T3-L1 CELLS.....	175
FIGURE 4. 44	SECONDARY ANTIBODY CONTROL IN IMMUOSTAINING OF PERILIPIN IN 3T3-L1 CELLS.....	176
FIGURE 4. 45	ELF 97 STAINING OF ALP ACTIVITY AND IMMUOSTAINING OF PERILIPIN IN 3T3-L1 CELLS .....	177
FIGURE 4. 46	CONTROL FOR ELF 97 STAINING OF ALP ACTIVITY AND IMMUOSTAINING OF PERILIPIN IN 3T3-L1 CELLS .....	178
FIGURE 4. 47	IMMUNOLABELLING OF ADRP IN HEPG2 CELLS.....	180
FIGURE 4. 48	PRIMARY ANTIBODY CONTROL IN IMMUOSTAINING OF ADRP IN HEPG2 CELLS.....	181
FIGURE 4. 49	SECONDARY ANTIBODY CONTROL IN IMMUOSTAINING OF ADRP IN HEPG2 CELLS.....	182
FIGURE 4. 50	ELF 97 STAINING OF ALP ACTIVITY AND IMMUOSTAINING OF ADRP IN HEPG2 CELLS. ....	183
FIGURE 4. 51	CONTROL FOR ELF 97 STAINING OF ALP ACTIVITY AND IMMUOSTAINING OF ADRP IN HEPG2 CELLS. .....	184
FIGURE 4. 52	ELF 97 ALP STAINING AND ADRP LABELING IN NON-TRANSFORMED HEPG2 CELLS. ....	185
FIGURE 4. 53	AGAROSE GEL IMAGE OF PCR PRODUCTS FOR THE 7 SETS OF PRIMERS (S1- S7) USED TO AMPLIFY THE PROMOTER REGION OF THE HUMAN <i>TNSALP</i> GENE. ....	187
FIGURE 4. 54	CHROMATOGRAM OF A SEQUENCED PCR PRODUCT (GENOMIC DNA AS A TEMPLATE) USING PCR PRIMER SET 3.....	188
FIGURE 5. 1	TRIACYLGLYCEROL BIOSYNTHESIS.....	205

## LIST OF TABLES

TABLE 2. 1	TNSALP GENE MUTATIONS .....	21
TABLE 2. 2	CLUSTERS OF GENES BY THE UPGMA VERSION OF THE AVERAGE LINKAGE ALGORITHM (ABRIDGED VERSION).....	45
TABLE 3.1	EARLE’S MINIMAL ESSENTIAL MEDIUM (10% EMEM) -100ML .....	60
TABLE 3. 2	DULBECCO’S MODIFIED EAGLE’S MEDIUM (10% DMEM) -100ML .....	61
TABLE 3. 3	ALP/PROTEIN EXTRACTION SOLUTION .....	66
TABLE 3. 4	PROTEIN STANDARDS FOR CALIBRATION CURVE.....	69
TABLE 3. 5	PCR PRIMERS FOR <i>PPAR<math>\gamma</math></i> AND <i>TBP</i> GENES IN HEPG2 CELLS.....	78
TABLE 3. 6	PCR COMPONENTS FOR 1 REACTION TUBE FOR <i>PPAR<math>\gamma</math></i> AND <i>TBP</i> GENES IN HEPG2 CELLS USING A BIORAD THERMOCYCLER.....	79
TABLE 3. 7	PCR COMPONENTS FOR 1 REACTION TUBE RUN ON THE ROTOR-GENE FOR <i>PPAR<math>\gamma</math></i> AND <i>TBP</i> GENES IN HEPG2 CELLS:.....	83
TABLE 3. 8	CONCENTRATION OF CDNA USED AS STANDARDS IN HEPG2 CELLS .....	84
TABLE 3. 9	EXAMPLE OF DILUTIONS AND CONCENTRATIONS OF CDNA USED IN A TYPICAL QUANTITATIVE REAL-TIME PCR (HEPG2 CELLS). DILUTED CDNA WAS OBTAINED BY DILUTING CDNA OBTAINED FROM THE REVERSE TRANSCRIPTION OF TOTAL RNA. ....	86
TABLE 3. 10	PCR PRIMERS FOR <i>PPAR<math>\gamma</math></i> AND <i>TBP</i> GENES (MOUSE). ....	87
TABLE 3. 11	CONCENTRATION OF CDNA USED AS STANDARDS .....	89
TABLE 3. 12	EXAMPLE OF DILUTIONS AND CONCENTRATIONS OF CDNA USED IN A TYPICAL QUANTITATIVE REAL-TIME PCR IN 3T3-L1 CELLS. DILUTED CDNA WAS OBTAINED BY DILUTING CDNA OBTAINED FROM THE REVERSE TRANSCRIPTION OF TOTAL RNA .....	90
TABLE 3. 13	PCR COMPONENTS FOR 1 REACTION TUBE RUN ON THE ROTOR-GENE 6000 FOR MAPK1 GENE IN HEPG2 AND 3T3-L1 CELLS.....	94
TABLE 3. 14	PCR PRIMERS FOR THE PROMOTER REGION OF THE HUMAN <i>TNSALP</i> GENE.....	106
TABLE 3. 15	VOLUME AND CONCENTRATION OF PCR COMPONENTS IN ONE TYPICAL PCR TUBE REACTION AND A MASTER MIX FOR 10 REACTIONS .....	108
TABLE 3. 16	OPTIMIZED PCR CONDITIONS FOR EACH OF THE AMPLIFIED SEGMENTS OF THE PROMOTER REGION OF THE HUMAN <i>TNSALP</i> GENE.....	109

# **CHAPTER ONE**

## **INTRODUCTION**

## 1.1 Introduction

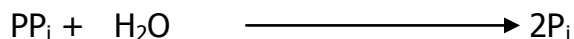
Alkaline phosphatases (ALPs) (orthophosphoric-monoester phosphohydrolase, EC.3.1.3.1) are a group of membrane-bound glycoproteins that hydrolyze a broad range of monophosphate esters at alkaline pH optima (McComb *et al.* 1979). ALP attaches itself to the surface of the cell membrane via a phosphatidyl inositol glycan (PI-G) tail which is attached to the carboxyl terminus of the protein (Jemmerson and Low 1987). ALPs are widely distributed in nature ranging from prokaryotes to higher eukaryotes (Hass *et al.* 1979). *In vitro* studies have shown that the specific activity for each of the forms of the enzymes show substrate dependence (Fishman 1989). ALP also catalyzes the removal of 5' phosphate groups from proteins, DNA, RNA, ribo- and deoxyribonucleotide triphosphates. As such ALPs have been used in nucleic acid manipulations (Primrose and Twyman 2005).

The reactions catalyzed by ALP can be summarized as follows (Price 1993):

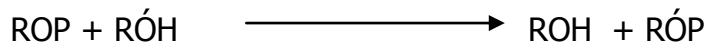
*Orthophosphatase*



*Pyrophosphatase*



*Phosphotransferase*



Measurements of total ALP and its isoenzymes in human body fluids are used in routine clinical practice to differentiate liver and bone diseases.

Recently, Ali *et al.* (2003) showed the presence of ALP in a murine preadipocyte cell line (3T3-L1) and human preadipocytes where it was shown to be involved in the control of adipogenesis (intracellular lipid accumulation). The same study also showed that ethnic differences were present in the activity of ALP isolated from human preadipocytes, with levels being much higher in preadipocytes isolated from black than white females.

The molecular control mechanisms for the intracellular lipid accumulation in a variety of tissues within the human body are still largely unknown. A number of factors are now known to be involved in the regulation of this process. These include PPAR $\gamma$  and a number of other transcription factors, IGF-1, fatty acids and cytokines. Environmental factors like age, gender and lifestyle also seem to play a role (Frubeck *et al.* 2001).

Unregulated increase in fat cell number and size may lead to obesity. Obesity is a common and serious medical problem especially in industrialized and developing economies (Rosen and Spiegelman 2000).

An understanding of the molecular events involved in adipogenesis may give a better insight into the modalities of interventions that can be used to reduce the accumulation of lipids within the lipid-storing cell types in humans and other animals. This study was carried out to determine whether ALP is present and involved in intracellular lipid accumulation in cell types that are known to be able to accumulate lipid for example, hepatocytes and preadipocytes.



This study also provides additional insight into the subcellular localization of ALP in the different lipid-storing cell types using immunocytochemical techniques. Additionally, the study looked at the expression pattern of the peroxisome proliferator activated receptor gamma (*PPAR $\gamma$* ) gene (an important transcriptional regulator of adipogenesis) and determined the effect of inhibiting ALP activity (chemically or through RNA interference pathway) on intracellular lipid accumulation and the expression of the *PPAR $\gamma$*  gene in 3T3-L1 cells and in an human hepatocarcinoma cell line (HepG2). Lastly, this study also investigated the role that single nucleotide changes in the promoter region of the human tissue non-specific ALP may play in the control of ALP expression. Differences in the activity of ALP were observed in cell extracts from preadipocytes isolated from black and white subjects in South Africa with the former ethnic group showing higher levels than the latter group (Ali *et al.* 2006).

The remainder of this thesis is organized in the order as follows: Firstly, a review of the literature relevant to the study is presented. Secondly, an outline of the materials and the methods used in the study is followed by the results section and lastly but not least the discussion of the results and the conclusions drawn from the study are given.

**CHAPTER TWO**  
**LITERATURE REVIEW**

## 2.1 The Biochemistry of ALPs

The ALPs are widely distributed in nature ranging from prokaryotes to higher eukaryotes. They have a homology to a large number of other enzymes and are part of the nucleoside pyrophosphatase/phosphodiesterase superfamily of enzymes (Gijsbers *et al.* 2002). With few exceptions, ALPs are homodimeric enzymes and each catalytic site contains three metal ions, that is two zinc and one magnesium ion, which are necessary for enzymatic activity.

ALPs hydrolyze a wide range of monophosphate esters at alkali pH optima (McComb *et al.* 1979). These enzymes also hydrolyze inorganic pyrophosphates and exhibit transphorylation activity. The transphorylation involves direct transfer of phosphate from substrate to an acceptor alcohol such as diethanolamine and 2-amino-2-methyl-1-propanol (Price 1993).

ALPs also catalyse the removal of phosphate groups on the 5' end of nucleic acids. Removing these phosphates prevents the DNA from self-ligating, thereby keeping DNA molecules linear until the next step of the process for which they are prepared (Primrose and Twyman 2005).

Phosphorylation of ALP occurs mainly at serine residue 102 in the active centre of the ALP molecule (Han and Coleman 1995). The phosphorylation of ALP may activate its catalytic activity and enable it to participate in hydrolysis (dephosphorylation) of molecules containing phosphate groups (Galperin and Jedizejas 2001).

## 2.2 Human ALP isoenzymes

Isoenzymes are distinctive genetically determined forms of an enzyme. Though these enzymes may essentially catalyze similar biochemical transformations, they have distinguishable physical and biochemical properties (Moss 1982). Different forms of enzymes having a common gene locus are called isoforms.

There are four genes encoding the protein moieties of the ALP enzymes: the tissue non-specific (TNSALP), the intestinal (I-ALP), the placental (P-ALP) and the germ-cell (G-ALP) isoenzymes (Fig. 2.1). These four classes of ALP have been identified by differences in protein structure as determined by peptide 'maps', partial sequence analysis and immunological analysis (Mulivor *et al.* 1978; McKenna *et al.* 1979; Whitaker and Moss 1979; Hua *et al.* 1986).

It has been proposed that the human ALPs are members of a multi-gene enzyme family that arose by successive duplication from a common ancestral gene (Harris 1982). While there are only four true isoenzymes recognized at present there are many more variants of the enzymes thus far described (Crofton *et al.* 1979; Okazaki *et al.* 2004).

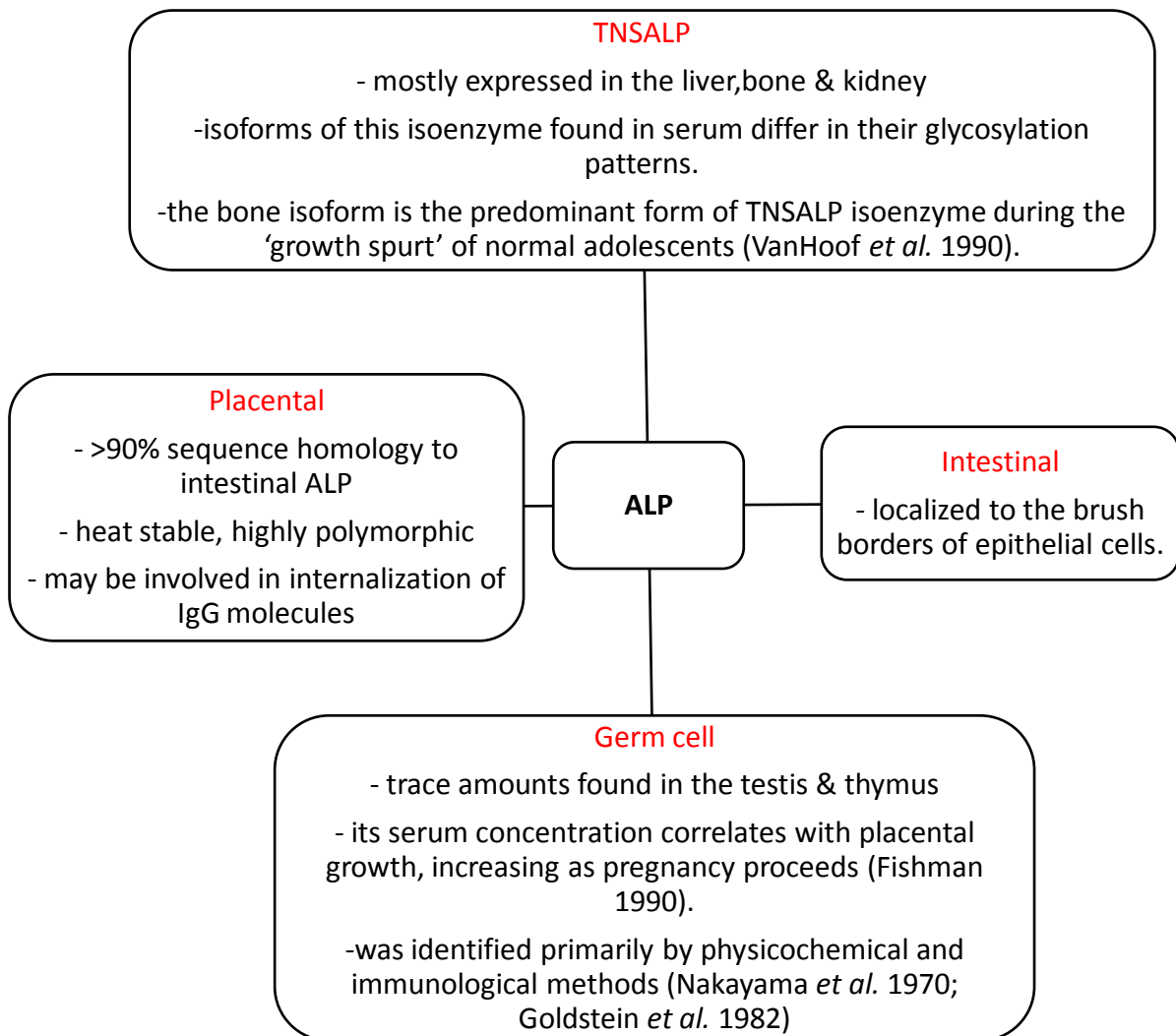


**Figure 2. 1** Human ALP isoenzymes.

*The gene loci for the P-ALP, I-ALP and G-ALP occupy adjacent position on the long arm of chromosome 2 (Griffin *et al.* 1987) while the locus for the TNSALP (also called liver/bone/kidney [L/B/K]) gene is on chromosome 1[1p36.1-p34] (Smith *et al.* 1988).*

### 2.3 Physiological roles of ALP

The presence of ALP in many species suggests its involvement in fundamental biological processes. However, the exact biological functions of these glycoproteins in normal metabolism is not yet known (Harris 1990). The only exception to this statement comes from the work on hypophosphatasia which clearly indicates that the bone isoform of the TNSALP isoenzyme is necessary for bone mineralization (Posen *et al.* 1977; Whyte 1994).

It is not clear what TNSALP does on the cell surface of most other cell types in the body. However, the localization of ALP to membranes suggests that it may be involved in the active transport of substances across these membranes.

Some of the proposed roles that ALP play in the human body are shown in Fig.

2.2.

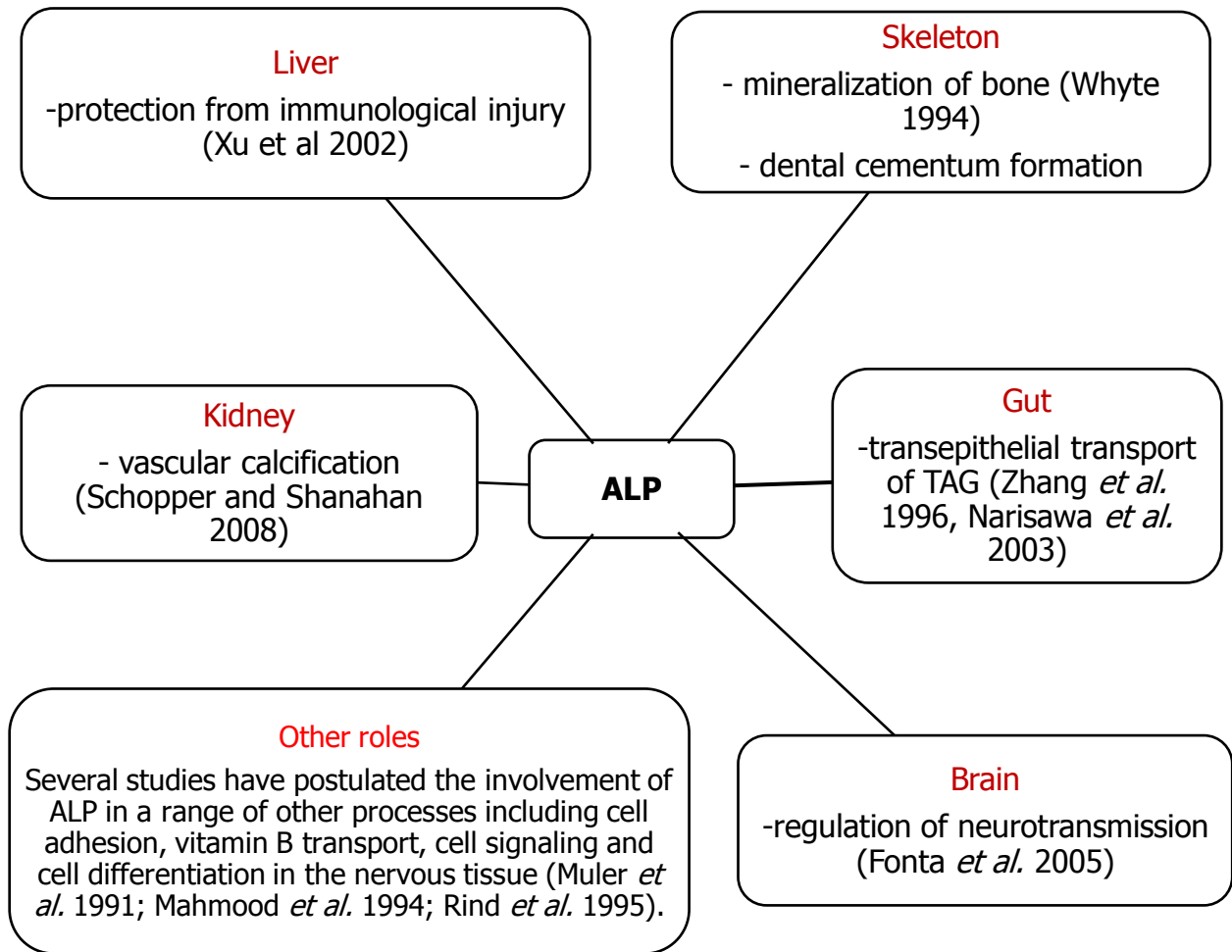


**Figure 2. 2** Roles of ALP in different tissues in the human body.

*The most well characterized biological function of ALP is its role in mineralization of the skeleton.*

## 2.4 Attached and soluble forms of ALP

ALP attaches to the surface of cell membranes via a phosphatidyl inositol glycan (PI-G) tail. The biogenesis and transfer of the PI-G structure has been called glypiation (Harris 1990). The detailed processes involved in glypiation are still somewhat uncertain. It is thought that co- or post-translationally a hydrophobic, carboxyl terminal region of the nascent protein is removed and the glycolipid is attached to the carboxyl terminus (Harris 1990). It is thought that damage to ALP rich cell surface microvilli, which coat the lumens of tissues like intestines, kidney, liver, bone and placenta would result in the entry of ALP into the systemic circulation. Defects in PI-G synthetic mechanisms could also result in an increased entry of ALP into the circulation (Fishman 1990).

So called 'soluble' forms of ALP also occur for example, in serum and are derived from the membrane bound forms by the action of a specific phospholipase C or D (Harris 1990). The 'soluble' forms are dimers while the membrane bound forms are more likely tetramers (Hawrylak and Stinson 1988).

Much less is known about the structures of the carbohydrate moieties of these glycoproteins than of the protein moieties. However, the patterns of the ALP glycosylation appear to be organ specific and not species specific, an important result which has been exploited in measuring the different forms of ALPs in serum (McCarthy *et al.* 1998).



## 2.5 Discrimination and quantification of total serum ALP and its isoenzymes

Most colorimetric and kinetic assays that measure total ALP activity (units are U/L) utilize *p*-nitrophenyl phosphate as a substrate that is hydrolyzed by ALP into a yellow coloured compound with maximal absorbance at 405nm in an alkaline buffer. The rate of the reaction is directly proportional to the enzyme activity and this basic kinetic procedure can be adapted for a number of automated platforms (Rosalki and Foo 1984).

Various biochemical and immunological methods have been used to discriminate and selectively assay the different ALPs in serum. In clinical practice the drive has been to develop techniques that can adequately resolve the bone, liver and kidney isoforms. Briefly, three general methods have proved particularly useful in isolating and measuring ALP isoenzymes in different biological materials (Harris 1990). These methods will not be covered at any length in this thesis.

These methods include the various forms of electrophoresis (Jennings *et al.* 1970; Hagerstrand and Skude 1976; Siede and Steiffert 1977; Moss and Edward 1984; Rosalki and Foo 1984; Siriha *et al.* 1986; Cocco *et al.* 1987; Griffiths and Black 1987); immunoassays (McKenna *et al.* 1979; Lehman 1980; Slaughter *et al.* 1981; Hendrix *et al.* 1990; Masuhara *et al.* 1992) and chromatography (Schoenau *et al.* 1986; Bielby and Chin 1987; Gonchoroff *et al.* 1989; Severini *et al.* 1991).

## 2.6 Genetics of ALP isoenzymes

There are presently four known gene loci encoding the protein moieties of the alkaline phosphatase glycoproteins. The I-ALP, P-ALP and G-ALP loci are closely linked and located near the end of the long arm of chromosome 2 [q34-q37] (Griffin *et al.* 1987). In contrast the TNSALP locus is located near the end of the short arm of chromosome 1 [p36.1-p34] (Smith *et al.* 1988). The reasons for the tissue specific differences in the expression of the various ALP genes is not known (Harris 1990).

### 2.6.1 Gene structures

The human *TNSALP* gene appears to exist as a single copy in the haploid genome and is composed of 12 exons distributed over more than 50kb being at least five times larger than the intestinal and placental ALP genes mainly due to intron size differences. Exon sequences were first localized by hybridization of radio-labelled TNSALP cDNA to restriction digests of cloned genomic DNAs. Intron-exon boundaries were precisely defined by DNA sequence analysis of appropriate genomic fragments (Weiss *et al.* 1988).

The sequence of the coding region is about 1572-1602bp and the mature polypeptide chain is about 507-513 amino acids long. The nucleotide sequence at the 5' end of TNSALP gene is also known and it is in the region upstream of this site where promoter activity resides (refer to section 2.6.2 for a detailed discussion on the role of this promoter region in ALP gene regulation).

Intestinal ALP is one of the linked genes on the long arm of chromosome 2. In intestinal and *TNSALP* genes the introns occur at analogous positions (Henthorn *et al.* 1987). The I-ALP gene in its entirety is 5291bp long. A 125bp fragment located 5' to the first exon can function as a promoter in mammalian cells. Two recognized transcription signals, a TATA-like sequence and a consensus binding site for the transcriptional factor Sp1 are found in this region (Henthorn *et al.* 1988). The placental ALP gene is one of the three closely related genes that are on the long arm of chromosome 2 in man. The expression of the placental and intestinal ALP genes is highly tissue specific in spite of nearly 90% sequence similarity within their exons.

A comparison of the placental ALP 5' flanking sequence (up to -540bp) with the analogous sequence of the I-ALP gene revealed several deletions/substitutions which could be important in determining the tissue-specific expression of these genes.

The sequences of the coding regions of the different genes are all very similar in length (1572-1602bp). They each include at their 5' ends a short sequence coding for a signal peptide (17-21 amino acids) which is cleaved off in protein synthesis leaving mature polypeptide chains 507-513 amino acids long. The P-ALP and G-ALP isoenzymes each comprise 513 amino acids with a positional identity of 98%. In the case of I-ALP the mature polypeptide predicted from its cDNA sequence comprises 509 amino acids and after allowing for small gaps shows 87% positional identity with both the placental and placental-like sequences. The amino acid sequence of the mature TNSALP (507 amino acids) only show about 50-60% positional identity with the other

three ALPs. These four genes appear to have evolved from a common ancestral gene by a series of successive gene duplications (Harris 1990).

### 2.6.2 Regulation of ALP gene expression

A promoter region has been identified in each of the four genes and there is currently much interest in finding out how differences in sequence in this region may play a role in determining the differences in the expression of the various genes in different tissues.

In this report regulation of gene expression will be discussed with particular emphasis on the *TNSALP* gene. In order to examine the promoter activity of DNA within the 5' region of the *TNSALP* gene, a 672bp *Ava*II fragment corresponding to bases -801 to -129 upstream of the first base of the ATG initiation codon was inserted upstream of the promoterless bacterial chloramphenicol acetyltransferase gene in derivatives of the plasmid psVOcat (Kadesch and Kildjian 1990). For the labelling of the bases in the gene sequence and important regulatory motifs refer to Fig. 2.3 below.

```

-805  GGTCCCCTTCTGCTTCTTCTTGCGGTAGCCAGGGAGGCAGCCCACGGGCAGGGAAGCG
      GGGGTGGGGGTGCAGAGGTGCACGTGGACAGAGACA

-705  GAGAAGAGACAGGGACGTGGGCAGAGACCGGATAAAGACAGACACCAGAGAAGCCAG
      ATATGTTGACAGACACAGAGACAGACGCCAGAGAGGAAGGCAG

-605  ACAAAGAGACGGGTGGAGACAAAGACTCCCACCAAGAGACGCAGAAGGAAGATGCCGA
      CGGTAAGACAAAACAGGAGACGCGCGCAAGGAGCACGTCAG

-505  AGCCCAGGCTCGCTGAGAGAGGAAGGGCTCCCCTGGGGCAGCCCGGAGGCAGAGAGA
      CCGAGAGTGCGGGGCGGGCGGGCGAGGGACGCCAGGGCCGCGTCACC

-405  CCAGCCCGTTCCTAGCTCCGCTCCCGGCAGGGGGCGCCCTGGCCTCGTGGCACGACCG
      GCCCGCGGGGCGCGGGCTCGGGCCGGGGGCGGGGCCGGGGC

-305  CTGGCTGGAGGGGTTGGGGCCGGGGGCGGGGGAGGGGGCGGGCTGCCCGGGCC
      ♦♦
      TCACTCGGGCCCCGCGCCGCCTTTATAAGGCGGCGGGGGTGGTG
      ♦♦♦
      ***
-205  GCCCGGGCCGCGTTCGCTCCCGCCACTCCGCGCCCGCTATCCTGGCTCCGTGCTCCC
      *****
      ACGCGCTTGTGCCTGGACGGACCCTCGCCAGTGCTCTGCGCA

-105  gtaaggattcgacgctccccgcgcctggtccccagggcccagcggacgtggtccatccccttctgcatcctcc
      gctggccccgtggtgaactttaatggc.....Intron 1 (>25 kb) .....
      ttaatttctagGATTGGAACATCAGTTAACATCTGACCACT

-74   GCCAGCCCACCCCTCCACCCACGTTCGATTGCATCTCTGGGCTCCAGGGATAAAGCAG
      GTCTTGGGGTGCACCATG...
      +1

```

**Figure 2. 3** The 5'-end of the *TNSALP* gene.

*The nucleotide sequence is oriented with transcription proceeding from left to right and numbered with the first base of the ATG initiation codon designated as +1. Nucleotides 5' to this position are indicated by negative numbers, disregarding positions within the first intron. Nucleotides within the 5' flanking region and first and second exons are shown in upper case letters; those within the first intron are shown in lower case. The major start sites of transcription initiation are shown as \*; those above the line were mapped by primer extension, those below by S1 nuclease protection. Similarly, ♦ indicate a minor transcription start site. Four copies of the core consensus for SP binding are highlighted yellow. A TATA box is shown in red. Multiple copies of an imperfect purine-rich repeat are shown in green. An 11-*

*bp direct repeat within the 5' flanking region and the first exon is highlighted in purple. A 15-bp direct repeat within the 5' flanking region is highlighted in grey - (adapted from Weiss et al. 1988).*

The ability of these constructs to express chloramphenicol acetyltransferase activity was measured 48 hours after transfection into SAOS-2 human osteosarcoma cells. The TNSALP promoter was found to be four to 10 times more active than the enhancer-less SV40 promoter in SaOS-2 cell line based on the mRNA levels (Kadesch and Kildjian 1990).

A 672 bp DNA segment situated 5' to the TNSALP gene can direct chloramphenicol acetyltransferase gene expression in mammalian cells. It is reasonable to assume that this activity is due to the TNSALP gene promoter. This region contains three types of DNA sequence elements worth noting (Fig. 2.3). First, an A/T rich sequence is present between nucleotides -228 and -222, about 25bp upstream of the major transcription start site. Similar sequences referred to as TATA boxes are found at analogous positions in many eukaryotic genes and are thought to be important in positioning the start of transcription initiation (Dyanan and Tjian 1985; Serfling *et al.* 1985). Second, four copies of the consensus sequence (GGGCGG) for binding transcription factor Sp1 are present at nucleotides positions -437, -320, -280, and -268 (Kadonaga *et al.* 1986). This sequence exists within the promoter of a diverse group of cellular and viral genes. Third, between nucleotides -740 and -460, there is a group of short purine-rich, imperfect direct repeats of the consensus sequence (GGGCGG), the significance of which is not known (Weiss *et al.* 1988).

The promoter region of the TNSALP gene is quite distinct from the intestinal and the placental ALP gene promoters. The former contains a G/C – rich promoter and a CpG island at its 5' end. In contrast, the latter genes contain G/C residues that do not qualify as CpG clusters (Henthorn *et al.* 1988). The features that have been described for the promoter region of the TNSALP gene have been observed in many other genes that exhibit a wide tissue distribution notably the 'housekeeping' genes (Kadesch and Kildjian 1990).

An increasing number of factors have been described that bind to various sites in the promoter region of the TNSALP gene and are thus involved in the regulation of its expression. A few examples of the transcription factors that regulate the expression of the TNSALP gene are given below.

The androgen receptor controls an integrated gene expression program required for bone mineralization, as shown by the delayed mineralization of skull and reduced bone volume and surface area observed in androgen receptor deficient mice (Kang *et al.* 2008). Androgen receptor dimers have been shown to bind to an Sp1 binding site situated between -437 and -432 upstream of the TNSALP gene (Orimo and Shimada 2005).

Bone morphogenic protein-2 (BMP-2) is one of the most potent bone inducing agents in osteoblast differentiation. The promoter region of the TNSALP gene contains a Dlx-5 binding *cis*-element to which the BMP-2 receptor dimer binds. Increased ALP activity was induced by BMP-2 stimulation in myogenic murine C2C12 cells (Kim *et al.*

2004). It is likely that this *cis*-element is one of the Sp1 binding sites shown in Figure 2.3.

Orimo and Shimado (2005) used the human osteosarcoma cell line (SaOS-2) to study the effect of *all-trans*-retinoic acid on the expression of human TNSALP gene. It was shown in this study that *all-trans*-retinoic acid upregulates human *TNSALP* gene expression and catalytic activity in SaOS-2 cells. Retinoic acid is the active form of vitamin A that stimulates cellular differentiation via the retinoic acid receptor (RAR)-retinoid X receptor (RXR) heterodimers. This complex binds to a specific *cis*-element, the retinoic acid response element (RARE) found in vitamin A-response genes (Mangelsdorf *et al.* 1995). A RARE has been found in the promoter region of the human TNSALP gene (Orimo and Shimada 2005). Using supershift assays, Orimo and Shimado (2005) found heterodimers of RXR and RAR bound to the RARE suggesting that the complex enhanced TNSALP expression. Agents such as *all-trans-retinoic acid* that bind to the RARE in the promoter region therefore enhances TNSALP expression and activity. It is known that *all-trans*-retinoic acid is a key regulator of bone formation. TNSALP plays a key role in bone mineralization by formation of hydroxyapatite crystals in osteoblast matrix (Whyte 1994).

Regulation of the murine *TNSALP* gene by retinoic acid occurs in a similar way (Escalente *et al.* 1996).

Weston *et al.*(2003) reported that *all-trans*-retinoic acid may be involved in ossification by inhibiting early differentiation of mesenchymal stem cells (MSCs) into other cell lineages but stimulating chondrocyte proliferation and hypertrophy, which



results in increased ossification of the cartilage during osteogenesis (Weston *et al.* 2003). Chondrocytes are the major type of cell found in the cartilage matrix. They are derived from a population of adult stem cells, mesenchymal stem cells. MSCs have the ability to differentiate into other cell lineages, for example, osteoblasts, chondrocytes and adipocytes, depending on the differentiation factors to which they are exposed (Vaananen 2005; Nardi and da Silva Meirelles 2006).

Forkhead transcription factor (FKHR) is involved in the regulation of multiple genes including those that code for glucose metabolic enzymes, proapoptotic factors and cell regulators (Carlsson and Mahlapuu 2002 ). The expression of FKHR in osteogenic cells (MC3T3-E1) was measured by RT-PCR and immunoblotting assays. Furthermore, it was shown via reporter and electrophoretic mobility shift assays that ALP gene transcription was stimulated through a Forkhead receptor element [FRE] lying within the promoter region of the TNSALP gene (Hatta *et al.* 2002).

Smad-interacting protein 1 (SIP1) is one of the members of the two-handed zinc finger protein family that bind to E4-box sequences present in the promoter of the mouse TNSALP gene.

SIP1 represses TNSALP promoter activity in C2C12 cells by binding *in vitro* to a CACCCT/CACCTG sequence (Tylzanowski *et al.* 2001). This sequence is located in the promoter region, upstream of exon 1 near the TATA box. A similar distribution of these sites is seen in the human TNSALP gene. The binding of SIP1 to a CACCT/CACCTG sequence is responsible for the repression of reporter constructs

carrying a TNSALP promoter fragment. Tylzanowski *et al.* (2001) suggest that SIP1 could therefore be a candidate repressor protein for the TNSALP gene.

These studies demonstrate that the TNSALP gene promoter has a number of different regulatory elements that modulate transcription of the gene. Thus, it is possible that the level of TNSALP expression in preadipocytes is dependent on the level of particular transcription factors and that polymorphisms within the promoter region may attenuate or enhance TNSALP gene expression.

## 2.7 Mutations in the TNSALP gene

Hypophosphatasia is a rare inborn error of metabolism associated with a low serum ALP and characterized by abnormal skeletal mineralization. The expression of the *TNSALP* isoenzyme is defective although that of the intestinal and placental isoenzymes appear normal (Mueller *et al.* 1983).

It has been suggested that inorganic pyrophosphate controls the mineralization process in bone. Its accumulation in hypophosphatasia might therefore be the immediate cause of the defect in bone mineralization. The condition appears to be inherited as an autosomal recessive disorder (Whyte 1994).

Hypophosphatasia shows much variation in clinical expression and it is customary to classify the patients into four main forms. A detailed review of the clinical classification is provided by Mornet (2007). The perinatal form results in still birth or death a few days after birth due to extensive hypomineralisation and deformity of bones. Infantile hypophosphatasia presents in the first 6 months of life and includes rickets, craniosynostosis and nephrocalcinosis.

After the first year, childhood hypophosphatasia presents with rickets causing short stature, delayed walking, premature shedding of deciduous teeth. Adult hypophosphatasia is characterized by osteomalacia and bony deformities during middle age in patients with a history of mild rickets in childhood.

The clinical severity of the disease can be predicted by measurements of the immunoreactivity and catalytic activity of the bone isoenzyme. The lower the immunoreactivity index the more severe the skeletal disease (Iqbal *et al.* 2000). Heterozygotes are in most cases clinically unaffected though they show reduced serum levels of the TNSALP isoform.

Genetic linkage studies using polymorphic probes for the TNSALP locus and flanking markers are consistent with a primary abnormality in the TNSALP gene in bone hypophosphatasic kindreds (Greenberg *et al.* 1990). However, the mutations that give rise to hypophosphatasia may also involve defects in the regulation of structurally intact TNSALP gene. The first defect in the *TNSALP* gene was identified on cDNA isolated from a patient-derived fibroblast line (Weiss *et al.* 1989).

The gene defect causes a lethal form of hypophosphatasia and involves a point mutation that converts amino acid 162 of the mature TNSALP from alanine to threonine.

Since then a number of mutations of the *TNSALP* gene have been published in patients with hypophosphatasia (Henthorn *et al.* 1992; Mornet *et al.* 1998; Taillandier *et al.* 2001; Watanabe *et al.* 2001; Herasse *et al.* 2002; Mumm *et al.* 2002; Orimo *et al.* 2002; Draguet *et al.* 2004; Watanabe *et al.* 2005).

TNSALP with an Asp<sup>289</sup>→Val mutation fails to reach the cell surface and undergoes proteasome-mediated degradation and accumulates intracellularly (Ishida *et al.* 2003). A frame shift mutant protein of TNSALP has also been described that results in a delayed secretion of the enzyme and the enzyme easily undergoes proteosomal degradation (Komaru *et al.* 2005).

A website ([http://www.sesep.uvsq.fr/03\\_hypo\\_mutations.php#mutations](http://www.sesep.uvsq.fr/03_hypo_mutations.php#mutations)) for human ALP gene mutations is available and below is a summary of the documented mutations in this gene responsible for hypophosphatasia (Table 2.1). The last update was on 30<sup>th</sup> September, 2010.

**Table 2. 1** *TNSALP* gene mutations

Missense mutations are the most frequently occurring while mutations in the regulatory part of the gene are the rarest.

<b>Type</b>	<b>Number</b>	<b>%</b>
Missense	177	79.4
Nonsense	6	2.7
Splicing	9	4.0
Small insertions	4	1.8
Small deletions	22	9.9
Large deletions	3	1.0
Insertion/deletion	1	0.5
Regulatory	1	0.5
<b>Total</b>	<b>222</b>	<b>100</b>

In all the cases of hypophosphatasia that have been reported no mention of the patient's anthropometric data are given. This information would be useful in the light of claims about the role of ALP in intracellular lipid accumulation in human and rodent adipocytes (Ali *et al.* 2006). However, it is interesting to note that transgenic mice carrying a TNSALP gene knock-out are reported to have very little adipose tissue (Narisawa *et al.* 1997).

## 2.8 Intracellular lipid accumulation

Lipids are a large and diverse group of naturally occurring organic compounds that are related only by their solubility in polar organic solvents (such as ether, chloroform, acetone) and general insolubility in water (Koon 2009).

In circulation lipids are transported in combination with proteins (these complexes are called lipoproteins). In living organisms, lipids are used for energy storage, serve as structural components of cell membranes and are important hormones or contain essential fatty acids. The major form in which the lipids are stored in the body is triacylglycerides (made up of a glycerol backbone to which 3 fatty acids are esterified).

Free fatty acids may be liberated from lipoproteins by lipoprotein lipase (LPL) and these may enter cells of various tissues where they are reassembled into triglycerides. Cells of different tissues of the body have varying capacities to accumulate lipids.

### 2.8.1 Lipid droplet formation

The lipid droplet (LD) is one of the numerous terms that have been used to describe cytoplasmic lipid inclusions that are surrounded by a limiting osmophilic boundary generally thought to be a phospholipid monolayer (Murphy 2001). Recently, the terms lipid body and adiposome have been proposed as alternative names for these organelles (Liu *et al.* 2004). These discrete lipid storage droplets are made up of a core of triacylglycerol (TAG) and cholesterol esters.

The ability to package neutral lipids into discrete lipid storing droplets is a general property of most cells (Martin and Parton 2006).

In cultured cells and *in vivo* LDs form in response to elevated fatty acid levels (Pol *et al.* 2004). In one model of LD formation (Fig. 2.4) neutral lipids are synthesized between leaflets of the ER membrane.

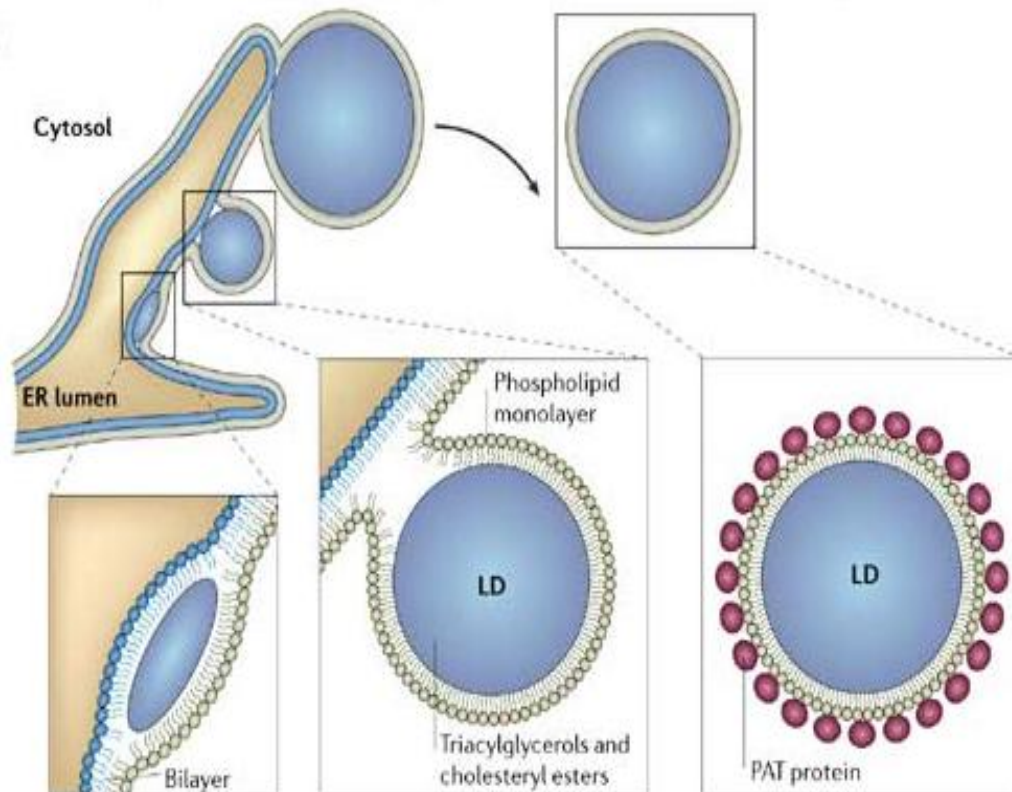


**Figure 2. 4** Lipid droplet formation and motility.

*In this model of LD formation, neutral lipids are synthesized between the leaflets of the ER membrane. The mature LD is then thought to bud from the ER membrane to form an independent organelle that is bounded by a limiting monolayer of phospholipids and LD-associated proteins. Some of the best understood LD-associated proteins are members of the PAT (perilipin, ADRP and TIP47-related protein)-domain family of proteins.*

*(Adapted from Martin and Parton 2006).*

These LDs are not just isolated storage depots in the cell but they can physically interact with several organelles over short or long durations via the cytoskeleton (Goodman 2008) [see Fig. 2.5].

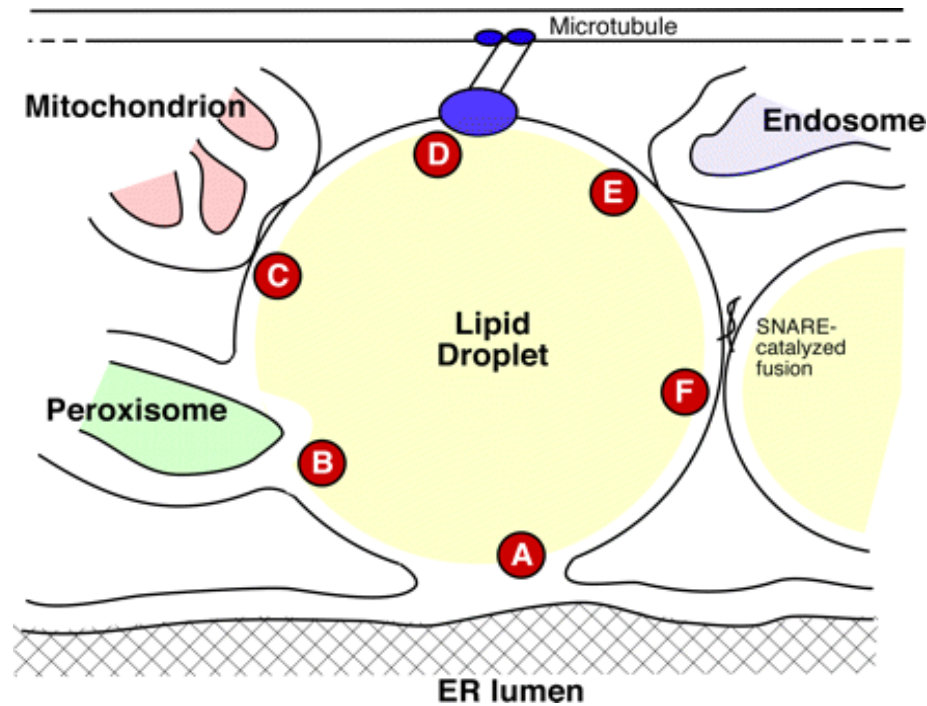


**Figure 2. 5** Lipid droplet-organelle associations.

*A, most droplets remain attached to the ER. It is not clear whether the phospholipid monolayer is continuous with the cytoplasmic monolayer of the ER, as shown, or whether the leaflets are separate. B, peroxisomes frequently associate with droplets and can insert pexopodia into the core of the droplet. C, mitochondrial associations allow flux of fatty acyl-CoAs for oxidation; other communication also exists. D, microtubule motors associate with droplets, allowing bidirectional transport (one motor is shown). E, endosomes probably associate transiently with droplets, transferring proteins and lipids. F, droplets can undergo SNARE-mediated homotypic fusion. (Adapted from Goodman 2008).*

Immunocytochemical studies (Brasaemle *et al.* 1997) revealed that lipid storage droplets are associated with specific proteins. Adipose differentiation-related protein (ADRP, also called adipophilin) is one of them. This protein is ubiquitously expressed in many different mammalian cell types and culture cell lines (including the murine



3T3-L1 preadipocytes, Chinese hamster ovary fibroblasts, HepG2 cells and the murine MA-10 Leydig cells) (Heid *et al.* 1998). Adipocytes and steroidogenic cells also express perilipins (Brasaemle *et al.* 1997), a family of lipid droplet-associated proteins that share a highly related sequence domain with ADRP. This group of proteins has been termed PAT (perilipin, ADRP and TIP47-related proteins). The proteins on the surface of LDs provide stability to the organelle and prevent their coalescing (Greenberg *et al.* 1991).

Cloning of perilipin cDNA from a rat adipocyte expression library revealed two forms of the protein. Perilipin A, a 56kDa protein is the most abundant and coats lipid droplets in both adipose and steroidogenic cells. Perilipin B, a 47kDa protein is less abundant than perilipin A and occurs primarily in adipose cells (Londos *et al.* 1999). The two isoforms are produced by alternative RNA splicing and are identical through their first 406 N-terminal amino acids but contain unrelated C-termini (Mackie-Branchette *et al.* 1995). Another form of perilipin (perilipin C) is relatively abundant in steroid producing cells but undetectable in adipocytes by Western blotting (Servetnick *et al.* 1995). This species of perilipin appears to differ from perilipin A and B at both its N- and C- terminus.

Perilipin and ADRP co-localize on lipid droplets of some cell types such as Leydig cells while in other cell types for example, mature adipocytes ADRP is not present.

The specific localization of ADRP and perilipins to lipid droplets in a wide variety of cells suggests that they may play a role in management of neutral lipid stores.

It is now known that perilipins protect the lipid droplet from hydrolysis that is mediated by the hormone-sensitive lipase/cholesterol esterase class of enzymes (Servetnick *et al.* 1995; Londos *et al.* 1996).

The amount of TAG stored in non-adipose tissue is minimal and very tightly regulated. Various rodent models of obesity have shown that cytosolic TAG accumulates excessively in these organs when this regulation is disrupted. This accumulation has been implicated in activating adverse signalling cascades that culminate in irreversible cell death (lipotoxicity) and lead to several well recognized clinical syndromes. It may arise in the setting of high plasma fatty acids or TAG in blood. Alternatively, lipid overload may result from mismatch between free fatty acid import and utilization (Lelliott and Vidal-Paig 2004). Evidence from both human and animal studies suggests that lipid accumulation in the heart, skeletal muscle, pancreas, liver and kidney play important roles in the pathogenesis of obesity-related disorders (Arulmozhi *et al.* 2007).

### 2.8.2 Tissues involved in lipid accumulation

Fat depots are scattered throughout the body, generally occurring in areas mainly composed of loose connective tissue such as the subcutaneous layers between muscle and dermis (Rosen and Spiegelman 2000). However, fat deposits are also found around the heart, kidneys and other internal organs.

- Adipose tissue

Adipose tissue is found mainly under the skin but also in depots between the muscles, in the intestines and in their membrane folds, around the heart and the liver. Its main role is to store energy in the form of fat, although it also cushions and insulates the body. It has an important endocrine function in producing hormones/factors such as leptin, prostaglandins, adiponectin, resistin, TNF $\alpha$ , IL-6, and adiponectin (Frubeck *et al.* 2001).

White fat (which is the more common type of adipose cell) is found in a wide variety of locations in the mammalian body. Brown fat is mainly found in subscapular, interscapular and mediastinal areas. Brown adipose cells are associated with thermogenesis mainly in hibernating and newborn mammals, although recent studies using  $^{18}\text{F}$ -fluorodeoxyglucose ( $^{18}\text{F}$ -FDG) positron-emission tomographic and computed tomographic (PET-CT) scans show that brown fat is present in adult humans. Brown adipose tissue regions were present more frequently in women than in men and the amount of brown adipose tissue correlated negatively with body-mass index especially in older people (Cypess *et al.* 2009).

It seems that higher levels of brown adipose tissue may protect against age-related obesity. This might also explain the gender differences in the prevalence of obesity in some population groups.

Brown and white adipocytes are morphologically different. Thus, brown adipocytes have cytoplasmic lipids arranged as numerous small membrane-bound droplets (multilocularity), while white adipocytes have cytoplasmic lipids arranged in a

single vacuole (unilocularity) (Cinti 2002). The mitochondria of brown adipocytes are packed with cristae and contain the thermogenic uncoupling protein 1 (UCP1) (Garlid *et al.* 1998). *In vivo* and *in vitro* studies have shown that the differentiation process of the two types of adipocytes show distinctive features. The origin of the adipocyte precursor is however, still unknown. White adipocytes have been shown to transdifferentiate into brown adipocytes and *vice-versa* (Cinti 2002).

The differentiation of preadipocytes into mature adipocytes, which includes the expression of mature cell markers and a concomitant accumulation of intracellular lipid, is called adipogenesis. A detailed discussion of adipogenesis is given in section 2.9 of this report.

Obesity is defined as a state of increased body fat tissue mass that arises from an imbalance between energy intake and expenditure. It is associated with increased fat cell size and number. It is considered a chronic illness, increasing worldwide and is known to be a major risk factor for type 2 diabetes, cardiovascular disease, and a number of many other disorders (Flegal *et al.* 2005).

Body fat is composed of two major fat depots: visceral and subcutaneous. Visceral fat is located around internal body organs (inside the peritoneal cavity) whilst subcutaneous fat is found beneath the epidermis. Visceral fat is composed of several adipose depots and portends greater risk for diabetes, dyslipidemia, hypertension and coronary artery disease than does subcutaneous fat (Reaven *et al.* 2004). It has been suggested that the high lipolytic rate of visceral adipocytes and their higher secretory

rate of factors that modify whole-body insulin sensitivity may play a role in this disease association (Bergman *et al.* 2006).

- The liver

In the liver, fat is located within hepatocytes (Szczepanick *et al.* 1999) and also in Ito cells [also known as hepatic stellate cells] (Hautekeete and Geerts 1997). In animals, the liver has been shown to have a high capacity to accumulate TAG and the size of this pool can change several-fold within hours (Duce *et al.* 1985). Triglycerides may accumulate either as small or large lipid deposits (micro- or macrovesicular steatosis) (Fong *et al.* 2000). Microvesicular steatosis is often associated with severe liver dysfunction and is a more severe condition than macrovesicular steatosis (Burt *et al.* 1998). Causes of macrovesicular steatosis include excessive alcohol intake and other causes such as total parenteral nutrition (TPN) and jejunal bypass. The pathogenesis of TPN-induced liver steatosis remains unknown (Wang *et al.* 2006).

Chronic ingestion of ethanol inhibits both the oxidation of fatty acids in the liver and release of very low-density lipoprotein (VLDL) into the blood. All of these mechanisms favour steatosis (Day and Yeaman 1994; Ismail 2008).

It has been shown that the regulation of lipogenesis and the accumulation of lipids in hepatocytes is mediated by PPAR $\gamma$  (Inoue *et al.* 2005). Zhao *et al.* (2004) showed that in a rat model of fatty liver disease PPAR $\gamma$  expression decreased in rats fed on alcohol. The fall in PPAR $\gamma$  correlated with an increase in inflammation, necrosis and fibrosis. Therefore, the investigators hypothesised that the ability of alcohol to inhibit PPAR $\gamma$  activity may promote liver fibrosis and necrosis (Zhao *et al.* 2004).

Diabetologists and hepatologists continue to see a rise in incidence of fatty liver disease (Yki-Jarvinen and Westerbacka 2005). Non-alcoholic steatohepatitis (NASH) is liver disease that occurs in people who drink little or no alcohol. The major feature of NASH is fat in the liver, associated with inflammation (Chitturi *et al.* 2004). About 20% of NASH progresses to cirrhosis over approximately 5-7 years (Powell *et al.* 1990). The cause of NASH is still not clear. The incidence of NASH is on the rise and seems to be linked to the global epidemic of obesity and type 2 diabetes mellitus (Farrel 2003). Visceral fat and insulin resistance have been proposed as predictors of NASH (Sobhonslidsuk *et al.* 2007; Ohki *et al.* 2009) but it is not known how they cause this disease. The definitive test for the diagnosis of NASH is histology of a liver biopsy. At present there is no specific therapy for NASH except interventions that control conditions associated with NASH such as diabetes and hyperlipidemia.

Clinical trials with the thiazolidinediones have shown improvements in liver pathology in NASH patients (Reynaert *et al.* 2005; Argo *et al.* 2009).

- Steroidogenic cells

Cholesteryl esters account for most of the stored lipids in adrenal cells and there is some accumulation of triacylglycerols and free fatty acids as well. Adrenal cells use this stored cholesterol as a substrate for steroid hormone synthesis or, as with other cells for membrane synthesis. Electron microscopy studies show that lipid droplets in adrenal cells are surrounded by a layer of an electron-dense substance known as the 'capsule' (Almahbobi *et al.* 1992). This adrenal lipid droplet capsule can be

demonstrated by immunostaining with a monoclonal antibody which recognizes a 160kda protein on the lipid droplet surface (Wang and Fong 1995).

Cultured adrenal cells contain many small lipid droplets that cannot be readily quantified by Oil Red O staining. The size of the lipid droplets can, however, be increased by incubating cells with culture medium containing an oleic acid/albumin mixture (Brasaemle *et al.* 1997).

Leydig cells are found adjacent to the seminiferous tubules in the testes. They synthesize and release androgens (C19 steroids). Lipids, mainly cholesteryl esters are stored in lipid droplets in Leydig cells (Sinha *et al.* 1997) and act as the precursors for the androgens. Adrenal cortical and Leydig cells both contain perilipin C which is not detected in adipocytes (Servetnick *et al.* 1995).

- Accumulation of lipids in macrophages

Lipids in macrophages are stored in cytosolic lipid droplets which have been suggested to consist of a core of neutral lipids (cholesterol esters or TAG) surrounded by a monolayer of amphipathic structures such as phospholipids and proteins. Perilipin and ADRP are the most well known of these proteins. The latter is the predominant protein of the lipid droplets in macrophages (Lu *et al.* 2001).

The uptake of modified low-density lipoprotein (LDL) by macrophages via the scavenger receptors results in lipid droplet accumulation and foam cell formation (Brown and Goldstein 1983; Draude and Reinhard 2000). This process plays an important role in the development of atherosclerosis. The atherosclerotic lesion is characterized by regions of hypoxia (Bostrom *et al.* 2006; Xu 2006). Hypoxia causes

an accumulation of triglyceride-containing cytosolic lipid droplets in the cell by increasing the expression of ADRP and the rate of TAG biosynthesis and by reducing the rate of  $\beta$ -oxidation of fatty acids (Bostrom *et al.* 2006).

In macrophages, induction of adipophilin expression by modified LDL promotes intra-cellular lipid accumulation and prevents lipid efflux from the macrophage cell line, THP-1. Therefore, adipophilin may contribute to lipid accumulation in the intima of the arterial wall (Larigauderie *et al.* 2004).

The peroxisome proliferator activated receptors ( $\alpha$ ,  $\gamma$  and  $\delta$ ) are a family of fatty acid-activated transcription factors which control lipid homeostasis and cellular differentiation.

It was reported (Vosper *et al.* 2001) that PPAR $\delta$  mRNA and protein levels are dramatically elevated during macrophage differentiation and provide pharmacological evidence that PPAR $\delta$  is a positive effector of lipid accumulation in human macrophage cultures.

- Accumulation of lipids in muscle,  $\beta$ -cells and cardiomyocytes

Lipid contained within skeletal muscle as TAG is thought to be an important link between obesity, insulin resistance and type 2 diabetes (Szczepanick *et al.* 1999; Goodpaster and Wolf 2004). It is thought that the oversupply of lipids to skeletal muscle causes insulin resistance by promoting the accumulation of lipid-derived metabolites (e.g. ceramide) that inhibit insulin signalling (Schmitz 2000; Sebastian *et al.* 2007).



The regulation of cholesterol and TAG metabolism in muscle cells is believed to involve liver X receptors (LXR). These play an important role in fatty acid metabolism by controlling the gene expression of sterol regulatory element binding protein-1c (SREBP-1c) and fatty acid synthase.

The  $\beta$ -cells of the islets of Langerhans synthesize and secrete insulin. Studies in the Zucker diabetic fatty rat have led to the concept that chronically elevated free fatty acid levels can cause apoptosis of TAG-laden pancreatic  $\beta$ -cells as a result of the formation of ceramides which induce nitric oxide-dependent cell death (Lee *et al.* 1994). This lipotoxicity could explain the development of type 2 diabetes in obesity. The ability of normal  $\beta$ -cells to accumulate cytoplasmic TAG might serve as a cytoprotective mechanism against FFA-induced apoptosis by preventing a cellular rise in toxic free fatty acyl moieties. It is known that this capacity is lost or insufficient in cells with a prolonged TAG accumulation as may occur *in vivo* (Cnop *et al.* 2001). Rat and human  $\beta$ -cells express high affinity receptors for LDL and VLDL and can internalize both lipoproteins. These receptors were not observed in islet  $\alpha$ -cells. In human  $\beta$ -cells LDL and VLDL uptake may contribute to the intracellular lipid accumulation observed in the aging  $\beta$ -cell population (Cnop *et al.* 2002).

Excessive deposition of lipids within myocardial tissue is an important cause of non-ischaemic dilated cardiomyopathy in humans (McGavock *et al.* 2006). Overexpression of long-chain acyl-CoA synthetase, a key enzyme involved in TAG synthesis, produces cardiac-restricted steatosis. Increased protein expression of acyl-CoA synthetase in the myocardium disrupts the balance between lipid import and

export which results in diffuse lipid accumulation in heart cells (McGavock *et al.* 2006). Current thinking suggests that cardiomyopathy is not a direct consequence of TAG accumulation alone but that it develops secondary to accumulation of by-products of lipid metabolism just like in muscle cells and interferes with intracellular signaling pathways (Schaffer 2003).

It is not yet clear whether the intracellular lipids that accumulate in  $\beta$ -cells, muscle or heart are membrane bound like in adipocytes and hepatocytes.

TNSALP is expressed in adipocytes (Ali *et al.* 2006) and hepatocytes (Nowrouzi and Yazdanparast, 2005) both of which are known to accumulate lipids. If TNSALP is an important factor in intracellular lipid accumulation it would be expected to also be expressed in the tissues described above.

However, no studies have specifically analysed whether these tissues do contain TNSALP, and this must be a question for future studies.

### 2.8.3 Cell line models used in studying lipid metabolism

Approximately one third of the adipose tissue mass within mammals is made up by mature adipocytes. The remaining two thirds of adipose tissue mass is made up by small blood vessels, nerve tissues, fibroblasts and preadipocytes in various stages of development (Geloan *et al.* 1989). Preadipocytes then make up a very small proportion of adipose tissue (Ntambi and Kim 2000). Preadipocytes and fibroblasts are not easily distinguishable and the inability to align preadipocytes at similar developmental stages confounds detailed *in vivo* studies (Ntambi and Kim 2000). In addition, primary cultures have a limited life span in culture. Some of these difficulties were partially

circumvented in the 1970s when Green and his colleagues established immortal fibroblast cell lines that readily differentiated into adipocytes when appropriate hormonal inducers were added (Green and Kehinde 1975). These cell lines provide an experimentally accessible system *in vitro*, which faithfully recapitulate the features of adipogenesis observed *in vivo*.

### 2.8.3.1 Preadipocyte cell lines

Adipocyte precursor cell lines can be divided into two classes: pluripotent fibroblasts and unipotent preadipocytes. The pluripotent fibroblasts have the ability to be converted into several cell types (Cornelius *et al.* 1994). 10T1/2 fibroblasts which were derived from CH3 mouse embryos can be converted to preadipose, pre-muscle and precartilaginous tissue upon treatment with 5-azacytidine, an inhibitor of DNA methylation. Other pluripotent fibroblasts cell lines are Balb/c 3T3, 1246, RCJ3.1 and CHEF/18. These pluripotent fibroblasts act as good models for understanding the events responsible for cellular determination of the separate cell fates.

Unipotent preadipocytes (3T3-L1, 3T3-F442A, Ob1771 and 1256) are cells that have undergone determination and can only differentiate to adipocytes. These cell lines are ideal for studying the molecular events responsible for the conversion of preadipocytes into adipocytes (Ntambi and Kim 2000). There are some differences in the differentiation requirements of each of these cell lines and it is thought that this is due to variations in the developmental stage at which cells were arrested when immortalised (Ntambi and Kim 2000).

The 3T3-L1 and 3T3-F442A culture lines are the most widely used with the former cell line being the most well-characterized and reliable model for studying the differentiation process (Takahashi *et al.* 2008). The 3T3-L1 cell line was derived from the Swiss 3T3 cell line prepared from disaggregated 17-19 day old Swiss mouse embryos (Green and Kehinde 1975). The 3T3-L1 cells show strong contact inhibition *in vitro* that is, their rate of growth is reduced as soon as cell-to-cell contacts are established. When the growth of the cells is arrested, a certain portion will convert to adipose cells (Aaranson and Todaro 1968).

There are advantages and disadvantages to using cell lines to study preadipocyte development. A cell line derived from cloning provides a homogenous cell population that contains cells all at the same stage of differentiation. This allows for a definitive response to various treatments. Furthermore, these cells can be passaged indefinitely, which provides a consistent source of cells (Ntambi and Kim 2000). It is, however, clear that preadipocytic cell lines are not true analogues of primary adipocytes (MacDougald and Mandrup 2002). In interpreting results it must also be kept in mind that with preadipocyte cell lines, all cells are exclusively differentiated white adipose tissue while in mammals a second type of fat cell (brown adipocytes) also exists. Another very important limitation to the exclusive use of established preadipocyte cell lines is that they have not allowed an assessment of depot-specific differences in fat cell behaviour and preadipocytes isolated from different fat depots are known to have different adipogenic potential, the molecular basis of which is not fully understood (Lefebvre *et al.* 1998).

### 2.8.3.2 Other lipid accumulating cell lines

HepG2 is an adherent cell line derived from a human hepatocellular liver carcinoma. The cells are epithelial in morphology. This cell line has been found to express a wide variety of liver-specific functions. Among these functions are those related to cholesterol and TAG metabolism. Intracellular lipid storage is increased by the addition of oleic acid coupled to bovine serum albumin to the culture medium to allow quantification of lipid accumulation (Brasaemle *et al.* 1997).

Y-1 is a cell line derived from the mouse adrenal cortex tumour. It also has an adherent growth mode and epithelial morphology. It produces steroid hormones at a high rate and pronounced morphological transformation under ACTH stimulation (Bounassisi *et al.* 1962). It accumulates small lipid droplets that do not stain deeply with oil red O stain. In order to enhance lipid accumulation it is necessary to add oleic acid/albumin to the culture medium (Brasaemle *et al.* 1997).

## 2.9 Regulation of lipid accumulation in selected cell types

### 2.9.1 Adipocytes

Adipocytes are thought to originate from fibroblast-like precursor cells that differentiate into mature adipocytes under appropriate stimulatory conditions (Cornelius *et al.* 1994). These precursor cells do not possess any morphological or enzymatic marker that can be used to determine whether they will be adipocytes (Albright and Stem 1998). The criteria used to identify preadipocytes depends on lipid accumulation after clonal expansion has stopped. This makes early identification of the preadipocytic state *in vivo* difficult (Gregoire *et al.* 1998). In humans much of

preadipocyte differentiation occurs shortly after birth (Burd *et al.* 1985). This allows the newborn to cope more efficiently with intervals between nutrient intake (MacDougald and Lane 1995).

During the first two years of life, adipose tissue mass grows by an increase in both size and number, initially by cell enlargement and then after 6-12 months by an increase in both size and number (Salans *et al.* 1973). Cell number increases slowly from two years of age until close to the onset of puberty, and during adolescence, there is another sharp elevation in cell number that accounts for a spurt in the growth of adipose tissue (Ailhaud *et al.* 1992). In the infant and young children there is a continuous subcutaneous layer of fat over the whole body. In the adult this thins out in some regions but persists and grows thicker in certain sites of predilection (Bjorntorp 1974). These differ in the two sexes and are largely responsible for the characteristic differences in the body form of females and males.

The adipogenic program

Adipogenesis is a term used to describe all the processes that lead to the appearance and accumulation of lipid droplets in adipocytes. It is a two-step developmental process by which an undifferentiated mesenchymal cell is committed into a preadipocyte, which then undergoes a secondary differentiation step to become a lipid-filled adipocyte (Fig. 2.6). The undifferentiated mesenchymal cell can develop along a number of different lineages such as myocyte, chondrocyte or osteocyte (Gregoire *et al.* 1998; MacDougald and Mandrup 2002).

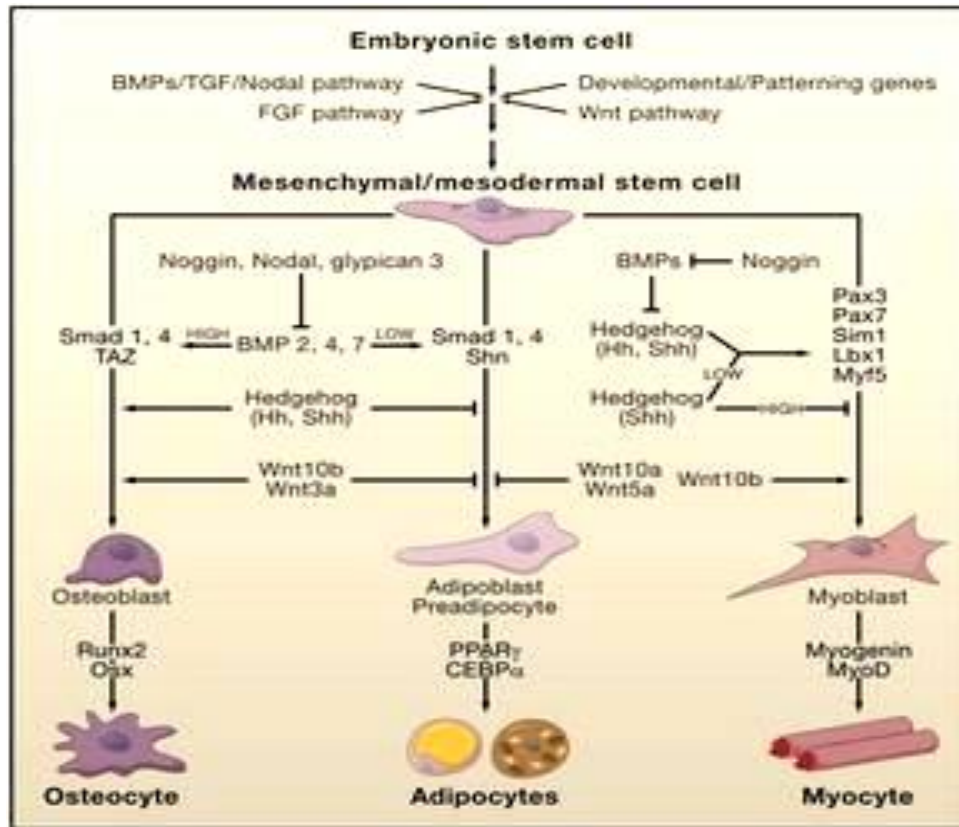


**Figure 2. 6** Development of mesenchymal/mesodermal derivatives.

*Mesenchymal stem cells (MSCs) develop from the mesoderm and then commit into different lineages influenced by a number of factors. Bone morphogenic proteins (BMPs) through their intracellular mediators (Smad proteins) can trigger MSCs to enter the osteogenic or adipogenic while preventing commitment into the myogenic lineage. Intracellular proteins such as TAZ and Schnurri-2 modify the action of BMP in the determination of the osteogenic or adipogenic lineages. In addition the actions of BMP can be modulated by Noggin, Nodal and glypican-3. Wnt and Hedgehog proteins are important for MSCs commitment in myogenic and osteogenic lineages and prevent commitment into adipogenic lineages. Adapted from (Gesta et al. 2007).*

- Adipocyte determination

Determination is the irreversible commitment of a cell to a pathway of differentiation (Whittaker 1973; Maduro 2010). Determination always comes before differentiation. Autonomous determination is when the cell holds all the information that it needs to direct its differentiation. When a cell depends on instructions from neighbours to direct its differentiation, it is called interactive determination (Lau *et al.* 2010). The fertilized egg and its early daughter cells are totipotent but as development proceeds, these cells give rise to progressively more specialised cells which have a less extensive developmental repertoire but can still develop into multiple cell types (Mayani 2003). In the end the cells become restricted to their ultimate fate, meaning that they become committed to a particular type of differentiation. This commitment or determination involves a gradual reduction of developmental options that ultimately renders the cells capable of becoming only a single cell type (Taghert *et al.* 1984).

Determination most likely involves the expression of one or few regulatory genes that control the subsequent expression of many other genes in the hierarchy. These restrictions of gene expression can be considered to be developmental. These decisions occur without any apparent change in the phenotype of the cells. Therefore one cannot establish whether a cell has become committed until after determination has occurred. The early molecular events that induce determination of the primitive mesenchymal precursor cells to the adipocyte lineage remain unknown though the transcriptional pathways that are important in the later stages of adipose differentiation have largely been identified (Rosen *et al.* 2000).



- Adipocyte differentiation

Adipocyte differentiation is the process whereby a relatively unspecialized cell acquires specialized features of an adipocyte. This transition involves four stages (growth arrest, clonal expansion, early and terminal differentiation). The first stage in the differentiation of fat cells and most cell lineages, is growth arrest (Bernlohr *et al.* 1985). In cultured cell lines growth arrest occurs after contact inhibition although experiments using very low density plating in serum-free medium demonstrate that cell-cell contact is not an absolute requirement for growth arrest to occur (Gregoire *et al.* 1998). In cultured cell models, growth arrest also requires the addition of a differentiation-inducing hormone mixture, usually insulin and a glucocorticoid and is followed by one or two rounds of clonal expansion (Camp *et al.* 2002). This process ceases with the expression of the transcriptional factors PPAR $\gamma$  and CCAAT/enhancer binding protein  $\alpha$ (C/EBP $\alpha$ ) (Shao and Lazaar 1997; Morrison and Farmer 1999) which leads to a permanent period of unusual growth arrest called G<sub>D</sub> (Scott *et al.* 1982) followed by the expression of the fully differentiated adipocyte phenotype (Cornelius *et al.* 1994). The cells then assume a more rounded shape, accumulate fat droplets and become terminally differentiated adipocytes by day 5-7 (Ntambi and Kim 2000).

The first sign of adipocyte differentiation is the appearance of lipid droplets in the cytoplasm. This is a much easier and more sensitive criterion than measuring enzymatic or chemical changes in culture because of asynchrony of participating cells. There is a dramatic alteration in cell shape as the cell converts from fibroblastic to a spherical shape.

The distinct shape results from different arrangements of the various cytoskeletal components inside the cell including microtubules and intermediate filaments. Rearrangement of the vimentin cytoskeleton has been observed during the transformation of preadipocytes into adipocytes in cell culture (Franke *et al.* 1987).

Studies have shown that the capacity of the preadipocytes to differentiate and accumulate lipid deteriorates with aging (Kirkland *et al.* 1993). Preadipocytes collected from old rats and humans accumulate less lipid and have lower lipogenic enzyme activities when exposed to a variety of conditions that induce differentiation than preadipocytes from younger individuals.

#### 2.9.1.1 Genes involved in adipocyte differentiation

Ntambi and Kim (2000) described the time course of the genetic events involved in adipocyte differentiation (Fig. 2.7). Very early markers of adipocyte differentiation are expressed when 3T3-L1 cells reach confluence. The cell to cell contact stimulates the expression of lipoprotein lipase and type VI collagen genes (Cornelius *et al.* 1988). Within an hour after the addition of transformation cocktail, the expression of c-fos, c-jun, c-mys and C/EBP $\alpha$  and  $\delta$  is observed (Cornelius *et al.* 1994). Between day 3-4, the activity of C/EBP $\alpha$  and PPAR $\gamma$  is maximum and induce the transcription of many adipocyte genes encoding proteins and enzymes involved in creating and maintaining the adipocyte phenotype (Gregoire *et al.* 1998). Interestingly, several genes associated with adipocyte differentiation are found to be aberrantly expressed in transgenic or naturally occurring mouse models of obesity and metabolic diseases (Robinson *et al.* 2000).

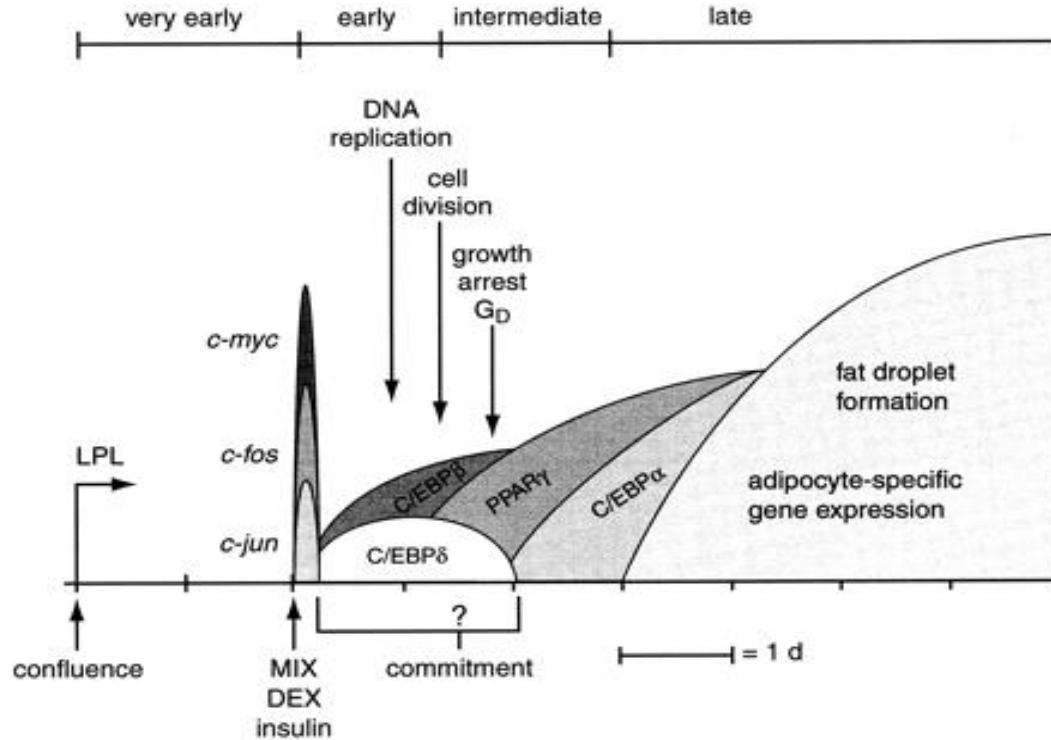


**Figure 2. 7** Progression of 3T3-L1 preadipocyte differentiation.

The major identified events of preadipocyte differentiation are presented chronologically. Areas labeled by gene names represent periods of gene expression during the differentiation program. The distinct stages of differentiation (very early, early, intermediate and late) are also provided. LPL, lipoprotein lipase; C/EBP, CCAAT/enhancer binding protein, PPAR, peroxisome proliferator-activated receptor; MIX, methylisobutylxanthine; DEX, dexamethasone (Ntambi and Kim 2000).

In another study, 579 genes were identified as genes that changed reliably and consistently during adipocyte differentiation (Gerhold *et al.* 2002). These genes were clustered into 32 distinct groups using the UPGMA (Unweighted group method with arithmetic mean) clustering algorithm (Table 2.2). Large portions of genes in clusters 26-32 are adipocyte specific.

**Table 2. 2** Clusters of genes by the UPGMA version of the average linkage algorithm (abridged version).

The genes shown in *bold* were confirmed with quantitative PCR analysis. Adapted from (Gerhold *et al.* 2002).

Cluster	No. of genes	Accession no.	Representative genes	Function
1	1	L12030	Stromal cell-derived factor 1	Cytokine and cytokine receptor
2	5	X83536	Matrix metalloproteinase 14	Extracellular matrix/cell adhesion
		M32490	Cysteine-rich protein 61	Cell growth/cycle regulator
		X65128	Growth arrest-specific gene	Cell growth/cycle regulator
		U43076	Cell division cycle 37	Cell growth/cycle regulator
		M70641	FISP12	Cell growth/cycle regulator
3	22	<b>X04367</b>	<b>PDGF receptor, <math>\beta</math>-polypeptide</b>	Cell growth/cycle regulator
		M63725	Activating transcription factor 1	Transcription factor
8	2	X70298	SRY box-containing gene 4	Nucleic acid binding
10	171	W99875	Pyruvate kinase 3	Metabolism
		M13445/X04663	$\alpha_1$ -Tubulin/ $\beta$ 5-tubulin	Structural protein
		L07803	Thrombospondin 2	Extracellular matrix/cell adhesion
25	1	AA067813	Glutamate-cysteine ligase	Protein synthesis
26	1	M93275	Adipose differentiation-related protein	Lipid metabolism
		<b>U01841</b>	<b>PPAR<math>\gamma</math></b>	Nuclear receptor
		D00466	Apolipoprotein E	Lipid metabolism
		<b>W36455</b>	<b>Adipsin</b>	Lipid metabolism

		W13632	Angiotensinogen	Secreted protein
		M33324	GH receptor	Cell growth/cycle regulator
27	29	U08188	Hormone sensitive lipase	Lipid metabolism
		<b>X13135</b>	<b>Fatty acid synthase</b>	Lipid metabolism
		AA016431	Fatty acid-binding protein 5	Lipid metabolism
		X85983	Carnitine acetyltransferase	Lipid metabolism
		W85270	Apolipoprotein CI	Lipid metabolism
		<b>U15977</b>	<b>Long-chain acyl-CoA synthase</b>	Lipid metabolism
		U41497	Very long-chain acyl-CoA dehydrogenase	Lipid metabolism
		L11163	Short-chain acetyl-CoA dehydrogenase	Lipid metabolism
31	2	M21285	Stearoyl-CoA desaturase	Lipid metabolism
32	1	<b>W29562</b>	<b>Adipocyte protein aP2</b>	Lipid metabolism

The role of TNSALP in the control of adipocyte differentiation is not fully understood. Its inhibition does block intracellular lipid accumulation (Ali *et al.* 2005) however, whether this inhibition involves the down regulation of the major transcription factors involved in the molecular control of adipogenesis, is not known.

#### 2.9.1.2 Transcriptional regulation of adipogenesis

Three classes of transcriptional factors have been identified that directly influence fat cell development. These include PPAR $\gamma$ , C/EBPs and the basic helix-loop-helix family of transcription factors (ADD1/SREBP1c).

- Peroxisome proliferator activated receptor- $\gamma$  (PPAR $\gamma$ )

PPAR $\gamma$  belongs to a superfamily of nuclear hormone receptors and like many members of this class of transcriptional factors, PPAR $\gamma$  must heterodimerize with a partner (the retinoid X receptor  $\alpha$ ) to bind DNA and be transcriptionally active (Kliwer *et al.* 1994; Tontonoz *et al.* 1994; Zhu *et al.* 1995). The basic mechanism of action of PPAR $\gamma$  and some of its ligands are illustrated in Fig. 2.8. The target genes of PPAR $\gamma$  and  $\alpha$  are those that are mostly involved in lipid and carbohydrate metabolism

Two other distinct members of the PPAR subfamily have been described:  $\alpha$  and  $\delta$  (Dreyer *et al.* 1992). Two isoforms of PPAR $\gamma$  exist (PPAR $\gamma$  1 and PPAR $\gamma$  2), both of them being a result of alternative promoter usage and differential RNA splicing of the PPAR $\gamma$  gene at the 5' end (Zhu *et al.* 1995). PPAR $\gamma$ 1 is the dominant isoform found in fat cells. PPAR $\gamma$ 2 is 30 amino acids longer than PPAR $\gamma$ 1 and is present at lower levels in adipose tissue and in a variety of other cell types (Tontonoz *et al.* 1994; Brun *et al.* 1996). The actions of PPARs at the cellular level are summarized in Fig. 2.8.

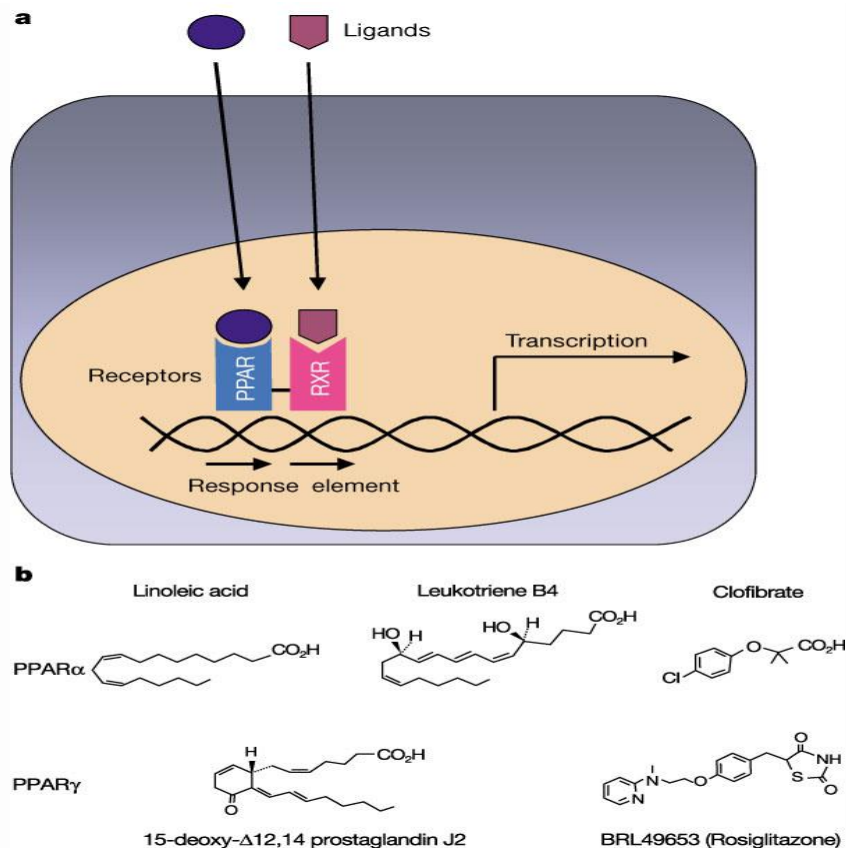


**Figure 2. 8** Basic mechanism of action of nuclear hormone receptors.

**a**, Nuclear hormone receptors bind to a specific sequence in the promoter of target genes (called hormone response elements), and activate transcription upon binding of ligand. Several nuclear hormone receptors, including the retinoic acid receptor, the vitamin D receptor and PPAR, can bind to DNA only as a heterodimer with the retinoid X receptor, RXR, as shown. **b**, Structure of some PPAR $\alpha$  and PPAR $\gamma$  ligands (Kersten et al. 2000).

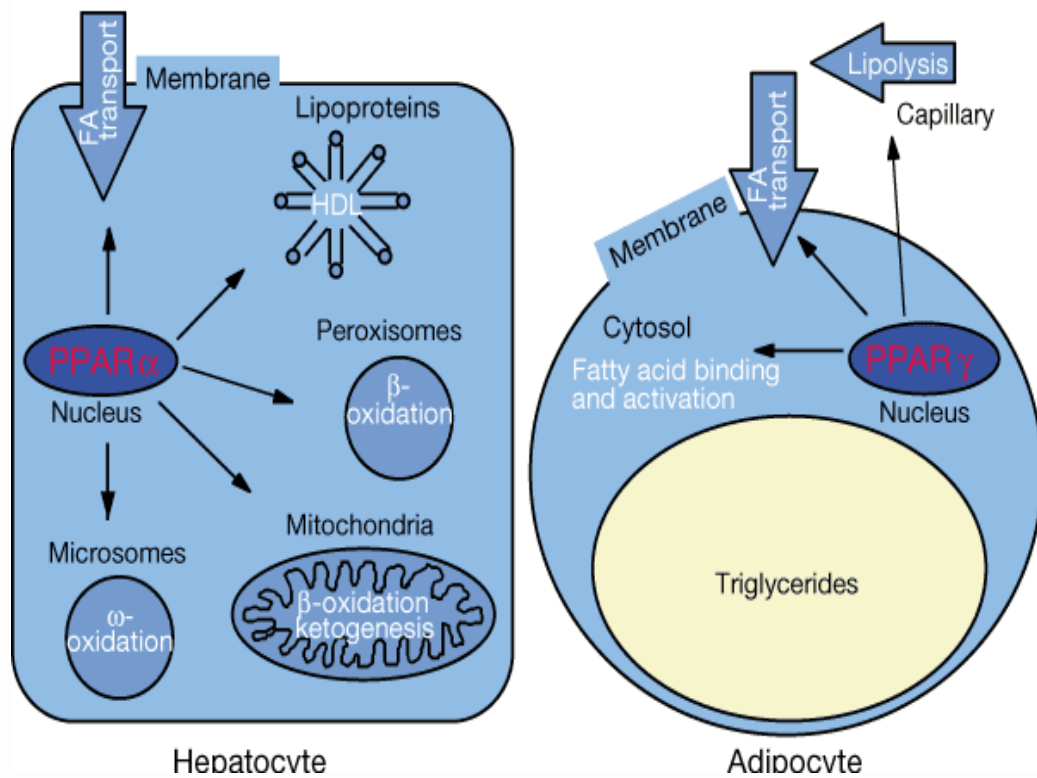


**Figure 2. 9** Actions of PPARs at the cellular level.

*PPAR $\alpha$*  stimulates oxidation of fatty acids in various organelles, such as mitochondria, peroxisomes and microsomes. It also stimulates uptake of fatty acids and synthesis of lipoproteins. *PPAR $\gamma$*  stimulates lipolysis of circulating triglycerides and the subsequent uptake of fatty acids into the adipose cell. It also stimulates binding and activation of fatty acids in the cytosol, events that are required for synthesis of triglycerides. FA, fatty acid; HDL, high density lipoprotein (Kersten *et al.* 2000).

#### Roles of PPAR $\gamma$ in mammalian metabolism

The role of PPAR $\gamma$  in adipogenesis has been illustrated in studies that have deleted this gene in mice. *PPAR $\gamma$*   $-/-$  mice are completely devoid of adipose tissue and *PPAR $\gamma$*   $+/-$  mice are characterized by a decreased adipose tissue mass (Kubota *et al.* 1999).



*In vitro* data shows that embryonic stem cells lacking both copies of *PPAR*<sub>γ</sub> fail to differentiate into adipocytes after appropriate treatment (Rosen *et al.* 1999).

In humans several mutations in the *PPAR*<sub>γ</sub> gene have so far been described. A rare Pro115Gln mutation in the NH<sub>2</sub> terminal domain of *PPAR*<sub>γ</sub> was found in four very obese subjects (Ristow *et al.* 1998). This mutation results in a permanently active *PPAR*<sub>γ</sub> and leads to increased adipocyte differentiation and obesity. The *PPAR*<sub>γ</sub> gene is mapped to chromosome 3(3p2s; OMIM number 601487).

High affinity selective *PPAR*<sub>γ</sub> agonists such as the thiazolidinediones (TZD) have been used to mediate differentiation in fibroblastic cells leading to lipid accumulation and the expression of many endogenous genes characteristic of the adipocyte (Sandouk *et al.* 1993). Some of the genes induced are lipoprotein lipase, type VI collagen, acylCoA synthetase, glucose transporter (Glut) 4 and fatty acid transport protein-1 (Cornelius *et al.* 1988).

A loss of function, missense mutation in *PPAR*<sub>γ</sub> has been reported in two patients with severe insulin resistance and diabetes (Barroso *et al.* 1999) indicating the role of *PPAR*<sub>γ</sub> in glucose homeostasis.

In one study, *PPAR*<sub>γ</sub> was shown to regulate bone metabolism *in vivo* with *PPAR*<sub>γ</sub>-deficient embryonic stem cells failing to differentiate into adipocytes, but spontaneously differentiating into osteoblasts. The adipocyte phenotype was restored by re-introduction of the *PPAR*<sub>γ</sub> gene (Akune *et al.* 2004).

### Regulation of PPAR $\gamma$ activity

PPAR $\gamma$  is activated through the binding of ligands to its carboxy-terminal ligand-binding domain. The thiazolidinedione (TZD) class of anti-diabetic drugs are recognized as potent synthetic ligands for PPAR $\gamma$  (Lehmann *et al.* 1995). These compounds are effective at promoting adipogenesis in culture and *in vivo*.

The first natural PPAR $\gamma$  ligand to be identified was a prostanoid, 15-deoxy- $\Delta^{12,14}$  prostaglandin J<sub>2</sub> [15d PGJ<sub>2</sub>] (Forman *et al.* 1995; Kliewer *et al.* 1995). Eicosanoids, polyunsaturated fatty acids (oleate and linoleate) and their derivatives also bind PPAR $\gamma$  (Forman *et al.* 1997; Kliewer *et al.* 1997). These natural ligands however bind PPAR $\gamma$  with affinities much lower than synthetic ligands (Kliewer *et al.* 1997).

PPAR $\gamma$  is inhibited by a number of inflammatory cytokines. The ligand-dependent transcriptional activity of PPAR $\gamma$  is thus inhibited by TNF- $\alpha$  (Zhang *et al.* 1996). In the TNF- $\alpha$  signaling pathways, activation of IKK and ERK were reported to inhibit the transcriptional activity of PPAR $\gamma$  (Ruan *et al.* 2003; Gao *et al.* 2006).

The association of PPAR $\gamma$  activity and atherosclerosis remains unclear (Kersten *et al.* 2000) although PPAR $\gamma$  seems to stimulate the uptake of oxidized LDL, an important component in foam cell formation.

- C/EBP family

Three members of the C/EBP family of transcription factors i.e. C/EBP $\alpha$ , C/EBP $\beta$  and C/EBP $\delta$  have been implicated in the induction of adipocyte differentiation. Their tissue distribution is, however, not limited to adipose tissue. These transcription factors have C-terminal basic region/leucine zipper (bZIP) domains which confer DNA binding and

the ability to dimerize either as homodimers or as heterodimers with other family members (Mandrup and Lane 1997). C/EBP also regulates the activity of PPAR $\gamma$  as shown in Figure 2.8 and described below.

C/EBP $\beta$  and C/EBP $\delta$  mRNA and protein levels rise early and transiently in cultured preadipocytes to which transformation cocktail has been added (Christy *et al.* 1991) whilst C/EBP $\alpha$  is induced later in the differentiation process, slightly preceding the induction of most genes involved in fat cell metabolism and the expression of PPAR $\gamma$  (Yew *et al.* 1995). Its function seems to be the maintenance of the terminally differentiated state through autoactivation of its own genes (Mandrup and Lane 1997).

Ectopic expression of C/EBP $\beta$  is sufficient to induce the differentiation of 3T3-L1 cells without the addition of hormonal inducers. Embryonic fibroblasts lacking both C/EBP $\beta$  and  $\delta$  were severely impeded from developing as adipocytes. C/EBP $\delta$  has a much lower adipogenic potential than C/EBP $\beta$  and it is thought that it may act synergistically with C/EBP $\alpha$  in the induction of PPAR $\gamma$ .

- ADD1/SREBP1

Adipocyte determination and differentiation factor 1 (ADD1) belongs to a family of the basic helix-loop-helix transcription factors (Tontonoz *et al.* 1993). This group of transcription factors has been implicated in tissue-specific gene regulation particularly in muscle, which shares a mesodermal origin with adipose tissue. It is mostly expressed in brown fat, followed by liver, white fat and kidney. It binds to an E-box motif (CANNTG) and also has an ability to bind to a sterol regulatory element (SRE) and hence it is also named SREBP-1 (Yokoyama *et al.* 1993). The expression of mRNA

encoding this factor is induced dramatically as cultured preadipocytic cell lines are stimulated to undergo differentiation. The mechanisms by which ADD1 exercises its adipogenic function remains unknown (Kim and Spiegelman 1996).

Adipogenesis is often portrayed as a wave of transcriptional events. The first wave involves a rise in the levels of C/EBP $\beta$  and  $\delta$  and these transcriptional factors activate the second wave which includes the transcription factors PPAR $\gamma$  and C/EBP $\alpha$ . It seems that the second wave of transcription factor stimulation is particularly susceptible to negative regulation. Factors that inhibit adipogenesis include: Wnts, TGF- $\beta$ , GH, resistin, inflammatory cytokines and PGF $_{2\alpha}$  (MacDougald and Mandrup 2002).

### 2.9.1.3 Hormonal regulation of adipogenesis

Various hormonal agents, chosen largely through empirical means, have been used to induce differentiation in preadipocytic cell lines.

Thus, early *in vitro* studies revealed that insulin was necessary for differentiation. Insulin increases the proportion of cells that differentiate and also increases the amount of lipid accumulation in each fat cell (Girard *et al.* 1994). Interestingly, preadipocytes express few, if any, insulin receptors (Reed and Lane 1979) and the effect of insulin on differentiation has been shown to occur through cross-activation of the IGF-1 receptor (Ferryhough *et al.* 2007). IGF-1 and insulin stimulate several specific downstream signal transduction pathways, any or all of which could mediate the adipogenic effects of these hormones (Smas and Sul 1995).

Glucocorticoids also induce differentiation of cultured preadipocyte cell lines and primary adipocytes. In most of these studies, glucocorticoids are given in the form of dexamethasone (DEX) (Rosen and Spiegelman 2000). DEX is believed to operate through the activation of the glucocorticoid receptor which is a nuclear hormone receptor in the same large family as PPAR $\gamma$ . DEX has been shown to induce C/EBP $\delta$ , which may account for some of its adipogenic activity (Wu *et al.* 1996).

Very early studies of cultured preadipocytic cell lines revealed that the addition of isobutylmethylxanthine (IBMX) enhances differentiation. IBMX acts by increasing cAMP levels and activation of  $\alpha$ -glycerolphosphatase dehydrogenase activity which is a lipogenic enzyme (Ellis and Manganiello 1985). A combination of IBMX, insulin and DEX is still the preferred regimen for inducing fat cell formation in 3T3-L1 cells. When IBMX is replaced by synthetic analogues of cAMP, adipogenesis is still enhanced.

### 2.9.2 Hepatocytes

PPAR $\gamma$ 2 is abundantly expressed in mature adipocytes and is elevated in the livers of animals that develop fatty livers. In the hepatic cell line AMC-12, PPAR $\gamma$ 2 selectively upregulated several adipogenic and lipogenic genes including ADRP, SREBP1 and FAS whose expression levels are known to increase in steatotic livers of ob/ob mice. PPAR $\gamma$ 2 regulated induction of both SREBP1 and FAS that paralleled an increase in *de novo* TAG synthesis in hepatocytes. These observations propose a role for PPAR $\gamma$  as an inducer of steatosis in hepatocytes (Schadinger *et al.* 2005). Macrophages resident in the liver (Kupffer cells), play a role in the physiological regulation of lipid metabolism of the adjacent hepatocytes. Inhibition of Kupffer cell

activity decreased prostaglandin E2 release into the liver tissue and this contributed to lipid accumulation in hepatocytes (Neyricnck *et al.* 2004). Under normal conditions quiescent Kupffer cells would therefore stimulate lipid accumulation. This effect is counteracted by the production of prostaglandins by other non-parenchymal cells in the liver such as, sinusoidal endothelial cells (Decker 1985). Prostaglandins stimulate the clearance of FFAs from the liver by increasing the production and secretion of VLDL (Feingold *et al.* 1989).

#### 2.10 ALP and adipogenesis

A direct role for ALP in the differentiation of the murine preadipocyte cell line, 3T3-L1 was demonstrated in a study by Ali *et al.* (2005). Inhibition of ALP activity by levamisole or histidine reduced intracellular TAG accumulation in the cells. Human TNSALP is inhibited by levamisole or histidine but not Phe-Gly-Gly which inhibits the tissue specific forms of ALP. Thus, Phe-Gly-Gly did not inhibit adipogenesis in the 3T3-L1 cell line (Ali *et al.* 2005). It is very likely therefore that it is the TNSALP isoenzyme that is involved in adipogenesis in the 3T3-L1 cells. ALP activity also increased during adipogenesis. The mechanism by which ALP may influence adipogenesis in the 3T3-L1 cells is not yet known. Increased adipogenesis was associated with increased ALP activity in primary cells, paralleling data from the 3T3-L1 preadipocytes (Ali *et al.* 2005).

Ali *et al.* (2006a) also showed that there was a difference in the activity of ALP in human preadipocytes from black and white females, which was paralleled by a higher level of adipogenesis in the preadipocytes taken from the black female

subjects. The reason for the higher level of ALP activity in this ethnic group is not known but possible causes include increased gene transcription due to differences in the promoter region gene sequence, increased levels of transcriptional factors controlling ALP gene expression and polymorphisms in the ALP exons coding for the catalytic site.

It would be worthwhile to further study the association of ALP activity and lipid accumulation in other cell lines e.g. Y-1 and HepG2 cells, but particularly in the latter cells since they are known to express TNSALP (Nowrouzi and Yazdanparast, 2005) and accumulate lipids (Brasaemle *et al.* 1997).

### 2.11 ALP gene silencing by RNA interference

It is recognized that the ALP inhibitors used by Ali *et al.* (2003) may not have had specific inhibitory effects on ALP activity. The definitive way to demonstrate the role of ALP in adipogenesis would be to knock-down (silence) the gene that codes for this protein in 3T3-L1 preadipocytes and HepG2 cells and study the progression of lipid droplet accumulation in these cells.

The appearance of double-stranded RNA within a cell, for example as a result of viral infection, triggers an RNA interference response. The cellular enzyme Dicer binds to the double stranded RNA and cuts it into short pieces of 20 or so nucleotides in length, known as small interfering RNAs or siRNA. These molecules then bind to a cellular enzyme complex RISC (RNA induced silencing complex) that uses one strand of the siRNA to bind to the complementary single-stranded mRNA molecules (Fig.

2.10). RISC then degrades the mRNA, thus silencing the expression of the viral gene (Downward 2004).

RNA interference has been exploited artificially to inhibit the expression of any gene of interest (Fire *et al.* 1998; Meister and Tuschli 2004).

The main systems for achieving RNA interference are short synthetic double stranded RNA molecules and gene expression vectors that direct their production in the cell (Siomi and Siomi 2009). Libraries of RNA interference have been constructed that allow the analysis of gene function on a genome-wide scale. It is envisaged that soon RNA interference will be exploited for therapy and a number of such agents are being tested in clinical trials (Wall and Shi 2003).



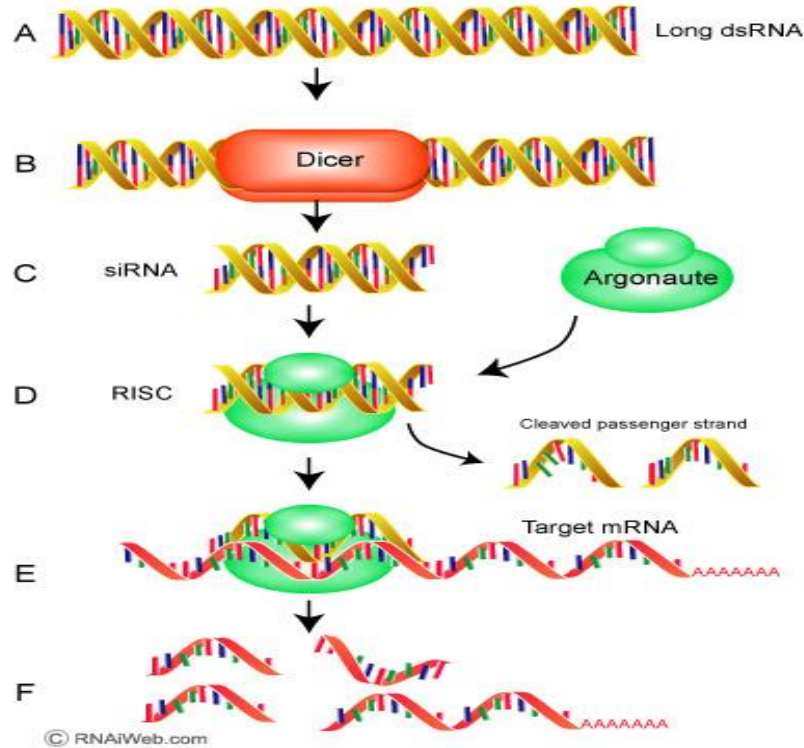


**Figure 2. 10** The RNAi pathway.

([http://www.rnaiweb.com/RNAi/What\\_is\\_RNAi/index.html](http://www.rnaiweb.com/RNAi/What_is_RNAi/index.html))

*A. On entering the cell, long dsRNAs act as a trigger of RNAi process.*

*B. It is first processed by the RNase III enzyme Dicer in an ATP-dependent reaction.*

*C. Dicer processes dsRNAs into 21-23 nucleotides (nt) short interfering RNA (siRNA) with 2-nt 3' overhangs. siRNA can also be synthesized outside the cell and then be introduced into a cell.*

*D. The siRNAs are incorporated into the RNA-inducing silencing complex (RISC) which consists of an Argonaute (Ago) protein as one of its main components. Ago cleaves and discards the passenger (sense) strand of the siRNA duplex leading to activation of the RISC.*

*E and F. The remaining guide (antisense) strand of the siRNA guides RISC to its homologous mRNA, resulting in the endonucleolytic cleavage of the target mRNA.*

**2.12 Aims of the study**

- (i) To study the relationship between ALP activity and intracellular lipid droplet accumulation in HepG2 as compared to 3T3-L1 cells and to determine the effect of inhibiting ALP activity on lipid droplet accumulation in HepG2 as compared to 3T3-L1 cells using *TNSALP* inhibitors.
- (ii) To determine the subcellular localization of ALP activity in HepG2 and 3T3-L1 cells.
- (iii) To study the expression pattern of the *PPAR $\gamma$*  gene with the induction of lipid droplet accumulation in the above cell types and what effects inhibition of ALP has on this process.
- (iv) To demonstrate the effect of post-transcriptional silencing of the *TNSALP* gene on lipid droplet accumulation in HepG2 and 3T3-L1 cells.
- (v) To study the role that single nucleotide polymorphisms (SNPs) in the promoter region of the human *TNSALP* gene play in the differential expression of ALP activity in two ethnic groups (black and white South African women).

# **CHAPTER THREE**

## **MATERIALS and METHODS**

3.1 ALP activity and protein measurements in HepG2 and 3T3-L1 cells with the progression of lipid droplet accumulation

3.1.1 3T3-L1 and HepG2 cell culture

HepG2 cells were obtained from the American Type Culture Collection (product number CRL-1197), as were the 3T3-L1 cells (product number CL-173). A frozen aliquot of the cells was thawed and seeded into a 25cm<sup>2</sup> culture flask (Corning®) containing Earle's Minimum Essential Medium (EMEM) supplemented with 10% fetal calf serum for the HepG2 cells and Dulbecco's Modified Eagle's Medium (DMEM) for the 3T3-L1's. The media were prepared as shown in Table 3.1 and 3.2 and were sterilized using a syringe fitted with a 0.22 micron filter. The flasks were incubated at 37<sup>0</sup>C in a 5% CO<sub>2</sub> atmosphere. Maintenance medium (EMEM or DMEM) was replaced after every 3 days until the cells were ready for experiments, passaging or freezing.

**Table 3.1** Earle's Minimal Essential Medium (10% EMEM) -100ml

<b>Reagent</b>	<b>Volume (ml)</b>
Earle's Minimum Essential Medium (BioWhittaker)	86.0
Sodium pyruvate (100mM, Gibco)	1.0
Pen/Strep (1000U/ml/1000µg/ml, BioWhittaker)	1.0
L-Glutamine (200mM,Gibco)	1.0
Non-essential amino acids (100X, BioWhittaker)	1.0
Fetal calf serum (Gibco BRL)	10.0

**Table 3. 2** Dulbecco's Modified Eagle's Medium (10% DMEM) -100ml

<b>Reagent</b>	<b>Volume (ml)</b>
DMEM (GibCo, 1X)	88
Fetal bovine serum (GibCo)	10
Pen/Strep (1000U/ml/1000µg/ml , BioWhittaker)	1
Glutamine (100X; 200mM,GibCo)	1

#### Passaging HepG2 and 3T3-L1 cells

When cells were approximately 70-80% confluent they were seeded into new flasks. Spent medium was removed from culture flask and the cell monolayer was washed twice with 3ml of ice cold sterile phosphate buffered saline (PBS [pH 7.2], GibCo Invitrogen). Then 1ml of 0.25% Trypsin-EDTA (GibCO) was added to the flask and incubated at 37<sup>0</sup>C for at least 20 minutes. When the cells were visibly detached from the surface of the flask, they were pipetted up and down to loosen them. Four ml of the growth medium was then added to the flask to stop the trypsinization process after which aliquots of the cell suspension were added to growth medium placed in new culture flasks.

#### Freezing cells

In order to create stocks of frozen HepG2 and 3T3-L1 cells, confluent cells in 25cm<sup>2</sup> culture flasks were washed twice with sterile PBS and detached by incubating with 1ml per flask of 0.25% Trypsin-EDTA at 37<sup>0</sup>C for 20 minutes.

Four ml of 10% culture medium was added to the trypsinized cells in each flask and the suspension was transferred into a 10ml centrifuge tube which was spun at 3000g for 5 minutes. The supernatant was discarded and the cell pellet was resuspended with 1.5ml of freezing medium (culture medium containing 10% dimethyl sulphoxide [(DMSO), Sigma]. This solution was then dispensed into cryovials, 1 ml per tube and kept overnight at -70<sup>0</sup>C. For long term storage the vials were transferred into the vapour phase of liquid nitrogen.

#### Thawing cells

Cells were re-cultured by removing vials from liquid nitrogen storage and placing them in a water bath equilibrated at 37<sup>0</sup>C. Cells were thawed quickly with shaking and transferred into a 25cm<sup>2</sup> culture flask containing 5ml of the growth medium. The cells were maintained in an incubator at 37<sup>0</sup>C in a 5% CO<sub>2</sub> atmosphere.

Newly thawed aliquots of cells were tested for *Mycoplasma* contamination using a <sup>™</sup>MycoAlert Mycoplasma kit (LONZA, USA). Aliquots of cells that were negative for *Mycoplasma* contamination were used in experiments.

#### 3.1.3 Induction of adipogenesis in 3T3-L1 Cells

3T3-L1 cells were grown and maintained under the conditions described in section 3.1.2 above. The cells were induced (transformed) to accumulate lipid droplets using a transformation cocktail prepared as below. After 3 days of initial incubation with transformation medium, the cells were maintained in DMEM<sub>D10</sub> containing insulin only

for a further 3 days after which it was replaced with DMEM every third day until the cells were harvested for experiments.

#### Transformation cocktail – 50ml

- 3-isobutyl-1-methyl-xanthine (IBMX)[Sigma]

50mg of IBMX was dissolved in 1ml of warm methanol (BDH) and 110 $\mu$ l of this was added to 50ml DMEM<sub>D10</sub> to give a final concentration of 495 $\mu$ M.

- Dexamethasone

1mg of dexamethasone was dissolved in 1ml of absolute ethanol (Univar). This was then diluted to 20ml with previously sterilized PBS (pH7.2) and 100 $\mu$ l of the solution was added to 50ml of DMEM<sub>D10</sub> to give a final concentration of 255nM.

- Insulin

An aliquot of 137 $\mu$ l of insulin (100IU/ml, Actrapid HM, Novo Nordisk) was added to 50ml of DMEM<sub>D10</sub> to give a final concentration of 1.83 $\mu$ M.

#### 3.1.4 Induction of lipid droplet accumulation in HepG2 cells

When the cells were approximately 70-80% confluent, 660 $\mu$ l of oleic acid-albumin mixture [ 6:1 moles of oleate:mole of albumin] (Sigma-Aldrich, UK) was added to 5ml of maintenance medium to give a final concentration of 400 $\mu$ M. Oleic acid-albumin was replaced after every third day until the cells were used for experiments.

Measurement of lipid accumulation in cells was done by using Oil Red O staining at day 0, 4, 7 and 11 after the addition of the oleic acid-albumin. On each of

these time intervals, cell counting was also done. Lipid accumulation was also assessed in cells in which oleic acid-albumin mixture was not added.

### 3.1.5 Measurement of lipid droplet accumulation in 3T3-L1 and HepG2 cells - Oil Red O staining

Intracellular lipid accumulation was determined using the Oil Red O staining procedure. Neutral lipid droplets have the ability to collect Oil Red O stain when it is added to them. The amount of the bound dye extracted (which is an approximation of the lipid content of the cells) is measured spectrophotometrically at 510nm (Ramirez-Zacarius *et al.* 1992).

#### Preparation of reagents

- 420mg of Oil Red O (Sigma) was dissolved in 120ml of absolute isopropyl alcohol (propan-2-ol, Univar). The solution was gently shaken at room temperature overnight. The solution was then filtered twice through a Whatman filter paper No.1 and then 90ml of distilled water was added to the filtrate. This working solution was kept at 4<sup>0</sup>C until used.
- Fixative - 3% glutaraldehyde (Merck) was prepared by adding 3ml of stock solution to 97ml distilled water.
- 60% isopropyl alcohol was prepared by adding 6 parts of absolute isopropyl alcohol to 4 parts of distilled water.



### Procedure

- Spent medium was removed from the culture flask and 2.5ml of fixative was added to the flask and left at room temperature for 2 hours.
- The fixative was replaced with 3ml of 60% propan-2-ol and after 5 minutes the alcohol was allowed to evaporate by opening the flask at room temperature for at least 10 minutes.
- 2.5ml Oil Red O stain solution was added to stain the cells at room temperature for 2 hours. The stain was removed and the cells rinsed with 3ml of 60% propan-2-ol for 5 seconds. The alcohol was removed.
- 3ml of 60% propan-2-ol was added to the flask to extract the dye with constant shaking (90rpm for 2 hours) on a Labcon Platform shaker (LabDesign, RSA).
- The amount of dye extracted was quantified by measurement of absorbance on the Labsystems Multiskan Ascent Multiplate Reader (Research Technologies, Finland) at 510nm using propanol:water (4:3) as a blank.

Images of the stained cells were also taken at the specified time intervals using a Nikon CoolPix 995 digital camera (Japan) that was mounted on an inverted phase microscope (Nikon TMS, Japan).

### Cell counting procedure

- Cells were trypsinized in the flasks sacrificed for cell counting at the appropriate time interval and 4ml of maintenance medium was added to the trypsinized cells and pipetted up and down to mix.

- A hemacytometer cover slip was mounted over the counting chamber (Hemacytometer, Neubauer double 0.10mm depth BrightLine AO Instrument Co.) and about 10 $\mu$ l of the suspended cells was dispensed to the underside of the cover slip until the whole of the chamber was covered with the suspension.
- The number of cells in each of the 4 fields (squares) was counted using the 10x objective on a Nikon TMS microscope, (Japan). The average of the cell count was multiplied by 10<sup>4</sup> cells to give the number of cells per ml of the suspension.

### 3.1.6 ALP and protein extraction of cultured cells

ALP and total protein were extracted from cells on day 0 (baseline), day 4 and day 11 (after induction of lipid droplet accumulation) using an extraction solution prepared as described in Table 3.3 below. Aliquots of the extract were used for ALP activity and total protein measurement.

**Table 3. 3** ALP/protein extraction solution

<b>Substance</b>	<b>Amount</b>
Tris-base [hydroxymethyl aminomethane] – (Merck)	157.6mg 1 ml
Triton-X 100 (BDH)	35mg
Phenylmethylsulphonyl fluoride (Sigma)	99ml
Distilled water	

Distilled water (80 ml) was added to the Tris–base, phenylmethylsulphonyl fluoride and Triton-X100 and stirred on a magnetic stirrer until the base was completely dissolved. The pH of the solution was adjusted to 7.2 using HCl and then the solution made up to 100ml. Aliquots of this solution were kept at -20 °C until use.

- Spent medium was removed from culture flask and cells were washed twice with 4ml ice cold PBS (pH7.2)
- 1ml of ALP/protein cell extraction solution was added to the flask and incubated for 15 minutes at 37°C until the cell monolayer was visibly detached from the flask.
- The cells were mixed by pipetting up and down and then the suspension transferred into 1.5ml Eppendorf tube. A 10µl aliquot of this suspension was used for approximating cell count.
- The tube was then centrifuged at 15000 RCF for 10 minutes at room temperature in a Mikro 22R Zentrifugen centrifuge.
- A 300µl aliquot of the supernatant was transferred into a tube and kept on ice ready for ALP measurement on the Modular Analyzer (Roche) in the Routine Chemistry Lab whilst 300µl of the supernatant was reserved for protein determination.

### 3.1.7 ALP activity measurement

ALP activity was measured in the routine Chemistry Laboratory (Johannesburg General Hospital) using a Cobas kit on the Roche Modular Analyzer P800 (Japan). ALP activity was also measured on the extraction solution and a zero reading was

obtained. The colorimetric assay uses pNPP as a substrate and monitors the change in optical density as a coloured product is formed when ALP hydrolyses its substrate. The amount of the coloured product that is formed is directly proportional to the amount of the enzyme present in a sample. ALP activity was expressed in IU/ $\mu$ g protein. The performance of the assay was checked by the simultaneous run of internal controls twice a day.

### 3.1.8 Total protein measurement using the Bradford method

This assay is based on the observation that absorbance maximum for an acidic solution of Coomassie Brilliant G-250 shifts from 465 to 595nm when binding to protein occurs (Bradford 1976).

#### Preparation of the Bradford Reagent

A 100mg of Coomassie Blue (G-250) was dissolved in 100ml 85% phosphoric acid. Then, 50ml of 95% ethanol was added to the mixture. The mixture was shaken until the G-250 was completely dissolved. The solution was made up to 1 litre. It was then filtered through a Whatman Filter No.1 to get rid of the blue particles of G-250.

#### Protein standard curve

Bovine serum albumin (BSA; 200mg) was dissolved in 100ml distilled water to give a stock of 2mg/ml. Standards were prepared from the stock as shown in Table 3.4.

**Table 3. 4** Protein standards for calibration curve

	<b>Volume of BSA stock (<math>\mu</math>l)</b>	<b>Volume of H<sub>2</sub>O (<math>\mu</math>l)</b>	<b>Final protein concentration (<math>\mu</math>g/mL)</b>
<b>Blank</b>	0	1000	0
<b>Std 1</b>	250	750	500
<b>Std 2</b>	375	625	750
<b>Std 3</b>	500	500	1000
<b>Std 4</b>	750	250	1500
<b>Std 6</b>	1000	0	2000

#### Measurements on the multiplate reader (Labsystem)

A 500 $\mu$ l aliquot of Bradford reagent was added to 10 $\mu$ l of each of the standards/samples. Samples (cell extracts) were each initially diluted 1 in 20 with distilled water before being added to the Bradford reagent. The Bradford reagent and samples were allowed to equilibrate at room temperature for at least 20 minutes before being mixed.

Samples that did not give absorbance readings between the lowest and the highest standards were appropriately diluted until they gave a reading that was within the standard curve.

A 300 $\mu$ l aliquot of the Bradford-standards/sample mixtures were pipetted into a 96 well plate and the optical densities read on the Labsystems Multiskan Ascent Multiplate Reader (Research Technologies, Finland) at 595nm within an hour after

addition of reagent to samples or standards. Concentrations of samples were calculated by the reader taking into account all the appropriate dilutions that may have been done on the samples.

3.2 The effect of ALP inhibitors on the progression of lipid droplet accumulation and ALP activity in HepG2 & 3T3-L1 cells

3.2.1 Cell culture

3T3-L1 and HepG2 cells were grown and maintained under conditions described earlier in section 3.1. When the cells were approximately 80% confluent, they were induced to accumulate lipid droplets using protocols described in sections 3.1.3 & 3.1.4 respectively.

The transformation and maintenance medium were spiked with the two ALP inhibitors (Levamisole and Histidine) and changed at the appropriate time intervals as described earlier in the same sections.

#### 3T3-L1 cells

The two inhibitors were used as described below (as reported by Ali *et. al.* 2005):

*Levamisole* (L-tetramisole hydrochloride, Sigma): 0.048g was dissolved in 2ml PBS (pH7.2) and 100 $\mu$ l of this solution was added to 5ml of the culture medium to give a final concentration of 2.0mM.

*Histidine* (C<sub>6</sub>H<sub>9</sub>O<sub>2</sub>, Merck): 0.465g was dissolved in 60ml culture medium and 5ml of this was aliquoted into 25cm<sup>2</sup> tissue culture flask. This gave a final concentration of 50mM.

### HepG2 cells

The two inhibitors were used at the following concentration after a dose-response curve was performed:

*Levamisole* (L-tetramisole hydrochloride, Sigma): 0.072g was dissolved in 2ml PBS (pH7.2) and 100 $\mu$ l of this solution was added to 5ml of the culture medium to give a final concentration of 3.0mM.

*Histidine* (C<sub>6</sub>H<sub>9</sub>O<sub>2</sub>, Merck): 0.58g was dissolved in 60ml culture medium and 5ml of this was allocated into 25cm<sup>2</sup> tissue culture flask to give a final concentration of 74.8mM.

### 3.3 *Peroxisome Proliferator Activated Receptor gamma (PPAR $\gamma$ )* gene expression studies in HepG2 & 3T3-L1 cells.

HepG2 and 3T3-L1 cells were grown and maintained under the conditions described in section 3.1.1. The cells were induced to accumulate lipid droplets using the procedure described earlier in this chapter. Isolation of total RNA was done on day 0, 4 and 7 post induction of lipid droplet formation. *PPAR $\gamma$*  gene expression was also studied in cell cultures in the presence of the two ALP inhibitors as used in section 3.2.1.

#### 3.3.1 Isolation of total RNA using the Qiagen<sup>®</sup>RNeasy Mini Kit (Germany)

### Harvesting cells

The cell monolayer was washed twice with cold PBS buffer (pH 7.2) having removed the culture medium from the flask. The cells were trypsinized using 1ml of 0.25%

Trypsin-EDTA. After cells were detached from the flask 1ml of growth medium was added to the flask and mixed by pipetting up and down. The cell suspension was transferred into an RNase-free polypropylene centrifuge tube and spun at 280 xg for 5 minutes at room temperature. The supernatant was completely removed and the cell pellet was loosened by flicking the tube. Cells were disrupted by the addition of 350 $\mu$ l of RLT buffer supplied in the kit and later homogenized by centrifuging the lysed cells in a shredder column also supplied in the kit at 8000 xg for 15 seconds.

#### Isolation of total RNA

- 350 $\mu$ l of 70% ethanol was added to the homogenized lysate and mixed well by pipetting.
- 700 $\mu$ l of the lysate was applied onto an RNeasy mini column placed into a 2ml collection tube and the tube centrifuged at 8000 xg for 15 seconds. The flow through was discarded.
- 700 $\mu$ l of wash buffer RW1 was added to the column and centrifuged as above. The collection tube and the flow through were discarded. The column was placed into a new 2ml collection tube.
- 500 $\mu$ l of buffer RPE was applied onto the column and the tube centrifuged at 8000 xg for 15 seconds. The flow through was discarded.
- Another 500 $\mu$ l of buffer RPE was added to the column and the tube centrifuged for 2 minutes at 8000 xg to dry the tube. The column was transferred to a new collection tube and spun for one minute at 14,000 xg.



- The column was placed in a new 1.5ml collection tube and 35µl of RNase-free water was pipetted directly into the RNeasy silica-gel membrane. The tube was centrifuged for 1 minute at 8000 xg to elute. This was repeated with a similar volume of RNase-free water.
- The eluate was kept on ice and contains the RNA template required for complementary DNA (cDNA) synthesis.

The concentration of total RNA isolated was determined on the NanoDrop® 1000 spectrophotometer (Thermo Scientific, USA) using RNase-free water as a blank (units were ng/µl). Total RNA isolated from cells was separated by agarose gel electrophoresis using Tris Boric acid EDTA (TBE) as running buffer and viewed under UV light to check its quality (Appendix I). Intact total RNA should give two bright bands representing the 28S and 18S ribosomal RNA. Secondly, the 260/280 ratio on the NanoDrop was used to determine the integrity of RNA (Pfaffl *et al.* 2002; McCurdy *et al.* 2008).

A ratio of 2.0 is generally considered good for RNA (NanoDrop ND1000 Full-spectrum UV/Vis spectrophotometer User's Manual 2005, NanoDrop technologies Inc. Wilmington, DE USA).

### 3.3.2 Reverse Transcriptase PCR (RT-PCR)

Complementary DNA (cDNA) was synthesized from RNA (isolated as described above) using moloney murine leukaemia virus (MMuLV) Reverse Transcriptase kit (Promega, USA). The procedure is summarized below.

## Step 1

<u>Reagent</u>	<u>Volume (<math>\mu</math>l)</u>	
Total RNA	2.5 $\mu$ g	} Incubated at 65 <sup>0</sup> C for 5 minutes
Oligo dT primer (0.2 $\mu$ mol/ $\mu$ l)	1.0	
dNTPs (5mM)	1.0	
Water (RNA/DNase - free)	added to make up 30 $\mu$ l	

## Step 2, put on ice and the following were added

RT buffer (5X)	4.0	} Incubated at 37 <sup>0</sup> C for 2 min
Diethrethitol (DTT), 0.1M	2.0	
RNAse inhibitor (100U/ $\mu$ l)	1.0	

## Step 3, added

MMuLV Rev Transcriptase	1.0	} Incubated at 37 <sup>0</sup> C for 50 min then at 70 for 15 min
-------------------------	-----	---

**Total volume                      30 $\mu$ l**

A tube containing no RNA but all the reagents required in the RT-PCR was set up to be used as a blank when determining the concentration of the cDNA on the NanoDrop® (Lossos *et al.* 2003).

The amount of RNA used in each tube for cDNA synthesis was 2.5µg. A total reaction volume of 30µl was set up for each of the time points.

'DNase digestion is optional with RNeasy kits since RNeasy silica-membrane technology efficiently removes most of the DNA without DNase treatment' – (RNeasy Mini Handbook [Qiagen, Germany], 4<sup>th</sup> edition; April 2006 page 23).

RNase inhibitor was supplied by Roche, (Germany); MMuLV RT by Promega, (USA); DTT by Sigma Aldrich (UK) and Oligo dTs by Inqaba, (RSA).

### 3.3.3 Amplification of *PPAR $\gamma$* and *TBP* genes and optimization of PCR conditions using a Biorad Thermocycler and the Rotor-Gene 6000 light cyclers

Amplification and optimization of PCR conditions for the *PPAR $\gamma$*  gene was done on the MyCycler thermocycler (BioRad, Italy). The *TATA box binding protein (TBP)* gene was used as an endogenous internal control for the gene expression studies. The use of an endogenous reference corrects for variation in nucleic acid recovery, differences in sample handling, presence of inhibitors and variation in RNA content. TBP gene has been used as a reference gene in a number of papers (Vandesompele *et al.* 2002; Kok *et al.* 2005; Foldager *et al.* 2009). Phan *et al.* (2004) reported that TBP gave results similar to hypoxanthine phosphoribosyltransferase (HGPRT) gene [a commonly used housekeeping gene] as the normalization control in 3T3-L1 cells. Unchanged expression of TBP gene in 3T3-L1 cells that was monitored by Western blot has also been reported (Vankoningsloo *et al.* 2006).

In HepG2 cell line, TBP gene has also been used as a reference gene where it has given results similar to the ones obtained in other cell lines (Wong *et al.* 2003; Sivertsson *et al.* 2010). In my work, TBP was shown to be a good reference gene because the expression of this gene does not fluctuate significantly during the period of experiments when both the HepG2 and 3T3-L1 cells were subjected to different treatments (Figures 4.15, 4.16, 4.24, 4.25, 4.30, 4.31, 4.35, 4.36 and 4.37).

Optimization of PCR conditions on both the Biorad thermocycler and the Rotor-Gene light cyclers involved manipulation of PCR parameters like the annealing temperature/time; primer concentrations & number of cycles followed by gel

electrophoresis of the PCR products to check for the quality of the PCR products (in terms of primer dimers, brightness of bands and unspecific products). The starting conditions were those provided by the manufacturers of the enzymes that were used in the PCRs. Conditions that gave the best PCR products (in terms of brightness of bands and lack of or less primer dimers) upon gel electrophoresis were chosen and in the following sections of this thesis these set of conditions are referred to as 'optimal conditions'.

Optimization of PCR conditions using a conventional thermocycler is cheaper (especially when an option of temperature gradient is available) than using a light cycler (real-time PCR machine) and the PCR products from a conventional thermocycler are visualized better on agarose gels than those from a light cycler.

**(i)** HepG2 cells

Primer design

The gene sequence of the human *PPAR $\gamma$*  gene is available in the GenBank Database under the accession number L40904 (appendix IA). The accession number for the human *TBP* gene is NM003194 and the sequences of the two genes are shown in appendix IB. Primer sequences for the two genes were designed using the GeneRunner software [Hastings Software Inc, Las Vegas, USA] (Lima and Garces 2006). To check how specific the primers were for a target, their sequences were compared to sequences in GenBank (<http://blast.ncbi.nlm.nih.gov/Blast.cgi>) using the basic local alignment search tool (BLAST).

Sequencher Version 4.7 (Gene Codes Corp USA) was used to align the primers with the target gene. Primer synthesis was done at Inqaba Biotec, RSA. Synthesized lyophilized primers were reconstituted with RNA/DNase-free water to give a stock solution of 100 $\mu$ M.

**Table 3. 5** PCR primers for *PPAR $\gamma$*  and *TBP* genes in HepG2 cells.

Gene	Primer sequence	bases	Tm (°C)	Expected product size (bp)
<i>PPAR<math>\gamma</math></i>	For 5'- GGT TGA CAC AGA GAT GCC A -3'	19	60.2	
	Rev 5'- CAA AGG AGT GGG AGT GGT C -3'	19	62.3	88bp
<i>TBP</i>	For 5'- CAG TGA CCC AGC AGC ATC -3'	18	62.2	277bp
	Rev 5'- GTC AGT CCA GTG CCA TAA GG -3'	20	62.5	

PCR reactions for each of the two genes were set up in separate tubes using their specific primer sets (Table 3.6). PCR products were visualized having been separated by gel electrophoresis as described in section 3.3.4 below. Negative template control (NTC) contained all the reagents of the PCR except the DNA template.

**Table 3. 6** PCR components for 1 reaction tube for *PPAR $\gamma$*  and *TBP* genes in HepG2 cells using a BioRad Thermocycler.

Reagent	Vol ( $\mu$ l)	Initial concentration	Final concentration
Buffer (SuperTherm Gold with 15mM MgCl <sub>2</sub> , [JMR UK])	1.00	10X	0.8X
dNTPs (Bioline, UK)	0.80	10mM each	0.7mM
Taq polymerase (SuperTherm Gold, JRM UK)	0.15	5U/ $\mu$ l	0.07U/ $\mu$ l
Forward primer ( <i>PPAR<math>\gamma</math></i> )	0.10	25 $\mu$ M	0.21 $\mu$ M
Forward primer ( <i>TBP</i> )	0.10	25 $\mu$ M	0.21 $\mu$ M
Reverse primer ( <i>PPAR<math>\gamma</math></i> )	0.10	25 $\mu$ M	0.21 $\mu$ M
Reverse primer ( <i>TBP</i> )	0.10	25 $\mu$ M	0.21 $\mu$ M
Distilled water	9.25		
DNA template	0.50		
<b>Total volume/tube</b>	<b>12.00</b>		

Thermal cycling

Initial denaturation	94 <sup>0</sup> C, 11 min	x1
Denaturation	94 <sup>0</sup> C, 45 sec	} x35
Annealing	60 <sup>0</sup> C, 30sec	
Extension	72 <sup>0</sup> C, 45sec	
Final extension	72 <sup>0</sup> C, 10min	x1

### 3.3.4 Gel electrophoresis

Agarose gel electrophoresis was used to separate and analyse PCR products. To visualise DNA, 2.5 $\mu$ l ethidium bromide (10mg/ml) was added to 50ml of molten agarose that was prepared as described below. Ethidium bromide binds to DNA by intercalating between bases and absorbs invisible UV light and transmits the energy as visible blue light. A 2 $\mu$ l aliquot of 6X Fermentas loading dye (made up of 10mM Tris-HCl, 0.15% orange G, 0.03% xylene cyanol FF, 60% glycerol and 60mM EDTA) was mixed with the sample/molecular weight marker and loaded into the wells of the agarose gel.

#### Preparation of running buffer and agarose gel

- 1X Tris Boric acid EDTA (TBE) buffer was prepared by dissolving 10.8g Tris (hydroxymethylaminomethane, Merck Germany) and 5.5g boric acid (Merck Germany) in 500ml distilled water. Four ml of 0.5M EDTA (Sigma, Germany) was added to the solution and the volume was made up to 1 litre in a volumetric flask with distilled water. The 0.5M EDTA was prepared by dissolving 9.3g of EDTA in 50ml distilled water and the pH adjusted to 8.0 on a Beckman  $\phi$ 32 pH meter.
- A 2% (w/v) agarose solution was prepared by dissolving 2 agarose tablets (equivalent to 1g) (Bioline, Germany) into 50ml TBE buffer.
- When the tablets were completely dissolved, the solution was heated in a microwave to a clear solution. The solution was allowed to cool and 2.5 $\mu$ l (10mg/ml) of ethidium bromide was added.



- A gel comb was fitted into a gel casting tray and the agarose solution was poured into it and allowed to set for about 25 minutes.
- The gel was then placed into the electrophoresis tank containing 1xTBE buffer with the wells facing the negative electrode.
- 2 $\mu$ l of loading dye was mixed with 4 $\mu$ l of PCR product and then loaded into the wells. The same volume of the loading dye was also mixed with 1 $\mu$ l molecular weight marker (O' Gene Ruler 50 bp, Fermentas [Lithuania]) and loaded into a separate well.

Electrophoresis was run at 95V (constant current) till the samples ran to about  $\frac{3}{4}$  of the length of the gel after which the current was switched off. The gel was then viewed under UV light using a Biorad Gel Doc XR Imaging System (Italy).

### 3.3.5 Quantitative real-time PCR (qPCR) in HepG2 cells.

The quantification of the levels of expression of the *PPAR $\gamma$*  and *TBP* genes was carried out using a Rotor-Gene 6000 (Corbett Life Sciences Research, NSW Australia) real-time cycler. A SensiMix™ dT kit (Quantace Ltd, London) was used for the PCR reactions (Table 3.7). PCR conditions were optimized as outlined in section 3.3.3.

Quantification of the levels of mRNA was done using the two standard curve method [one curve each for the reference and gene of interest] (Rotor-Gene 6000 Operator Manual 1.7.87 Corbett Research 2006 Australia: page 75-78). Absolute quantification determines the input copy number, usually by relating the PCR signal to a standard curve.

### Standard curve

Equal volumes of each of the standard (of known concentration) made from the 'cDNA pool' was added to a PCR tube containing specific primers for a gene and its concentration entered into the Rotorgene software. Depending on the concentration units entered, the software would then determine its own value for each of the standards. Triplicates were run. Change in fluorescence in each of the standards was plotted against cycle number. The threshold values were then calculated. This is the cycle number at the point where the fluorescence curve crosses a limit of detection (ten times the SD of the baseline fluorescence). The threshold ( $C_T$ ) values were thus calculated for each standard and plotted against cDNA concentration to yield the standard curve.

### Unknown samples

In order to use the same amount of cDNA in PCR (for example 50ng), samples were diluted if necessary to concentrations that would give 50ng in a volume between 0.5-1 $\mu$ l. These tubes (triplicates) were then run alongside the tubes containing the standards making note of any dilutions made on the sample.

The Rotorgene software would then determine the concentration of the unknown samples by reading them off the standard curve. The final result was calculated by multiplying the concentration of the sample with the dilution factor if any dilutions were made.

**Table 3. 7** PCR components for 1 reaction tube run on the Rotor-Gene for *PPAR $\gamma$*  and *TBP* genes in HepG2 cells:

Reagent	Vol ( $\mu$ l)	Initial concentration	Final concentration
SensiMix dT	6.5	2X	1.1X
SYBR® Green I	0.5	50X	2.1X
For primer ( <i>PPAR<math>\gamma</math></i> )	0.1	25 $\mu$ M	0.17 $\mu$ M
For primer ( <i>TBP</i> )	0.1	25 $\mu$ M	0.17 $\mu$ M
Rev primer ( <i>PPAR<math>\gamma</math></i> )	0.1	25 $\mu$ M	0.17 $\mu$ M
Rev primer ( <i>TBP</i> )	0.1	25 $\mu$ M	0.17 $\mu$ M
Water	variable		
cDNA template	variable		
Total volume/tube	<b>12.00</b>		

#### Cycling parameters

Initial denaturation	95 <sup>0</sup> C, 10 min	x1
Denaturation	95 <sup>0</sup> C, 10 sec	} x40
Annealing	57 <sup>0</sup> C, 15sec	
Extension	72 <sup>0</sup> C, 20sec	

Data was acquired after step 3 (extension).

Preparation of a standard curve

A cDNA pool was made by thoroughly mixing cDNA samples synthesized from RNA isolated from the cell cultures on day 0, 4 and 7. This cDNA was then serially diluted to give standards that were used in the real-time PCR. The cDNA pool is representative in terms of quality and concentration range of the cDNA likely to be found in the samples under study. Similarly, in order to generate a standard curve to use in qRT-PCR, Orimo and Shimado (2005) sequentially diluted cDNA made from mRNA isolated from SaOS-2 cells to estimate the levels of ALP mRNA in these same cells.

Five graded series of cDNA dilutions were done on the cDNA pool using DNase-free water and the concentrations were determined on the NanoDrop 1000 spectrophotometer (Thermo Scientific, USA) using water as a blank. The graded cDNA dilutions were used as calibrators.

**Table 3. 8** Concentration of cDNA used as standards in HepG2 cells

<b>Standard</b>	<b>Concentration (ng/<math>\mu</math>l)</b>
Std1	291.2
Std2	145.8
Std3	68.8
Std4	35.7
Std5	16.3

Triplicates of PCR reaction tubes containing each of the standards were set up for the two genes. PCR was carried out using the cycling parameters described earlier in this section.

#### Quantitative real-time PCR run

The concentration of cDNA synthesized from RNA isolated from HepG2 cells was determined on the NanoDrop 1000 spectrophotometer. The concentrations of cDNA synthesized on day 0, 4 and day 7 post addition of oleic acid was diluted with DNase-free water to give a similar starting amount of DNA per volume of sample using the formula  $C_1V_1=C_2V_2$  (where  $C_1$  is the initial concentration of cDNA and  $V_1$  the volume of the aliquot to be diluted,  $C_2$  and  $V_2$  are the concentration and volume respectively of the final solution). Using the Sensimix dT kit,  $\geq 100$ ng of cDNA is the optimal amount for one PCR reaction mixture. Samples were therefore diluted so that an equivalent of this amount was present in a microlitre or less of sample.

**Table 3. 9** Example of dilutions and concentrations of cDNA used in a typical quantitative real-time PCR (HepG2 cells). Diluted cDNA was obtained by diluting cDNA obtained from the reverse transcription of total RNA.

	<b>Sample</b>	<b>Initial [cDNA] (ng/<math>\mu</math>l)</b>	<b>Diluted [cDNA] (ng/<math>\mu</math>l)</b>	<b>Volume required to give 50ng of cDNA (<math>\mu</math>l)</b>
	Day 0	1213.5	75.6	<b>0.66</b>
<b>Expt 1</b>	Day 4	932.4	69.7	<b>0.72</b>
	Day 7	530.1	85.4	<b>0.59</b>
	Day 0	604.0	61.7	<b>0.81</b>
<b>Expt 2</b>	Day 4	419.8	52.1	<b>0.95</b>
	Day 7	432.3	80.5	<b>0.62</b>
	Day 0	75.7	75.7	<b>0.66</b>
<b>Expt 3</b>	Day 4	104.4	85.8	<b>0.58</b>
	Day 7	182.4	63.1	<b>0.79</b>

For each experiment, master mixes were set up for each of the 3 time points and for each of the two genes using their specific primers, to give a total of 6 master mixes. Each PCR run included triplicates for each of the standards and each of the samples.

**(ii) 3T3-L1 cells**Primer design

The gene sequence of the mouse *PPAR $\gamma$*  gene is available in the GenBank database under the accession number NM011146.3 (appendix IC). The accession number for the mouse *TBP* gene is NM013684 (appendix ID). Primer design, synthesis and storage were carried out as described in section 3.3.3 (i).

**Table 3. 10** PCR primers for *PPAR $\gamma$*  and *TBP* genes (mouse).

Gene	Primer sequence	bases	T <sub>m</sub> (°C)	Expected product size
	For 5'- CCA GAG CAT GGT GCC TTC GCT -3'	21	68	
<b><i>PPAR<math>\gamma</math></i></b>	Rev 5'- CAG CAA CCA TTG GGT CAG CTC -3'	21	60	240 bp
	For 5'- ACC CTT CAC CAA TGA CTC CTA TG -3'	23	68	
<b><i>TBP</i></b>	Rev 5'- ATG ATG ACT GCA GCA AAT CGC -3'	21	62	189 bp

The following conditions were determined optimal for the amplification process. PCR reactions for each of the two genes were set up in separate tubes using their specific primer sets as shown in Table 3.6

Thermal cycling

Initial denaturation	94 <sup>0</sup> C, 11 min	x1
Denaturation	94 <sup>0</sup> C, 45 sec	} x35
Annealing	64 <sup>0</sup> C, 30sec	
Extension	72 <sup>0</sup> C, 45sec	
Final extension	72 <sup>0</sup> C, 10min	x1

PCR products were visualized having been separated by gel electrophoresis as described in section 3.3.4. Optimization of PCR conditions using a conventional thermocycler were done in the same way as given in section 3.3.3

## 3.3.6 Quantitative real-time PCR (qPCR) in 3T3-L1 cells

The quantification of the levels of expression of the *PPAR $\gamma$*  and *TBP* genes was carried out using a Rotor-Gene 6000 (Corbett Life Sciences Research) real time cycler. A SensiMix™ dT kit (Quantace, UK) was used for the PCR reactions.

Optimization of PCR conditions

The following conditions were found optimal for the amplification of the two genes on the Rotor-Gene 6000. PCR reactions for each of the two genes were set up in separate tubes using their specific primer sets. PCR components for 1 reaction tube were set up as shown in Table 3.7 but using an initial concentration of the primers of 20nM.



Cycling parameters

Initial denaturation	95 <sup>0</sup> C, 10 min	x1
Denaturation	95 <sup>0</sup> C, 10 sec	} x40
Annealing	60 <sup>0</sup> C, 15sec	
Extension	72 <sup>0</sup> C, 20sec	

Data was acquired after step 3 (extension).

Preparation of a standard curve

The standard curve was prepared as described in section 3.3.5, sub-section "Preparation of a standard curve".

**Table 3. 11** Concentration of cDNA used as standards

<b>Standard</b>	<b>Concentration (ng/<math>\mu</math>l)</b>
Std1	272.4
Std2	130.8
Std3	60.5
Std4	29.8
Std5	14.1

Triplicates of PCR reaction tubes containing each of the standards were set up for the two genes. PCR was carried out using the cycling parameters described earlier in this section.

Quantitative real-time PCR in 3T3-L1 cells.

Sample preparation was carried out as described in section 3.3.5, sub-section "Quantitative real-time PCR run".

**Table 3. 12** Example of dilutions and concentrations of cDNA used in a typical quantitative real-time PCR in 3T3-L1 cells. Diluted cDNA was obtained by diluting cDNA obtained from the reverse transcription of total RNA

	<b>Sample</b>	<b>Initial [cDNA] (ng/<math>\mu</math>l)</b>	<b>Diluted [cDNA] (ng/<math>\mu</math>l)</b>	<b>Volume required to give 63.2ng of cDNA (<math>\mu</math>l)</b>
	Day 0	85.7	-	<b>0.70</b>
<b>Expt 1</b>	Day 4	238.0	-	<b>0.27</b>
	Day 7	212.0	-	<b>0.30</b>
	Day 0	86.9	-	<b>0.73</b>
<b>Expt 2</b>	Day 4	790.9	206.0	<b>0.31</b>
	Day 7	369.5	-	<b>0.17</b>
	Day 0	157.5	-	<b>0.40</b>
<b>Expt 3</b>	Day 4	906.9	186.7	<b>0.31</b>
	Day 7	150.3	-	<b>0.42</b>

Only 2 samples (Day 4, expt 2 and Day 4, expt 3) were diluted because the initial concentration of cDNA at these time points were too high to give 63.2ng of cDNA from 1 $\mu$ l or less of their respective samples.

For each experiment, master mixes were set up for each of the 3 time points and for each of the two genes using their specific primers, to give a total of 6 master mixes. Each PCR run included triplicates for each of the standards and the samples.

### 3.4 RNAi studies for the TNSALP gene in HepG2 and 3T3-L1 cells

Establishment and optimization of gene silencing conditions in a human (HepG2) and a mouse cell line (3T3-L1) was done using the RNAi Human/Mouse starter kit (Qiagen, Germany Cat No. 301799). The kit contains positive and negative siRNA controls, HiPerFect transfection reagent and protocols intended as starting points for RNAi experiments.

Short interfering RNA (siRNA) targeted against the protein kinase MAPK1 (Erk 2) is the positive (silencing) control that is included in the kit. The sequence of this positive siRNA control is homologous to both the human and mouse MAPK1 mRNA sequences (GeneBank accession numbers NM002745 [human] and NM011949 [mouse] respectively).

The negative control siRNA (<sup>®</sup>AllStars negative) included in the kit is a highly validated siRNA that has no known homology to any mammalian gene and is therefore used to control for non-specific silencing effects. The AllStars negative siRNA included in the kit is labeled with Alexa Fluor 488. This label allows easy monitoring of transfection efficiency and enables optimization of transfection conditions. qPCR was used to monitor the efficiency of gene silencing using PCR primers (QuantiTect) specific for the MAPK1 gene in both cell lines.

Primer assays used for amplification of the MAPK1 gene were different for HepG2 and 3T3-L1 cells. It was expected that the amplicons would be of different sizes and therefore different melting peaks. The sequences of the primers were however, not provided by the manufacturers (Qiagen, Germany).

Optimization of siRNA transfection included manipulation of the following parameters: amount of siRNA, ratio of HiPerfect reagent to siRNA and cell density.

#### 3.4.1 Optimized transfection conditions using the Fast-Forward protocol

##### a) Preparation of siRNA working solution

RNase-free water (250 $\mu$ l) was added to each tube containing 5nmol lyophilized siRNA (negative and positive controls) to obtain a 20 $\mu$ M solution. This solution is equivalent to approximately 250ng/ $\mu$ l siRNA. 20 $\mu$ l aliquots were prepared and kept at -20°C until use.

##### b) Cell culture

HepG2 and 3T3-L1 cells were seeded and grown in 25cm<sup>2</sup> Nunc culture flasks and maintained under conditions described in sections 3.1.1 and 3.1.2 respectively.

#### Procedure

1. Shortly before transfection  $\sim 6 \times 10^4$  cells were seeded into wells of a 24-well plate in 0.5ml of an appropriate growth medium (10% EMEM for HepG2 and 10% DMEM for 3T3-L1 cells).
2. For the short time until transfection ( $\sim 4$  hours), the cells were incubated under conditions described in sections 3.1.1 and 3.1.2.

3. A 125ng aliquot of siRNA (0.5 $\mu$ l of the reconstituted siRNA) was diluted in 100 $\mu$ l culture medium containing no serum to give a final siRNA concentration of 16.5nM. Then 3 $\mu$ l of HiPerFect transfection reagent was added to the diluted siRNA and mixed by vortexing.
4. The samples were incubated at room temperature (15-25°C) for 5-10 minutes to allow the formation of transfection complexes.
5. The transfection complexes were then added drop-wise into the cells, gently swirling the plate to ensure uniform distribution of the complexes.
6. The culture plates containing the cells were incubated under conditions described earlier and gene silencing was monitored 72 hours after transfection.

#### 3.4.2 Transfection efficiency

Efficiency of transfection was monitored using a confocal fluorescence microscope (Carl Zeiss 100M, German) by following the emission spectra of Alexa Fluor 488. Cells that were transfected (having green fluorescent dots) were counted and expressed as a percentage of the total number of cells in a given field.

#### 3.4.3 Gene knockdown efficiency

Total RNA was isolated from cell cultures that were treated with the AllStars negative siRNA and the positive (silencing) siRNA. Concentration of the total RNA was determined on the NanoDrop ND 1000 spectrophotometer. cDNA synthesis was done

using the MMuLV RT kit as described in section 3.3.2. The same amounts of total RNA were used as templates in cDNA synthesis from both sets of cell cultures.

#### Quantitative real-time PCR

qPCR was performed on the Rotor-Gene 6000. Volumes and concentration of PCR components used are shown in Table 3.13. QuantiTect primer assay for MAPK1 (mouse Catalogue number QT 00133840, human Catalogue number QT 00065933) were used at a final concentration of 1X. The primer assays for the MAPK1 gene in human and mouse are different. The cycling parameters were similar to those described in section 3.3.5 but with an annealing temperature of 60°C.

**Table 3. 13** PCR components for 1 reaction tube run on the Rotor-Gene 6000 for MAPK1 gene in HepG2 and 3T3-L1 cells

<b>Reagent</b>	<b>Vol (<math>\mu</math>l)</b>	<b>Initial concentration</b>	<b>Final concentration</b>
SensiMix dT	6.0	2x	1X
SYBR® Green I	0.24	50X	1X
Primer assay	1.2	10X	1X
Water	variable		
cDNA template	variable		
Total volume/tube	<b>12.00</b>		

#### 3.4.4 Post-transcriptional silencing of the *TNSALP* gene in 3T3-L1 and HepG2 cells using the long-term transfection protocol

##### Cell culture

On the day before first transfection, 3T3-L1 and HepG2 cells were seeded into 24-well Nunc plates at an approximate density of  $6 \times 10^4$  cells per well and maintained under conditions described in sections 3.1.1 and 3.1.2 respectively.

##### Transfection

Lyophilized pellets of the siRNA for the *TNSALP* gene for the mouse and the human cell lines were prepared and used as described in section 3.4.1. Transformation cocktail was added to the cells as they were transfected for the first time. New transfection complexes were added to the cells with change of culture medium. No transfection complexes were added to cells that acted as controls.

Non-silencing siRNA (<sup>®</sup>AllStars negative) transfection complexes were added to cells to control for the non-specific effects of siRNA transfection.

The following were the parameters of the HP GenomeWide siRNA (Qiagen, Germany):

##### (i) mouse (3T3-L1) cells

Catalogue number: SI02666132

Gene accession: NM 007431

Gene symbol: Alpl

Gene ID: 11647

nmol/tube: 5

MW (K-salt): 13310.124  
Purity: High-performance purity (HPP)  
Target sequence: 5'-CAGGATCGGAACGTCAATTAA-3'  
Sense strand: 5'-GGAUCGGAACGUCAAUUAATT-3'  
Antisense strand: 5'-UUAUUUGACGUUCCGAUCCTG-3'  
Type of overhang: DNA

(ii) human (HepG2) cells

Catalogue number: SI02658600  
Gene accession: NM 000478  
Gene symbol: Alpl  
Gene ID: 249  
nmol/tube: 5  
MW (K-salt): 13365.164  
Purity: High-performance purity (HPP)  
Target sequence: 5'-CCGGGACTGGTACTCAGACAA -3'  
Sense strand: 5'-GGAACUGGUACUCAGACAATT -3'  
Antisense strand: 5'-UUGUCUGAGUACCAGUCCCGG-3'  
Type of overhang: DNA



### Total RNA isolation, ALP activity measurement and determination of intracellular lipid accumulation in transfected/untransfected cells

Total RNA was isolated from 3T3-L1 cell cultures on day 0, 7 and 11 post-addition of transfection complexes and on day 0, 4, 7 and 11 from HepG2 cells using the procedures outlined in section 3.3.1. cDNA synthesis was done with the isolated RNA as template using the procedure described in section 3.3.2. ALP was extracted from the cultures using the extraction solution prepared as shown in Table 3.2 and ALP activity measured using the pNPP method as noted in section 3.1.7. Total protein was determined on the cell extracts using the Bradford method (section 3.1.8) but the protein standards were diluted 1:1000 to allow measurements of lower protein concentrations as the cells were now grown in 24 well plates. Intracellular lipid accumulation was assessed using the Oil Red O staining procedure (section 3.1.5).

### Efficiency of *TNSALP* gene knockdown

cDNA synthesized from the total RNA on the various time points was used for the *TNSALP* gene expression studies using the Rotor-Gene 6000. QuantiTect primer assays ([mouse] catalogue number QT 01740221 and [human] catalogue number QT 00012957) each designed for the specific site on the mRNA transcript for the *TNSALP* gene for the two cell types, were used. PCR reaction volumes were as shown in Table 3.13. The cycling parameters were also the same as used in section 3.3.5 but the annealing temperature was 60°C.

### 3.5 Subcellular localization of ALP in HepG2 cells

#### 3.5.1 Cell culture

3T3-L1 cells were grown on 22x22mm cover slips placed in a 6 well Nunc culture plate and incubated at 37°C in a 5% CO<sub>2</sub>/ 95% air in DMEM containing no phenol red. Phenol red-free medium reduces autofluorescence of culture cells (Querido and Chartranda 2008). The cover slips were pre-incubated with 2% (w/v) gelatine solution (BDH Chemicals, Poole England) for 15 minutes and then allowed to air dry for 30 minutes before cells were added on top of them. Gelatine enhances attachment of cells to the cover slips. At confluence, the cell monolayer was washed twice (5 minutes each) with PBS (pH 7.4). Differentiation was induced using the protocol previously described and immunolabeling was done 8 days post-transformation.

HepG2 cells were also cultured on 22x22mm cover slips placed in a 12 well Nunc culture plate and incubated at 37°C in a 5% CO<sub>2</sub>/ 95% air in EMEM containing no phenol red. The cover slips were also pre-incubated with 2% (w/v) Gelatin solution. Lipid accumulation was induced in confluent cells by the addition of 660µl oleic acid coupled to serum bovine albumin (6:1 moles of oleate:mole of albumin) in 5ml of maintenance medium.

#### 3.5.2 Preparation of reagents

- 1X Phosphate buffered saline (PBS): 8.0g sodium chloride (NaCl, Merck RSA), 0.2g potassium chloride (KCl, Univar RSA), 1.4g dibasic sodium phosphate (Na<sub>2</sub>HPO<sub>4</sub>, Merck RSA) and 0.24g monobasic potassium phosphate (KH<sub>2</sub>PO<sub>4</sub>, Merck

RSA) were added to 950ml distilled water. The pH of the solution was adjusted to 7.4 and the volume made up to 1L.

- Antibody dilution buffer: To prepare 10ml, 1.0ml purified Goat IgG [Invitrogen Corporation, CA USA] was added to 9.0ml 1X PBS (pH 7.4, BioWhitaker Lonza MD USA) and while stirring 1mg Saponin (Sigma Aldrich UK) was added until completely dissolved.
- Blocking buffer: 0.15g of glycine [0.2M](Proanalysis, RSA) was dissolved in 10ml antibody dilution buffer.
- 3% (w/v) paraformaldehyde-PBS solution: 3g of paraformaldehyde (Sigma Germany) was dissolved in 100ml 1X PBS (pH 7.4, BioWhitaker Lonza MD USA) and stirred on a magnetic stirrer at a low heat setting in a fume hood until the solution became clear. The pH of the solution was then adjusted to 7.4.
- 4', 6-Diamidino-2-phenylindole (DAPI) (Invitrogen, CA USA): 10.9mM of DAPI dilactate stock was diluted in 1X PBS (pH 7.4, BioWhitaker Lonza MD USA) and used at a final concentration of 300nM.
- 2% (w/v) gelatine solution: 10g of gelatin (BDH Chemicals Poole England) was dissolved in 500ml of deionised water. The solution was autoclaved for 30 minutes and then cooled at room temperature before storage at 4-8<sup>0</sup>C.

All the reagents prepared above were syringe filtered through a 0.22 micron filter before use.

- Normal rabbit and guinea pig serum [abD Serotec UK]: for use as negative controls for primary antibodies. These were used at the same dilution (see below) as the primary antibodies which they were replacing.
- Fluorsave reagent (CalBiochem Merck, Germany): for mounting cover slips on slides.

#### Primary antibodies

- Rabbit monoclonal anti-perilipin (D1D8 XP) antibody obtained from Cell Signalling Technology, Inc USA (catalogue number 9349) was diluted 1:100 with antibody dilution buffer before use.
- Guinea pig polyclonal (GP40, hCTA/B) anti-adipophilin/ADRP antibody obtained from Progen Biotechnik, Heidelberg Germany was diluted 1:100 with antibody dilution buffer before use.

#### Secondary antibodies

- Alexa Fluor 594-coupled goat anti-rabbit IgG (H&L chains) antibody [Invitrogen Molecular Probes, CA USA] (stock 2000 $\mu$ g/mL; absorption maxima 590nm and emission maxima 717nm) was used at a concentration of 10 $\mu$ g/mL as the secondary antibody to the primary rabbit anti-perilipin antibody.
- Alexa Fluor 488-coupled goat anti-guinea pig IgG [H&L chains] antibody [Invitrogen Molecular Probes, CA USA] (stock 2000 $\mu$ g/mL; absorption maxima 495nm and emission maxima 519nm) was used at a concentration of 10 $\mu$ g/mL and used as the secondary antibody to the guinea pig anti-ADRP antibody.

### 3.5.3 Specificity of the immunocytochemical methods

#### 3.5.3.1 Negative controls

In order to show that the staining of the cells is specifically due to the primary antibodies (Perilipin/ADRP), the two primary antibodies were replaced with similarly diluted normal serum from the species in which the primary antibodies were raised (that is rabbit and guinea pig serum respectively) keeping all the other steps outlined in the protocol in section 3.5.2.2 (Burry 2000), the same. Fluorescence was also checked in cells in which the secondary antibodies were omitted from the procedure. In this case, the secondary antibody was replaced with the antibody dilution buffer.

#### 3.5.4 Indirect immunolabeling of perilipin and ELF 97 staining of ALP in differentiated 3T3-L1 cells.

- Maintenance medium was aspirated from the wells of the culture plates and cells were washed twice for 5 minutes each with 2ml 1X PBS (pH 7.4).
- Cells were fixed on the microscope slide cover slip by addition of 1ml of 3% freshly prepared formaldehyde-1X PBS solution for 10 minutes at room temperature. The fixative was then removed. Cells were then rinsed three times in 2ml 1X PBS for 5 minutes each.
- Cells were incubated at room temperature for 45 minutes in 200µl blocking buffer containing glycine, saponin and goat IgG. Glycine was used to quench background fluorescence due to aldehydes; saponin was used to permeabilize the cells and purified goat IgG was used to block non-specific antibody binding

(DiDonata and Brasaemle 2003). Cells were then washed once with 1X PBS (pH 7.4) for 5 minutes.

- 100  $\mu$ l containing anti-perilipin antibody (1:100 dilution in antibody dilution buffer) was added to fixed cells and maintained in a humid chamber at 4<sup>0</sup>C overnight. The cells were then allowed to warm up at room temperature for 30 minutes.
- 100 $\mu$ l of Alexa Fluor 594-coupled goat anti-rabbit antibody (10 $\mu$ g/ml) in antibody diluent was then added to the cover slip and incubated in the dark for 1 hour at room temp. The cells were then washed three times with 2ml 1X PBS for 10 minutes each and stained for ALP activity as described below. If no ALP staining was necessary cell nuclei were counterstained with DAPI (300nM in PBS) and the cover slip was then mounted on a microscope slide using Fluorsave reagent (CalBiochem, Merck Germany). The slide was then allowed to dry at room temperature for 20 minutes before visualization.

ALP staining using the ELF 97 endogenous phosphatase kit

ALP staining in 3T3-L1 cells was done using the enzyme linked fluorescence (ELF 97) kit (Invitrogen Molecular Probes, Leiden The Netherlands). This was due to failure to find antibodies that could specifically and clearly label ALP in the cells that were studied.

- Excess PBS from the cover slip was shaken off.
- 100 $\mu$ l of the diluted (1:20) ELF 97 substrate [2-(5'-chloro-2-phosphoryloxyphenyl-6-chloro-4(3H)-guinazolinone) was filtered through ELF

97 spin filter (0.2µm pore size) by centrifuging at 300xg for 5 minutes in a Mikro 22 Centrifuge (Germany). The filtrate was then added to the cover slip that was placed on top of a microscope glass slide. For the control slide, a known inhibitor of ALP (Levamisole, 7mM in PBS) was added and incubated for an hour at room temperature before this step.

- The reaction was monitored on an Olympus BX 41 microscope using a DAPI filter. After 15 minutes, once sufficient reaction product was formed, the reaction was quenched by submerging the cover slip in wash buffer (25mM EDTA, 5mM Levamisole in PBS, pH 8.0). Cleavage of the ELF 97 substrate generates a yellow green precipitate at the site of ALP activity. Omission of the ELF 97 substrate did not give any ALP signal.
- The cover slip was then washed with two changes of the wash buffer between 10-15 minutes with gentle agitation.
- The wash buffer was then removed and the cover slip was then mounted on a microscope slide using the ELF 97 mounting medium (Invitrogen Molecular Probes, Leiden The Netherlands). It was then allowed to dry overnight at room temperature away from light before visualization.

Visualization was through DAPI/fluorescein/red filters. Images were captured using an Olympus XM10 camera mounted on an Olympus 1X71 microscope (Hamburg, Germany). The images were processed using Analysis LS Research Soft Imaging Solutions (Münster, Germany).

### 3.5.5 Indirect immunolabeling of ADRP and ELF 97 staining of ALP in HepG2 cells

The procedure described in section 3.5.4 was also used to label adipose differentiation related protein (ADRP) and ALP in HepG2 cells 7 days after the addition of oleic acid–albumin mixture. Non-transformed cells were also labeled. ADRP (adipophilin) belongs to a group of proteins (PAT family) that closely associates with the lipid droplet membrane in many types of cells (Londos *et al.* 1999; Ohsaki *et al.* 2005). Motomura *et al.* (2006) demonstrated the staining of ADRP in human hepatocytes. Perilipin is not expressed in HepG2 cells (Servetnick *et al.* 1995; Straub *et al.* 2008).

ADRP antibody was used at a dilution of 1:100. The concentration of the secondary antibody (Alexa Fluor 488-coupled goat anti-guinea pig IgG) used was 10µg/mL.

### 3.6 Analysis of single nucleotide polymorphisms (SNPs) in the promoter region of the human *TNSALP* gene

The nucleotide sequence of the coding region of the human *TNSALP* gene and its 5' upstream region is available in the DDBJ/EMBL/GenBank databases under the accession number AB176449. The 5' upstream region is 3.84kb in size and its nucleotide sequence is shown in appendix IE. For the naming of the bases in this region of the gene, refer to Fig.2.3 (Weiss *et al.* 1988).

Ethical clearance for this part of the study was obtained from the Human Research Ethics Committee (Medical), WITS University (Protocol No. M070214).



### 3.6.1 Primer design and synthesis

To design primers for use in amplifying the promoter region of the human *TNSALP* gene, Gene Runner software (version 3.05, Hastings Software USA) was used.

In order to make analysis of sequenced fragments easier, 7 sets of primers were designed for amplification of the whole fragment Table 3.14. The segments overlapped to avoid elimination of some bases during amplification.

Primer sequences were sent to Inqaba Biotec (RSA) for synthesis. The lyophilized primers were reconstituted with an appropriate volume of DNA/RNase-free water to give a stock solution of 100 $\mu$ M.

Polymerase chain reaction (PCR) was used to amplify the segments of the promoter region and control DNA (isolated from a subject who did not participate in the study) was used to optimize PCR conditions.

**Table 3. 14** PCR primers for the promoter region of the human *TNSALP* gene

Segment	Primer sequence	bases	T <sub>m</sub> (°C)	Expected product size
1- 550bp	For 5'- <i>ACT GGG ATT ACA GGC GTG TG</i> -3'	20	64.6	549 bp
	Rev 5'- <i>ACC TAC AGC CCC ACC TTT AAC</i> -3'	21	64.8	
471-1000	For 5'- <i>GCT GCT TCG GCT GTC GTA GTC TC</i> -3'	23	72.5	529 bp
	Rev 5'- <i>AGG CTG AGG CAC GAG AAA GCC</i> -3'	21	73.5	
971-1591	For 5'- <i>AGG GTT CAA GCG TTT CTC GTG CC</i> -3'	23	75.9	620 bp
	Rev 5'- <i>GTG GGC AGG GCA GGT GTT TAC</i> -3'	21	70.8	
1531-2050	For 5'- <i>CTA TCT CTG GCC TTG GTG TA</i> -3'	20	59.1	519 bp
	Rev 5'- <i>CAC CCT CAA ACC CTC TTA CT</i> -3'	20	60.0	
2031-2751	For 5'- <i>AGT AAG AGG GTT TGA GGG TGG</i> -3'	21	64.4	720 bp
	Rev 5'- <i>AGC ACT GGC CCT AAA ACA TGG</i> -3'	21	68.6	
2731-3270	For 5'- <i>CCA TGT TTT AGG CCC AGT GC</i> -3'	20	67.2	539 bp
	Rev 5'- <i>GCT CTG TTT GAA TGC CTC CA</i> -3'	20	64.9	
3251- 3780	For 5'- <i>TGG AGG CAT TCA AAC AGA GC</i> -3'	20	64.9	521 bp
	Rev 5'- <i>GCT ACC GCA AGA AGA AGC AC</i> -3'	20	62.5	

### 3.6.2 DNA extraction

Whole blood (4.5ml) from 6 black females (BMI  $33.0 \pm 4.6$ ; age  $49.7 \pm 6.3$  years) and 6 white females (BMI  $31.5 \pm 4.5$ ; age  $39.5 \pm 11.9$  years) was collected into an EDTA tube and centrifuged in a Labofuge 200 centrifuge (Heraeus Sepatech, USA) at 2500xg for 10 minutes at room temperature. Three layers were formed with the middle layer being the buffy coat. The buffy coat layer was then carefully pipetted out of the tube. DNA was extracted using the QIAamp DNA mini Kit (Qiagen, Germany; [www.qiagen.com/literature/default.aspx?Term=QIAquickextraction+kit&](http://www.qiagen.com/literature/default.aspx?Term=QIAquickextraction+kit&)) according to the manufacture's instructions.

The eluate containing genomic DNA was stored at  $-20^{\circ}\text{C}$  until use. To determine the concentration of the isolated DNA, a NanoDrop spectrometer ND1000 (NanoDrop Technologies Inc, USA) was used.

### 3.6.3 Optimization of the PCR conditions for the promoter region of the human *TNSALP* gene

#### Preparation of the master mix

The master mix contains all the components of PCR except the template DNA.

Taq polymerase (Supertherm Gold) and its buffer (containing 15mM  $\text{MgCl}_2$ ) were supplied by JMR Holdings (UK); dNTPs were supplied by Bioline and the primers were synthesized by Inqaba, (RSA).

**Table 3. 15** Volume and concentration of PCR components in one typical PCR tube reaction and a master mix for 10 reactions

<b>Reagent</b>	<b>Vol (<math>\mu</math>l)</b>	<b>Initial concentration</b>	<b>Final concentration</b>	<b>Master mix for 10 reactions</b>
Buffer	1.0	10X	1X	10.0
dNTPs	0.8	10mM each	0.7mM	8.0
Taq polymerase (ST Gold)	0.15	5U/ $\mu$ l	0.06U/ $\mu$ l	1.5
Forward primer	0.1	100 $\mu$ M	0.8 $\mu$ M	1.0
Reverse primer	0.1	100 $\mu$ M	0.8 $\mu$ M	1.0
Distilled water	7.85			78.5
DNA template	2.0			
Total volume/tube	<b>12.0</b>			

Thermal cycling

The reaction tubes were then placed in a thermal cycler (<sup>TM</sup>My Cycler thermocycler, Biorad [Italy]) that was programmed using the parameters below. Optimization of the PCR conditions usually involved manipulation of the annealing temperature/time and or adjustment of primer concentration. Negative control contained all reagents for the PCR excluding the DNA template.

**Table 3. 16** Optimized PCR conditions for each of the amplified segments of the promoter region of the human *TNSALP* gene

Segment	Annealing temp/time	Extension time	[Primer]
1 (1-550bp)	67°C/30sec	35 sec	50mM
2 (471-1000bp)	60°C /30sec	35 sec	100 mM
3 (971-1591bp)	77°C /30sec	45sec	50 mM
4 (1531-2050bp)	59°C /30sec	35sec	100 mM
5 (2031-2751bp)	64°C /30sec	35 sec	50 mM
6 (2731-3270bp)	64°C /30sec	1min	50 mM
7 (3251- 3780)	58°C /30sec	1min	100 mM

The initial denaturation temperature was 94°C for 11minutes while the extension temperature was 72°C for 10 minutes for all the PCR reactions.

Cycling conditions were 94°C for 40 seconds, annealing temperature  $x$  for  $y$  seconds (Table 3.16). These steps were repeated 30 times in sequence.

#### 3.6.4 Gel electrophoresis of PCR products for the promoter region of the human *TNSALP* gene

Electrophoresis on agarose gel was used to separate and analyze PCR products as described in section 3.3.4 above.

### 3.6.5 DNA sequencing

#### Purification of PCR products

PCR products were purified using the QIAquick PCR purification kit (Qiagen, Germany; [www.qiagen.com/literature/default.aspx?Term=QIAquickpurification+kit&](http://www.qiagen.com/literature/default.aspx?Term=QIAquickpurification+kit&)) as per manufacturer's recommendations before the samples were sent for sequencing.

#### DNA sequencing

PCR products were sent to Inqaba Biotec (RSA) for sequencing. A Genetic Analysis System method on a Spectrumedix SCE 2410 (Spectrumedix ILL, USA) was used to sequence the PCR products.

#### Mutation analysis of sequenced samples

A total of 168 sequence results (14 for each of the 12 samples) were received from Inqaba Biotec. Sequencher version 4.7 was used to align the reference gene (GeneBank accession number AB 176449) sequence with the sequenced results and checked for single nucleotide differences.

Forward and reverse sequences for each of the segments sequenced were checked for background noise at the beginning and end of the sequence and those parts of the chromatogram that did not show well defined peaks were edited before the sequences were analyzed. Starting from the 5' end both sequences were inspected for any nucleotide base differences.

### 3.7 Statistical analysis

All experiments were repeated 3 times unless otherwise stated. Mean and standard error of the mean (SEM) were calculated from the 3 repeats for each of the variables under study. Each data point in the figures shown in the next chapter is a mean of 3 experiments unless otherwise stated.

Students paired t-test was used to compare the difference between means calculated for each of the variables in the experiments.

A p-value of equal or less than 0.05 was considered a statistically significant difference between means for any of the variables studied.

All the statistical tests were performed using <sup>®</sup>Microsoft Excel (2003).

# **CHAPTER FOUR**

## **RESULTS**



The data contained within this chapter derives from experiments performed to answer a number of questions. The first was to determine whether TNSALP is expressed within HepG2 cells and whether its level increases during intracellular lipid accumulation, using the 3T3-L1 preadipocyte cell line as a comparator. Secondly, TNSALP inhibitors were used to determine whether this isoenzyme is required for lipid accumulation and whether inhibition of ALP activity would also affect the expression of the key adipogenic regulator, PPAR $\gamma$  in both cell lines. The third question was would more specific inhibitors of TNSALP i.e. siRNA, block intracellular lipid accumulation in both 3T3-L1 and HepG2 cells. The fourth question was, what is the intracellular localization of TNSALP in these two cells lines, and how is it related spatially to the lipid droplet-specific proteins? The final question was whether the marked ethnic difference in TNSALP activity in preadipocytes from white and black subjects (Ali *et al.* 2006a) was related to polymorphisms within the promoter region of the TNSALP gene.

#### 4.1 ALP activity and intracellular lipid droplet accumulation in HepG2 & 3T3-L1 cells

In order to determine the relationship between lipid droplet accumulation and ALP activity in HepG2 and 3T3-L1 cells, total ALP activity and lipid accumulation was measured in cells that were induced to accumulate intracellular lipids over a time course of 11 days.

#### 4.1.1 Intracellular lipid accumulation

Intracellular lipid accumulation was measured as optical density (OD) of the Oil Red O stain that was back extracted from cells after induction of intracellular lipid droplet accumulation and was expressed as OD units per 200,000 cells. The images of cells are shown in Fig. 4.1.

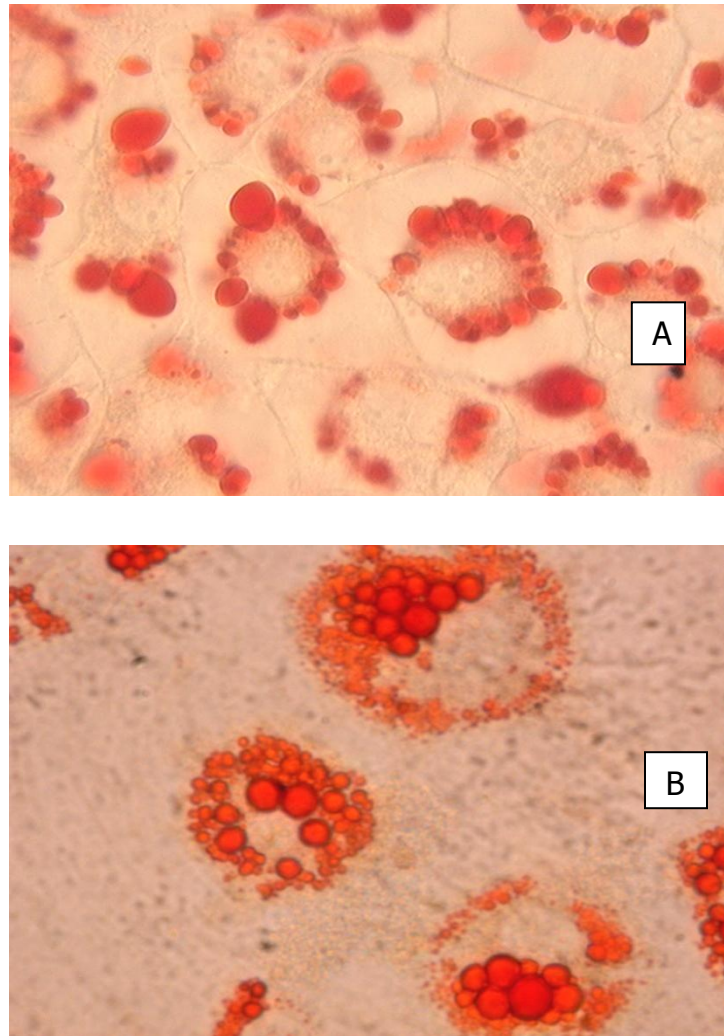


**Figure 4. 1** Photographs of 3T3-L1 & HepG2 cells (stained with Oil Red O).

*A- 3T3-L1 cells and B- HepG2 cells 11 days post-induction of lipid accumulation (x40 magnification). In both cell types the lipid droplets appear to form a necklace around the nucleus but in the HepG2s there are lots of small lipid droplets.*

In 3T3-L1 cells, statistically significant increases in lipid accumulation were observed on day 7 and 11 ( $p < 0.005$ ) post-induction of lipid droplet aggregation compared to day 0 (Fig.4.2). In HepG2 cells, statistically significant increases in lipid accumulation were also observed on day 7 ( $p < 0.05$ ) and day 11 ( $p < 0.005$ ) post-induction of lipid droplet formation compared to day 0 (Fig.4.3).

#### 4.1.2 ALP activity in HepG2 and 3T3-L1 cells

ALP activity of cell extracts (expressed in IU/ $\mu$ g protein) increased from day 0 to day 4 parallel to lipid accumulation in both cell types. Statistically significant increases in ALP activity were observed on day 4, 7 and 11 compared to day 0 in 3T3-L1 cells ( $p < 0.05$ ; Fig.4.2) and on day 4 ( $p < 0.005$ ; Fig.4.3) in HepG2 cells. ALP activity, however, declined earlier in HepG2 (at day 7) than in 3T3-L1 cells (Fig.4.2 and 4.3).

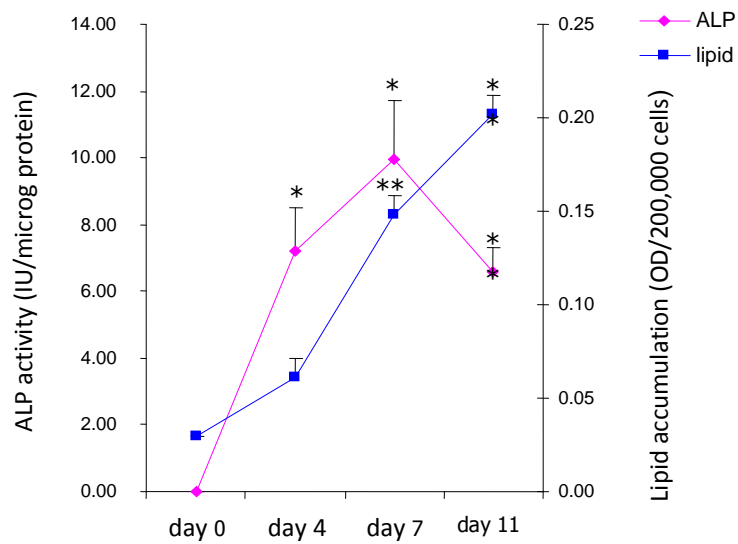


**Figure 4. 2** ALP activity and lipid accumulation in 3T3-L1 cells.

*ALP activity reaches a peak on day 7 after which it declines. Lipid accumulation increases parallel to ALP activity but continues to rise until day 11. Data expressed as mean  $\pm$  SEM; each point represents the mean of 4 experiments; \* $p < 0.05$  vs day 0; \*\* $p < 0.005$  vs day 0.*

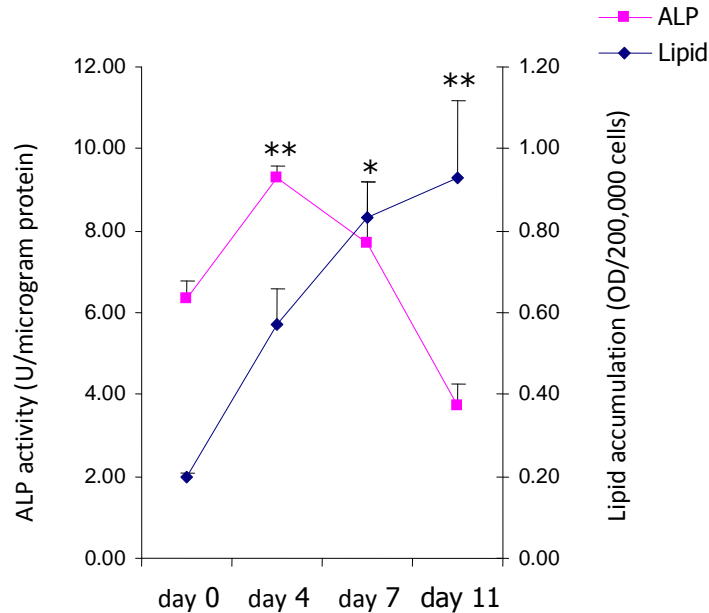


**Figure 4. 3** ALP activity and lipid accumulation in HepG2 cells.

*ALP activity reaches a peak on day 4 after which it declines. Lipid accumulation increases parallel to ALP activity but continues to increase until day 11. Data expressed as mean  $\pm$  SEM; each point represents the mean of 4 experiments; \* $p < 0.05$  vs day 0; \*\* $p < 0.005$  vs day 0.*

#### 4.2 Effect of ALP inhibitors (levamisole & histidine) on intracellular lipid accumulation in HepG2 and 3T3-L1 cells.

In order to study the effect of two ALP inhibitors on lipid accumulation, HepG2 and 3T3-L1 cells were induced to accumulate lipid droplets in the presence and absence of levamisole and histidine. Lipid accumulation and ALP activity were determined in cells treated with the two inhibitors and in cells in which no inhibitor was added.

#### 4.2.1 Lipid accumulation

Differences in intracellular lipid content in the presence and absence of the two ALP inhibitors in HepG2 and 3T3-L1 cells are shown as images in Fig. 4.4 & 4.5 respectively.

Triglyceride content of HepG2 and 3T3-L1 cells in the absence of the two inhibitors was significantly higher on day 7 ( $p < 0.005$  in 3T3-L1 cells;  $p < 0.05$  in HepG2 cells) and 11 ( $p < 0.005$  in 3T3-L1 cells;  $p < 0.005$  in HepG2 cells) compared to day 0 (Fig.4.6 & 4.7).

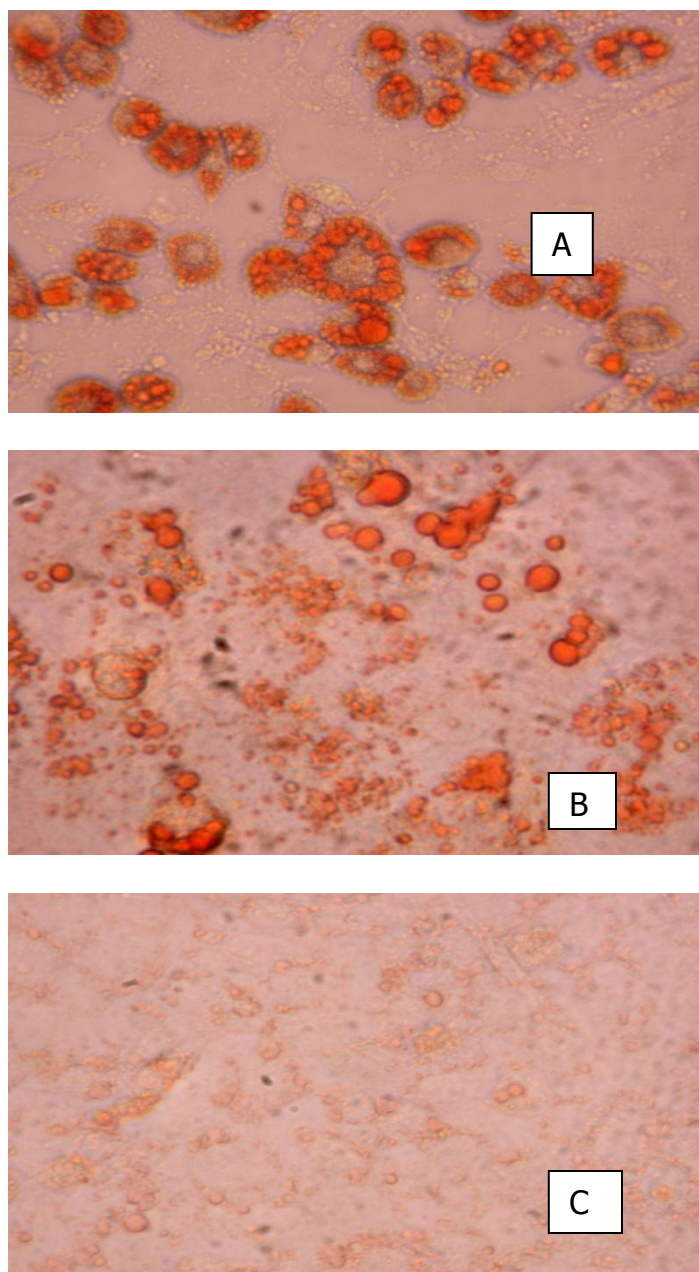


**Figure 4. 4** Oil Red O stain photographs of HepG2 cells.

*A - No inhibitor, B - Treated with levamisole [3.0mM] and C - Treated with histidine [74.8mM] (11 days post-induction of lipid droplet accumulation). All images x 40 magnification.*

*Histidine-treated cells accumulated less lipid than levamisole-treated cells. Untreated cells accumulated more lipid than the inhibitor-treated cells.*



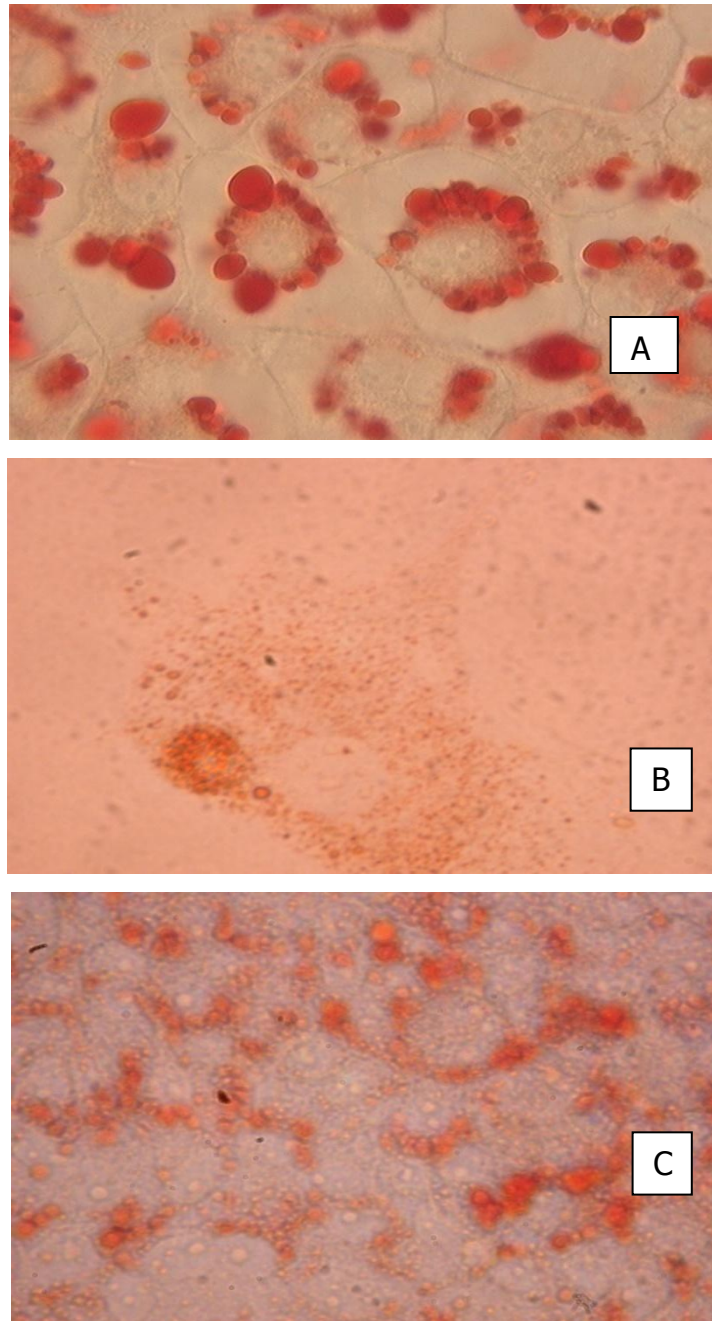


**Figure 4. 5** Oil Red O stain photographs of 3T3-L1 cells.

*A - No inhibitor, B - Treated with histidine [50mM] and C - Treated with levamisole [2.0mM] (11 days post-induction of lipid droplet accumulation). All images x 40 magnification.*

*Histidine-treated cells accumulated less lipid than levamisole-treated cells. Untreated cells accumulated more lipid than the inhibitor-treated cells.*

In the presence of histidine (in both cell types), a statistically significantly lower level of intracellular lipid was observed on day 7 and 11 ( $p < 0.05$ ) when compared to the untreated cells. In HepG2 cells, a statistically significantly higher level of intracellular lipid was observed only on day 4 ( $p < 0.05$ ) when compared to day 0 in the presence of histidine (Fig.4.6). No statistically significant differences in intracellular lipid content were observed between histidine-treated cells and cells on day 0 in 3T3-L1 cells (Fig.4.7). Inhibition of intracellular lipid accumulation by histidine was nearly complete in 3T3-L1 cells.

In the presence of levamisole, a statistically significant lower lipid content was noted on day 11 in HepG2 cells ( $p < 0.05$ ) compared to untreated cells (Fig.4.6). In 3T3-L1 cells, a statistically significant lower lipid content in the presence of levamisole was noted on day 4 and day 11 (both  $p < 0.05$ ) compared to the untreated cells (Fig.4.7). In HepG2 cells, a statistically significant higher level of intracellular lipid was observed on day 7 and day 11 ( $p < 0.05$ ) when compared to day 0 in the presence of levamisole. In 3T3-L1 cells a statistically significant higher level of intracellular lipid was observed on day 11 compared to day 0 in the presence of levamisole (Fig.4.7).

In both cell types significantly lower levels of lipid were seen in cells treated with histidine when compared to levamisole. In HepG2 cells, this difference in intracellular lipid content was observed on day 7 and 11 ( $p < 0.05$ ; Fig.4.6) while in 3T3-L1 cells the difference between the treatments was observed on day 7 only ( $p < 0.05$ ; Fig.4.7).

In the presence of histidine in HepG2 cells a significant increase in lipid accumulation occurred at day 4 only compared to day 0. In 3T3-L1 cells no significant increase in lipid accumulation was observed at day 4, 7 and 11 compared to day 0. Histidine inhibited lipid accumulation earlier and more strongly in 3T3-L1 than in HepG2 cells.

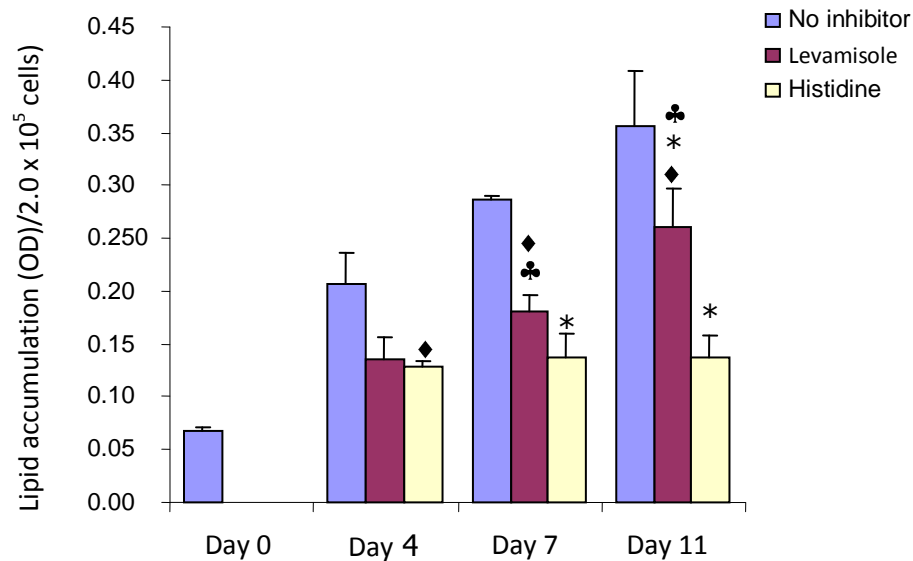


**Figure 4. 6** The effect of histidine and levamisole treatment on intracellular lipid accumulation in HepG2 cells.

*Histidine [74.8mM] reduced lipid accumulation from day 4 to day 11 while the inhibitory effect of levamisole [3.0mM] was seen from day 7. Histidine inhibited lipid accumulation much more strongly than levamisole. Data expressed as mean  $\pm$  SEM; \* $p < 0.05$  vs untreated cells; ♦ $p < 0.05$  vs day 0; ♣ $p < 0.05$  vs histidine.*

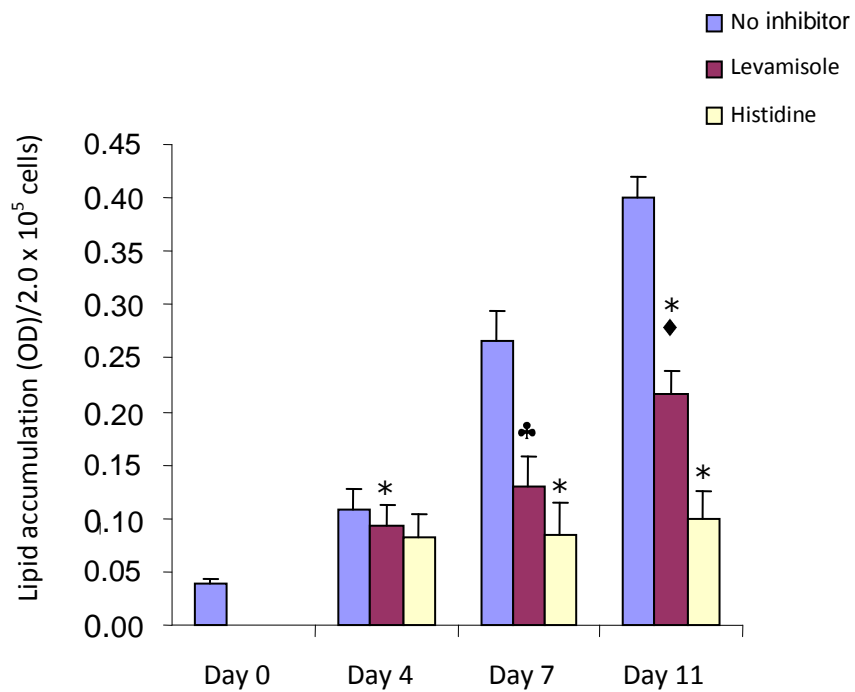


**Figure 4. 7** The effect of histidine and levamisole treatment on intracellular lipid accumulation in 3T3-L1 cells.

*Less lipids accumulated in histidine-treated cells from day 7-11 compared to untreated cells while the inhibitory effect of levamisole was observed on day 11 only when compared to untreated cells. Histidine [50mM] inhibited lipid accumulation much more strongly than levamisole [2.0mM]. Data expressed as mean  $\pm$  SEM; \* $p < 0.05$  vs untreated cells;  $\blacklozenge p < 0.05$  vs day 0;  $\clubsuit p < 0.05$  vs histidine.*

#### 4.2.2 ALP activity in the presence and absence of histidine and levamisole.

In the absence of the two inhibitors, a statistically significant increase in ALP activity was observed on day 4 ( $p < 0.05$ ) in HepG2 cells compared to day 0 (Fig.4.8). On day 7, however, the  $p$ -value was less than 0.05 when compared to day 0. Statistically significant differences in ALP activity were observed on day 4, 7 ( $p < 0.05$ ) and 11 ( $p < 0.005$ ) compared to day 0 in 3T3-L1 cells (Fig.4.9).

In the presence of histidine, statistically significant decreases in ALP activity were observed on day 4 ( $p < 0.05$ ; Fig.4.8) in HepG2 cells compared to the untreated cells while in 3T3-L1 cells statistically significant decreases in ALP activity were observed on day 4 ( $p < 0.005$ ; Fig.4.9), day 7 and 11 ( $p < 0.05$ ; Fig.4.9). Histidine treatment maintained ALP activity on day 4, 7 and 11 at levels similar or lower to that observed on day 0 in both HepG2 cells (Fig.4.8) and 3T3-L1 cells (Fig.4.9).

In the presence of levamisole, a statistically significant decrease in ALP activity were observed on day 4 in HepG2 cells ( $p < 0.05$ ; Fig.4.8) and in 3T3-L1 cells ( $p < 0.05$ ; Fig.4.9) compared to untreated cells. On day 7, the decrease in ALP activity was not significant compared to untreated cells (HepG2) ( $p > 0.05$ ).

In the presence of histidine in both HepG2 and 3T3-L1 cells no statistically significant decrease in ALP activity was observed on days 4, 7 and 11 compared to day 0. Histidine treatment maintained ALP activity at a level similar to that seen on day 0.

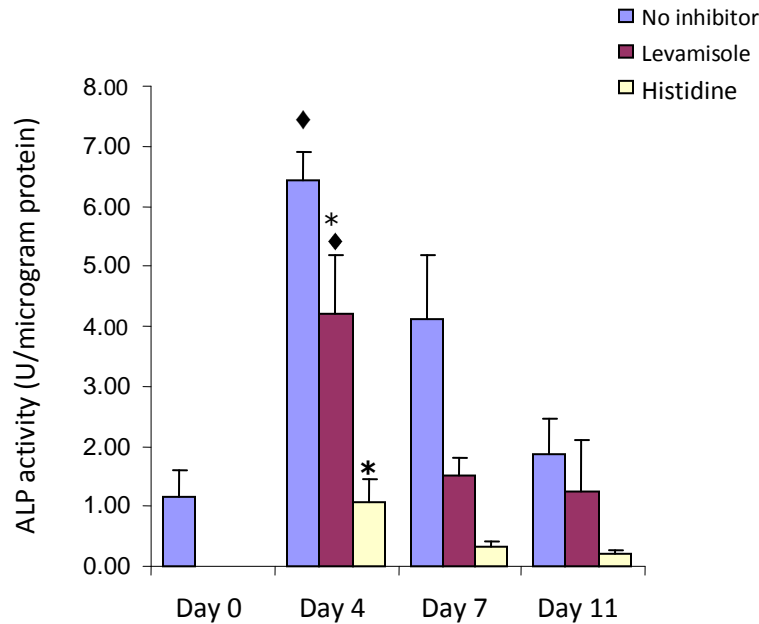


**Figure 4. 8** Effect of histidine and levamisole treatment on ALP activity in HepG2 cells.

*Histidine [74.8mM] and levamisole [3.0mM] reduced ALP activity on day 4 with the strongest inhibition seen in histidine-treated cells when compared to untreated cells. On day 7 & 11 ALP activity in histidine-treated cells was lower than that on day 0. Data expressed as mean  $\pm$  SEM; \* $p < 0.05$  vs untreated cells; ♦ $p < 0.05$  vs day 0.*

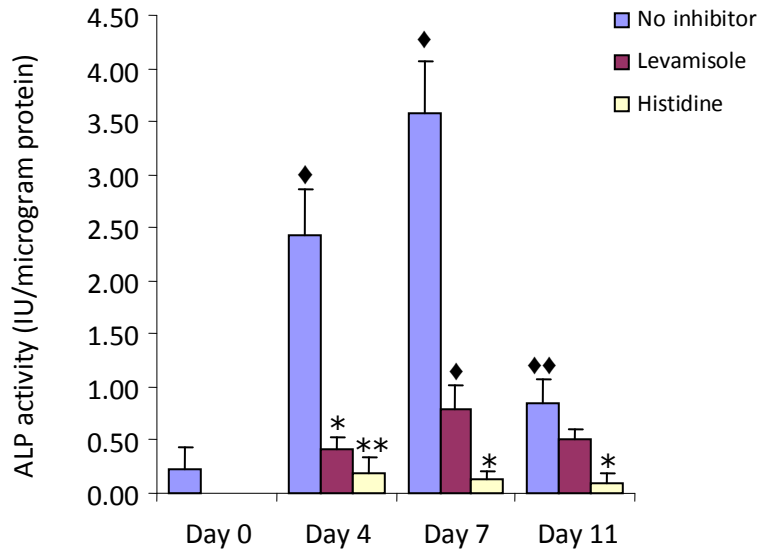


**Figure 4. 9** Effect of histidine and levamisole treatment on ALP activity in 3T3-L1 cells.

*ALP activity was reduced by histidine [50mM] and levamisole [2.0mM] from day 4 to 11 compared to untreated cells. An almost complete block in ALP activity was seen in histidine-treated cells. Data expressed as mean  $\pm$  SEM; \* $p < 0.05$  vs untreated cells; \*\* $p < 0.005$  vs untreated cells; ♦ $p < 0.05$  vs day 0; ♦♦ $p < 0.005$  vs day 0.*

4.3 The expression of the *PPAR $\gamma$*  gene in the absence and presence of histidine and levamisole

In order to determine the effect that the two ALP inhibitors have on the expression of the *PPAR $\gamma$*  gene, total RNA isolated from HepG2 and 3T3-L1 cells on day 0, 4 and 7 was reverse transcribed into cDNA which was then used in conventional and real-time

PCR to indirectly quantify the PPAR $\gamma$  mRNA levels. Total RNA was isolated from cells grown in the presence and absence of levamisole and histidine.

#### 4.3.1 Conventional PCR

During conventional PCR, the *PPAR $\gamma$*  gene was amplified and resulted in an 88 base pair band in HepG2 cells and a 241 base pair band in 3T3-L1 cells. The *TATA-box binding protein (TBP)* gene gave 277 and 189 base pair products for HepG2 and 3T3-L1 cells respectively after amplification (image in Fig.4.10 & 4.11). The latter was used as the reference gene. All bands corresponded to the predicted fragment sizes. For the no template control (NTC), DNase-free water was added instead of cDNA. Primer location and region of amplification of the two sets of primers are shown in Appendix I.



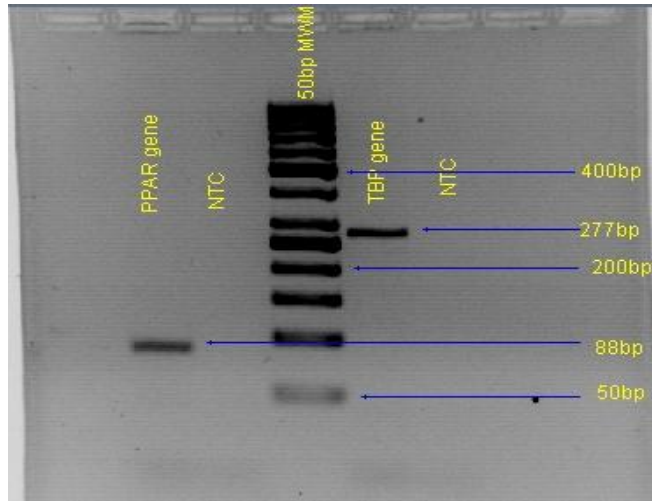


**Figure 4. 10** Agarose gel image of PCR products from HepG2 cells.

*Separation of PCR products on a 2% agarose gel stained with ethidium bromide showed a 88bp band for PPAR $\gamma$  gene and a 277bp band for the TBP gene using a 50bp DNA molecular weight marker. NTC is the no template control.*

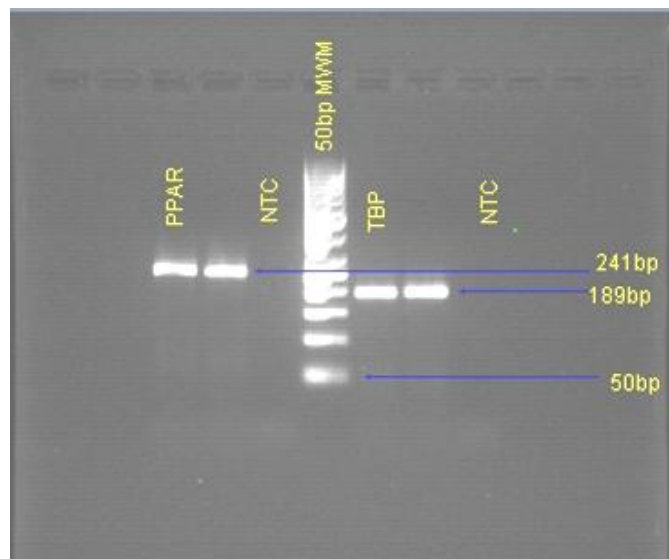


**Figure 4. 11** Agarose gel image of PCR products from 3T3-L1 cells.

*Separation of PCR products on a 2% agarose gel stained with ethidium bromide showed a 241bp band for PPAR $\gamma$  gene and a 189bp band for the TBP gene using a 50bp DNA molecular weight marker. NTC is the no template control.*

4.3.2 Optimized conditions for quantitative real-time PCR on Rotor-Gene 6000 DNA synthesized from mRNA extracted from both HepG2 and 3T3-L1 cells showed excellent amplification during real-time PCR (Fig.4.12 & 4.13 respectively). Clear, single peaks on the melting curve plot indicated precise amplification with no unspecific products. For the no template control (NTC), DNase free water was added instead of cDNA. The mean melting peak temperature for TBP in HepG2 cells (reference gene) was  $83.4 \pm 0.1$  (range 83.3-83.7), N=20. The mean melting peak temperature for TBP in 3T3-L1 cells was  $81.3 \pm 0.2$  (range 81.2-81.5), N=20.

The PCR product of the TBP in HepG2 and 3T3-L1 cells was sequenced to confirm its identity. The consensus sequence of the forward and the reverse sequences were blasted into GenBank and there was a 100% sequence similarity with the reference sequences for the two genes (Appendix I).

Quantification of the levels of mRNA was done using the two standard curves on the Rotor-Gene 6000 as described in section 3.5.5. Efficiency of amplification of the standards are given in Appendix I. 100% efficiency corresponds to 1 using the Rotorgene software and this means the doubling (in amount) of PCR products after one cycle.

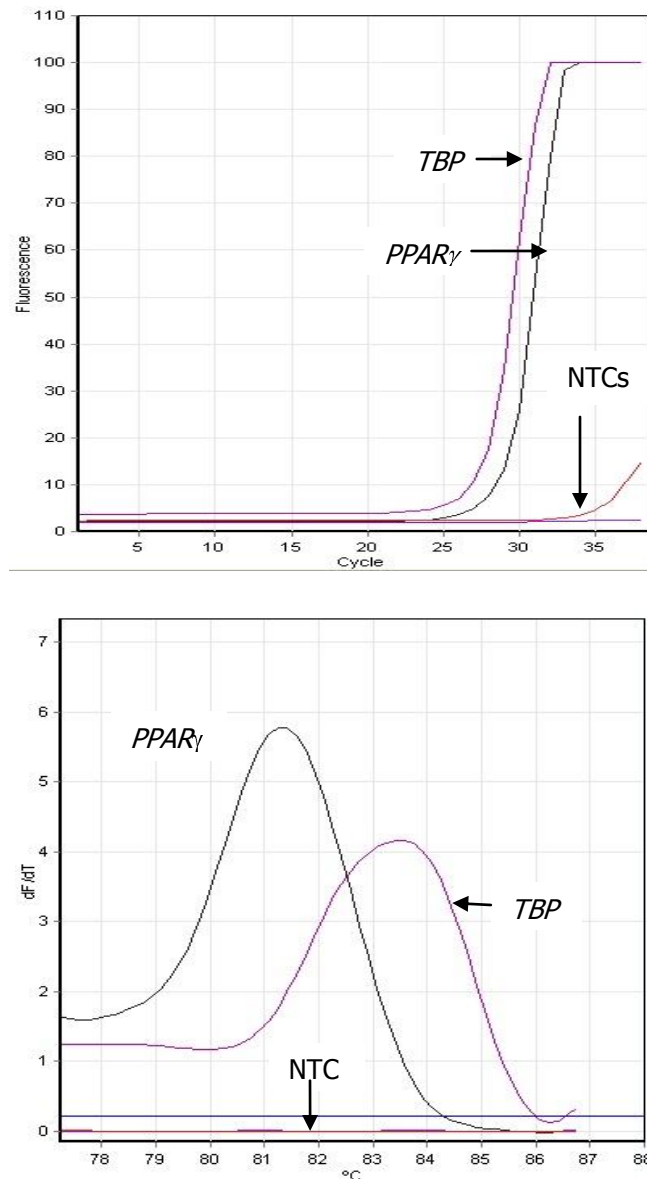


**Figure 4. 12** Real time amplification plot (top) and melting curve of PCR products for HepG2 cells.

*Specific amplification of the PPAR $\gamma$  and TBP genes are shown by single melting curves of their PCR products. The blue line is the threshold limit. NTCs are negative controls. Cycling parameters and PCR components are shown on page 83.*

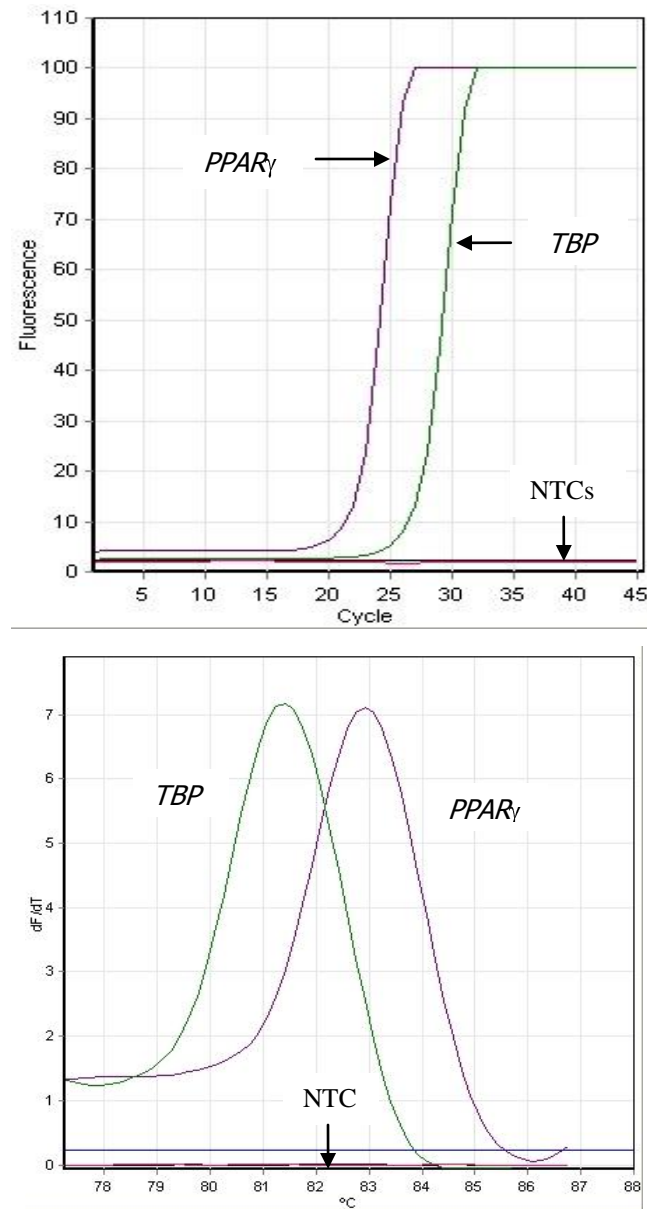


**Figure 4. 13** Real time amplification plot (top) and melting curve of PCR products for 3T3-L1 cells.

*Specific amplification of the  $PPAR\gamma$  and  $TBP$  genes are shown by single melting curves of their PCR products. The blue line is the threshold limit. NTCs are negative controls. Cycling parameters are shown on page 89 and PCR components are shown in Table 3.7.*

### 4.3.3 *PPAR*<sub>γ</sub> gene expression in HepG2 and 3T3-L1 cells.

A 4-fold increase in the expression of the *PPAR*<sub>γ</sub> gene after induction of lipid accumulation was observed between day 0 and day 4 in HepG2 cells after which it declined. The difference in the expression of the gene was statistically significant between day 0 and day 4 ( $p < 0.05$ ; Fig.4.14). In 3T3-L1 cells, a statistically significant 2.5-fold increase in the expression of the *PPAR*<sub>γ</sub> gene was observed between day 0 and day 4 ( $p < 0.05$ ; Fig.4.15). No statistically significant differences in the expression of the *TBP* gene were observed on all days in both cell types. The basal expression (day 0) of *PPAR*<sub>γ</sub> gene was higher in 3T3-L1 than in HepG2 cells. The difference was, however, not significant.

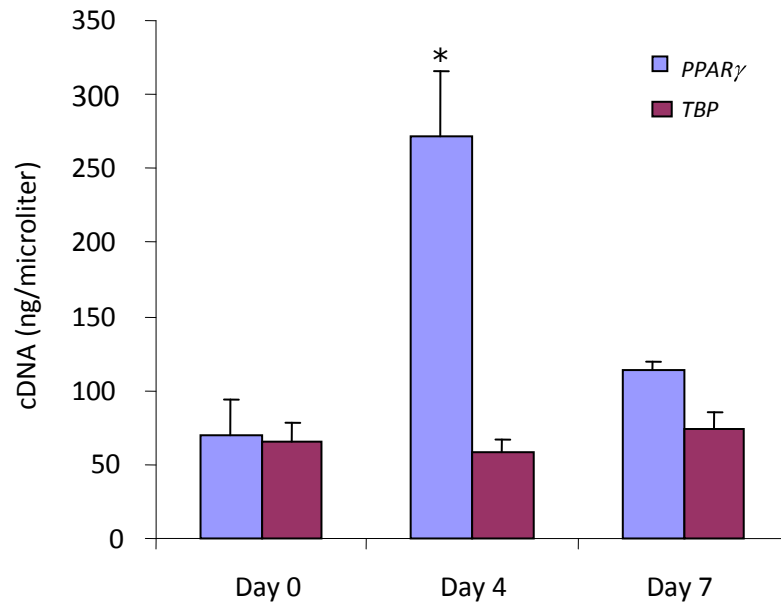


**Figure 4. 14** PPAR $\gamma$  gene expression in HepG2 cells.

*A 4-fold increase in the expression of PPAR $\gamma$  occurred 4 days after induction of lipid droplet accumulation. On day 7 the levels were lower than on day 4 but slightly higher than day 0. No significant changes in the expression of the TBP were observed during the 11 day period. Data expressed as mean  $\pm$  SEM; \* $p$ <0.05 vs day 0.*

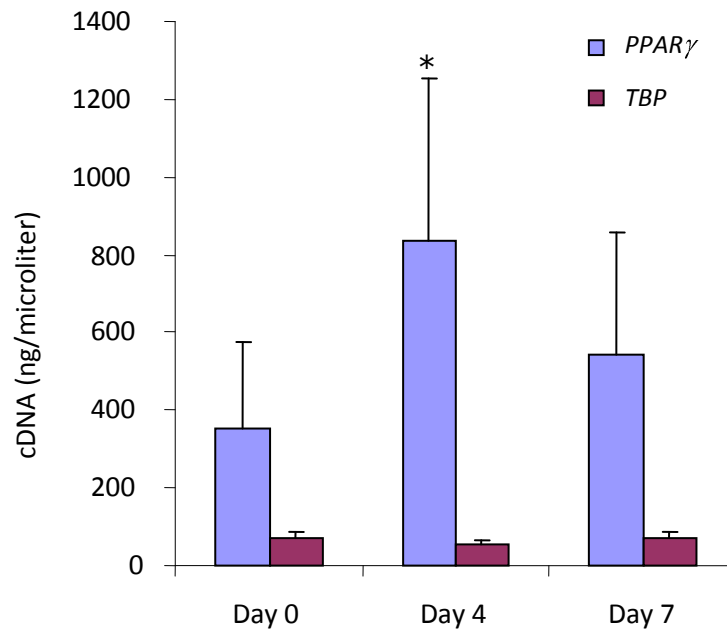


**Figure 4. 15** *PPAR $\gamma$*  gene expression in 3T3-L1 cells.

*A 2½-fold increase in the expression of PPAR $\gamma$  occurred day 4 after induction of adipogenesis. On day 7 the levels were lower than on day 4 but slightly higher than day 0. No significant changes in the expression of the TBP were observed during the 11 day period. Data expressed as mean  $\pm$  SEM; \* $p$ <0.05 vs day 0.*

#### 4.3.4 *PPAR $\gamma$* gene expression in the presence of histidine and levamisole in HepG2 and 3T3-L1 cells.

Histidine and levamisole did not alter the expression pattern of the *PPAR $\gamma$*  gene in either cell types. Thus, in the presence of levamisole, a 2-fold increase in the expression of the *PPAR $\gamma$*  gene was observed between day 0 and day 4 in HepG2 cells while in 3T3-L1 cells a 2½ -fold increase was observed over the same time period.

The increase in the expression of the *PPAR $\gamma$*  gene was statistically significant in both cell types between day 0 and day 4 ( $p < 0.05$ ; Fig.4.16 & 4.17). In the presence of histidine, a statistically significant 2-fold increase in the expression of the *PPAR $\gamma$*  gene occurred between day 0 and day 4 in both cell types ( $p < 0.05$ ; Fig.4.16 & 4.17). The level of expression of the *TBP* gene did not change significantly over the 7 day period. Histidine and levamisole were used at concentration mentioned on pages 119 and 120 in HepG2 and 3T3-L1 cells respectively.



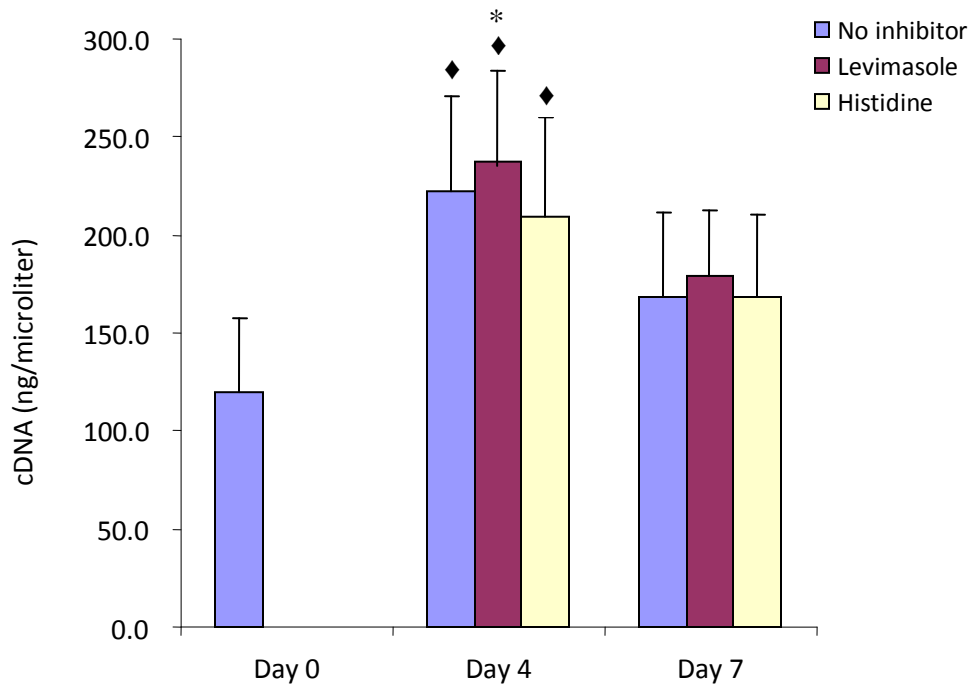


**Figure 4. 16** *PPAR $\gamma$*  gene expression in HepG2 cells grown in the presence of levamisole and histidine.

*An increase in PPAR $\gamma$  level occurred on day 4 after induction of lipid accumulation followed by a decline on day 7 in the presence of both levamisole [3.0mM] and histidine [74.8mM]. The two inhibitors did not alter the expression pattern of PPAR $\gamma$  seen in cells not treated with either of the two inhibitors. Data expressed as mean  $\pm$  SEM; \* $p < 0.005$  vs untreated; ♦ $p < 0.05$  vs day 0.*

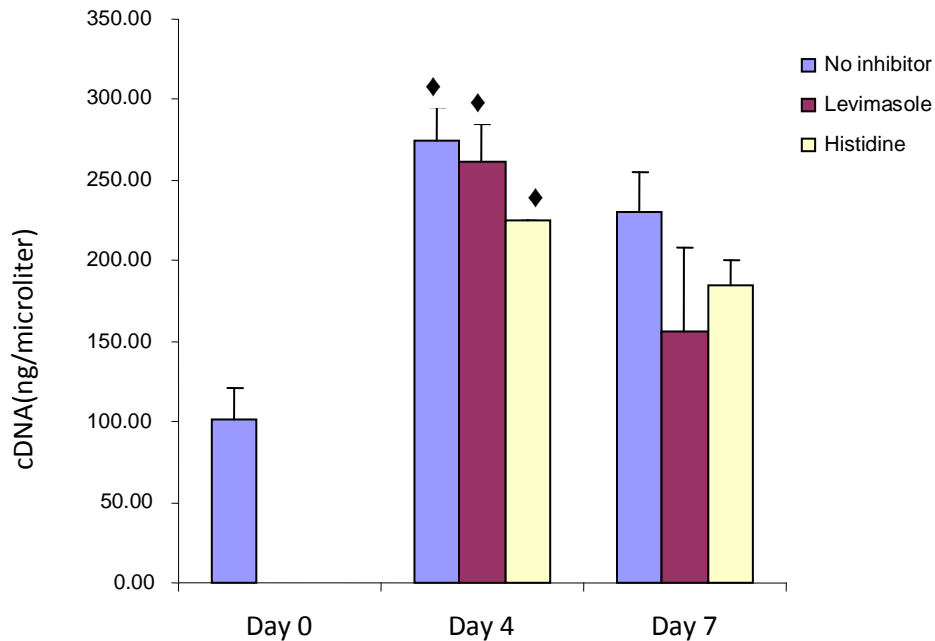


**Figure 4. 17** *PPAR $\gamma$*  gene expression in 3T3-L1 cells grown in the presence of levamisole and histidine.

*An increase in PPAR $\gamma$  level occurred on day 4 after induction of adipogenesis followed by a decline on day 7 in the presence of both levamisole [2.0mM] and histidine [50mM]. The two inhibitors did not alter the expression pattern of PPAR $\gamma$  seen in cells not treated with either levamisole or histidine. Data expressed as mean  $\pm$  SEM;  $\blacklozenge$   $p < 0.05$  vs day 0.*

#### 4.4 RNAi studies for the TNSALP gene in HepG2 and 3T3-L1 cells

In order to study the effect that the silencing of the TNSALP gene using siRNA oligos would have on intracellular lipid accumulation, transfected and untransfected HepG2 and 3T3-L1 cells were induced to accumulate lipid droplets over a 11 day period. Total ALP was measured in cell extracts at selected time points over the same period. Transfection conditions and efficiency of gene knockdown were established using fluorescently labelled anti-MAPK1 siRNA oligos. The RNAi human/mouse/rat starter kit (Qiagen, Germany) provides highly validated siRNA oligos, reagents, primer assays and guidelines for establishing transfection conditions.

##### 4.4.1 Transfection efficiency of siRNA oligos in 3T3-L1 and HepG2 cells using the RNAi human/mouse/rat starter kit

100 $\mu$ l of Anti-MAPK1 siRNA oligos (16.5nM) was added to confluent HepG2/3T3-L1 cells that were grown on a microscope slide cover slip and after 72 hours the cells were visualized on a fluorescence microscope to see the proportion of cells that were transfected. In this work the number of transfected cells (with green dots inside the cell) was manually counted and expressed as a percentage of the total number of cells seen in a given field. Two or more dots in a cell would be counted as one transfected cell. Eight fields were randomly selected and cells counted to gauge a measure of transfection efficiency. DAPI stain was used to count total number of cells in a given field. Approximately 120 cells were counted in each field. The efficiency of

transfection was determined at  $72.9\% \pm 1.6$  in 3T3-L1 and  $68.6\% \pm 0.8$  in HepG2 cells.

Confocal fluorescence microscope images of HepG2 and 3T3-L1 cells transfected with control siRNA and anti-MAPK1 siRNA are shown in Fig.4.18 & 4.19 respectively. The green dots are the fluorescently labeled siRNA in the cytoplasm of cells. Cells transfected with the control siRNA show green dots within cells while those transfected with the positive (silencing) siRNA do not show green dots in the cytoplasm of the cells. Pictures which were taken using a non-fluorescent filter are labelled as transilluminated pictures.

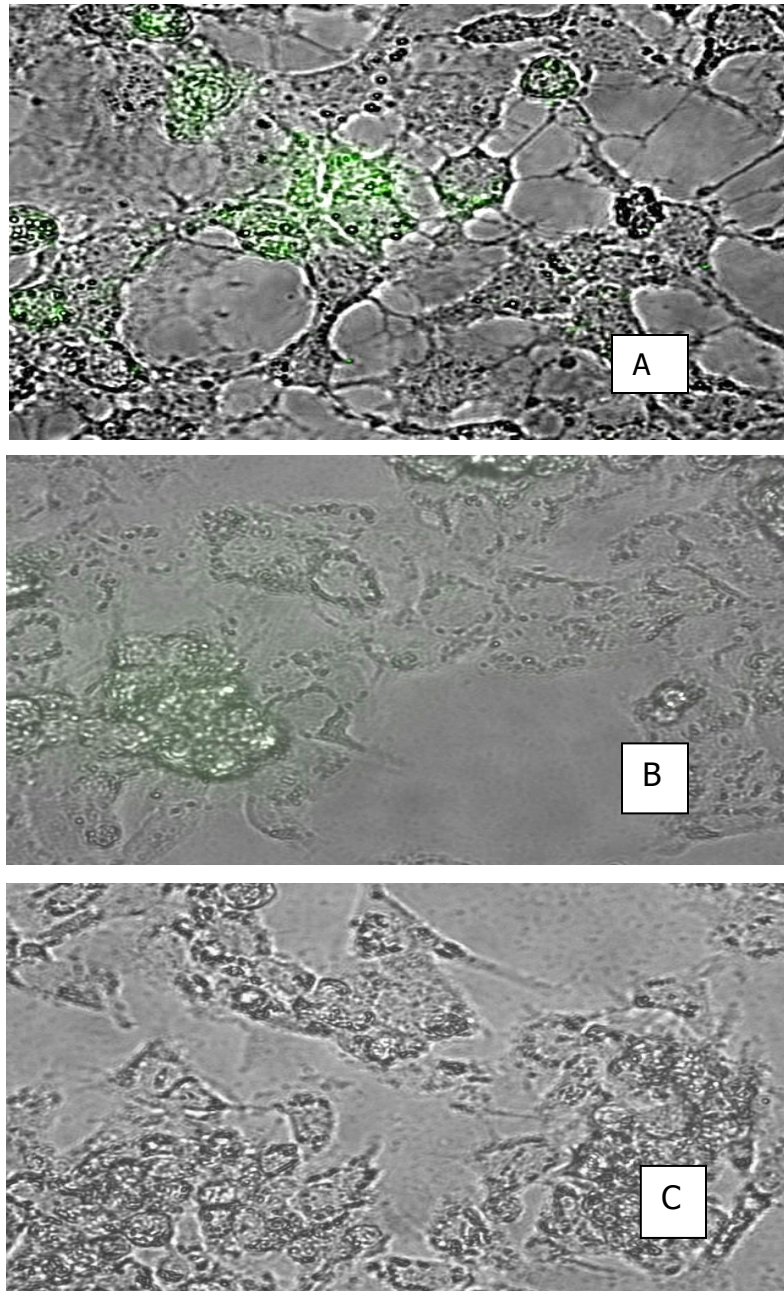


**Figure 4. 18** Confocal fluorescence picture of HepG2 cells.

*A - With control siRNA, B – With anti-MAPK1 siRNA and C -Transilluminated light (72 hours post-transfection x 63). 16.5nM of control and anti-MAPK1 siRNA were each added to cells grown on a microscope slide cover slip placed in a well of a culture plate containing 3ml culture medium.*

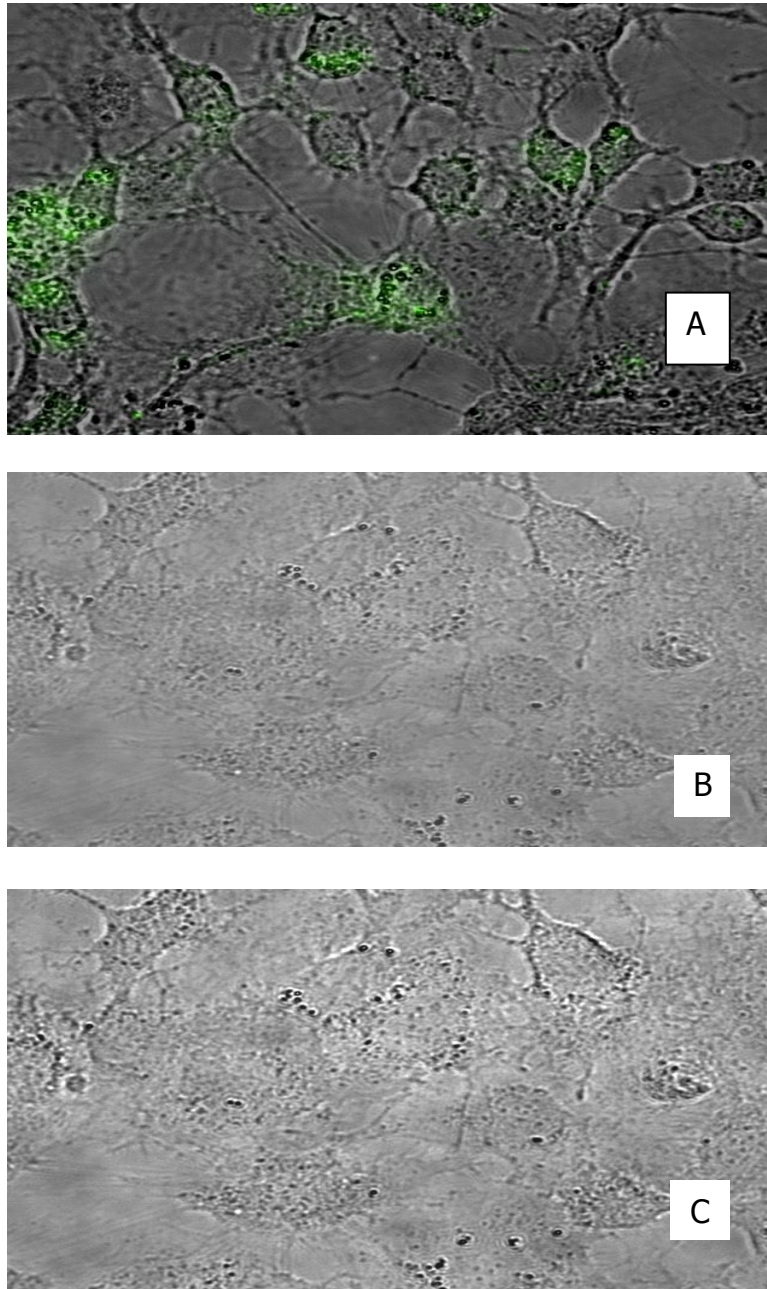


**Figure 4. 19** Confocal fluorescence picture of 3T3-L1 cells.

*A - With control siRNA, B – With anti-MAPK1 siRNA and C -Transilluminated light (72 hours post-transfection x 63). 16.5nM of control and anti-MAPK1 siRNA were each added to cells grown on a microscope slide cover slip placed in a well of a culture plate containing 3ml culture medium.*

#### 4.4.2 *MAPK1* gene knockdown efficiency

In order to determine the efficiency of knockdown of the MAPK1 gene in HepG2 and 3T3-L1 cells, total RNA isolated from cells before and after transfection with the control and Anti-MAPK1 siRNA oligos was reverse transcribed into cDNA and the MAPK1 mRNA levels indirectly quantified using real-time PCR with primers specific for the MAPK1 gene. Control siRNA oligos do not have any known homology with mouse or human mRNA sequences. Knockdown efficiency of MAPK1 gene helps to give an idea of efficiency of knockdown of gene of interest. The siRNA for genes of interest are provided without fluorescence tags.

##### 4.4.2.1 Optimized qPCR conditions on the Rotor-Gene 6000

PCR conditions for the amplification and quantification of the MAPK1 gene were optimized as described in section 3.3.3. The amplification plots and melting curves of the products obtained using the 'optimized conditions' are shown in Fig. 4.20 and 4.21 below. For the no template control (NTC), DNase free water was added instead of cDNA. Though the same gene was being amplified in the two cell types, PCR primers used for the amplification were different, hence the difference in the melting temperature of the two PCR products.

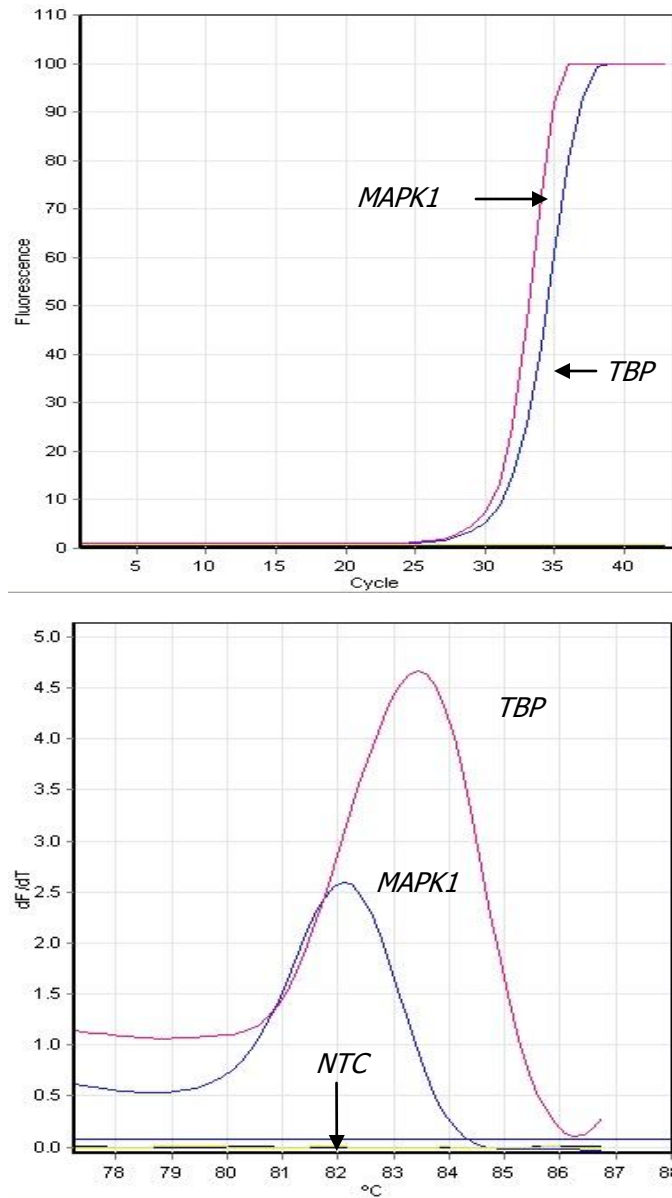


**Figure 4. 20** Real time PCR amplification plot (top) and melting curve of PCR products (*MAPK1* gene) for HepG2 cells.

*Specific amplification of MAPK1 and TBP genes are shown by single melting curves of their PCR products. The blue line is the threshold limit. NTCs are negative controls. Cycling parameters are shown on page 83 but with annealing temperature of 60°C and PCR components are shown in Table 3.13.*



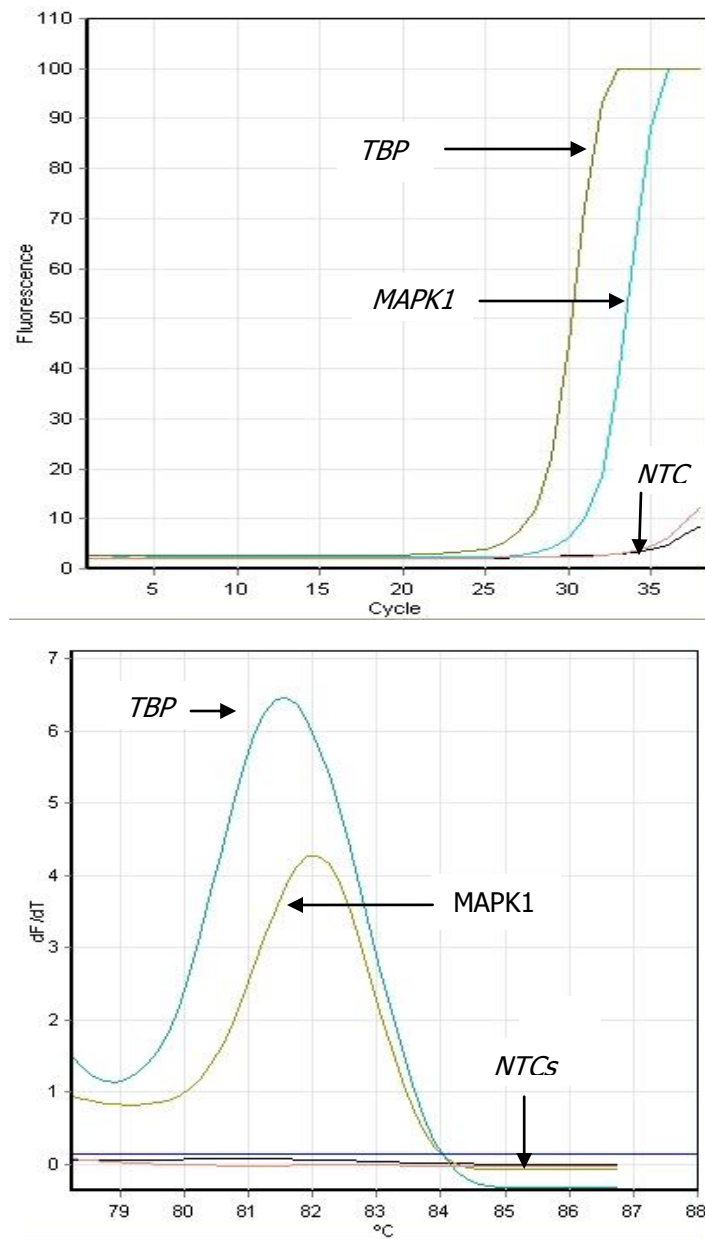


**Figure 4. 21** Real time PCR amplification plot (top) and melting curve of PCR products (*MAPK1* gene) for 3T3-L1 cells.

*Specific amplification of MAPK1 and TBP genes are shown by single melting curves of their PCR products. The blue line is the threshold limit. NTCs are negative controls. Cycling parameters are shown on page 83 but with annealing temperature of 60°C and PCR components are shown in Table 3.13.*

#### 4.4.2.2 *MAPK1* gene knockdown efficiency

Expression level of the *MAPK1* gene was determined using the two-standard curve method on the Rotor-Gene 6000 (described in section 3.3.5). Efficiency of gene knockdown was calculated as a percentage difference in the expression of the gene in cells treated with the control (non-silencing) siRNA and cells treated with the silencing (anti-*MAPK1*) siRNA. The expression of the two genes in cells not transfected with either of the siRNA was set at 100% relative to cells which were transfected with either the positive or negative siRNA. The percentage change in the expression of the *MAPK1* gene was significant in both cell lines ( $p < 0.005$ , Fig.4.22, 3T3-L1 cells;  $p < 0.05$ , Fig 4.23, HepG2 cells).

No significant change in the expression of the *TBP* gene was observed in either cell type between cells transfected with the anti-*MAPK1* siRNA and the control siRNA compared to untransfected cells. The knockdown efficiency of the *MAPK1* gene in 3T3-L1 cells was  $78.9\% \pm 5.9$  while in HepG2 cells it was  $68.6\% \pm 10.3$ .

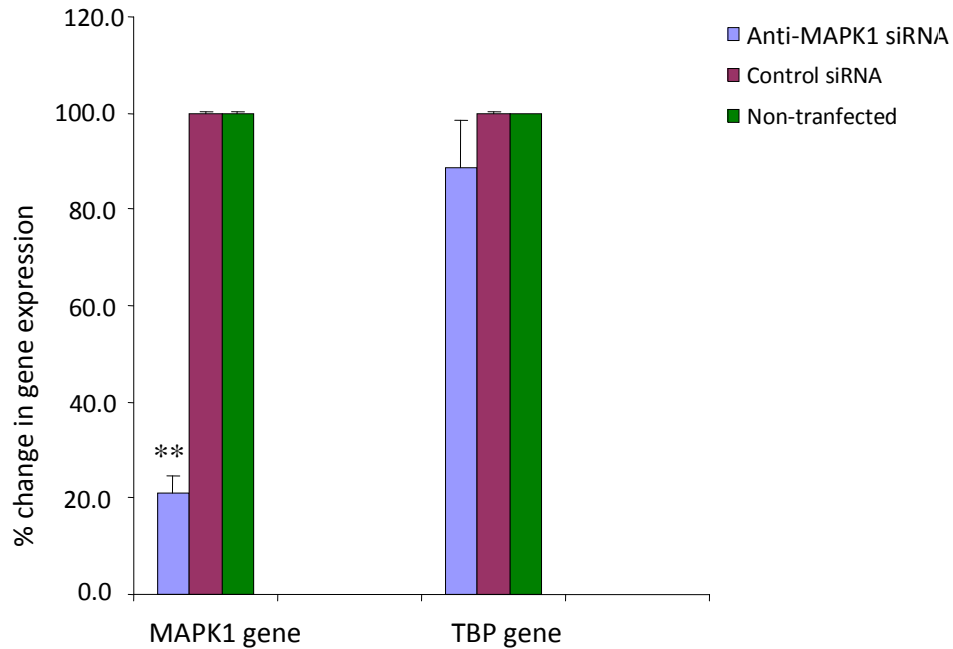


**Figure 4. 22** *MAPK1* gene expression in 3T3-L1 cells 72 hours post-transfection.

*An approximately 80% decline in gene expression was observed in cells transfected with anti-MAPK1 siRNA. No change in gene expression was seen in control and non-transfected cells. TBP gene expression did not significantly vary between the three types of treatments. Data are mean  $\pm$  SEM; \* $p < 0.05$  vs control & non-transfected; \*\* $p < 0.005$  vs control siRNA & non-transfected.*

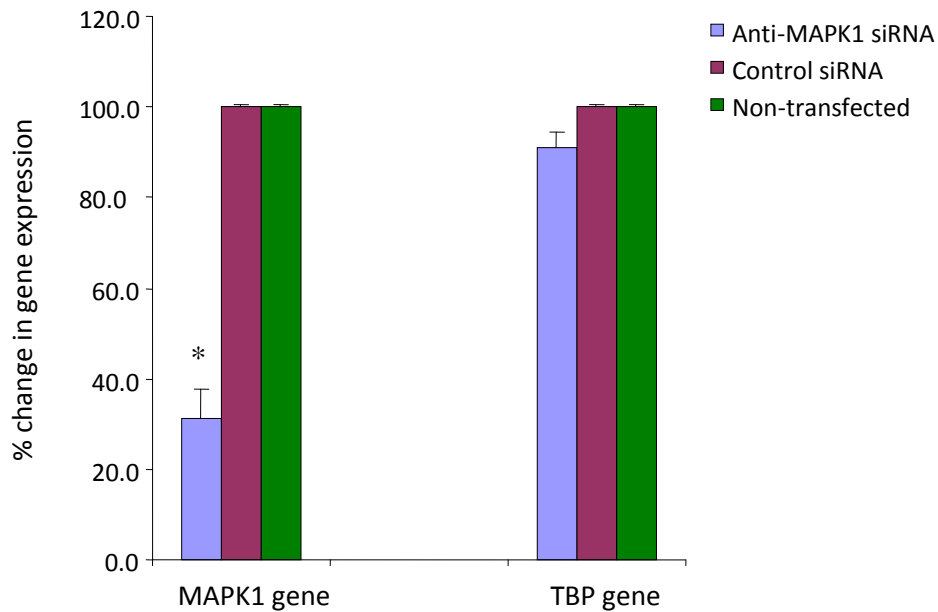


**Figure 4. 23** *MAPK1* gene expression in HepG2 cells 72 hours post-transfection.

*An approximately 70% decline in gene expression was observed in cells transfected with anti-MAPK1 siRNA. No change in gene expression was seen in control and non-transfected cells. TBP gene expression did not significantly vary between the three types of treatments. Data are mean  $\pm$  SEM; \* $p < 0.05$  vs control & non-transfected; \*\* $p < 0.005$  vs control siRNA & non-transfected.*

#### 4.4.3 Knockdown efficiency of the TNSALP gene in 3T3-L1 and HepG2 cells transfected with siRNA directed against TNSALP mRNA

The conditions of transfection (cell density and concentration of siRNA oligos) that were established using the control and anti-MAPK1 siRNA oligos were used in studying the effect of knocking down the TNSALP gene on intracellular lipid accumulation in cells that were induced to accumulate lipid droplets using the protocol previously described.

The quantity of *TNSALP* gene expression was determined using the cDNA reverse transcribed from the total RNA isolated from 3T3-L1 cell cultures on day 0, 7 and 11 and on day 0, 4, 7 and 11 from HepG2 cells using the Rotor-Gene 6000 real-time cycler. TBP was used as the reference gene. Total RNA was isolated from cells transfected with control siRNA, anti-ALP oligos and in untransfected cells.

PCR conditions for amplification of the TNSALP gene were determined using the 'optimization' strategy described in section 3.3.3. The amplification and melting plots of the PCR products using the QuantiTect primer assay (Qiagen QT 01740221) for the *TNSALP* gene in 3T3-L1 cells and QuantiTect primer assay (Qiagen QT 00012957) for the *TNSALP* gene in HepG2 cells respectively are shown in Fig. 4.24 and 4.25. For the no template control (NTC), DNase free water was added instead of cDNA.

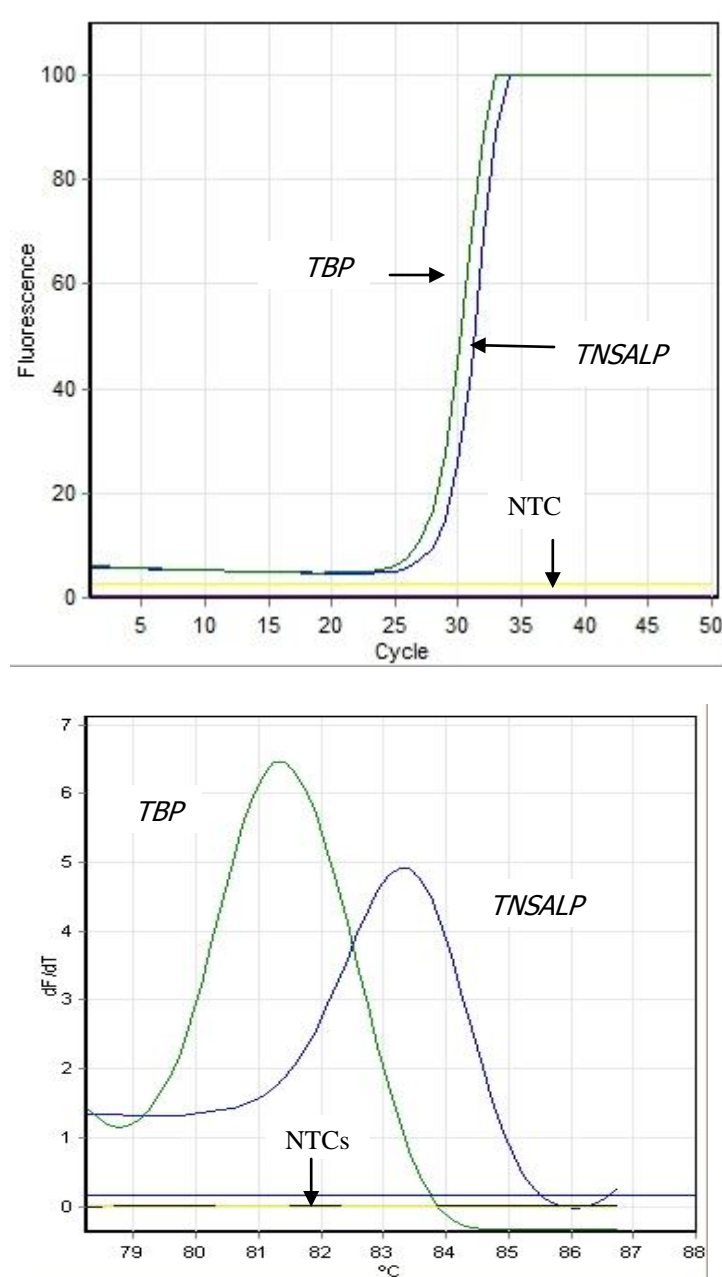


**Figure 4. 24** Real time PCR amplification (top) and melting curves for the *TNSALP* gene in 3T3-L1 cells.

*Specific amplification of the TNSALP and TBP genes are shown by single melting curves of their PCR products. The blue line is the threshold limit. NTCs are negative controls. Cycling parameters are shown on page 83 but with annealing temperature of 60°C and PCR components are shown in Table 3.13.*

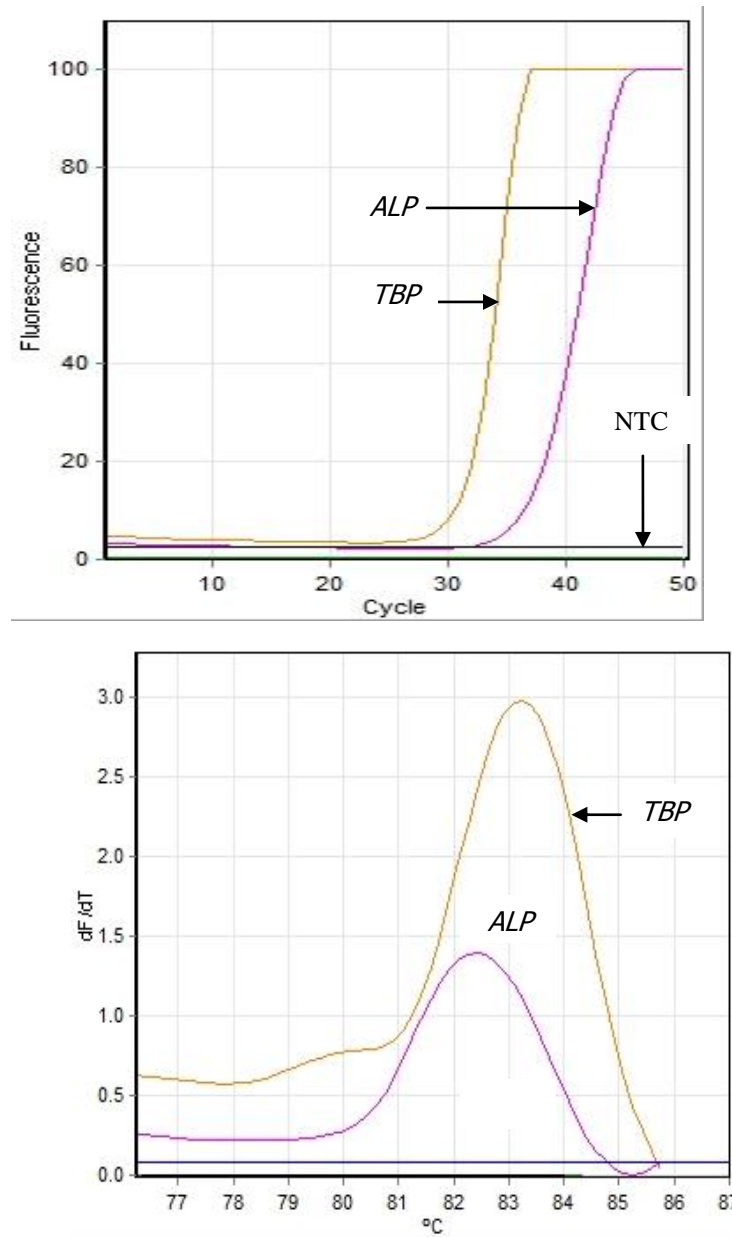


**Figure 4. 25** Real time PCR amplification (top) and melting curves for the *TNSALP* & *TBP* genes in HepG2 cells.

*Specific amplification of TNSALP and TBP genes are shown by single melting curves of their PCR products. The blue line is the threshold limit. NTCs are negative controls. Cycling parameters are shown on page 83 but with annealing temperature of 60°C and PCR components are shown in Table 3.13.*

Knockdown efficiency at a given time point (e.g. day 7) was calculated as the difference in the expression of ALP gene between non-transfected cells and cells transfected with anti-ALP siRNA expressed as a percentage of the level in non-transfected cells.

Expression of the ALP gene in 3T3-L1 cells reached a maximum on day 7 for the untransfected cells and for cells transfected with the anti-ALP siRNA and the control siRNA (data not shown). However, no significant differences in any of the mean values could be found as a result of the high SEM values. Therefore, expression levels of the *ALP* and *TBP* genes shown in the graphs that follow are given as a percentage of the level of expression in untransfected cells on day 7 or day 11. The expression of the ALP and TBP genes in untransfected cells was set at 100%.

In the 3T3-L1 cells the percentage change in the ALP gene expression on day 7 between cells transfected with anti-ALP siRNA and those not transfected was significant ( $p < 0.05$ , Fig.4.26). A significantly lower level of gene expression was also observed when anti-ALP treated cells were compared to those cells transfected with the control siRNA ( $p < 0.05$ , Fig.4.26). On day 11, significantly lower levels of ALP gene expression were observed when cells transfected with anti-ALP siRNA were compared to cells transfected with the control (non-silencing) siRNA and those cells that were not transfected (Fig.4.27). On both day 7 and 11, significant increases in ALP gene expression were observed in cells transfected with anti-ALP siRNA compared to expression on day 0.



Significant increases in ALP gene expression (on day 7 and 11) were also observed when cells treated with the control siRNA were compared to cells on day 0 (Fig.4.26 & 4.27).

On day 7, the knockdown efficiency in 3T3-L1 cells was  $81.3\% \pm 2.7$  between untransfected cells and those cells transfected with the anti-TNSALP siRNA. At the same time point the efficiency of knockdown was  $80.5\% \pm 4.2$  (SEM) between 3T3-L1 cells that were transfected with the control (non-silencing) siRNA and those that were transfected with the anti-TNSALP siRNA.

There was no significant difference in the expression of the *TBP* gene between untransfected cells and those treated with the siRNA for the *TNSALP* gene and the non-silencing siRNA at day 7 and 11 (Fig.4.28 & 4.29). This was also the case when the three treatments on day 7 and 11 were compared to cells on day 0.

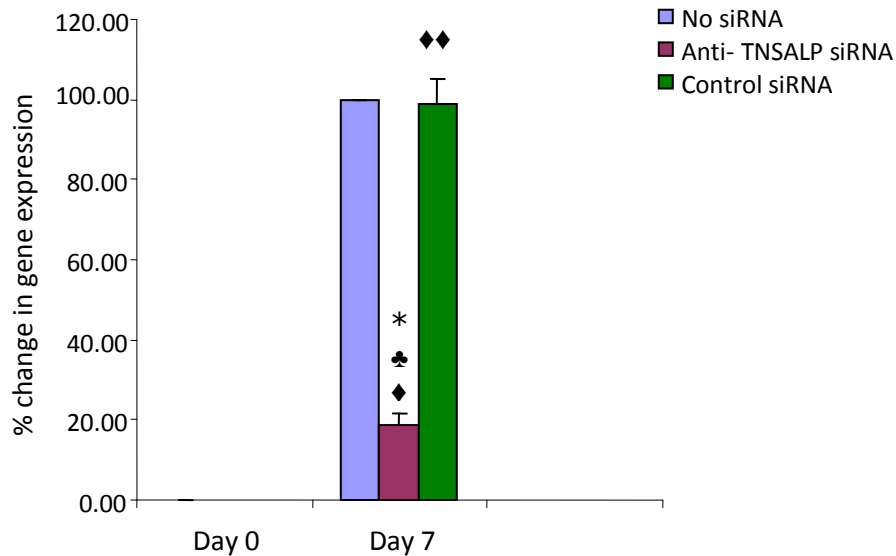


**Figure 4. 26** *TNSALP* gene expression in transfected 3T3-L1 cells 7 days post-transfection.

*Anti-ALP siRNA caused ~80% reduction in TNSALP gene expression on day 7 compared against control siRNA. The level of TNSALP gene expression in untransfected and control cells was not different. Data are mean  $\pm$  SEM; ◆ $p$ <0.05 vs Day 0; ◆◆ $p$ <0.005 vs Day 0; \* $p$ <0.05 vs No siRNA; ♣ $p$ <0.05 vs control siRNA.*

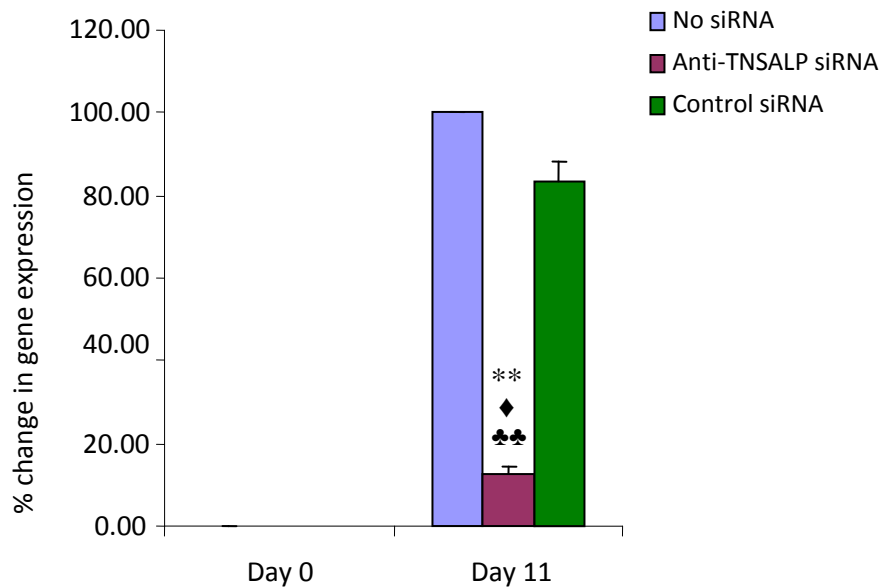


**Figure 4. 27** *TNSALP* gene expression in transfected 3T3-L1 cells 11 days post-transfection.

*Anti-ALP siRNA caused ~87% reduction in TNSALP gene expression on day 11 compared to control siRNA. The level of TNSALP gene expression in untransfected and control cells was not significantly different. Data are mean  $\pm$  SEM; ♦ $p < 0.05$  vs Day 0; ♦♦ $p < 0.005$  vs Day 0; \* $p < 0.05$  vs No siRNA; \*\* $p < 0.005$  vs No siRNA; ♣ $p < 0.05$  vs control; ♣♣ $p < 0.005$  vs control.*

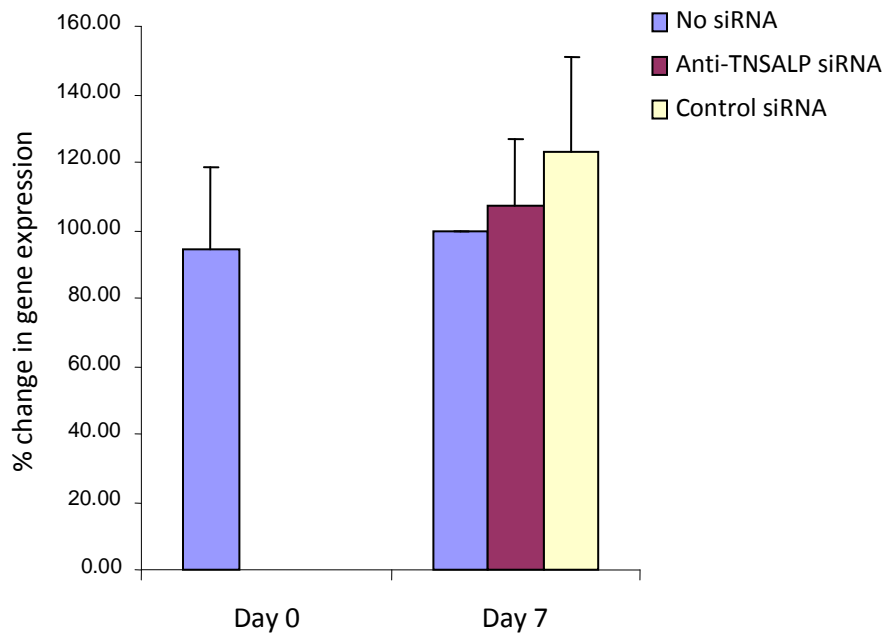


**Figure 4. 28** *TBP* gene expression in transfected 3T3-L1 cells 7 days post-transfection.

*No significant differences in expression of the TBP gene were seen on day 7 between untransfected cells and those transfected with either the control siRNA or anti-TNSALP siRNA. Data are mean  $\pm$  SEM.*

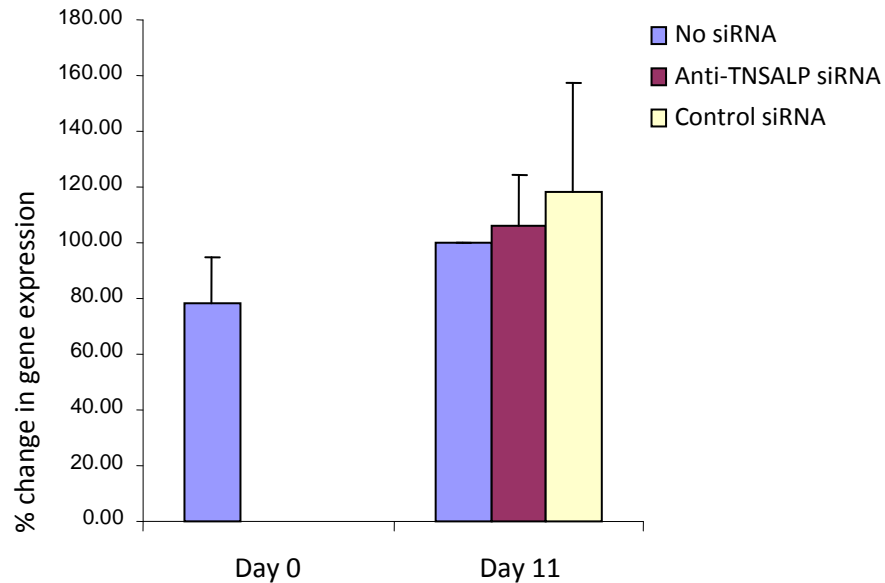


**Figure 4. 29** *TBP* gene expression in transfected 3T3-L1 cells 11 days post-transfection.

*No significant differences in expression of the TBP gene were seen on day 7 between untransfected cells and those transfected with either the control siRNA or anti-TNSALP siRNA. Data are mean  $\pm$  SEM.*

In the HepG2 cells ALP gene expression reached a maximum on day 4 and declined thereafter (data not shown). However, as with the 3T3-L1 cells no significant differences in the level of expression of the ALP gene could be observed due to the high SEM values. Therefore, the levels of expression of both the ALP and TBP genes were expressed as percentage values as described for the HepG2 cells.

In HepG2 cells, the percentage expression of the ALP gene increased from day 0 to 4 in untransfected cells. A significant decrease in ALP gene expression was observed on day 4 in cells transfected with the anti-ALP siRNA compared to untreated cells ( $p < 0.05$ , Fig.4.30). Compared to day 0, a significant increase in ALP gene expression was also observed on day 4 in cells treated with the control siRNA ( $p < 0.05$ , Fig.4.30). In contrast, no significant differences in ALP gene expression were observed between the cells transfected with the control siRNA and cells transfected with the anti-TNSALP siRNA on day 7 and 11 (Fig.4.31 & 4.42).

On day 4, the knockdown efficiency was  $80.0\% \pm 8.9$  between untransfected cells and those cells transfected with the anti-ALP siRNA. At the same time point the efficiency of knockdown was  $73.9\% \pm 15.7$  between HepG2 cells that were transfected with the control siRNA and those that were transfected with the anti-ALP siRNA. The expression of the *TBP* gene in HepG2 cells was not significantly influenced by any of the siRNAs (Fig.4.33, 4.34 & 4.35).

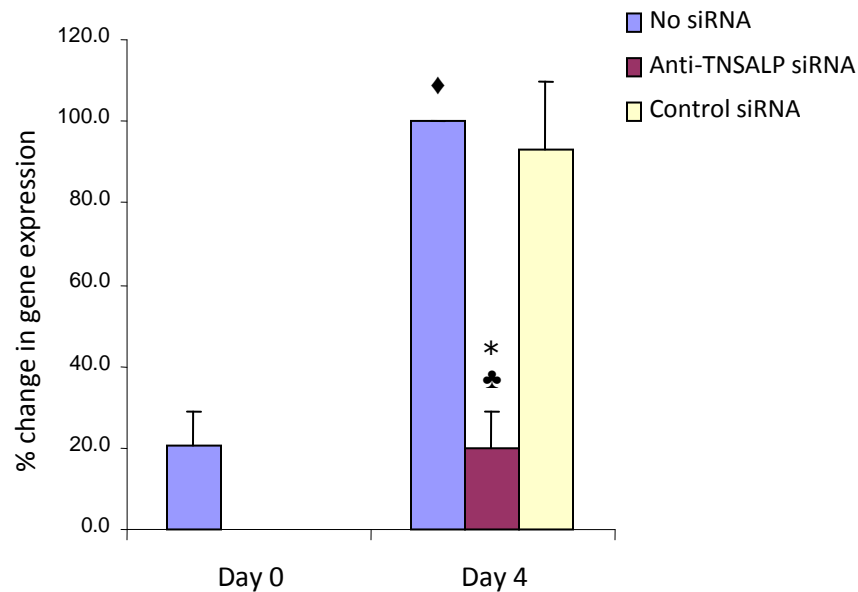


**Figure 4. 30** *TNSALP* gene expression in transfected HepG2 cells 4 days post-transfection.

*Anti-ALP siRNA* caused ~74% reduction in *TNSALP* gene expression on day 7 compared to control *siRNA*. The level of *TNSALP* gene expression in untransfected cells and cells transfected with control *siRNA* was not significantly different. Data are mean  $\pm$  SEM;  $\blacklozenge p < 0.05$  vs Day 0;  $*p < 0.05$  vs No *siRNA*;  $\clubsuit p < 0.05$  vs control *siRNA*.

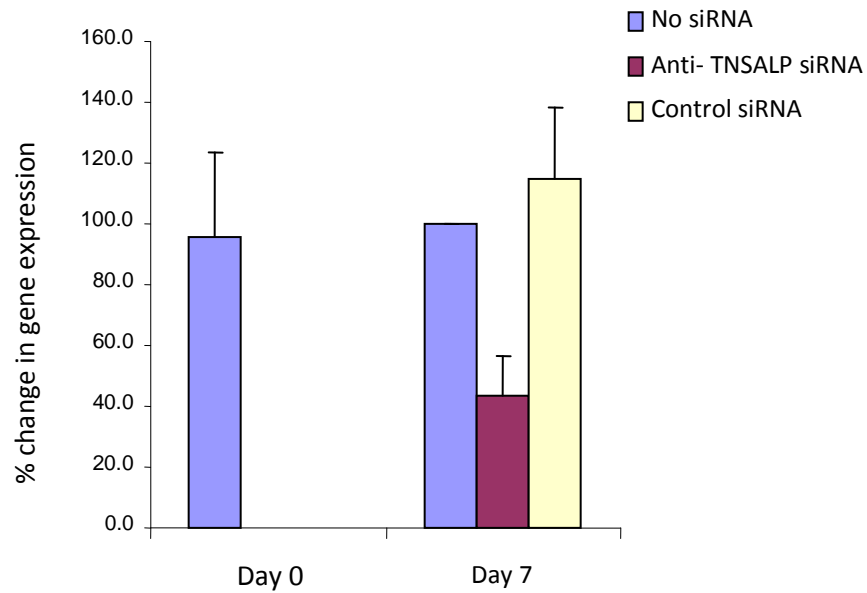


**Figure 4. 31** *TNSALP* gene expression in transfected HepG2 cells 7 days post-transfection.

*No significant differences in percentage change in gene expression were observed between cells transfected with anti-TNSALP siRNA and either untransfected cells or cells transfected with control siRNA on day 7. Data are mean  $\pm$  SEM.*



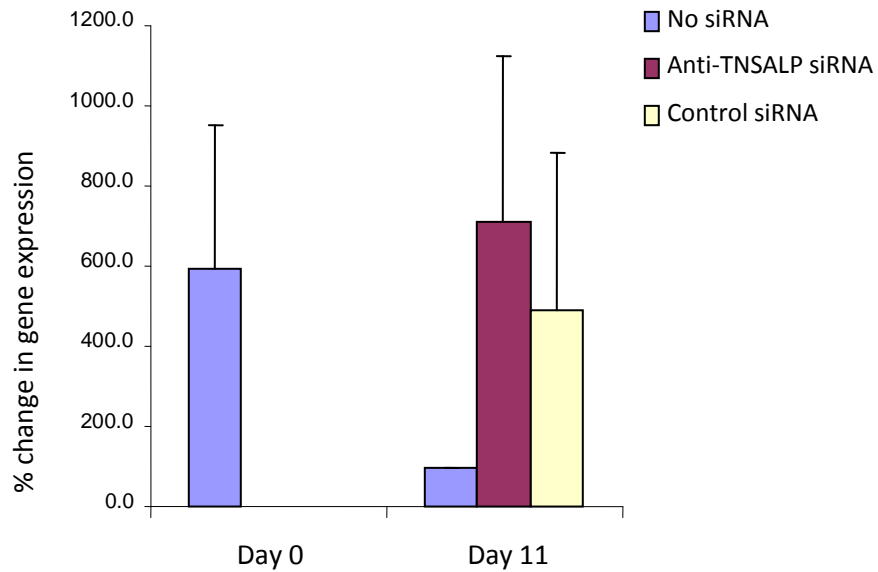


**Figure 4. 32** *TNSALP* gene expression in transfected HepG2 cells 11 days post-transfection.

*No significant differences in percentage change in gene expression were observed between cells transfected with anti-TNSALP siRNA and either untransfected cells or cells transfected with control siRNA on day 11. Data are mean  $\pm$  SEM.*

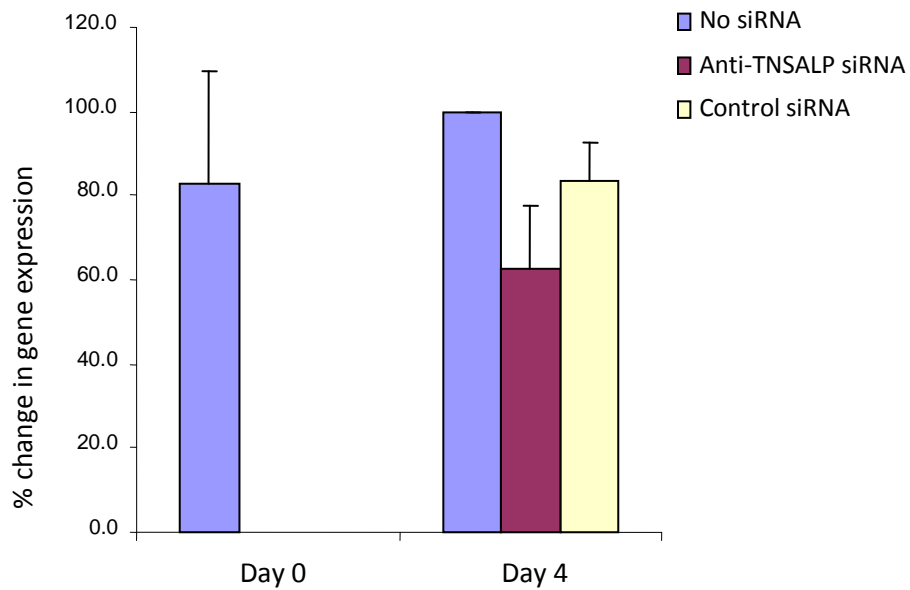


**Figure 4. 33** *TBP* gene expression in transfected HepG2 cells 4 days post-transfection.

*No significant differences in expression of the TBP gene were seen on day 4 between untransfected cells and those transfected with either the control siRNA or anti-TNSALP siRNA. Data are mean  $\pm$  SEM.*

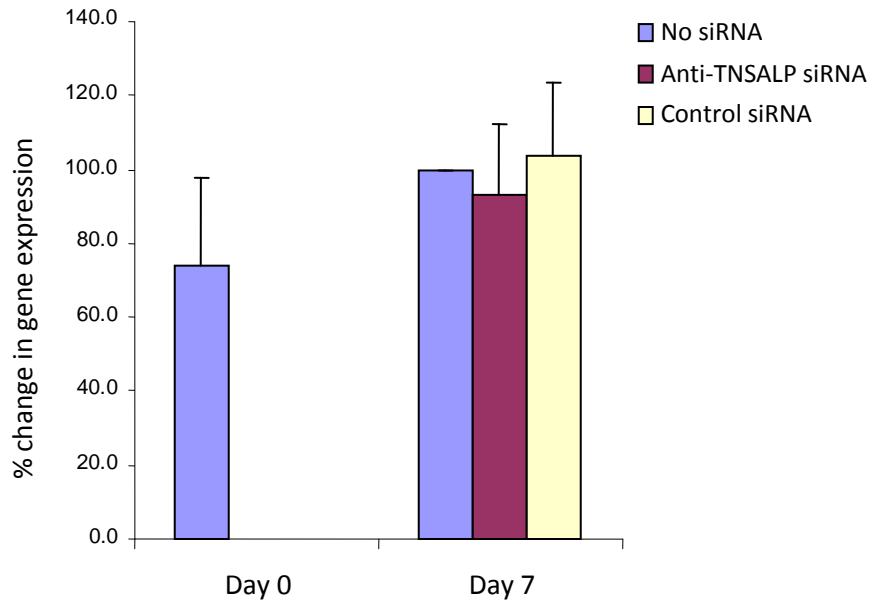


**Figure 4. 34** *TBP* gene expression in transfected HepG2 cells 7 days post-transfection.

*No significant differences in expression of the TBP gene were seen on day 7 between untransfected cells and those transfected with either the control siRNA or anti-TNSALP siRNA. Data are mean  $\pm$  SEM.*

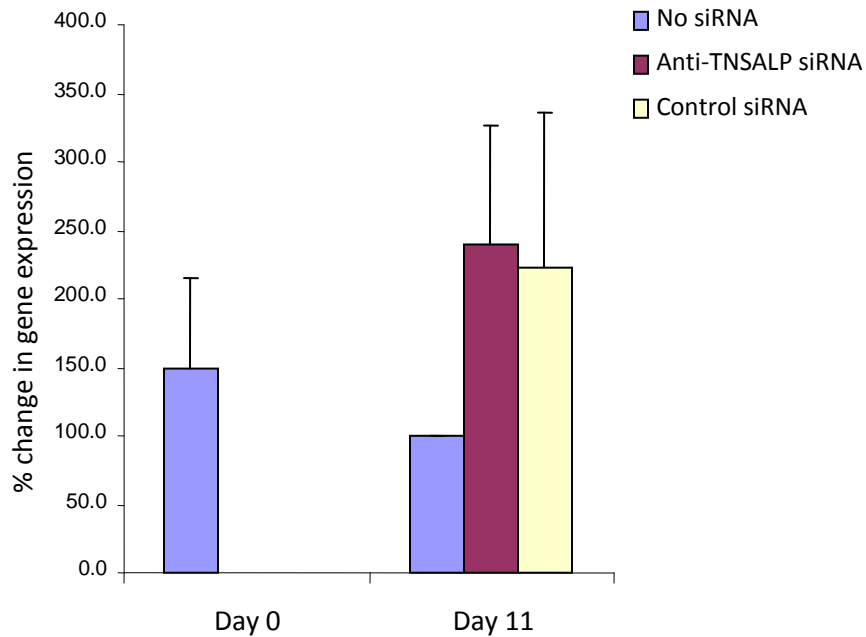


**Figure 4. 35** *TBP* gene expression in transfected HepG2 cells 11 days post-transfection.

*No significant differences in expression of the TBP gene were seen on day 11 between untransfected cells and those transfected with either the control siRNA or anti-TNSALP siRNA. Data are mean  $\pm$  SEM.*

#### 4.4.4 ALP activity in 3T3-L1 & HepG2 cells transfected with siRNA directed against *TNSALP* mRNA

In order to confirm if the knockdown of TNSALP gene worked, ALP activity was analyzed in cells transfected with anti-TNSALP siRNA, in cells transfected with control siRNA and in untransfected cells.

A five-fold higher level of ALP activity was observed in 3T3-L1 cells that were not treated with the siRNA for the *TNSALP* gene when compared to cells treated with the silencing siRNA on day 7. Similar results were observed in 3T3-L1 cells that were treated with the control siRNA (AllStars negative) compared to cells treated with the anti-TNSALP (silencing) siRNA. The differences in ALP activity on day 7 and 11 in cells transfected with the anti-ALP siRNA compared with the cells that were transfected with the negative siRNA and the untransfected cells were statistically significant ( $p < 0.05$ ; Fig.4.36). The activity of ALP in cells transfected with the control siRNA and in untreated cells on day 11 was significantly lower than on day 7 but were higher than the baseline levels [day 0] ( $p < 0.05$ ; Fig.4.36).

On day 4 ALP activity was four and half-fold higher in untransfected HepG2 cells and HepG2 cells treated with control siRNA when compared to cells treated with the anti-ALP siRNA (Fig.4.37). A significantly higher ALP activity was observed on day 4 ( $p < 0.05$ ; Fig.4.37) between untransfected cells and cells transfected with control siRNA compared with cells on day 0. On day 11, a significantly lower ALP activity ( $p < 0.05$ ; Fig.4.37) was observed in cells treated with anti-ALP siRNA compared to cells on day 0.

The differences in ALP activity between the cells transfected with the anti-ALP siRNA and the untreated cells (HepG2) were statistically significant on day 4, 7 and 11 ( $p < 0.05$ ). However, a statistically significant difference in ALP activity between cells transfected with the control siRNA and those transfected with the anti-ALP siRNA

was observed on day 4 only ( $p < 0.05$ ; Fig.4.37). In all the three types of treatments, ALP activity declined on day 7 and continued to do so until day 11 (Fig.4.36 & 4.37).

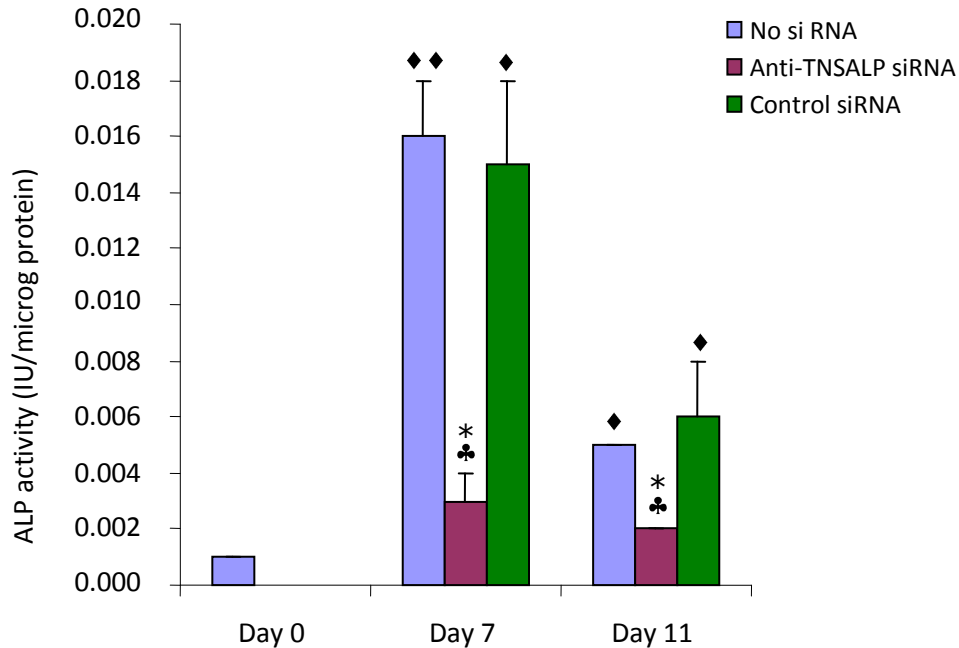


**Figure 4. 36** ALP activity in 3T3-L1 cells transfected with siRNA.

*A 5-fold reduction in ALP activity was seen on day 7 when anti-ALP transfected cells were compared to control cells. A 3-fold reduction was observed on day 11. Treatment with anti-ALP siRNA did not cause a significant increase in ALP activity from day 0. Data are mean  $\pm$  SEM' \* $p < 0.05$  vs untransfected cells;  $\blacklozenge p < 0.05$  vs day 0;  $\blacklozenge\blacklozenge p < 0.005$  vs day 0;  $\clubsuit p < 0.05$  vs control siRNA.*

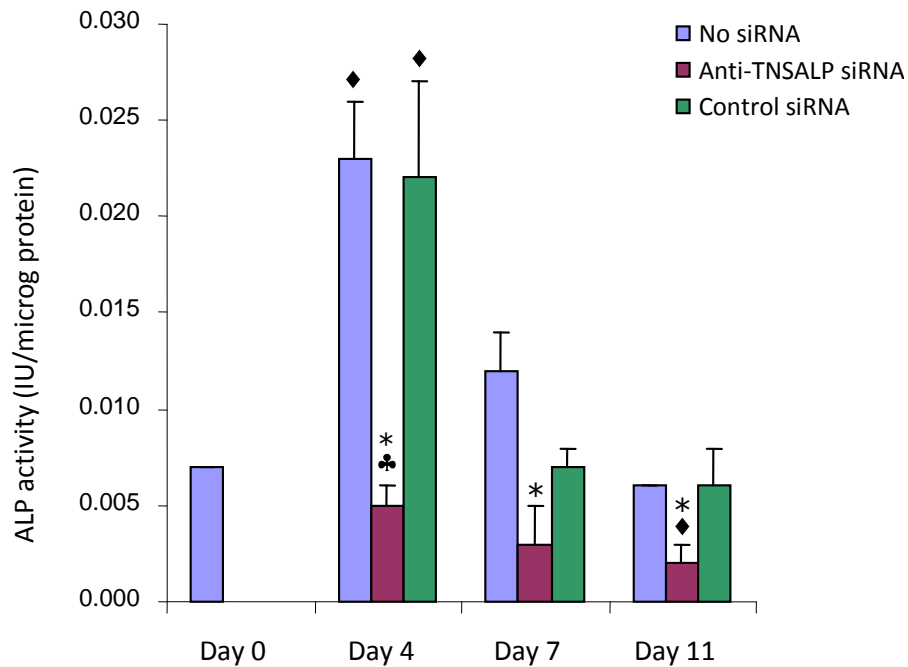


**Figure 4. 37** ALP activity in HepG2 cells transfected with siRNA.

*A 5-fold reduction in ALP activity was seen on day 4; a 2-fold reduction on day 7 and a 3-fold reduction on day 11 when anti-ALP transfected cells were compared to control cells. A significant increase in ALP activity from day 0 was observed only on day 11 in anti-TNSALP-treated cells. Data are mean  $\pm$  SEM; \* $p < 0.05$  vs untreated cells;  $\blacklozenge p < 0.05$  vs day 0;  $\blacklozenge\blacklozenge p < 0.005$  vs day 0;  $\clubsuit p < 0.05$  vs control siRNA.*

#### 4.4.5 Intracellular lipid droplet accumulation in 3T3-L1 & HepG2 cells transfected with siRNA directed against TNSALP mRNA

In order to demonstrate the effect that the transient silencing of the TNSALP gene had on lipid accumulation, HepG2 and 3T3-L1 cells were grown in medium to which the siRNA oligos were added. At confluency transformation cocktail was added to the cells as described in section 3.1.1 & 3.1.2.

In 3T3-L1 cells, intracellular lipid accumulation increased parallel to ALP activity in cells that were not treated with siRNA and in those that were treated with the control siRNA from day 0 to day 7. Unlike ALP activity, intracellular lipid accumulation continued to increase after day 7. Increases in lipid accumulation were statistically significant on day 7 ( $p < 0.005$ ) and day 11 ( $p < 0.05$ ) in cells transfected with the control siRNA or untreated cells compared to cells transfected with the anti-ALP siRNA (Fig.4.38). Significant increases in ALP activity were observed on day 7 and 11 in untreated cells and cells transfected with the control siRNA when compared to day 0 ( $p < 0.005$ ; Fig.4.38). A significant increase in ALP activity was also observed in cells transfected with the silencing siRNA compared to cells on day 0 ( $p < 0.05$ ; Fig.4.38). On day 7 and 11, cells transfected with the control siRNA showed a higher ALP activity than cells transfected with the anti-ALP siRNA ( $p < 0.05$ ; Fig.4.38).

In HepG2 cells, statistically significant differences in intracellular lipid accumulation were observed on day 7 ( $p < 0.05$ ; Fig.4.39) between cells treated with the anti-ALP siRNA and untreated cells. Untreated cells accumulated more intracellular lipid than cells transfected with the silencing siRNA. A similar difference



was also observed on day 11 ( $p < 0.005$ ; Fig.4.39). Statistically significant differences in intracellular lipid accumulation were also observed in cells transfected with the control siRNA compared to cells transfected with the anti-ALP siRNA on both day 7 ( $p < 0.05$ ) and 11 ( $p < 0.005$ ) [Fig.4.39].

Compared to cells on day 0, significant increases in intracellular lipid accumulation were observed on day 7 and 11 in cells transfected with the control siRNA and in untreated cells ( $p < 0.005$ ; Fig.4.39). In cells transfected with the anti-ALP siRNA a similar increase was observed on day 11 ( $p < 0.05$ ; Fig.4.39). Significantly higher intracellular lipid accumulation was observed in cells transfected with the control siRNA compared to cells transfected with the anti-ALP (silencing) siRNA on day 7 ( $p < 0.05$ ) and day 11 ( $p < 0.005$ ; Fig.4.39).

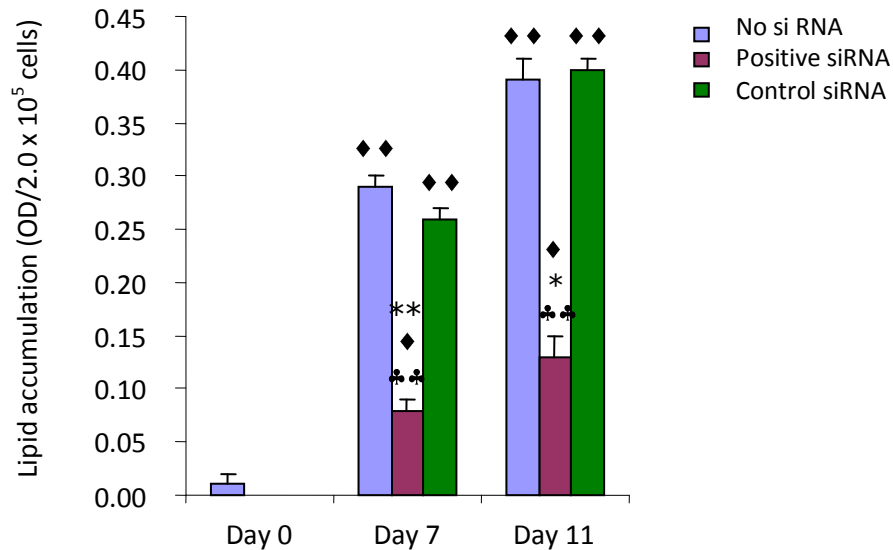


**Figure 4. 38** Intracellular lipid accumulation in 3T3-L1 cells transfected with anti- TNSALP siRNA oligos.

*On day 7 and 11, Anti-TNSALP treated cells accumulated 69 and 68% lower lipid levels respectively compared to control siRNA. On both day 7 and 11, significantly higher increases in lipid accumulation were observed between the three types of treatments and day 0. Data are mean  $\pm$  SEM; \* $p < 0.05$  vs untreated cells; ♦ $p < 0.05$  vs day 0; ♦♦ $p < 0.005$  vs day 0; ♣ $p < 0.05$  vs control siRNA; ♣♣ $p < 0.05$  vs control siRNA.*

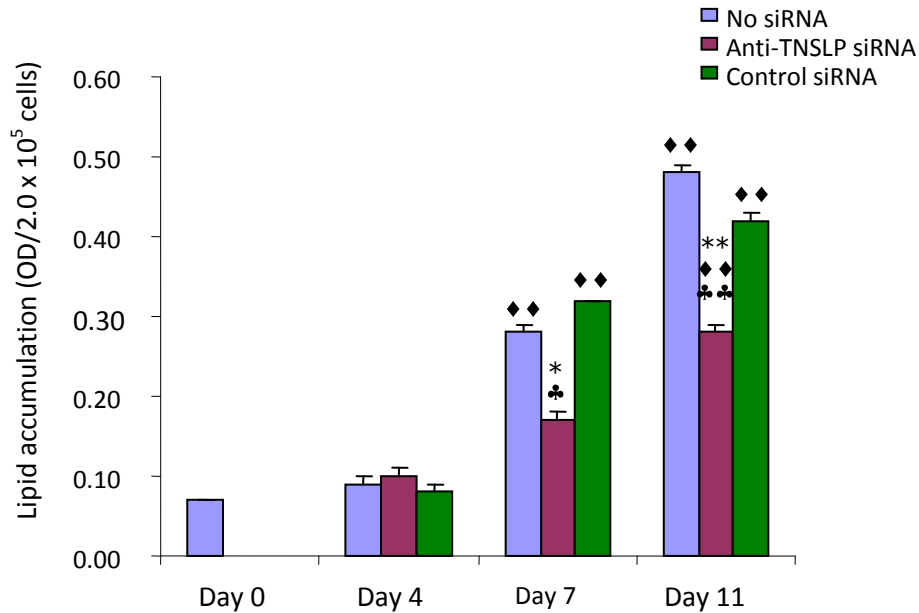


**Figure 4. 39** Intracellular lipid accumulation in HepG2 cells transfected with siRNA for *TNSALP* gene.

On day 7 and 11, Anti-TNSALP treated cells accumulated 40 and 34% lower lipid levels respectively compared to control siRNA. On both day 7 and 11, significant higher increases in lipid accumulation were observed between the three types of treatments and day 0. Data are mean  $\pm$  SEM; \* $p < 0.05$  vs untreated cells; ♦ $p < 0.05$  vs day 0; ♦♦ $p < 0.005$  vs day 0; ♣ $p < 0.05$  vs control siRNA; ♣♣ $p < 0.05$  vs control.

The inhibitory effect of the anti-ALP siRNA on intracellular lipid accumulation, as visualised using oil red O staining of the lipid droplets, in 3T3-L1 and HepG2 cells is shown in Fig. 4.40 & 4.41 respectively.

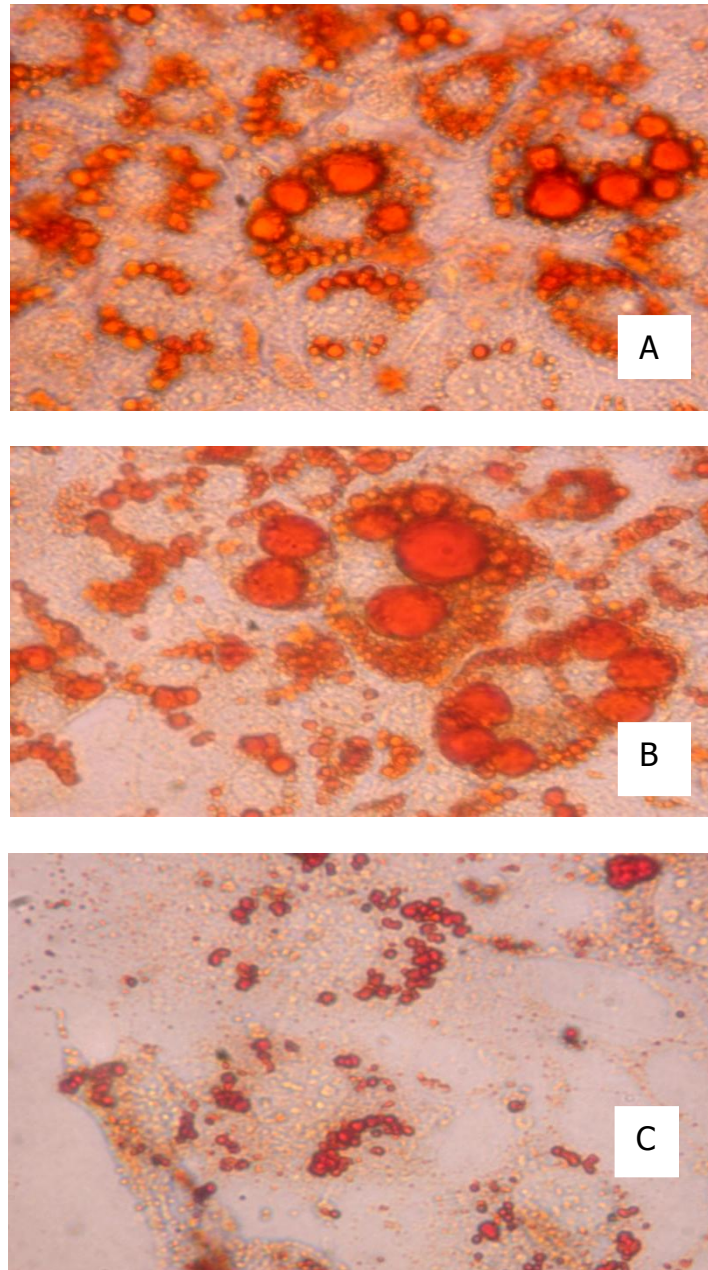


**Figure 4. 40** Oil Red O stain pictures of transfected 3T3-L1 cells.

*A - No siRNA, B - with control siRNA and C - with anti-ALP siRNA 11 days post-addition of transfection complexes (x 40 magnification). Reduced intracellular lipid droplet accumulation is observed in anti-ALP treated cells compared to control siRNA and untransfected cells. Cells were transfected post-confluency in culture medium containing transformation cocktail.*

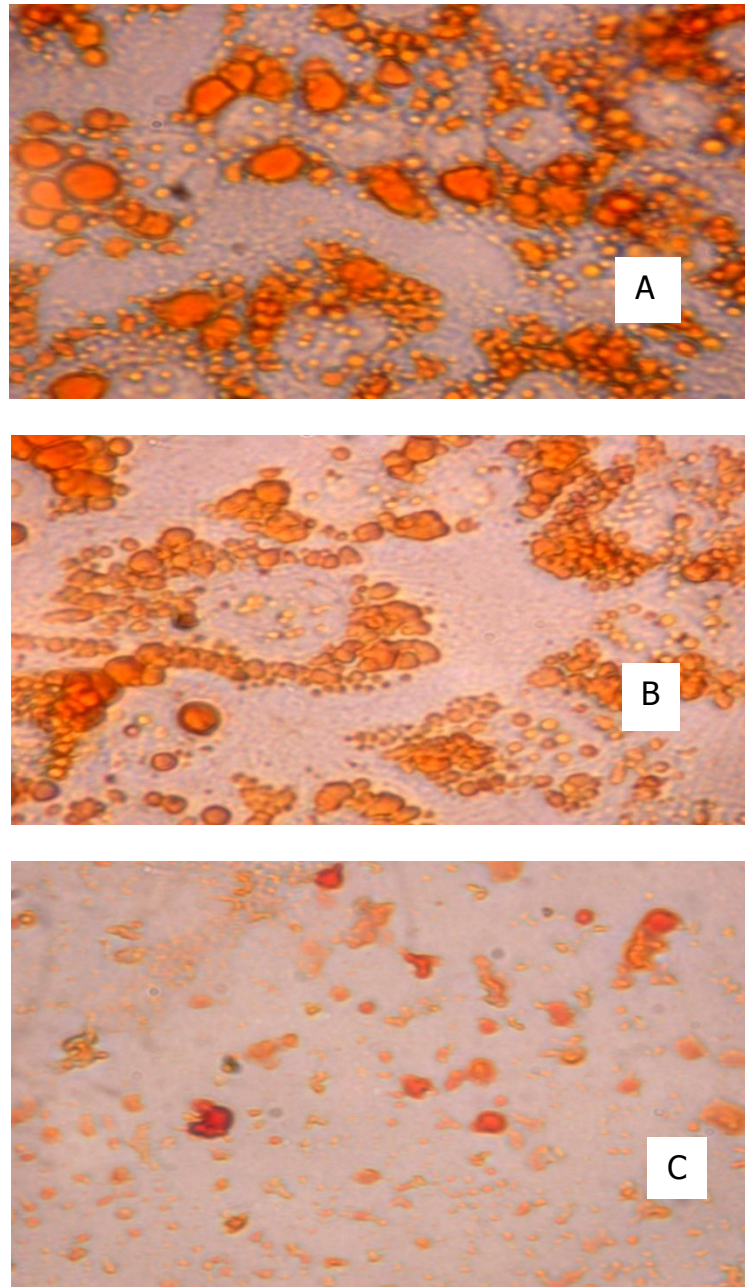


**Figure 4. 41** Oil Red O stain pictures of transfected HepG2 cells.

*A - No siRNA, B - with control siRNA and C - with anti-ALP siRNA 11 days post-addition of transfection complexes (x 40 magnification). Reduced intracellular lipid droplet accumulation is observed in anti-ALP treated cells compared to control siRNA and untransfected cells. Cells were transfected post-confluency in culture medium containing transformation cocktail.*

## 4.5 Subcellular localization of ALP in HepG2 & 3T3-L1 cells

### 4.5.1 Immunolabelling of perilipin and staining of ALP in 3T3-L1 cells

In order to show the localization of ALP activity within 3T3-L1 cells, transformed cells grown on a microscope cover slip were stained with ELF 97 phosphatase substrate having been immunolabelled for perilipin [Fig 4.42-4.46]. Alexa Fluor 594 goat conjugated anti-rabbit secondary antibody (red fluorescence) was used to locate the anti-perilipin antibody [Fig 4.42]. No fluorescence was visible in the primary antibody control, in which the secondary antibody was left out (Fig 4.43). Non-specific background staining was present in the secondary antibody control, in which the primary antibody was left out (Fig 4.44). Cleavage of ELF 97 phosphatase substrate by ALP produces a bright yellow/green colour when viewed using DAPI long pass filter [Fig 4.45]. The negative control for the ELF 97 substrate, which did not yield a signal, was produced by incubating cells with a known inhibitor of ALP (levamisole) [Fig 4.46B]. Levamisole had no effect on perilipin staining [Fig 4.46A].



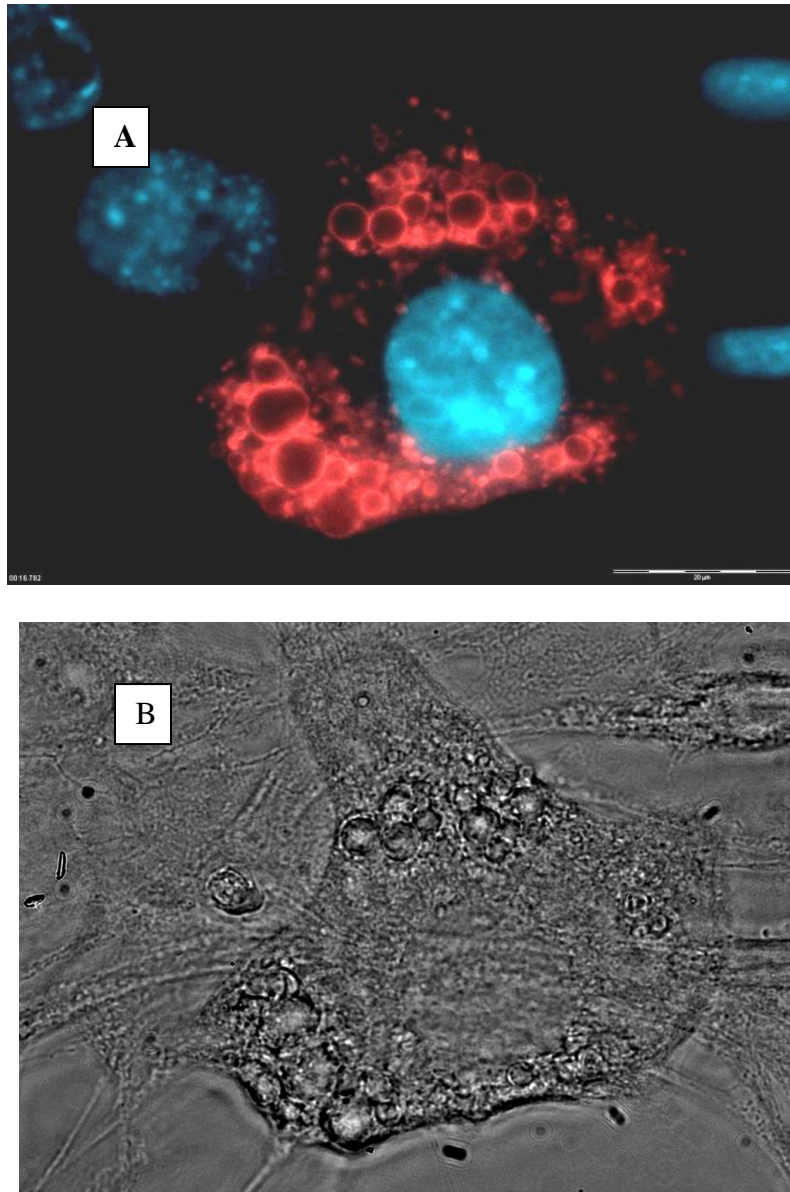


**Figure 4. 42** Immunolabelling of perilipin in 3T3-L1 cells.

*A- Staining of perilipin on the periphery of lipid droplet (red) using Alexa Fluor 594 goat conjugated anti-rabbit secondary antibody. Lipid droplets are seen intracytoplasmically. Cell nucleus was counterstained with DAPI (blue). B- Phase contrast image of cell shown in A. Scale bar =20μm. Original magnification x100.*

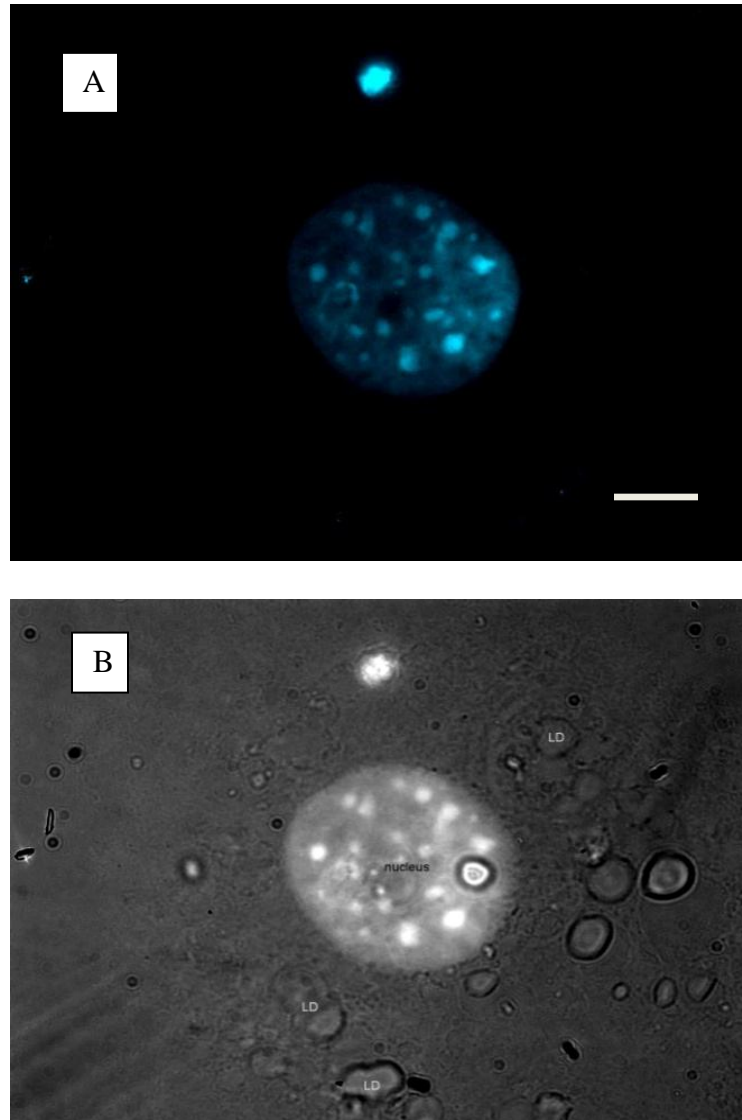


**Figure 4. 43** Primary antibody control in immunostaining of perilipin in 3T3-L1 cells.

*A - Cells were incubated with anti-perilipin antibody in the absence of the secondary antibody (Alexa Fluor 594 goat conjugated anti-rabbit secondary antibody). No fluorescence was visible. Cell nucleus was counterstained with DAPI (blue). B - Phase contrast image of cell shown in A. Scale bar =20 $\mu$ m. Original magnification x100.*



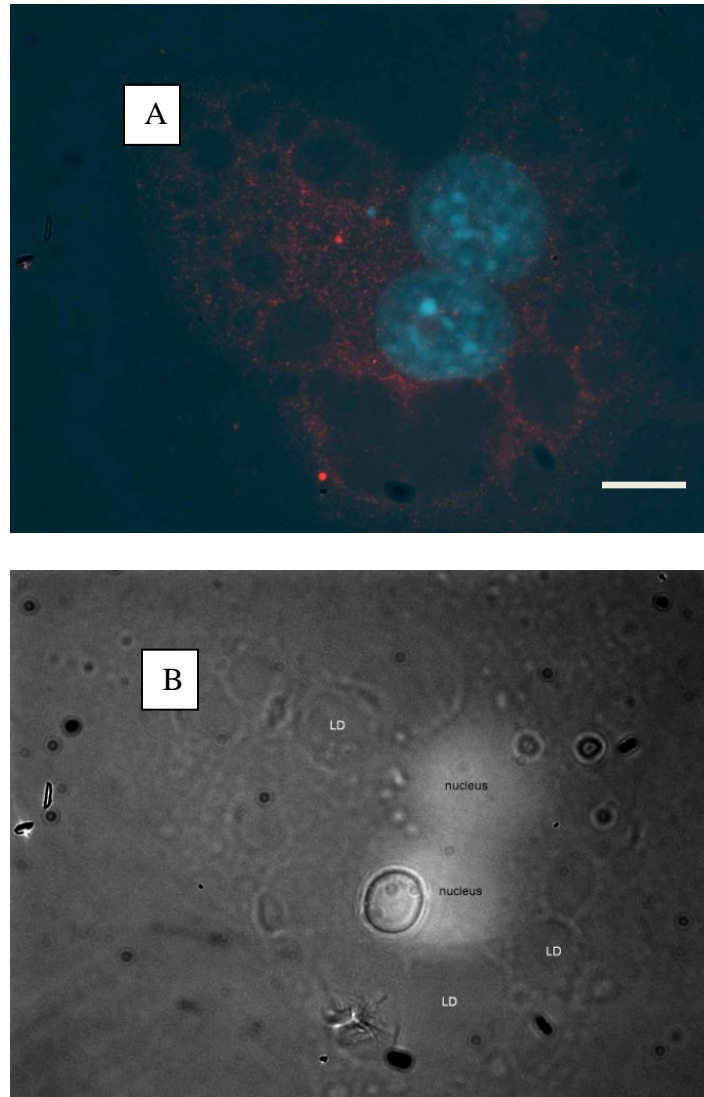


**Figure 4. 44** Secondary antibody control in immunostaining of perilipin in 3T3-L1 cells.

*A- Non specific background staining of the cytoplasm was noted for cells incubated with the secondary antibody (Alexa Fluor 594 goat conjugated anti-rabbit secondary antibody) in the absence of the anti-perilipin primary antibody. Note that no staining of the lipid droplet is visible. Cell nucleus was counterstained with DAPI (blue). B- Phase contrast image of cell shown in A. Scale bar =20 $\mu$ m. Original magnification x100.*

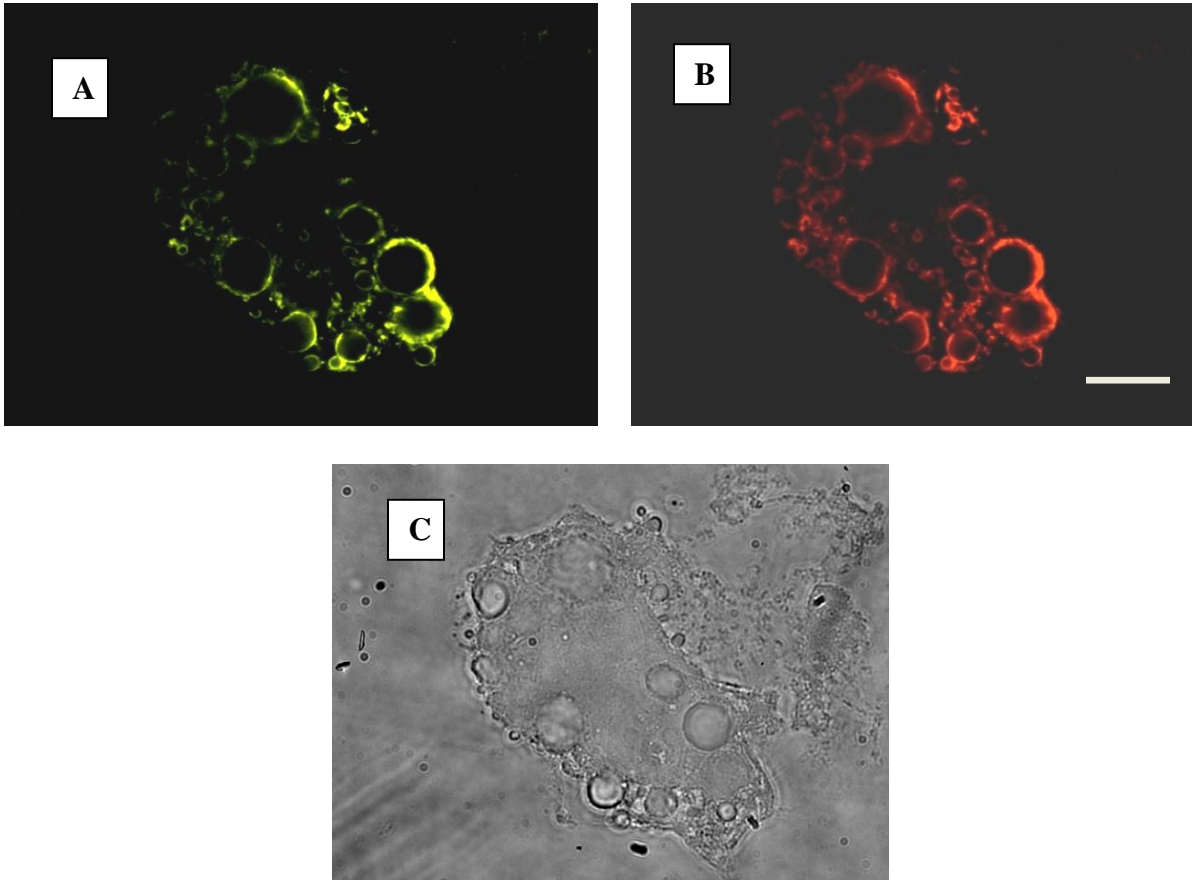


**Figure 4. 45** ELF 97 staining of ALP activity and immunostaining of perilipin in 3T3-L1 cells.

*A - Yellow/green staining of ALP activity captured using the DAPI long pass filter ( $A_{max}$  =345nm &  $E_{max}$ =455nm). B - Perilipin staining (Alexa Fluor 594 goat conjugated anti-rabbit secondary antibody). C - Phase contrast image of cell shown in A&B. Scale bar =20 $\mu$ m. Original magnification x100.*

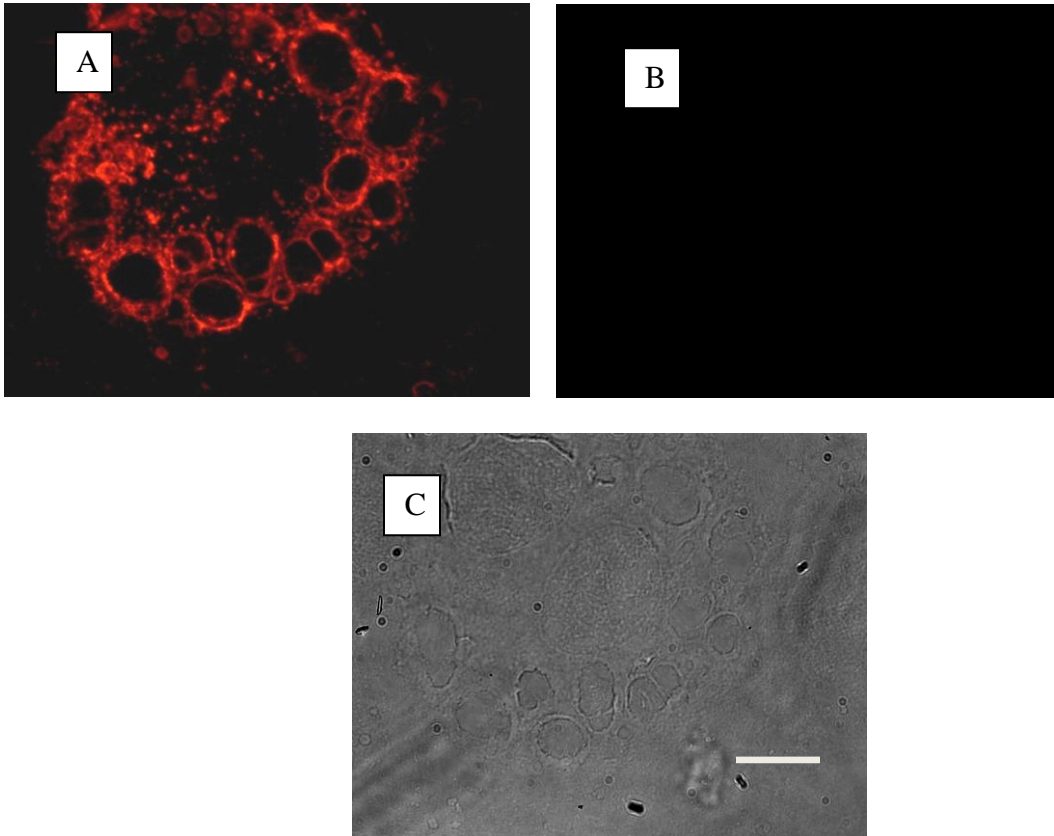


**Figure 4. 46** Control for ELF 97 staining of ALP activity and immunostaining of perilipin in 3T3-L1 cells.

*A - Perilipin staining (Alexa Fluor 594 goat conjugated anti-rabbit secondary antibody) and B - DAPI filter image after incubation with 7mM levamisole (inhibitor of ALP) for 1hour at room temperature. No ALP staining is visible in B. C - Phase contrast image of cell shown in A-B. Scale bar =20 $\mu$ m. Original magnification x100.*

#### 4.5.2 Immunolabelling of Adipose differentiation-related protein (ADRP) and staining of ALP in HepG2 cells

HepG2 cells were also immunolabeled for Adipose differentiation-related protein (ADRP) and stained for ALP [Fig 4.47-4.52].

Alexa Fluor 488 goat-coupled anti-guinea pig antibody (green fluorescence) was used to detect the primary anti-ADRP antibody [Fig 4.47]. No fluorescence was visible in the primary negative control (Fig 4.48). Non-specific background staining was present in the secondary antibody control (Fig 4.49). Cleavage of ELF 97 phosphatase substrate by ALP produces a bright yellow/green colour when viewed using a DAPI long pass filter [Fig 4.50]. The control for ELF 97 substrate, which did not yield a signal, was produced by incubating cells with a known inhibitor of ALP (levamisole) [Fig 4.51]. Non-transformed HepG2 cells were also stained for ALP and labelled for ADRP and neither ALP activity nor ADRP were visible [Fig 4.52].

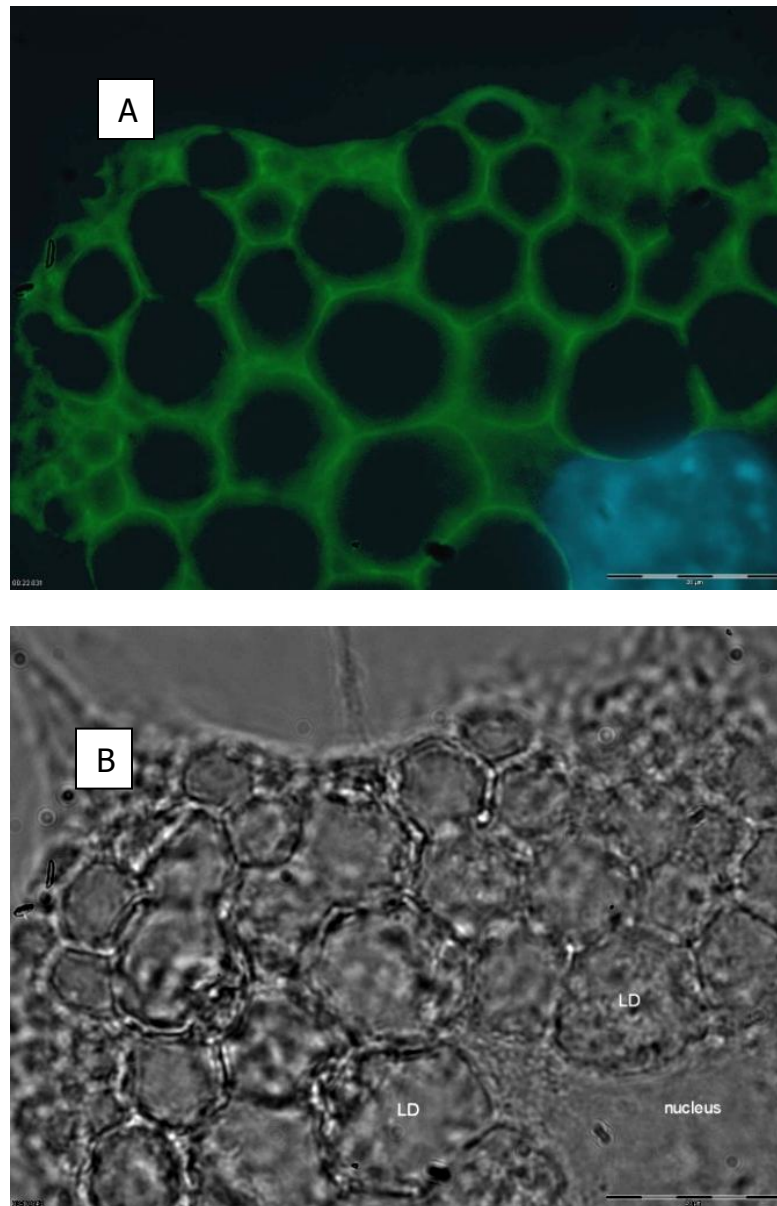


**Figure 4. 47** Immunolabelling of ADRP in HepG2 cells.

*A - Staining of ADRP on the periphery of lipid droplets (green) using Alexa Fluor 488 goat conjugated anti-guinea pig secondary antibody. Cell nucleus was counterstained with DAPI (blue). B - Phase contrast image of cell shown in A. LD= lipid droplet. Scale bar =20 $\mu$ m. Original magnification x100.*

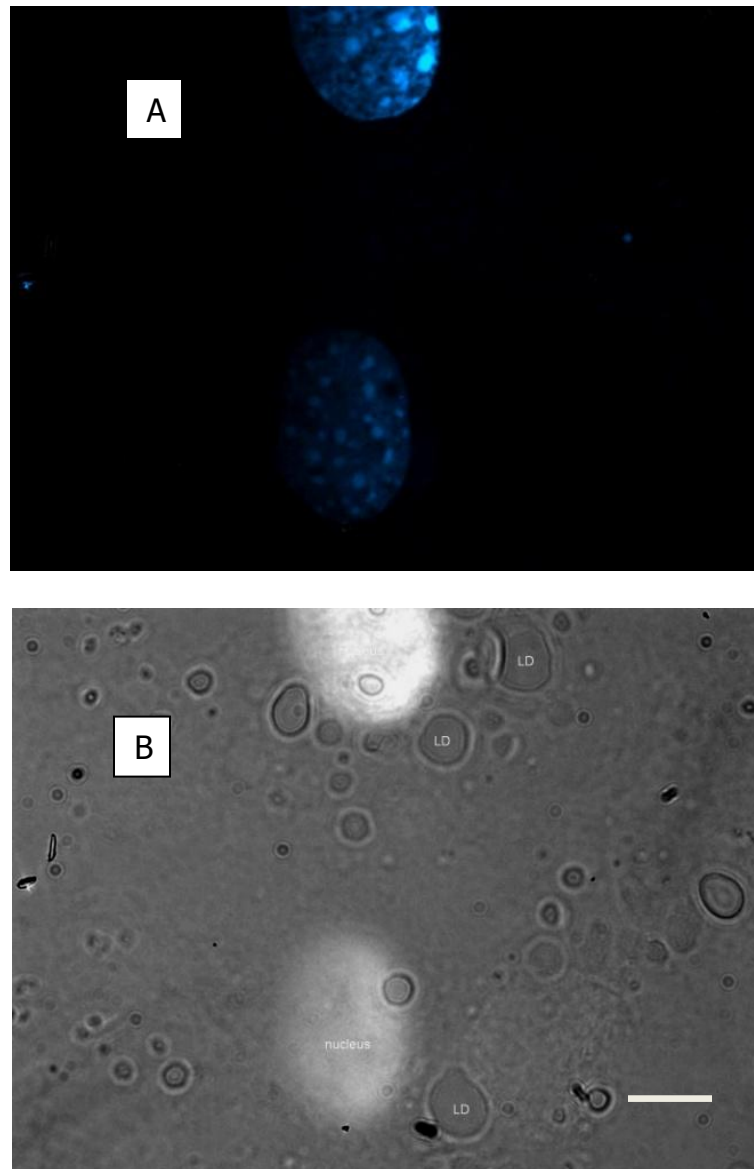


**Figure 4. 48** Primary antibody control in immunostaining of ADRP in HepG2 cells.

*A - Cells were incubated with anti-ADRP antibody in the absence of the secondary antibody (Alexa Fluor 488 goat conjugated anti-guinea pig secondary antibody). Fluorescence was not present. Cell nucleus was counterstained with DAPI (blue). B - Phase contrast image of cell shown in A. LD= lipid droplet. Scale bar =20 $\mu$ m. Original magnification x100.*

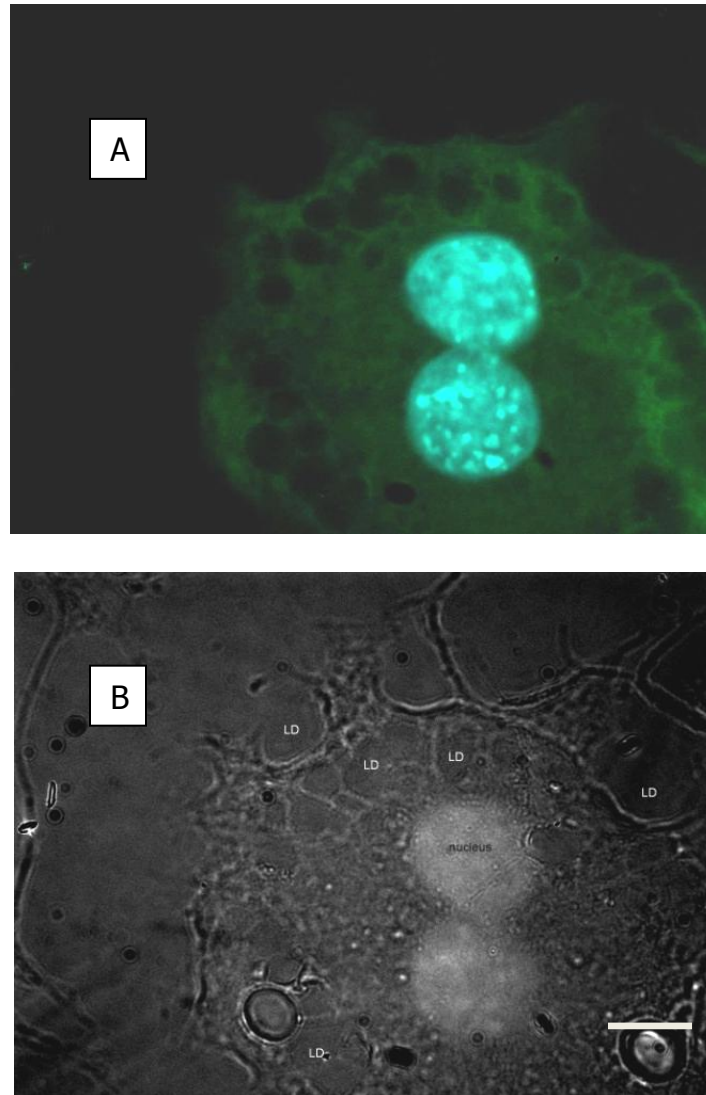


**Figure 4. 49** Secondary antibody control in immunostaining of ADRP in HepG2 cells.

*A – Non-specific background staining of cells incubated with the secondary antibody (Alexa Fluor 488 goat conjugated anti-guinea pig secondary antibody) in the absence of the anti-ADRP primary antibody. Staining is cytoplasmic. Cell nucleus was counterstained with DAPI (blue). B - Phase contrast image of cell shown in A . LD = lipid droplet. Scale bar =20 $\mu$ m. Original magnification x100.*



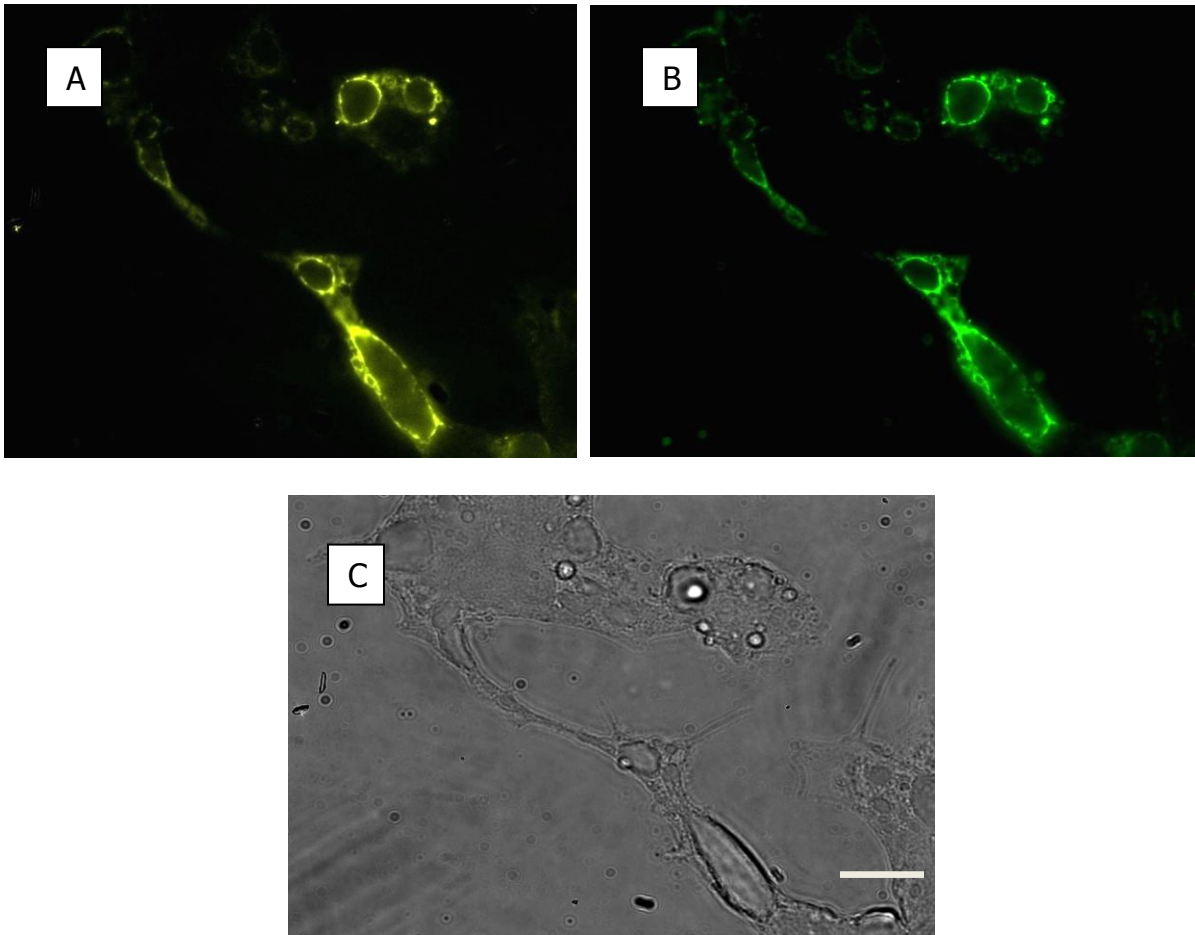


**Figure 4. 50** ELF 97 staining of ALP activity and immunostaining of ADRP in HepG2 cells.

*A - Yellow green staining of ALP activity captured using the DAPI long pass filter ( $A_{max}$  =345nm &  $E_{max}$ =455nm). B - ADRP staining (Alexa Fluor 488 goat conjugated anti-guinea pig secondary antibody). C - Phase contrast image of cell shown in A-B. Scale bar =20 $\mu$ m.*

*Original magnification x100.*



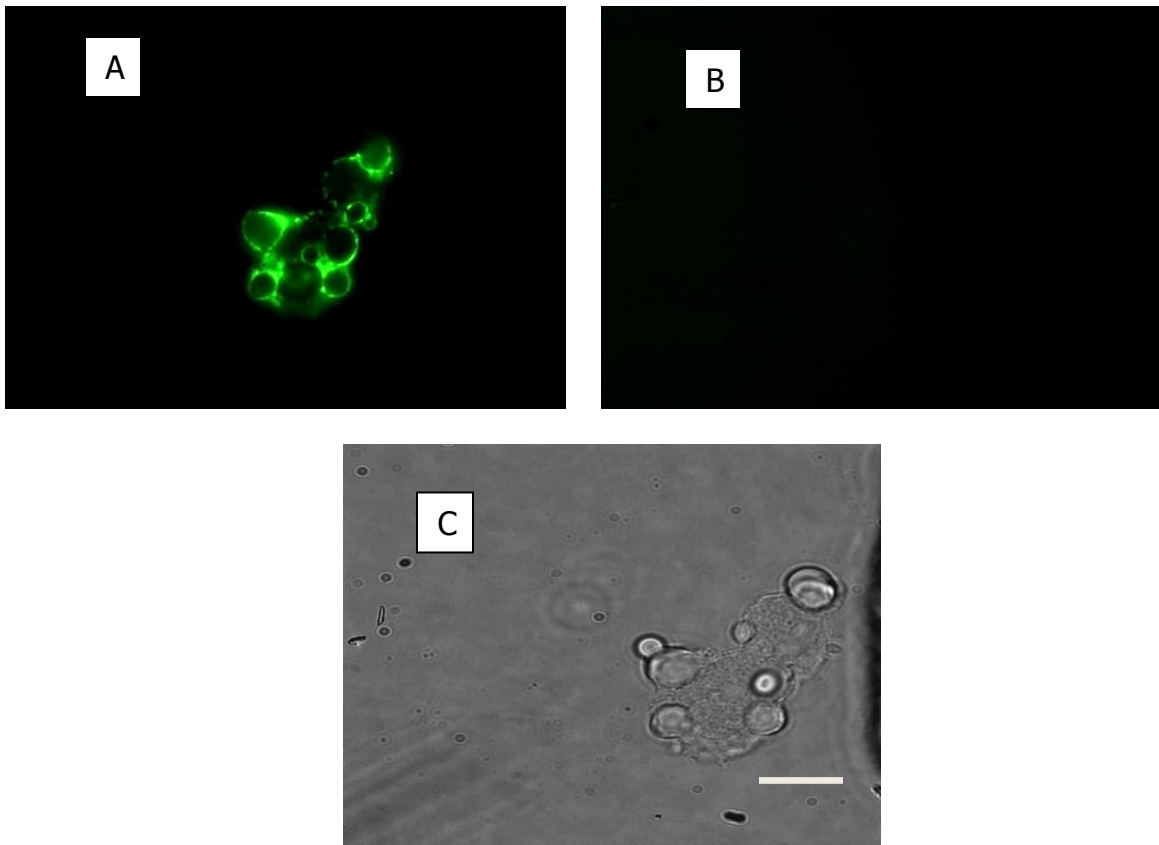


**Figure 4. 51** Control for ELF 97 staining of ALP activity and immunostaining of ADRP in HepG2 cells.

*A - ADRP staining (Alexa Fluor 488 goat conjugated anti-guinea pig secondary antibody). B - DAPI filter image after incubation with 7mM levamisole (inhibitor of ALP) for 1 hour at room temperature. C - Phase contrast image of cell shown in A-B. Scale bar =20 $\mu$ m. Original magnification x100.*

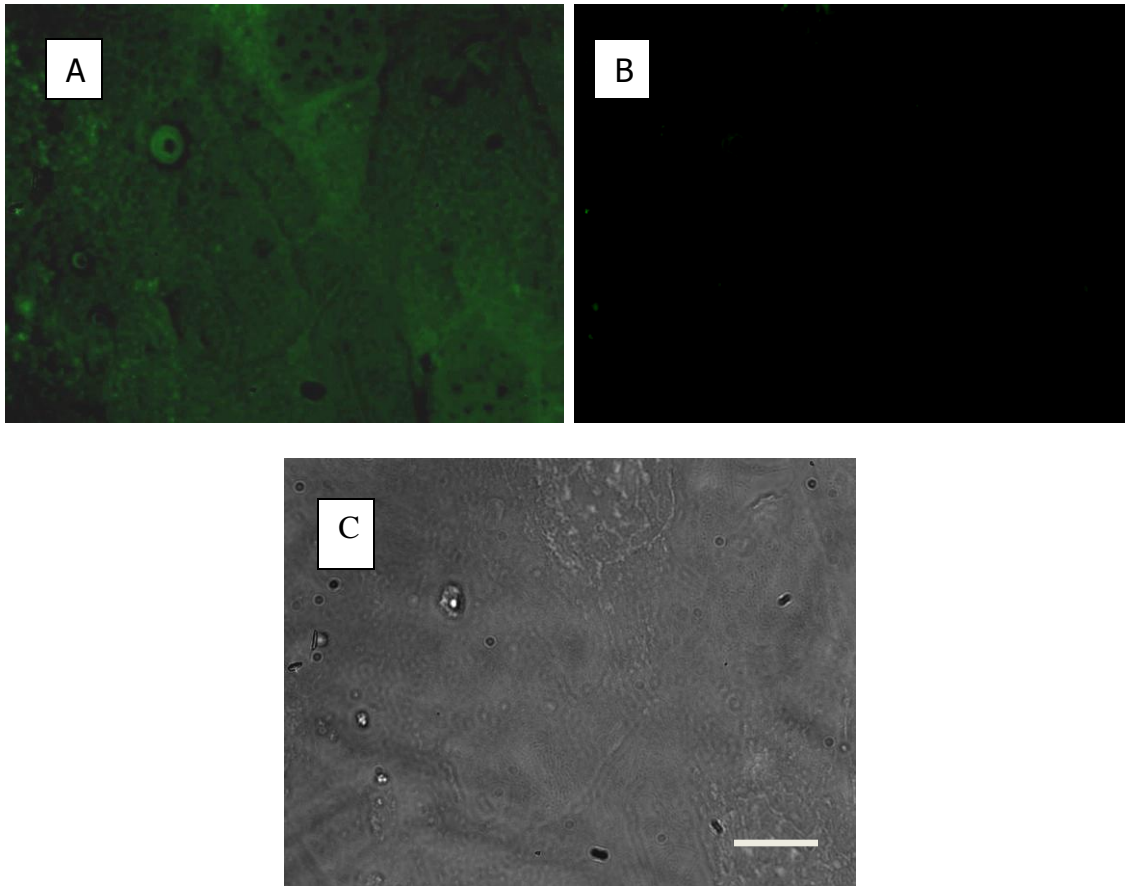


**Figure 4. 52** ELF 97 ALP staining and ADRP labeling in non-transformed HepG2 cells.

*A - Non specific background staining due to Alexa Fluor 488 goat conjugated anti-guinea pig secondary antibody. B - ALP activity staining was not present. C - Phase contrast image of cell shown in A. Scale bar =20 $\mu$ m. Original magnification x100.*

#### 4.6 Single nucleotide polymorphisms in the promoter region of the human *TNSALP* gene

The profound difference in pre-adipocyte ALP activity observed between white and black South African females (Ali *et al.* 2006) suggested that either the catalytic activity or the level of expression of the enzyme was much higher in the latter group.

It was therefore decided to analyse the promoter region of the ALP gene to determine if genomic sequence variation existed between the 2 ethnic groups.

Three important motifs to which specific transcription elements (Sp1, the RARE and Dlx 5 binding *cis*-element) bind have been described in the promoter region of the human TNSALP gene (Weiss *et al.* 1988). These motifs are scattered across the promoter region, so the whole promoter region was therefore sequenced to search for any nucleotide base changes that could play a role in regulating the rate of transcription. Seven sets of overlapping PCR primers were used to amplify the promoter region of the human TNSALP gene.

#### 4.6.1 Optimized PCR conditions and gel electrophoresis of PCR products

By changing one or several PCR parameters, conditions described in Table 3.15 and 3.16 were found optimal in amplifying the promoter region. An agarose gel image of PCR products after electrophoresis is shown in Fig. 4.53 below. All PCR products corresponded to the predicted PCR product sizes.

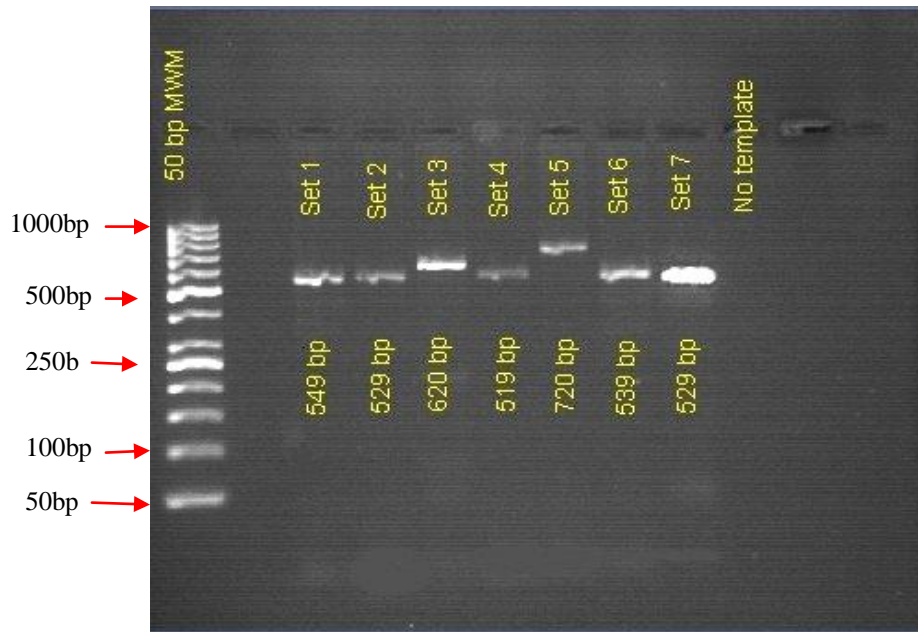


**Figure 4. 53** Agarose gel image of PCR products for the 7 sets of primers (S1-S7) used to amplify the promoter region of the human *TNSALP* gene.

*PCR products were separated on a 2% agarose gel stained with ethidium bromide. A 50bp MWM was used to size the PCR amplicons. Sizes of the molecular weight marker (MWM) are shown on the left hand side of the gel. No template is the negative control. PCR primer location on the gene is shown in Appendix I.*

#### 4.6.2 Sequencing of PCR products

Sequence results of the seven fragments of PCR products for each of the 12 subjects were aligned and compared with the reference sequence using Sequencher 4.7. No single nucleotide base changes were identified in the sequenced strands. Below is a chromatogram of one of the sequenced samples (Fig. 4.54).

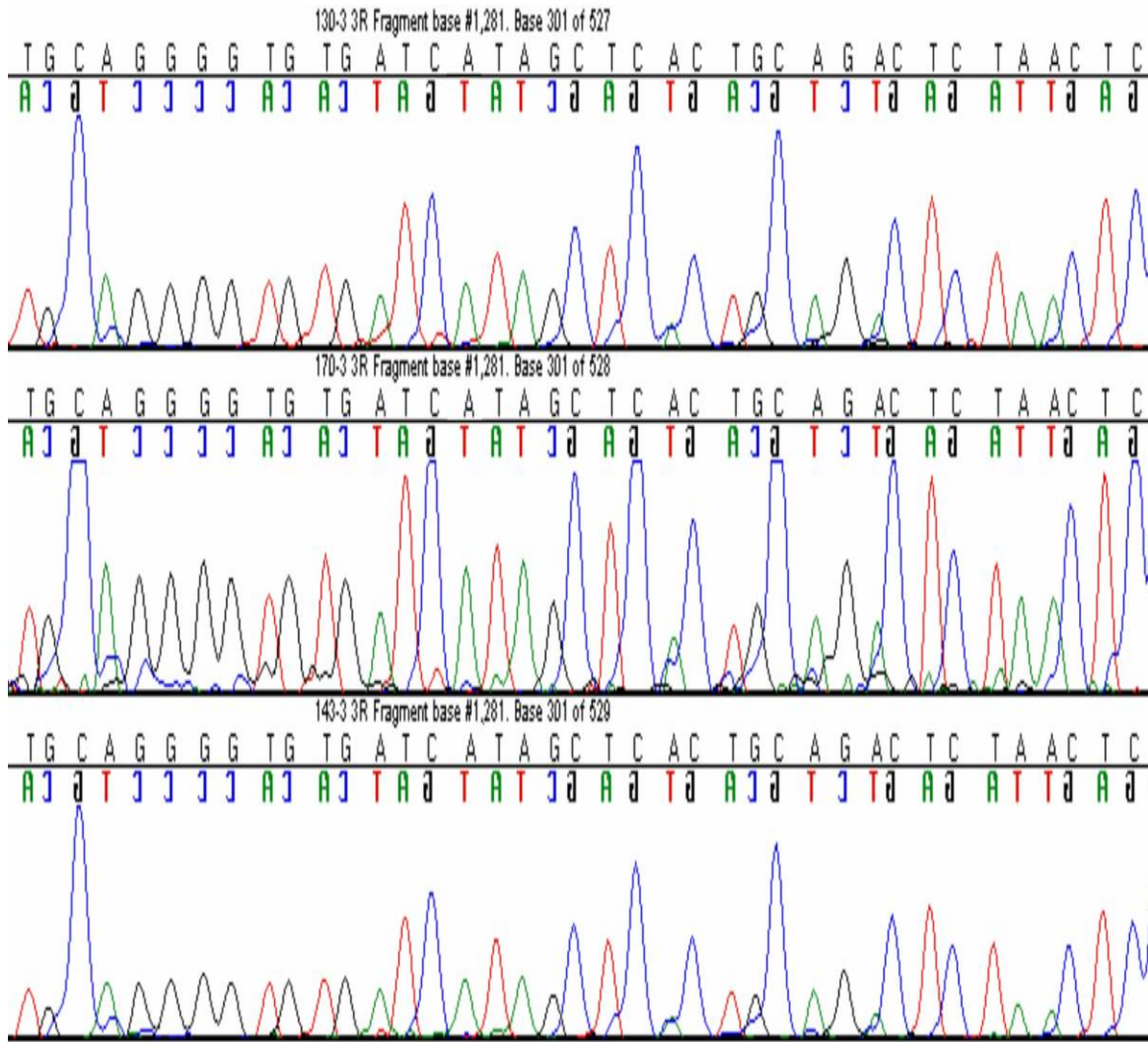


**Figure 4. 54** Chromatogram of a sequenced PCR product (genomic DNA as a template) using PCR primer set 3.

*No nucleotide base changes were identified when the sequenced strands were aligned with a Gene Bank reference sequence.*

# **CHAPTER FIVE**

## **DISCUSSION**

## 5.0 Introduction

Obesity is defined as a state of increased body fat tissue mass that arises from an imbalance between energy intake and expenditure. It is associated with increased fat cell size and number. An increase in fat cell number appears to correlate well with severity of human obesity even in late adult life (Hirsch and Batchelor 1976). Debate about whether obesity should be called a disease or simply a condition continues. The authors of one paper argue that because "obesity has a known aetiology and pathogenesis, it meets the criteria required to call it a disease" (Bray 2004). The prevalence of obesity is increasing worldwide and is known to be a major risk factor for type 2 diabetes, cardiovascular diseases and a number of many other disorders (Flegal *et al.* 2005). It is therefore, not surprising that over the past decade there has been an upsurge of knowledge about adipocyte biology mainly focusing on the factors and mechanisms that influence adipocyte determination and differentiation (Ruesch and Klem 1994; Gregoire *et al.* 1998; Fajas *et al.* 2001).

Ali *et al.* (2006) reported for the first time that ALP plays a role in the control of adipogenesis in the murine preadipocyte cell line, 3T3-L1 and in human preadipocytes and it was therefore suggested by the authors that this enzyme may be a prime candidate for the future development of therapeutic interventions for obesity and its related diseases.

The present study demonstrates that ALP that is expressed in a human hepatocarcinoma derived cell line (HepG2) plays a role in intracellular lipid accumulation.

This study also sheds more light on the characterization of the role that ALP plays in adipogenesis or lipid accumulation in both the 3T3-L1 and HepG2 cells in terms of determining the spatial relationship of ALP activity with the lipid droplets, studying the relationship between the expression of PPAR $\gamma$  gene with the progression of lipid droplet accumulation and determining the effects of inhibiting or blocking ALP activity on intracellular lipid accumulation in the two cell types.

### 5.1 ALP activity and intracellular lipid droplet accumulation in 3T3-L1 and HepG2 cells

The major morphological change that occurs during adipogenesis is intracellular lipid accumulation. This is preceded by characteristic changes in cell shapes from a more spindle-like shape into a circular shape that enables the cells to store the maximal amount of lipid (Smas and Sul 1995). The distinct shapes result from the rearrangements of the various cytoskeletal components inside the cell including microtubules and intermediate filaments (Chisholm 2002).

This study has shown for the first time that the ALP expressed in HepG2 cells plays a role in the formation of intracellular lipid droplets. It has been previously reported that the main ALP produced by HepG2 cells is the TNSALP (Nowrouzi and Yazdanparast 2005).

ALP activity increased parallel to lipid droplet accumulation in both 3T3-L1 and HepG2 cells. In 3T3-L1 cells ALP activity increased from day 0 (baseline) to day 7 and declined on day 11 post-induction of transformation. In HepG2 cells, the decline in ALP activity was earlier than in 3T3-L1 cells, that is day 4 post-induction of lipid droplet



accumulation. In both cell lines intracellular lipid accumulation continued to increase from day 0 to day 11.

ALP activity on day 0 (before induction of lipid droplet formation) was higher in HepG2 than in 3T3-L1 cells. This may be due to the fact that the HepG2 cells are terminally differentiated whilst 3T3-L1 cells are “immature” adipocytes. With differentiation, the level of ALP activity in the 3T3-L1 cells increases to levels similar to those seen in the HepG2 cells.

In the conversion of preadipocytes into adipocytes it seems that ALP is required at a later stage of this metabolic process and maybe involved in the initiation of lipid accumulation within the membrane-bound lipid droplet. Other genes have also been reported to be temporarily up-regulated when preadipocytes are induced to accumulate lipids *in vitro* and include: c-fos, c-jun, c-myc and C/EBP $\alpha$  and  $\delta$  (Cornelius *et al.* 1994), C/EBP $\alpha$  and PPAR $\gamma$  (Gregoire *et al.* 1998). Most of these peptides are transcription factors that induce adipogenesis and precede the expression of the genes that characterise a cell as a mature adipocyte.

Once pre-adipocytes are induced to accumulate lipids *in vitro*, the process is irreversible and the lipid droplets continue to increase in size even when the pro-differentiation medium is withdrawn. One study reported a high ALP activity in the small, multilobular pre-adipocytes isolated from human bone marrow but absent from the large, unilobular mature adipocytes (Bianco *et al.* 1988). It could therefore be hypothesised that in humans ALP is important only during the final stages of adipogenesis and is not required for mature adipocyte function.

This may explain the decrease in ALP activity after day 4 in HepG2 cells and day 7 in 3T3-L1 cells but an increase in lipid accumulation up to day 11 of the experiment. This would suggest that addition of ALP inhibitors after day 4 in HepG2 and day 7 in 3T3-L1 cells would have minimal or no effect on lipid accumulation compared to addition before these time points. The time course of ALP expression and its subcellular location suggest that it may be important in the initiation of lipid droplet formation but is not required for maintenance of the lipid droplet.

In normal physiology, it is possible that hepatocytes tend to 'protect' themselves from accumulating excessive intracellular lipids in order to maintain the fine cellular ultrastructure that is crucial to the many important biochemical pathways taking place in liver cells. This might be the reason why the ALP gene is downregulated earlier in HepG2 than in 3T3-L1 cells during the adipogenic process. Also, the adipose cells being the cells dedicated to fat storage and metabolism may have a better capacity to accumulate intracellular lipids than HepG2 cells.

In terms of lipid droplet size, 3T3-L1 cells accumulated bigger droplets than HepG2 cells. As the lipid droplets formed, they tended to coalesce into bigger structures often unilocular and formed a better defined ring shape in the cytoplasm (around the nucleus) in 3T3-L1 than in HepG2 cells. The characteristic change in cell shape observed in 3T3-L1 cells as they accumulated intracellular lipid (rounding up) was not observed in HepG2 cells. It is not yet clear if the differences observed could be due to the differences in the regimen used for inducing intracellular lipid formation in the two cell types.

To my knowledge, there are no reports of the use of transformation cocktails containing hormones such as insulin to stimulate lipid droplet accumulation in HepG2 cells *in vitro*. It would be worthwhile to study the liver ALP activity pattern in rodent models of NASH and find out if ALP is involved in the pathophysiology of the disease.

The possible mechanisms where TNSALP may be involved in intracellular accumulation of neutral lipids in some lipid-storing cells is discussed further in section 5.4.1.

5.2            Pharmacological inhibition of ALP activity blocks intracellular lipid accumulation in HepG2 cells and adipogenesis in 3T3-L1 cells.

Ali *et al.* (2003) showed that the ALP isoenzyme that is inhibited by levamisole and histidine but not Phe-Gly-Gly is expressed in the 3T3-L1 cells. This property is characteristic of the murine TNSALP isoenzyme (Ohkubo *et al.* 2000). The human TNSALP isoenzyme, shares 90% amino acid sequence homology with the murine TNSALP isoenzyme (Terao and Mintz 1987). Ali *et al.* (2003) reported in the same study that inhibition of ALP with histidine reduced intracellular lipid accumulation in 3T3-L1 cells and in human preadipocytes while levamisole inhibited ALP activity and intracellular lipid accumulation in 3T3-L1 cells but not in isolated human preadipocytes.

The present study has shown the inhibition of ALP activity by histidine and levamisole in HepG2 cells. Intracellular lipid droplet accumulation in HepG2 cells was significantly reduced by the two inhibitors.

At the concentrations used in this study, histidine showed a stronger inhibitory effect on ALP activity and a correspondingly greater reduction in intracellular lipid accumulation than levamisole (Fig.4.6 page 122). This suggests that all the machinery required for lipid accumulation is present within the cells but that reduced ALP activity dramatically slows down this process.

The ability of the two ALP inhibitors to reduce intracellular lipid accumulation in HepG2 suggests that ALP is involved in the metabolic processes related to intracellular lipid accumulation. However, it must be noted that both inhibitors have other effects that may also lead to the inhibition of lipid deposition, and these will be discussed below.

Levamisole is an agonist of both adrenergic and nicotinic receptors (Hsu 1980) and has been ascribed to increase the activity of enzymes like glycogen synthase in rat adipocytes (Basi *et al.* 1994) and pyruvate dehydrogenase in rat fat pads (Thomaskutty *et al.* 1993).

The transcriptional activity of ADD1/SREBP1c in murine 3T3-L1 cells is down-regulated by an increased expression of glycogen synthase (which is directly regulated by glycogen synthase kinase 3 [GSK3]) (Kim *et al.* 2004). ADD1 is a transcriptional factor that is involved in the stimulation of many lipogenic genes and it has been suggested that ADD1 plays a role in coordinating insulin-dependent lipid and glucose metabolism (Kim *et al.* 1998; Foretz *et al.* 1999). Increased activity of glycogen synthase therefore results in decreased intracellular lipid accumulation.

In one study, the decreased activity of pyruvate dehydrogenase complex (PDHc) was found to be associated with increased fat storage in pancreatic  $\beta$ -cells in rats (Pighin et al. 2003). Lipotoxicity leading to pancreatic  $\beta$ -cell dysfunction is well documented (Rossetti et al. 1990; McGarry and Dobbins 1999).

The participation of adrenergic receptors (ARs) in the regulation of adipose tissue development and metabolism is well known (Soloveva et al. 1997). Stimulation of the  $\beta_3$ -ARs in adipocytes leads to increased lipolysis primarily through the production of cAMP via coupling of G proteins to adenylyl cyclase and the activation of hormone-sensitive lipase whereas stimulation of  $\alpha_2$ -ARs leads to increased lipid storage through the inhibition of cAMP production (Lafontan and Berlan 1993). The net lipid mobilization depends on the balance between stimulatory and inhibitory effects of catecholamines on beta and alpha ARs respectively (Mauriege et al. 1987). Levamisole binds the  $\beta$ -adrenergic receptors and could therefore block intra-cellular lipid accumulation by increasing lipolysis.

Soloveva *et al.* (1997) reported a 2-fold increase in the level of  $\beta$ -AR transcripts in transgenic mice over-expressing  $\beta_1$ -AR and the activation of these receptors was reported to prevent excessive adiposity. In humans, a functional glutamine 27 glutamic acid (Gln27Glu) polymorphism in the beta2-AR gene has been associated with the male-type adiposity (increase in fat mass in the upper body region particularly in the abdomen) in women and thus an increased cardiovascular risk (Kunnas et al. 2009).

It is unlikely that levamisole blocks intra-cellular lipid accumulation via the nicotine acetylcholine receptor since activation of this receptor by nicotinic acid blocks lipolysis via the inhibition of cAMP accumulation in adipose tissue through mechanisms similar to those previously described for the  $\alpha$ -ARs (Tunaru et al. 2003).

Rae *et al.* (2003) reported the inhibition of the amino acid system A transporter (SAT2) by histidine (Rae *et al.* 2003). SAT2 is ubiquitously expressed and confers a  $\text{Na}^+$ -dependent ability for the transport of short-chain neutral amino acids. SAT2 is known to be expressed in 3T3-L1 cells (Hyde *et al.* 2001). It is not known how the inhibition of the SAT2 system could inhibit intracellular lipid accumulation, however it is known that SAT2 levels increase during adipogenesis in 3T3-L1 cells (Su *et al.* 1998) and may provide amino acids for increased protein synthesis.

Thus it is also possible that histidine may affect other biomolecules than ALP and by this mechanism block intracellular lipid accumulation.

Inhibition of ALP activity in the osteoblastic cell line (SV-HFO) using levamisole was shown to cause reduced cellular mineralization even in the presence of dexamethasone (Iba *et al.* 1995). As such ALP has been used as one of the early markers of osteoblast differentiation (Naito *et al.* 2005; Hsu *et al.* 2007; Wang *et al.* 2007). However, the use of ALP activity as a marker of differentiation of mesenchymal cells into osteoblasts is now questioned as a result of the evidence that ALP is also an important marker of the adipogenic process.

The present study has gone a step further by inhibiting ALP activity with siRNA designed against the TNSALP mRNA transcripts and studying its effects on intracellular lipid accumulation in both the 3T3-L1 and HepG2 cells.

### 5.3 The RNA interference pathway and the knockdown of specific mRNA transcripts

The interpretation of results on the effects of levamisole and histidine on ALP activity and lipid accumulation in 3T3-L1 and HepG2 cells is fraught with difficulty because of the lack of specificity of the two inhibitors on ALP activity, as already noted. Specific silencing of ALP activity using the RNA interference pathway could better clarify the involvement of this glycoprotein in intracellular lipid accumulation.

In the initial application of RNAi to study the expression of mammalian genes, the major setback was that the introduction of double stranded RNA greater than 30 nucleotides in length led to non-specific suppression of gene expression. However, as the RNAi system became better understood, scientists discovered that short interfering RNA oligos of 23 nucleotides could be used to mediate gene silencing in mammalian cells and no non-specific gene silencing effects were seen in mammalian cells using such siRNA species (Elbashir *et al.* 2001). At the same time it was confirmed that identically sized synthetic siRNAs can induce gene-specific inhibition of expression in *C.elegans*, human and mouse cells (Caplen *et al.* 2001). Consistent with this observation, numerous studies have since shown that double-stranded RNA-induced gene silencing occurs in a number of different eukaryotic species (Timmons and Fire

1998; Hammond *et al.* 2000; Li *et al.* 2000; Wianny and Zernicka-Goetz 2000; Semizarov *et al.* 2003).

The RNAi human/ mouse starter kit (Qiagen Technologies) is a good starting point for establishing unknown transfection conditions in cell lines. Use of the fluorescently-labelled siRNA provides convenient monitoring of transfection efficiency. When siRNAs are used at low concentrations any potential off-target effects are minimized.

#### 5.3.1 Effect of siRNA transfection on ALP activity and intracellular lipid accumulation.

Using siRNA directed against mRNA transcripts for TNSALP, we have shown for the first time that the inhibition of intracellular lipid accumulation in 3T3-L1 and HepG2 cells is mediated by TNSALP. Thus, the specific siRNA directed against the TNSALP transcript reduced ALP activity and lipid accumulation in both cell lines.

Western blots were not used to confirm the reduction of TNSALP protein levels because this was deemed unnecessary since ALP activity was measured in the cell extracts. The assessment of ALP activity is the most pertinent measure of the end result of TNSALP mRNA knockdown. Furthermore, the temporal profile of the transcript knockdown and the reduction of ALP activity were superimposable in both cell lines suggesting a direct link between these two events. It is impossible to explain these results without inferring that the knockdown of the TNSALP mRNA led to a reduction in the intracellular levels of the ALP enzyme.



The use of the AllStars negative siRNA was a good internal control to assess the non-specific off-target effects that the double-stranded RNA molecules could have on the cells in general and lipid metabolism in particular. Cells that were treated with Allstars negative siRNA gave results (in terms of ALP activity, mRNA expression levels and lipid accumulation) that were very similar to untreated cells. Furthermore, expression of the housekeeping TBP gene was not affected by the anti-TNSALP siRNA which also suggests that off-target effects of the siRNA were minimal.

### 5.3.2 Effect of siRNA transfection on *TNSALP* gene expression

The expression of the *TNSALP* gene determined indirectly through measuring the levels of its mRNA on day 0 was zero in 3T3-L1 cells. This is in keeping with the TNSALP protein activity which was also undetectable on day 0. On day 7 the knockdown efficiency was  $81.3\% \pm 2.7$  (SEM) in cells that were transiently transfected with the siRNA and this was mirrored by low ALP activity at this same time point. The expression of *TNSALP* declined on day 11 and again this is consistent with the ALP activity level determined at the same time point. In untransfected HepG2 cells, the expression of the TNSALP gene was highest on day 4 after which it declined. ALP activity was also highest on day 4 and a sharp decline was observed after this time point. In HepG2 cells transfected with the silencing siRNA, the suppression of ALP activity on day 4 was mirrored by a significant reduction in ALP mRNA levels determined on the same time point. On day 4, the knockdown efficiency of the TNSALP gene was  $80.0\% \pm 8.9$ .

There are no reports on the knockdown of the *TNSALP* gene in 3T3-L1 and HepG2 cells in the literature. However, one study showed that *TNSALP* knock-out mice developed epileptic seizures the origin of which has been linked to deficiency in pyridoxal-5-phosphate and GABA metabolism (Waymire *et al.* 1995). This study reported “that mice homozygous for the mutant *TNSALP* allele were indistinguishable from littermates at birth. During the first two weeks postnatally, the single gross difference between mutants and heterozygotes or wild-type littermates was their size, which ranged from 50% to 100% of that of control littermates” (Waymire *et al.* 1995). The authors, however, did not mention differences in other anthropometric measurements such as body fat and muscle mass. However, another study of *TNSALP* knockout mice described both reduced bone mineral density and the presence of very little adipose tissue (Narisawa *et al.* 1997).

Though the efficiency of transfection using siRNA for the *TNSALP* gene in both 3T3-L1 and HepG2 cells was not determined, based on the results of the *MAPK1* gene it can be argued that the efficiency of transfection was not 100% and this may explain the retention of low levels of *TNSALP* gene expression in the presence of the *TNSALP* siRNA in both cell types.

The knockdown of the *TNSALP* gene in 3T3-L1 and HepG2 cells and the resultant reduced intracellular lipid accumulation confirms the important role that ALP plays in adipogenesis.

The positioning of the *TNSALP* protein on the membrane of the lipid droplet in both HepG2 and 3T3-L1 cells and its expression late in the adipogenic process suggest

that it functions downstream of PPAR $\gamma$ . This is also implicated by the lack of effect of TNSALP inhibitors on PPAR $\gamma$  expression. It is therefore unlikely that the knock-down of TNSALP mRNA would affect the expression of other key transcription factors involved in gene regulation early in the adipogenic pathway e.g. SREBP1 or the C/EBPs. Future investigations must explore the effect of TNSALP mRNA knock-down on the expression of proteins that act as markers of the mature adipocyte such as hormone sensitive lipase or FABP1, as well as the transcriptional regulation of the TNSALP gene. This data would help to show the effect and relationship of ALP with proteins characteristic of developing adipocytes.

#### 5.4 Subcellular localization of ALP in HepG2 cells

A large body of evidence points out that ALP is a membrane-associated glycoprotein (Harris 1990; Detmers *et al.* 1995) and is anchored to cell membranes via a PI-G tail (Jemmerson and Low 1987; Kihn *et al.* 1990). A number of studies have also shown that the membrane surrounding the lipid droplet in a number of cell lines (for example, preadipocytes, murine MA-10 Leydig cells and adrenal Y-1 cells) contain perilipin, vimentin and ADRP (Greenberg *et al.* 1991; Servetnick *et al.* 1995; Brasaemle *et al.* 1997). All these proteins are known to be phosphoproteins. ADRP is the predominant protein of the lipid droplets in adrenal cells, macrophages and hepatocytes (Brasaemle *et al.* 1997; Lu *et al.* 2001; Motomura *et al.* 2006). It has been suggested that perilipin protects the lipid droplets from lipolytic enzymes and may play a role in management of neutral lipid stores (Servetnick *et al.* 1995).

The membrane of lipid droplets is closely associated with that of the endoplasmic reticulum and other secretory vesicles (Targett-Adams *et al.* 2003). This may enable shuttling of biomolecules between the lipid droplet compartment and the secretory vesicles. There is growing evidence that the association between lipid droplets and other vesicles point to novel functions of droplets in organelle communication. Droplet translocation through the cytoplasm and rapid movement on microtubules has been observed (Valetti *et al.* 1999).

The present study has shown for the first time that ALP localizes on the lipid droplet membrane in a human hepatocarcinoma cell line, HepG2 cells. It appears that this is the same locality within these cells where ADRP is also expressed. In 3T3-L1 cells, ALP activity was co-localised on the lipid droplet with perilipin.

ALP activity was demonstrated using the ELF 97 endogenous phosphatase detection kit (Molecular Probes). This method gives specific labelling of ALP activity and is compatible with other detection methods e.g. fluorescence staining (Cox and Singer 1999). One important aspect to observe in using the ELF 97 kit to detect endogenous phosphatases is to be able to demonstrate that no ALP signal is present when a specific inhibitor of ALP is incubated with the cells before the ELF 97 reaction. Inhibition of ALP activity by levamisole in this study blocked the ELF 97 signal, confirming that this technique was detecting ALP activity. No ALP activity was seen in non-transformed HepG2 cells using the ELF 97 substrate suggesting either that this method is not sensitive enough to detect ALP activity at this time point or that no ALP is present in these cells before the induction of lipid droplet formation. This seems

unlikely, because ALP activity could be measured in HepG2 cells before stimulation of intracellular lipid accumulation. A previous study has reported immunocytochemical localisation of ALP to the nucleus of HepG2 cells (Yamamoto *et al.* 2003) whilst a study of cultured rodent hepatocytes have shown localisation of ALP to the nuclear membrane, the endoplasmic reticulum, the Golgi apparatus and the plasma membrane (Asada-Kubota and Kanamura 1986).

Immunocytochemical analysis of ALP sub-cellular localisation was also attempted using ALP monoclonal antibodies. However, this method was unsuccessful with poor visualisation of the immunocytochemical stain and high non-specific binding of the antibodies.

The localization of ALP to the lipid droplet membrane supports the supposed role that ALP plays in intracellular lipid accumulation. However, it is not known what ALP does on the surface of the lipid droplet membrane. The following sections will discuss the possible role of ALP in intracellular lipid accumulation.

#### 5.4.1 Proposed mechanisms of TNSALP mediated intracellular lipid accumulation.

In light of the current body of information on the localization and activity of ALP in human tissue and a number of cell lines it is not easy to propose a unifying mechanism that clearly shows the role of ALP in intracellular lipid accumulation. Indeed, there are a number of possible mechanisms by which ALP may be involved and these will be discussed below.

#### 5.4.1.1 ALP in neutral lipid synthesis

It is possible that ALP may be involved in the intracytoplasmic synthesis of neutral lipids (TAG and cholesterol esters). An important and possibly rate-determining step in the biosynthesis of TAG in all eukaryotic cells is the conversion of phosphatidic acid into diacylglycerol [DAG] by *phosphatidic acid phosphatase* [PAP] (Bell and Coleman 1980; Carman and Han 2009). Stimulation of the activity of the cytoplasmic fraction of PAP in human liver tissue has been reported when the liver tissues were pre-incubated with ALP (Angelin *et al.* 1987). A previous study reported similar findings when rat liver tissues were used (Berglund *et al.* 1982). Dephosphorylation by ALP may therefore be of importance in regulating the activity of PAP in animals.

The pathway of TAG biosynthesis is shown in the scheme below:

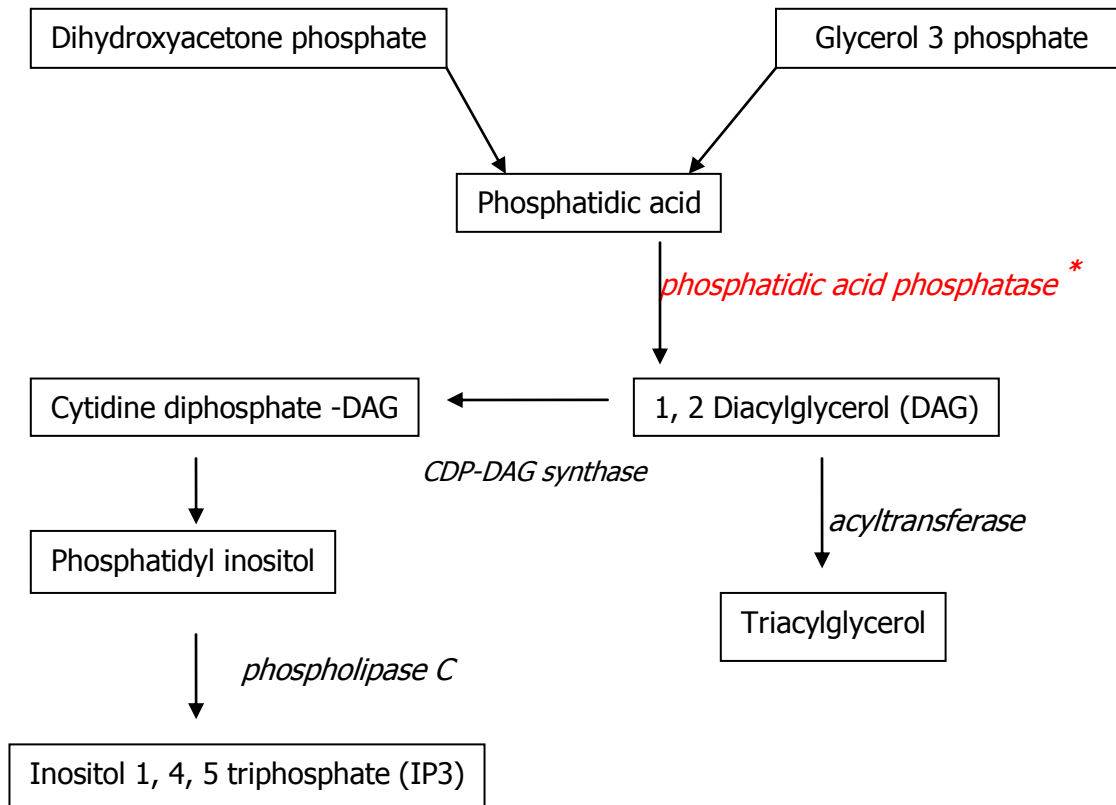


**Figure 5. 1** Triacylglycerol biosynthesis

An increase in ALP activity stimulates the activity of *PAP\** which results in the increased synthesis of DAG. DAG can be converted directly into TAG by DAG acyltransferase.

Alternatively, DAG can be shuttled into a pathway leading to the formation of inositol 1, 4, 5 triphosphate [IP3]. IP3 binds with the receptors in the membrane of the smooth endoplasmic reticulum [ER] where it helps opening of  $\text{Ca}^{2+}$  channels. The resulting increase in free cytoplasmic calcium synergizes with the action of DAG in activation of some forms of protein kinases and may activate many other calcium-dependent processes (Rhoades and Bell 2009). Protein kinase C is reported to phosphorylate receptor interacting protein 140 (RIP 140). RIP 140 is abundantly

expressed in adipocytes and is known to regulate lipolysis through its interaction with perilipin (Ho *et al.* 2011). In HepG2 cells however, activation of AMP-activated protein kinase  $\alpha$  (AMPK $\alpha$ ) reduced lipid accumulation caused by incubation of cells with palmitate (Liu *et al.* 2011).

In future it would be worthwhile to assay the activity of PAP in cell extracts in which ALP activity has been blocked by either siRNA oligos or chemical inhibitors to study the role that the two enzymes play in lipid accumulation.

#### 5.4.1.2 Interaction with lipid droplet associated proteins

TNSALP is a membrane-bound glycoprotein and therefore its supposed role in lipid droplet formation could possibly be exerted at the level of the lipid droplet membrane. This could involve the interaction of ALP with membrane receptors or phosphoproteins located on this membrane. Perilipins are the most abundant phosphoproteins that associate with the lipid droplet in a number of lipid storing-cell types (Londos *et al.* 1999).

Perilipins (especially Perilipin A) regulate TAG storage by reducing rates of basal lipolysis and facilitating hormonally stimulated lipolysis (Garcia *et al.* 2004). The phosphorylation of perilipins by protein kinases (PKA) causes a large increase in the rate of lipolysis (Souza *et al.* 2002; Tansey *et al.* 2003). One study has suggested that perilipins, in the phosphorylated state, may be hormone sensitive lipase (HSL)-binding proteins (Sztalryd *et al.* 2003) and are involved in docking the HSL at the surface of the lipid droplet membrane. Inhibition of ALP activity may therefore allow for lipolysis



by reducing de-phosphorylation of perilipin and thus increasing docking of HSL at the surface of the lipid droplet membrane.

The role of perilipin in lipid storage *in vivo* is supported by studies using perilipin knockout mice. Tansey et al. (2001) reported that perilipin null mice were leaner than wild type littermates and were resistant to diet induced obesity. Adipocytes isolated from perilipin null mice showed elevated basal lipolysis (Tansey et al. 2001).

If ALP is a phosphoprotein phosphatase, its localization on the lipid droplet membrane would suggest that ALP may be involved in maintaining perilipins and possibly other members of the PAT family of phosphoproteins in the de-phosphorylated state.

#### 5.4.1.3 TNSALP as a transport protein

Narisawa *et al.* (2003) presented evidence that intestinal ALP (I-ALP) is involved in the rate-limiting step during intestinal fat absorption in rats. Thus, I-ALP gene knockout rats showed an accelerated rate of fat absorption compared to the wild type rats when fed on a high fat diet (Narisawa *et al.* 2003). Furthermore, I-ALP was found on the surface of membrane bound lipid particles that are involved in the transport of lipids into and across enterocytes (Zhang *et al.* 1996). These data suggest that I-ALP is a prime regulator of fat absorption into the enterocytes lining the intestine and may give some indication of the possible role of TNSALP in preadipocytes and hepatocytes.

A physiological role for ALP in the regulation of organic cation transport at the blood brain barrier has been suggested in rat brain endothelial 4 (RBE4) cells (Calhau

*et al.* 2002). How the transport of organic cations may relate to the role of ALP in the control of intracellular lipid accumulation however, is not known.

In bacteria, the presence of phosphate groups usually prevents organic molecules from passing through the membrane. Dephosphorylating the membrane proteins is known to be important for bacterial uptake of organic compounds ([www.en.academic.ru.dic.nsf/enwik/](http://www.en.academic.ru.dic.nsf/enwik/)). If this happens in eukaryotes, then this may also be a possible mechanism through which ALP mediates lipid accumulation by facilitating passage of organic molecules that may be utilized in lipid synthesis.

Alternatively, ALP may be involved in the hydrolysis of ATP and this could be linked to the energy requiring process of lipid droplet formation (Shinozaki and Pritzker 1996).

#### 5.5 *PPAR*<sub>γ</sub> gene expression in 3T3-L1 and HepG2 cells

A number of studies have reported the involvement of *PPAR*<sub>γ</sub> in intracellular lipid accumulation in various cell lines and primary cells (Brun *et al.* 1996; Wu *et al.* 1997; Emma and Yousef 2003; Seargent *et al.* 2004; Schadinger *et al.* 2005).

Often referred to as the 'master regulator of adipogenesis', *PPAR*<sub>γ</sub> participates in the transcriptional activation of numerous adipogenic and lipogenic genes important for adipocyte maturation and lipid accumulation. Examples of such genes are *PEPCK* (Tontonoz *et al.* 1995), *fatty acid transport protein-1* (Martin *et al.* 1997), *Glut4* (Wu *et al.* 1998), *lipoprotein lipase* (Schoonjans *et al.* 1996) and *aP2* (Tontonoz *et al.* 1994).

There are a few reports of the involvement of the PPAR $\gamma$  gene in metabolism in hepatocytes. Some of the reports are discussed below and these studies were carried out in rodents.

A PPAR $\gamma$ -responsive element has been identified in mouse hepatocytes and these elements are important in the control of hepatocyte growth factor (HGF) gene transcription (Jiang *et al.* 2001). HGF promotes cell growth, cell motility and morphogenesis of its target cells (Michalopoulos and DeFrances 1997). Furthermore, studies have shown that treatment of rat hepatocytes with HGF leads to increased lipogenesis (Shao *et al.* 1996; Kaibori *et al.* 1998; Shiota *et al.* 2000).

Hepatic PPAR $\gamma$  protein expression measured immunohistochemically in mice with liver steatosis induced by a high fat diet revealed an increased expression compared to control mice (Inoue *et al.* 2005). This study shows that PPAR $\gamma$  activity is associated with lipid accumulation in liver cells.

One study has shown that PPAR $\gamma$  regulates lipogenesis and lipid accumulation in steatotic hepatocytes (Schadinger *et al.* 2005). This phenomenon is accompanied by a selective upregulation of several adipogenic and lipogenic genes including *ADRP*, *SREBP1* and *fatty acid synthase*.

These studies demonstrate that at least in rodents, PPAR $\gamma$  may be involved in the lipid accumulation observed in hepatocytes and may also modulate the steatohepatitis associated with obesity.

In this study we have shown for the first time that the expression of the PPAR $\gamma$  gene increases during lipid accumulation within the human derived liver cell line,

HepG2. The expression of the *PPAR $\gamma$*  gene was found to be highest four days after addition of transformation medium in both 3T3-L1 and HepG2 cells. After day 4 the expression declined to levels not significantly different from the baseline values. The expression of *PPAR $\gamma$*  has been reported to reach a maximum between day 3 and 4 after induction of lipid droplet accumulation in a number of other studies (Wu *et al.* 1995; Clarke *et al.* 1997; Jessen and Stevens 2002). Other studies have shown that the increase in *PPAR $\gamma$*  expression varies from 2 (Zizola *et al.* 2010) to 8 (Chung *et al.* 2010) fold over a 4 day period of adipogenesis in 3T3-L1 cells. In this study, *PPAR $\gamma$*  expression increased 2 to 3 fold in the 3T3-L1 cells, which is comparable to the literature.

Interestingly, ALP activity and *PPAR $\gamma$*  gene expression peak at the same time point in the hepatocyte cell line but in the preadipocytes *PPAR $\gamma$*  gene expression peaks before ALP activity. This suggests a difference in the time course of the principal events that control intracellular lipid accumulation in the two cell lines.

The decline in the activity of *PPAR $\gamma$*  after day 4 suggests the completion of the differentiation process and a lessening of the need for direction of new transcript synthesis (Jessen and Stevens 2002).

#### 5.5.1 Levamisole and histidine do not alter the expression pattern of the *PPAR $\gamma$* gene in 3T3-L1 and HepG2 cells

The question of whether the activation of the *PPAR $\gamma$*  gene precedes that of the *ALP* gene was addressed by incubating HepG2 and 3T3-L1 cells with ALP inhibitors and determining the effect of this treatment on the *PPAR $\gamma$*  gene expression. The

expression of the *PPAR $\gamma$*  gene peaked on day four after the induction of lipid droplet accumulation and declined to near base line levels on day 7 in the presence of the two ALP inhibitors (levamisole and histidine) in both cell types under study. This expression pattern is similar to the one observed when the cells were not treated with the two inhibitors. Use of the two ALP inhibitors nevertheless caused inhibition of both intracellular lipid accumulation and ALP activity as discussed in section 5.2.

These results suggest that in both HepG2 and 3T3-L1 cells *PPAR $\gamma$*  gene activation does not require the presence of functional ALP. It is therefore possible that ALP acts at a later stage in the adipogenic pathway than *PPAR $\gamma$*  or in a separate pathway to that of *PPAR $\gamma$*  and which is critical for intracellular lipid accumulation.

#### 5.6 Ethnic differences in ALP activity and the role of SNPs in the promoter region of the human *TNSALP* gene

A national survey has shown that obesity is more prevalent in South African black than white women (Puoane *et al.* 2002). In a study performed in our department significant differences in ALP activity and adipogenesis were seen in preadipocytes isolated from white and black women, the activity being higher in the latter group (Ali *et al.* 2006a). This may partly explain the higher prevalence of obesity in the black population group.

In the present study we hypothesized that the differences in ALP activity mentioned above could be due to differences in the rates of transcription of the ALP gene. The possible role that SNPs in the promoter region of the human *TNSALP* gene could play in moderating the transcription process was therefore investigated.

Sequencing results of the promoter region for the *TNSALP* gene amplified from 6 black women (BMI  $33.0 \pm 4.6$ ; age  $49.7 \pm 6.3$  years) and 6 white South African women (BMI  $31.5 \pm 4.5$ ; age  $39.5 \pm 11.9$  years) did not show any nucleotide changes. No significant difference in the fat mass was observed between black and white women who participated in the study (Appendix II).

In a study by Ali *et al.* (2006a) the difference in ALP activity in pre-adipocytes isolated from black and white women was so profound that if polymorphisms in the promoter region of the *TNSALP* gene were responsible for this difference, it should be present at a very high frequency in the one population group compared to the other and thus should be detectable even in a small group of subjects. Also, in the study of Ali *et al.* (2006a) the level of preadipocyte ALP activity was not related to BMI and therefore, the inability of the current study to identify an ALP promoter polymorphism cannot be due to the use of predominantly obese subjects. In the original study of Ali *et al.* (2006a) differences in ALP activity were observed between pre-adipocytes from 15 white and 13 black females before addition of the adipogenesis-inducing cocktail i.e. at day 0 ( $36.5 \pm 5.8$  versus  $136.4 \pm 10.9$  mU/mg protein, respectively;  $p < 0.0005$ ) and 12 days after ( $127 \pm 16$  versus  $278 \pm 27$  mU/mg protein, respectively;  $p < 0.0005$ ). In fact, at day 0, the lowest ALP activity detected in preadipocytes from the black females was higher than the highest ALP level detected in the preadipocytes from the white females. The same study reported that intracellular lipid accumulation was higher in pre-adipocytes isolated from black compared to white females which parallels the obesity prevalence rates in these population groups and also suggested

that the reason for the higher fat accumulation in pre-adipocytes isolated from black females may be related to the higher ALP activity (Ali *et al.* 2006).

These data suggest that the differences in preadipocytic ALP activity between black and white South African women might either be due to a post-translational modification of the ALP protein, differences in ALP mRNA stability, differences in the levels of molecules controlling ALP gene expression, involvement of altered levels or activity of upstream transcription factors that regulate TNSALP expression, differences in micro RNA involvement at the transcriptional level or differences in the genetic sequence of the ALP exon coding for the active site of the enzyme. Differences in the promoter region of the gene by methylation or chemical modifications of the histones that do not change the underlying DNA sequence but modifies the expression of a gene (Jaenisch and Bird 2003) may also explain the large difference in ALP activity observed between the two ethnic groups. Interestingly, methylated sites (CpG islands) are present in the promoter region of the human TNSALP gene (Weiss *et al.* 1988).

#### 5.6.1 Polymorphisms in TNSALP and ENPP1 genes and its association with biochemical features of obesity

A number of studies have shown that genetic polymorphisms in the gene of a known functional partner of TNSALP in bone mineralization called ectonucleotide pyrophosphatase/phosphodiesterase 1 (ENPP1) are significantly associated with obesity traits in humans of different ethnicity (El Achhab *et al.* 2009; Santoro *et al.* 2009). The ENPP1 gene is located on chromosome 6q22-q23 and its product has been identified as one of the principal regulators of extracellular pyrophosphate

(ePPi)/phosphate (Pi) equilibrium levels. It is through the metabolism of ePPi/Pi and calcium that TNSALP and ENPP1 modulate mineralization of bone (Zhang *et al.* 2007). Recently, DNA polymorphisms in the TNSALP gene and other genes involved in mineralization of bone (e.g. mouse progressive ankylosis gene, ANKH) have been shown to have strong associations with obesity related phenotypes in healthy Caucasian subjects. The obesity related phenotypes that were strongly associated with the TNSALP gene polymorphisms were waist-to-hip ratio (WHR) and serum levels of epidermal growth factor receptor (EGFR) (Korostishevsky *et al.* 2010).

A haplotype G-A (rs3738096 and rs1256331) located in the 3' UTR of the TNSALP gene showed the most significant association with WHR (Korostishevsky *et al.* 2010). The haplotype T-G (rs869179 and rs1472563) which is within the TNSALP promoter was associated with EGFR levels. *In vivo* and *in vitro* studies have shown that EGFR increases adipogenesis (Serrero *et al.* 1993; Adachi *et al.* 1994). The EGFR levels exhibited weak correlation with the WHR trait and other obesity phenotypes that were studied e.g. BMI and leptin (Korostishevsky *et al.* 2010).

This PhD study, however, did not identify any SNPs in the promoter region of the TNSALP gene in black and white South Africans. I believe that this could have been due to the small sample size that was studied (N=12). Furthermore, the purpose of this study was not to associate ALP SNPs with obesity but rather to determine if SNPs were present in the promoter region which may explain the difference in ALP levels observed in preadipocytes from white and black females.



The study by Korostishevsky *et al.* (2010) and work performed in this thesis strengthens the hypothesis that ALP plays some role in adipocyte biology and accumulation of intracellular lipids in a number of cell types.

## 5.7 Conclusions

The presence of ALP in many species of animals and its wide tissue distribution suggests its involvement in fundamental biological processes. To date, little is known with any certainty about the exact biological functions of these glycoproteins in normal metabolism (Harris 1990). The only exception to this statement comes from the work on hypophosphatasia which clearly indicates that the liver/bone/kidney isoenzyme is necessary for bone mineralization (Posen *et al.*, 1977; Whyte 1994). There are reports of the role of ALP in mammalian embryogenesis (McDougall *et al.* 1998) and in cell differentiation (Andracchi and Korte 1991). ALP may therefore continue to be a subject of intensive research in an attempt to understand more clearly some of its biological functions.

The presence of ALP activity in 3T3-L1 cells, human preadipocytes (from the mammary gland and subcutaneous abdominal fat) (Ali *et al.* 2006; Ali *et al.* 2006a) and in HepG2 cells suggests that ALP expression is a common feature of cells that accumulate cytoplasmic lipid droplets. The localization of ALP activity on the surface of the lipid droplet membrane in HepG2 and 3T3-L1 cells shown in this study certainly points to the involvement of ALP in some of the processes related to intracellular lipid accumulation.

By using a more specific approach of inhibiting ALP expression, RNAi, the present study has also strengthened the suggestion that ALP plays a role in cytoplasmic lipid droplet accumulation and the use of PCR primers specific for the

TNSALP isoenzyme indicates that it is the TNSALP isotype that is involved in intracellular lipid accumulation.

The increase in the expression of the PPAR $\gamma$  gene early in adipogenesis (3T3-L1 cells) and in intracellular lipid accumulation (HepG2 cells) suggests that PPAR $\gamma$  is an important factor in lipid accumulation in both preadipocytes and hepatocytes. Furthermore, the ability of ALP inhibitors to block intracellular lipid accumulation in both HepG2 and 3T3-L1 cells but to have no effect on PPAR $\gamma$  gene expression suggests that PPAR $\gamma$  either precedes ALP in the adipogenic pathway or exists on a separate but equally important pathway in the adipogenic process.

#### 5.8 Strategies for future work

Related to the work on ethnic differences in ALP activity observed in black and white South African women, future work would include increasing the sample size for sequencing studies to detect nucleotide base changes in other regions of the TNSALP gene (similar to work done by Kolostishevsky *et al.* 2010 in Caucasian population) and studying the methylation pattern of the promoter region of the gene in black and white subjects. Studies should also be performed to quantify ALP gene expression in preadipocytes isolated from both population groups.

To extend the ALP inhibitor studies (using pharmacological agents or siRNA) to another cell line known to accumulate intracellular lipid droplets i.e. adrenal Y-1 cells and Leydig cells.

Because both ALP and PPAR $\gamma$  are induced during intracellular lipid accumulation in 3T3-L1 and HepG2 cells, in order to show whether ALP is downstream of PPAR $\gamma$  or not, future studies will involve use of PPAR $\gamma$  agonist such as thiazolidinediones to test if stimulation of PPAR $\gamma$  will increase ALP activity.

The specific knock out of the ALP gene in adipocytes *in vivo* would be important to determine if this would lead to reduced adipose tissue.

It is possible that ALP controls the phosphorylation status of molecules that play an important role in adipogenesis. Therefore, the phosphorylation level of proteins isolated from preadipocytes incubated with  $^{32}\text{P}$  in the presence and absence of ALP inhibitors may help to identify the molecule(s) that are de-phosphorylated by ALP using phospho-specific antibodies (Tran *et al.* 2007) or immunoblotting (Iyer *et al.* 2005).

The ability of ALP to activate PAP could easily be investigated by incubating preadipocytes with TNSALP inhibitors or treat them with siRNA against TNSALP, and measure PAP activity and lipid accumulation in the presence and absence of the inhibitors.

## **APPENDIX I**

## APPENDIX I

### Appendix IA

#### **Homo sapiens peroxisome proliferator activated receptor gamma (*PPARG*) mRNA, complete cds**

LOCUS HUMPPARGB 1808 bp mRNA linear PRI 26-DEC-2001  
DEFINITION Homo sapiens peroxisome proliferator activated receptor gamma (*PPARG*) mRNA, complete cds.  
ACCESSION L40904  
VERSION L40904.2 GI:17978515  
SOURCE Homo sapiens (human)  
ORGANISM [Homo sapiens](#), Eukaryota; Metazoa; Chordata; Craniata; Vertebrata; Euteleostomi; Mammalia; Eutheria; Euarchontoglires; Primates; Haplorrhini; Catarrhini; Hominidae; Homo.

#### **Primer location and region of amplification of the *PPAR $\gamma$* gene in HepG2 cells**

(Forward primer is shown in red while the reverse primer is in blue, both are underlined; highlighted in yellow is the region that was amplified).

1ccgaccttaccaggcggccttgacgttggcttgcggcaggagacagcaccatggtg  
61ggttctctctgagtctgggaattcccagcccagccgcagccgcccctggggggcttg  
121ggtcggcctcgaggacaccggagagggggcgcacgcccgcctggccgcagaaatgacat  
181ggttgacacagagatgccattctgcccaccaacttgggatcagctccgtggatctctc  
241cgtaatggaagacctcccactccttgatatcaagccttcaactactgttgacttctc  
301cagcatttctactccacattacgaagacattccattcacagaacagatccagtggttgc  
361agattacaagtatgacctgaaactcaagagtaccaaagtcaatcaagtgaggcctgc  
421atctccaccttattattctgagaagactcagctctacaataagcctcatgaagagccttc  
481caactccctcatggcaattgaatgctgtgtctgtggagataaagcttctggattcacta  
541tggagttcatgctgtgaaggatgcaagggtttctccggagaacaatcagattgaagct  
601tatctatgacagatgtgatcttaactgctggatccacaaaaaagtagaaataaatgtca  
661gtactgtcggttcagaaatgccttgcaaggatgtctcataatgccatcaggtttgg  
721gcggatgccacaggccgagaaggagaagctgttggcggagatctccagtgatatcgacca  
781gctgaatccagagtcctgacctccggcctggcaaacatttgtatgactcatacat  
841aaagtccttcccgtgaccaaagcaaaggcgagggcgatcttgacaggaaagacaacaga  
901caaatcaccattcgttatctatgacatgaattcctaatgatgggagaagataaaatcaa  
961gttcaaacacatccccctgcaggagcagagcaaagaggtggccatccgcacatcttca  
1021gggctgccagtttgcctccgtggaggctgtgcaggagatcacagagtatgccaaaagcat  
1081tctgtgtttgtaaatcttgactgaacgaccaagtaactctcctcaaatatggagtcca  
1141cgagatcatttacacaatgctggcctcctgatgaataaagatggggttctcatatccga  
1201gggccaaggctcatgacaagggagtttctaaagagcctgcgaaagccttttggtgactt  
1261tatggagcccaagtttgagttgctgtgaagttcaatgcactggaattagatgacagcga  
1321cttggcaatatttctgtcattattctcagtgagaccgcccaggttctgctgaatgt  
1381gaagcccattgaagacattcaagacaacctgctacaagcctggagctccagctgaagct  
1441gaaccacctgagtcctcacagctgttggcaagctgctccagaaaatgacagacctcag  
1501acagattgtcacggaacacgtgcagctactgcaggtgatcaagaagacggagacagacat  
1561gagtcttaccgctcctgcaggagatctacaaggactgtactagcagagagctcctgag

1621ccactgccaacatttccttctccagttgcactattctgaggaaaatctgaccataag  
 1681aaatttactgtgaaaaagcggtttaaaaagaaaagggttagaatatgatctattttatg  
 1741catattgtttataaagacacatttacaatttacttttaataaaaaattaccatattat  
 1801gaaattgc

## Appendix IB

### Homo sapiens TATA box binding protein (*TBP*), mRNA

LOCUS NM\_003194 1867 bp mRNA linear PRI 20-SEP-2009  
 DEFINITION Homo sapiens TATA box binding protein (*TBP*), mRNA.  
 ACCESSION NM\_003194  
 VERSION NM\_003194.3 GI:61744433  
 SOURCE Homo sapiens (human)  
 ORGANISM [Homo sapiens](#) Eukaryota; Metazoa; Chordata; Craniata; Vertebrata;  
 Euteleostomi; Mammalia; Eutheria; Euarchontoglires; Primates; Haplorrhini;  
 Catarrhini; Hominidae; Homo.

### Primer location and region of amplification of the *TBP* gene in HepG2 cells

(Forward primer is shown in red while the reverse primer is in blue, both are underlined; highlighted in yellow is the region that was amplified).

01ggttcgctgtggcgggcgccctgggcccggctgtttaactcgttccgctggccata  
 61gtgatctttgcagtgaccagcagcactgtttcttggcgtgtgaagataaccaagg  
 121aattgaggaagtgtgagaagagtgtgctggagatgctctagaaaaaattgaatagt  
 181agacgagttccagcgaagggttctggttccaagaagaaagtgaacatcatggatca  
 241gaacaacagcctgccacctacgctcagggttggcctcccctcagggtgccatgactcc  
 301cggaatccctatcttagtccaatgatgccttatggcactggactgaccccacagcctat  
 361tcagaacaccaatagtctgtctatgttgaagagcaacaaggcagcagcagcaaca  
 421acagcagcagcagcagcagcagcaacagcaacagcagcagcagcagcagcagca  
 481gcagcagcagcagcagcagcagcagcagcagcaacaggcagtgccagctgcagccgtca  
 541gcagtaacgtcccagcaggcaacacagggaacctcaggccaggcaccacagctctcca  
 601ctcacagacttcacaactgcaccttgcgggaccactccactgtatccctccccat  
 661gactcccatgacccccatcactcctgccacgccagcttcggagagttctgggattgtacc  
 721gcagctgcaaaatattgtatccacagtgaatcttggtgtaaaactgacctaaagacct  
 781tgcactcgtgcccgaacgccgaatataatccaagcggtttgctgcgtaatcatgag  
 841gataagagagccacgaaccagggcactgatttcagttctgggaaaatggtgtgcacagg  
 901agccaagagtgaagaacagtccagactggcagcaagaaaatagctagagttgtacagaa  
 961gttgggtttccagctaagttctggactcaagattcagaataggtggggagctgtga  
 1021tgtgaagttctataaaggtagaaggccttgctcaccaccaacaatttagtagtta  
 1081tgagccagagttattctcgtttaaactacagaatgatcaaacccagaattgttctct  
 1141tattttgttctggaaaagttgtattaacaggtgctaaagtcagagcagaaaattatga  
 1201agcattgaaaacatctacctattctaaagggattcaggaagacgacgtaatggctctc  
 1261atgtaccttgctcccccccccttcttttttttaaacaaatcagtttgttt  
 1321ggtaccttaaatggtggtgttgagaagatggatgtgagtgagggtgtggacca  
 1381ggtgatgcccttctgaagtgccaccgaggatgccgggaaggggcattattgtgcac  
 1441tgagaacaccgcgcagcgtgactgtgagttgctcataccgtgctgctatctgggcagcgc  
 1501tgcccattatttatatgtagatttaaacactgctgttgacaagttggttgagggaga

1561aaactttaagtgttaaagccacctctataattgattggacttttaatttaagtgtttt  
 1621ccccatgaaccacagttttatatttctaccagaaaagtaaaaatctttttaaaagtgt  
 1681tgtttttctaattataactcctaggggttattctgtgccagacacattccacctctcc  
 1741agtattgcaggacagaatatatgtgtaaatgaaaatgaatggctgtacatattttttct  
 1801ttcttcagagtactctgtacaataaatgcagtttataaaaagtgttaaaaaaaaaaaaaa  
 1861aaaaaaa

## Appendix IC

### Mus musculus peroxisome proliferator activated receptor gamma (PPAR $\gamma$ ), transcript variant 2, mRNA

LOCUS NM\_011146 1769 bp mRNA linear ROD 05-OCT-2009  
 DEFINITION Mus musculus peroxisome proliferator activated receptor gamma (PPAR $\gamma$ ), transcript variant 2, mRNA.  
 ACCESSION NM\_011146  
 SOURCE Mus musculus (house mouse)  
 ORGANISM [Mus musculus](#), Eukaryota; Metazoa; Chordata; Craniata; Vertebrata; Euteleostomi; Mammalia; Eutheria; Euarchontoglires; Glires; Rodentia; Sciurognathi; Muroidea; Muridae; Murinae; Mus.

### Primer location and region of amplification of the PPAR $\gamma$ gene in 3T3-L1 cells

(Forward primer is shown in red while the reverse primer is in blue, both are underlined; highlighted in yellow is the region that was amplified).

1 caaacaccagtggaattacagcaaatctctgtttatgctgttatgggtgaaactctg  
 61ggagattctcctgttgac ccagagcatgggtccttcgctgatgcactgcctatgagcact  
 121tcacaagaaattaccatggttgacacagagatgccattctggcccaccaacttcggaatc  
 181agctctgtggacctctccgtgatggaagaccactcgcattccttgacatcaagccctt  
 241accacagttgatttctccagcatttctgctccacactatgaagacattccattcacaga  
 301ctgacccaatgggtgctgattacaaatatgacctgaagctccaagaataccaaagtgcg  
 361atcaaaagtagaacctgcactctccaccttattattctgaaaagaccagctctacaacagg  
 421cctcatgaagaaccttctaactccctcatggccattgagtgccgagtctgtggggataaa  
 481gcatcaggctccactatggagttcatgctgtgaaaggatgcaagggttttccgaaga  
 541accatccgattgaagcttattatgataggtgatcttaactgccggatccacaaaaa  
 601agtagaataaatgcagtagtctgctggttcagaagtgccttgctgtggggatgtctcac  
 661aatgccatcaggttggcgatgccacaggccgagaaggagaagctgttggcggagatc  
 721tccagtgatcgcaccagctgaaccagagctgctgatctgcgagccctggcaaagcat  
 781ttgtatgactcatacataaagtccctcccgtgaccaaagccaagcggaggcgatcttg  
 841acaggaaagacaacggacaatcaccattgtcatctacgacatgaattcctaatgatg  
 901ggagaagataaaaatcaagttcaaacatatccccctgcaggagcagagcaaagaggtg  
 961gccatccgaattttcaaggtgccagtttcgatccgtagaagccgtgcaagagatcaca  
 1021gagtagtccaaaatataccctggttcattaacctgattgaaatgaccaagtactctg  
 1081ctcaagtatggtgcatgagatcatctacacgatctggcctccctgatgaataaagat  
 1141ggagtcctcatctcagaggccaaggattcatgaccaggagttcctcaaagcctgcgg  
 1201aagcccttgggtgactttatggagcctaagtttgagtttgctgtgaagtcaatgactg  
 1261gaattagatgacagtgacttggctatattatagctgtcattattctcagtggagaccgc  
 1321ccaggcttgctgaacgtgaagccatcgaggacatccaagacaacctgctgcaggccctg



1381gaactgcagctcaagctgaatcaccagagtcctctcagctgttcgccaaggtgctccag  
 1441aagatgacagacctcaggcagatcgtcacagagcacgtgcagctactgcatgtgatcaag  
 1501aagacagagacagacatgagcctcaccctgctccaggagatctacaaggacttgat  
 1561tagcaggaaagtcccaccgctgacaacgtgttcctctattgattgactattatgtg  
 1621agggaaaaaatctgacacctaagaaattfactgtgaaaaagcatttaaaaacaaaaagt  
 1681tttagaacatgatctattttatgcatattgtttataaagatacatttacaatttactttt  
 1741aatattaaaaattaccacattataaaatt

**Appendix ID**

**Mus musculus TATA box binding protein (TBP), mRNA**

LOCUS NM\_013684 1842 bp mRNA linear ROD 23-AUG-2009  
 DEFINITION Mus musculus TATA box binding protein (TBP), mRNA.  
 ACCESSION NM\_013684  
 VERSION NM\_013684.3 GI:172073170  
 SOURCE Mus musculus (house mouse)  
 ORGANISM [Mus musculus](#) Eukaryota; Metazoa; Chordata; Craniata; Vertebrata;  
 Euteleostomi; Mammalia; Eutheria; Euarchontoglires; Glires;  
 Rodentia; Sciurognathi; Muroidea; Muridae; Murinae; Mus.

**Primer location and region of amplification of the TBP gene in 3T3-L1 cells**

(Forward primer is shown in red while the reverse primer is in blue, both are underlined; highlighted in yellow is the region that was amplified).

1 aagagcgcaactggcgggaagtgacggcatcagatgtgcgtcaggcgttcggtggatcgag  
 61 tccggtagcgggtggcgggtatctgctggcggttggctaggttctgcggtcgcgctcatt  
 121 ttctccgagtgcccagcatcactatttcaggtgtggaagataaccagaacattgaa  
 181 gacgtttctaaggagatattcagaggatgctctagggaagatctgagtactgaagaaagg  
 241 gagaatcatggaccagaacaacagcctccacctatgctcagggttgacctcccaca  
 301 gggcgccatgactcctggaattcccattttagccaatgatgccttacggcacaggact  
 361 tactccacagcctattcagaacaccaacagtctctctatgttgaagagcaacaaagaca  
 421 gcagcagcaacagcaacagcagcagcaacaacagcaggcagtagcaactgcagcagccte  
 481 agtacagcaatcaacatctcagcaaccacacagggtgcctcaggccagaccccacaact  
 541 cttcattctcaaaactgaccactgcaccgtgccaggcaccacccctgt**acccttc**  
 601 **accaatgactcctatg**accctatcactcctgccacaccagcttctgagagctctggaat  
 661 gtaccgcagcttcaaaatattgtatctaccgtgaatcttggtgtaaaactgacctaaa  
 721 gaccattgcacttcgtgcaagaaatgctgaatataatccca**agcgattgctcagctcat**  
 781 catgagaataagagagccacggacaactgcgttgattttcagttctgaaaaatggtgtg  
 841 cacaggagccaagagtgaagaacaatccagactagcagcaagaaaatagctagagttgt  
 901 gcagaagtgggcttcccagctaagttcttagactcaagatccagaacatggtggggag  
 961 ctgtgatgtgaagttccctataaggctggaaggccttgctgaccaccagcagttcag  
 1021 tagctatgagccagaattattcctggattaatctacagaatgatcaaccagaattgt  
 1081 tctcctatgtttctggaaaagtgtattaacaggtgctaaagttagagcagagat  
 1141 ttatgaagcattgaaaacatctacccatctaaaggattcaggaagaccacatagtt  
 1201 gtctgccatgttctcctgccttcctatccacgtgtttttaaaccagtcagtttgg  
 1261 accactgatggtacagttggtgaggacactcagttacaggtggcagcatgaagtgacact

1321gtgtgtcctactgcaggatactagaaaggtccccctctgcactgaaatcacctgcage  
 1381actactgtgagttgcttgctctgtgctgctacttggcggcactgccatttattatat  
 1441ttagatttaaacactgctgttggtgattggttaaggacagaacttaagtgtc  
 1501aagccacctgtacaattggacttttcatttaaatcttcccacacaagccagttttata  
 1561tttctaccagaaaagtaaaaatcttttttaaaagtgtgttttctagtttgaactctt  
 1621aggagttattttgtgccagatactccgccttcccagattgcaggactgaatagttg  
 1681tattaatcaaaacaatggctgtacatactttcttctcagagtactctgcacaaaaac  
 1741gcagcttgtaaattgtagattttgtataaatgataccttgtaagtcatgtgatcata  
 1801ctgtcaaagaaattatttttagatataatgcctgagaccatt

## Appendix IE

### Homo sapiens ALPL gene for alkaline phosphatase, promoter region

LOCUS AB176449 4388 bp DNA linear PRI 26-OCT-2006  
 DEFINITION Homo sapiens ALPL gene for alkaline phosphatase, promoter region  
 and exon 1.  
 ACCESSION AB176449  
 SOURCE Homo sapiens (human)  
 ORGANISM [Homo sapiens](#) Eukaryota; Metazoa; Chordata; Craniata; Vertebrata;  
 Euteleostomi; Mammalia; Eutheria; Euarchontoglires; Primates; Haplorrhini;  
 Catarrhini; Hominidae

### Primer location and region of amplification of the TNSALP gene promoter region in humans

(Forward primers are shown in red while the reverse primers in blue, highlighted in yellow are sites on the gene where forward and reverse primers share the same bases. All are underlined. The whole promoter region was amplified.

1 actgggattacagggcgtgtgccactgtgcccggccccctggtatcttactaacttacttat  
 61taatgtttggtgtttattatctaccttcccactaaagtgtcagttccgtgaggataaac  
 121attctgttttgctcactggatgtccagttcctagaaggggtgctgctgcagagcaggca  
 181tccaataaacatttgttgatgaataagggtgccaagtctgcctgggataacagcctgct  
 241cactggaaaggtgacgatgacaacagtgatgggtgctttgggtgtgagggaggagcaagt  
 301taaattctcacctataaagatctttccatcaggctgcagacacagagggagtccccagcaa  
 361caatagctcatatatgcttcagtttctcatccgtgaagagagaataaaaagtcocactt  
 421ttattagcgtccaattgcocctggccacggcagcattgtcgggttaatgatgctgcttcgg  
 481ctgtcgtagtctcttccacctcatgccttttggttcatttttaactgagttaaaggtgg  
 541ggctgtaggtggcactgggaatcaaattggctgaacttgtgctcaggcctgggcttgagat  
 601aaaatgacccttttagtccaagcatcaaaacagaccaaggtttcaggcccccttgccctt  
 661aaatagattttcagggattattttctccagccctagaccacagctgactcctcaccgctc  
 721tccacgaacagacctcagagttttgtttctctctctcctcctttctttctcctttatc  
 781tctgtctactgaggtcctggctgtccccctgccccaccctaccctatgctcttgggcttc  
 841tggcctcatctctaacttagcttctaatttttctcttcttttcttttctttttttgaaa  
 901cagagtctcactctgtcaccaggtgaggtgtagtggtgctgatctcagctcactgcaac  
 961ctctgcctccagggttcaagcgtttctcgtgctcagcctcccaagtagctgggactaca  
 1021gggtgtgcagtcaccttgcctggcctaatttttatgttttcagtagagacggggtttcaccg  
 1081tggtggccaggctggtctcaaacctccggacctcaggtgatccacctgcctagcctcccaa  
 1141agtgtctgggattacagggcatgagccaccacgcccggcctaacttagcttctaattcta  
 1201gcctgggtgaacctcttaaatttttttcccaagacaaagtctcactctgttggccaggc  
 1261tggagtgacaggggtgtgatcatagctcactgcagactctaactcctggacacaagagacc  
 1321ctcccatcttggcctcccaaagtgtgggattacagggcgtgagccaccatgcctggcctg  
 1381cctagtgaacttgaaggtctagcttgcggcacaggctcatggcatgcactaacagatac  
 1441ggaataaatggatgaatggaaaaagccctggactgggaatagtaaacctggtaaccaaac

1501ccagctctgaccctgacctgtaagtaactactatctctggccttggtgtaccccatgtat  
1561agtggggattgtaaacacctgacctgccaccttatgatactgctgtgagactcaaaaga  
1621catcattagctcttaggcacagggagcttggagggttaaattccaatttgcttagtttcaa  
1681caaggaagtgggtgccccagggacaatgatggagagaaatcgaatgtaatgagctggtgcc  
1741accagctgagtggtcctgaaatcatggcatctgggttgcaacttagagattgtccagttca  
1801aaaggccagaaggaatctgaacctcgatgggaaaagtgacttgctcagctccccagcaag  
1861ccagggcagagctggaggatggactggagtctcctgggtccaggtccaggacttctttcc  
1921gctgtgttgacagagccaggaggaggggcaaccggggagcaggggaggcaagggctgctg  
1981gatgccccatctcagttgaattctccttgagggaccagcccaggagcagagtaagaggg  
2041tttgaggggtggaaggtggcagggctggccaagcagatagtcctgctgctgataaccaa  
2101tccctgaaatcccaggtggagggacttgagggcaaatcacagacatgggggacctaatg  
2161ctggccatgtggtcaaccagaagtgcctgcccctcatagctttggggagatcagaagt  
2221agggatagggctgggtgtggtggctcatgcctgtaatccatcactttgggataaggagg  
2281caggggatcacttgagcttaggagttcgagaccagcctgagcaacatagcaaacctctg  
2341ttctttacaaaaaatacaaaaaattagccgggctggtgggtgcacacctgtagtcctggc  
2401tgctggggaggctgaggtgggaagatcacttgagcccgggaggctcgaggctgcagtgagc  
2461tgacatcatgctactgcattccagcctaggcaatagagtgggacctgtctcaaaaaaaa  
2521aaaaaaaaaagtccaggggtgctggccccatgataggtgcaatgggtgctccaattcct  
2581ctggctctgcctcccagcctctgtccaagcaacagggcagatTTTTccatgcctggggactt  
2641gccccctggctcactgatgatgataccatcttaagtctcctggaatccttaaaccttct  
2701tggcatttgtgagcaagtattgagccccctcccatgttttagggccagtgctgggtgcttt  
2761caactgcaatttcttacagaggatggtatttctaaactccattcatttgctaactccat  
2821gatttttgccatatcaccacccatgaaatacataaataaatagtatttactcaatatt  
2881ttgactcacttttaaaaaacataaaacttatctgaaaagggaaacctatgtcacgcctctaa  
2941ataaacagtatcaaccaaaaaatacaaaaagaaacaaaaataaatacaaaagacattcttgg  
3001ttctggcaccagggccccagttctggctccaaccttactgagaagtcacatgatctctctg  
3061ggcctcagttttctcctctggaaaatggagcttttggagttaatgcatgcacagtgct  
3121ggcctgagactggcatggagtgagtggaagagaggttgctgacctggctaaaattgg  
3181tctctgggcagacattttcccaagggccactgagaagaccctcctggttaggagtcagtga  
3241gctctgtcgctgaggcattcaaacagagcctgcggacttctcactgcgaagttgccag  
3301agaattcagtgctcagaggaaagggagtggttattccatcagagctgggtccccaggagc  
3361gggagcagggcctgtagcaccagcctctgtccctggctcccgtctatccgggattttag  
3421cgtttcctctgtagttttcaagcactgtctcatatgactctcgcaccagcagagggccag  
3481gggagatgggtgtctgcctgttaaagaggggcccggctgggtccacataggtcaagtgacttg  
3541gccaaggtcaccagagcagagttttgaaacttgagctgtctgactcaactgcctgggaagt  
3601gcctgccccctcctctggcatccagggagcatgtcctggggctctggctgggacatagccg  
3661gacacctgcgggcccctttacgtctctaaagagagaaagaggggaagggcccctgtctaggg  
3721gggtgggttccctccagatgccaccccctccgaggtccccttctgcttctcttgoggtagc  
3781cagggagggcagcccacgggcaggaagcgggggtgggggtgcagagtcagaggtgcacgt

**Appendix IF**

LOCUS NM\_000478 2606 bp mRNA linear PRI 25-SEP-2011  
DEFINITION Homo sapiens alkaline phosphatase, liver/bone/kidney (ALPL), transcript variant 1, mRNA.  
ACCESSION NM\_000478  
VERSION NM\_000478.4 GI:294712525  
KEYWORDS .  
SOURCE Homo sapiens (human)  
ORGANISM [Homo sapiens](#)  
Eukaryota; Metazoa; Chordata; Craniata; Vertebrata; Euteleostomi; Mammalia; Eutheria; Euarchontoglires; Primates; Haplorrhini; Catarrhini; Hominidae; Homo.  
REFERENCE 1 (bases 1 to 2606)  
AUTHORS Mentrup,B., Marschall,C., Barvencik,F., Amling,M., Plendl,H., Jakob,F. and Beck,C.  
TITLE Functional characterization of a novel mutation localized in the start codon of the tissue-nonspecific alkaline phosphatase gene  
JOURNAL Bone 48 (6), 1401-1408 (2011)

Location of the siRNA target sequence is shown in red.

CCGGGCCTCACTCGGGCCCCGCGGCCGCTTTATAAGGCGGCGGGGGTGGTGGCCCCGGGCCGCGTTGCGCTCCC  
GCCACTCCGCGCCCGCTATCCTGGCTCCGTGCTCCCACGCGCTTGTGCCTGGACGGACCCTCGCCAGTGCTCTGC  
GCAGGATTGGAACATCAGTTAACATCTGACCACTGCCAGCCCACCCCTCCCACCCACGTGATTGCATCTCTGGG  
CTCCAGGGATAAAGCAGGTCTTGGGGTGCACCATGATTTACCATTCTTAGTACTGGCCATTGGCACCTGCCTTAC  
TAACTCCTTAGTGCCAGAGAAAAGAGAAAAGACCCCAAGTACTGGCGAGACCAAGCGCAAGAGACACTGAAATATGCC  
CTGGAGCTTCAGAAGCTCAACACCAACGTGGCTAAGAATGTATCATGTTCTCTGGGAGATGGGATGGGTGTCTCC  
ACAGTGACGGCTGCCCCGATCCTCAAGGTGAGCTCCACCACAACCCTGGGGAGGAGACCAGGCTGGAGATGGAC  
AAGTTCCCCTTCGTGGCCCTCTCAAGACGTACAACACCAATGCCAGGTCCCTGACAGCGCCGGCACCCGCCACCG  
CCTACCTGTGTGGGGTGAAGGCCAATGAGGGCACCGTGGGGTAAGCGCAGCCACTGAGCGTTCCTGGTGAACA  
CCACCCAGGGGAACGAGGTACCTCCATCCTGCGCTGGGCCAAGGACGCTGGGAAATCTGTGGGCATTGTGACCA  
CCACGAGAGTGAACCATGCCACCCCAAGCGCCGCTACGCCACTCGGCTGA**CCGGGACTGGTACTCAGACAA**CGA  
GATGCCCCCTGAGGCCTTGAGCCAGGGCTGTAAGGACATCGCCTACCAGCTCATGCATAACATCAGGGACATTGAC  
GTGATCATGGGGGGTGGCCGAAATACATGTACCCCAAGAATAAACTGATGTGGAGTATGAGAGTGACGAGAAA  
GCCAGGGGCACGAGGCTGGACGGCTGGACCTCGTTGACACCTGGAAGAGCTTCAAACCGAGATAACAAGCACTCC  
CACTTCATCTGGAACCGCACGGAACCTCTGACCCTTGACCCCAACAATGTGGACTACCTATTGGGTCTCTCGAGC  
CAGGGGACATGCAGTACGAGCTGAACAGGAACAACGTGACGGACCCGTCCTCTCCGAGATGGTGGTGGTGGCCA  
TCCAGATCCTGCGGAAGAACCCCAAAGGCTTCTTCTTGCTGGTGGAAAGGAGGCAGAAATTGACCACGGGCACCATG  
AAGGAAAAGCCAAGCAGGCCCTGCATGAGGCGGTGGAGATGGACCGGGCCATCGGGCAGGCAGGCAGCTTGACC  
TCCTCGGAAGACACTCTGACCGTGGTCACTGCGGACCATTCCCAGCTTTCACATTTGGTGGATACACCCCCCGTG  
GCAACTCTATCTTTGGTCTGGCCCCATGCTGAGTGACACAGACAAGAAGCCCTTCACTGCCATCCTGTATGGCAA  
TGGGCTGGCTACAAGGTGGTGGGCGGTGAACGAGAGAATGTCTCCATGGTGGACTATGCTCACAACTACCA  
GGCGCAGTCTGCTGTGCCCTGCGCCACGAGACCCACGGCGGGGAGGACGTGGCCGTCTTCTCAAGGGCCCCAT  
GGCGCACCTGCTGCACGGCGTCCACGAGCAGAACTACGTCCCCACGTGATGGCGTATGCAGCCTGCATCGGGGC  
CAACCTCGGCCACTGTGCTCCTGCCAGCTCGGCAGGCAGCCTTGTGCAAGGCCCTGCTGCTCGCGCTGGCCCT  
CTACCCCTGAGCGTCTGTTCTGAGGGCCCAGGGCCCCGGGCACCCACAAGCCCGTGACAGATGCCAACTTCCCAC  
ACGGCAGCCCCCCCCCTCAAGGGGCAGGGAGGTGGGGGCTCCTCAGCCTTGCAACTGCAAGAAAGGGGACCCAA  
GAAACCAAAGTCTGCCGCCACCTCGCTCCCCTCTGGAATCTTCCCAAGGGCCAAACCCACTTCTGGCCTCCAGC  
CTTTGCTCCCTCCCCGCTGCCCTTTGGCCAACAGGGTAGATTTCTCTTGGGCAGGCAGAGAGTACAGACTGCAGAC  
ATTCTCAAAGCCTCTTATTTTCTAGCGAACGATTTCTCCAGACCCAGAGGCCCTGAAGCCTCCGTGGAACATTCT  
GGATCTGACCCTCCAGTCTCATCTCCTGACCCTCCCACTCCCATCTCCTTACCTCTGGAACCCCCCAGGCCCTACA

ATGCTCATGTCCCTGTCCCCAGGCCAGCCCTCCTTCAAGGGAGTTGAGGTCTTTCTCCTCAGGACAAGGCCTTGC  
TCACTCACTCACTCCAAGACCACCAGGGTCCCAGGAAGCCGGTGCCTGGGTGGCCATCCTACCCAGCGTGGCCCA  
GGCCGGAAGAGCCACCTGGCAGGGCTCACACTCCTGGGCTCTGAACACACACGCCAGCTCCTCTCTGAAGCGAC  
TCTCCTGTTTGAACGGCAAAAAAAAAATTTTTTTTTCTCTTTTTGGTGGTAAAGGGAACACAAAACATTTAA  
ATAAACTTTCAAATATTTCCGAGGACAAAAAAAAAAAA

**Appendix IG**

LOCUS NM\_007431 2521 bp mRNA linear ROD 25-SEP-2011  
DEFINITION Mus musculus alkaline phosphatase, liver/bone/kidney (Alpl), mRNA.  
ACCESSION NM\_007431  
VERSION NM\_007431.2 GI:160333225  
KEYWORDS .  
SOURCE Mus musculus (house mouse)  
ORGANISM [Mus musculus](#)  
Eukaryota; Metazoa; Chordata; Craniata; Vertebrata; Euteleostomi; Mammalia; Eutheria; Euarchontoglires; Glires; Rodentia; Sciurognathi; Muroidea; Muridae; Murinae; Mus; Mus.  
REFERENCE 1 (bases 1 to 2521)  
AUTHORS Dubose,A.J., Smith,E.Y., Yang,T.P., Johnstone,K.A. and Resnick,J.L.  
TITLE A new deletion refines the boundaries of the murine Prader-Willi syndrome imprinting center  
JOURNAL Hum. Mol. Genet. 20 (17), 3461-3466 (2011)  
PUBMED [21659337](#)  
REFERENCE 2 (bases 1 to 2521)  
AUTHORS Hirota,T., Ohta,H., Shigeta,M., Niwa,H. and Saitou,M.  
TITLE Drug-inducible gene recombination by the Dppa3-MER Cre MER transgene in the developmental cycle of the germ cell lineage in mice  
JOURNAL Biol. Reprod. 85 (2), 367-377 (2011)

Location of the siRNA target sequence on the mouse TNSALP gene is shown in red.

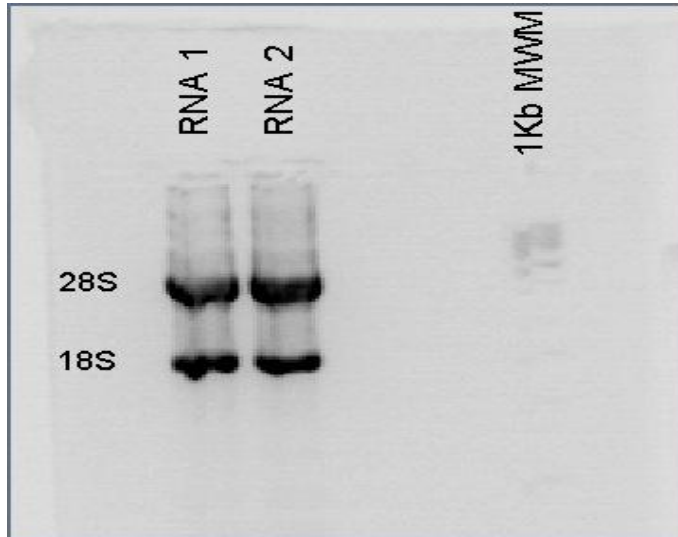
GAGGCCGGCGGGTGTCTCGGCCAGGCCCTTCATAAGCAGGCGGGGAGGTGGCCGCCAGAGTACGCTCC  
CGCCACTGCGCTCCTTAGGGCTGCCGCTCGCGAGCCGGAACAGACCCTCCCACGAGTGCCTG**CAGGATC**  
**GGAACGTCAATTAA**CGTCAATTAACATCTGACGCTGCCCCCCCCCCCCCTCTCCACCATCTGGGCTCCA  
GCGAGGGACGAATCTCAGGGTACACCATGATCTCACCATTTTTAGTACTGGCCATCGGCACCTGCCTTAC  
CAACTCTTTTGTGCCAGAGAAAAGAGAGACCCAGTTACTGGCGACAGCAAGCCCAAGAGACCTTGAAA  
AATGCCCTGAAACTCCAAAAGCTCAACACCAATGTAGCCAAGAATGTCATCATGTTCTGGGAGATGGTA  
TGGGCGTCTCCACGTAACCGCTGCCCGAATCCTTAAGGGCCAGCTACACCACAACACGGGCGAGGAGAC  
CCGGCTGGAGATGGACAAATTTCCCTTTGTGGCCCTCTCCAAGACATATAACACCAACGCTCAGGTCCCT  
GACAGCGCGGGCACTGCCACTGCCTACTTGTGTGGCGTGAAGGCCAACGAGGGCACAGTGGGAGTGAGCG  
CAGCCACAGAGCGCACGCGATGCAACACCACTCAGGGCAATGAGGTCACATCCATCCTGCGCTGGGCCAA  
GGATGCTGGGAAGTCCGTGGGCATTGTGACTACCACTCGGGTGAACCACGCCACACCCAGTGCAGCCTAC  
GCACACTCGGCCGATCGGGACTGGTACTCGGATAACGAGATGCCACCAGAGGCTCTGAGCCAGGGCTGCA  
AGGACATCGCATATCAGCTAATGCACAATATCAAGGATATCGACGTGATCATGGGTGGCGGCCGAAATA  
CATGTACCCGAAGAACAGAACTGATGTGGAATACGAACTGGATGAGAAGGCCAGGGGTACAAGGCTAGAT  
GGCCTGGATCTCATCAGTATTTGGAAGAGCTTTAAACCCAGACACAAGCATTCCCCTATGTCTGGAACC  
GCACTGAACTGCTGGCCCTTGACCCCTCCAGGGTGGACTACCTCTTAGGTCTTTGAGCCCGGGGACAT  
GCAGTATGAATTGAATCGGAACAACCTGACTGACCCTTCGCTCTCCGAGATGGTGGAGGTGGCCCTCCGG

ATCCTGACCAAAAACCTCAAAGGCTTCTTCTTGCTGGTGGAAAGGAGGCAGGATTGACCACGGACATCATG  
AGGGTAAGGCCAAGCAGGCTCTGCATGAAGCAGTGGAGATGGACCAGGCCATTGGCAAGGCAGGCGCCAT  
GACATCCCAGAAAAGACACCTTGACTGTGGTTACTGCTGATCATTCCCACGTTTTACATTGGTGGATAC  
ACCCCCGGGGCAACTCCATCTTTGGTCTGGCTCCCATGGTGGAGCGACACGGACAAGAAGCCCTTACGG  
CCATCCTATATGGTAACGGGCCTGGCTACAAGGTGGTGGACGGTGAACGGGAAAATGTCTCCATGGTAGA  
TTAGCTCACAACAACCTACCAGGCCAGTCCGCTGTTCCCTGCGCCATGAGACCCACGGTGGAGAAGAC  
GTGGCGGTCTTTGCCAAGGGCCCGATGGCACACCTGTTACGGCGTCCATGAGCAGAACTACATTCCCC  
ATGTGATGGCGTATGCCTCCTGCATTGGGGCCAACCTTGACCACTGTGCCTGGGCCGGCTCTGGGAGCGC  
ACCCTCCCCAGGGGCCCTGCTGCTTCCACTGGCTGTGCTCTCCCTACGCACCCTGTTCTGAGGGTGCAGG  
TCCCACAAGCCCGCAATGGACAGCCAGCTCCCCTCCTTTGTGGCCCACCACCGGGCAGCCCACACTCAA  
GGGAGAGGTCCAGGCAACTTCCAGCAGGAACAGAAAGTTCGCTATCTGCCTTGCCTGTATCTGGAATCCTC  
CATGGGCCAGATTCTGGCTCTGCCTTTATCCCTAGTTATTGCCCTTTGGCCAGCAGGTTTCTCTTG  
GGCAGGCAAGACACAGACTGCACAGATTCCCAAAGCACCTTATTTTTCTACCAAATATATTCTCCAGACC  
CTGCAACCTCCATGGAACATTCCAGATCTGACCTTCTCTCCTCCATCCCTTCCCTTCCCTCTGGAACACT  
GGGCCCCATAGTCACGGCCAGTCTCAAGCCCAACCCTCCCTGGGGGGAAGACCAGGTCTGCTCAGGATG  
AGACTCCCAGGAAGCCACCTCCGGGGTTGGCTGTCTACCCAGGGTTGCCAAGCTGGGAAGAACACTCCAG  
CCGGACAGGACACACACACACTCCCCACCCAATTGCAGAGACTCGCCAACCCTTCACTGAAGTGGCTC  
TCCTGTTTGAATAGCGGGTGGGGTGGGGGAGAAGAAAGAAAGAAAAAATTTTTAATTTCTCT  
TTTTGGTGTGGTTAAAAGGGAACACAAGACATTTAATAAAACATCCCAAATATTTCTGAGGCCAAAAA

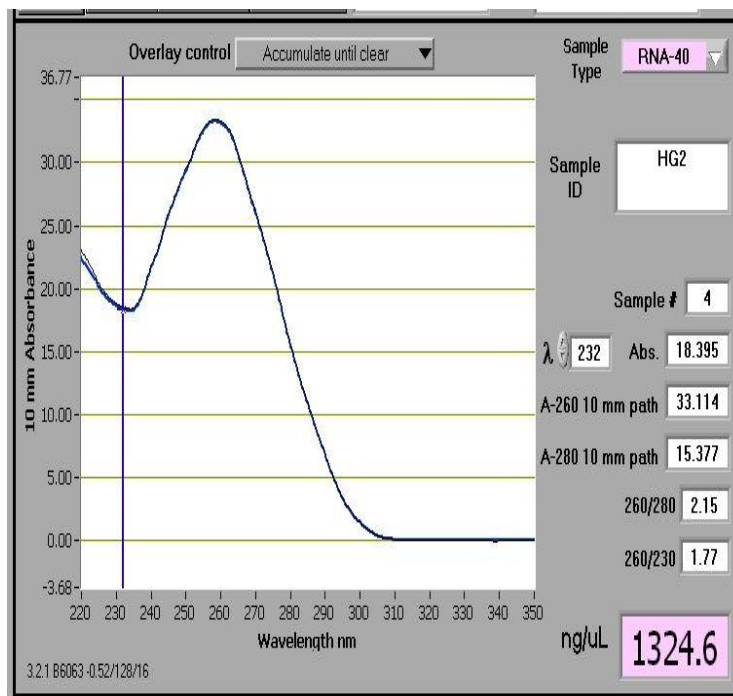
A

**Appendix IH**

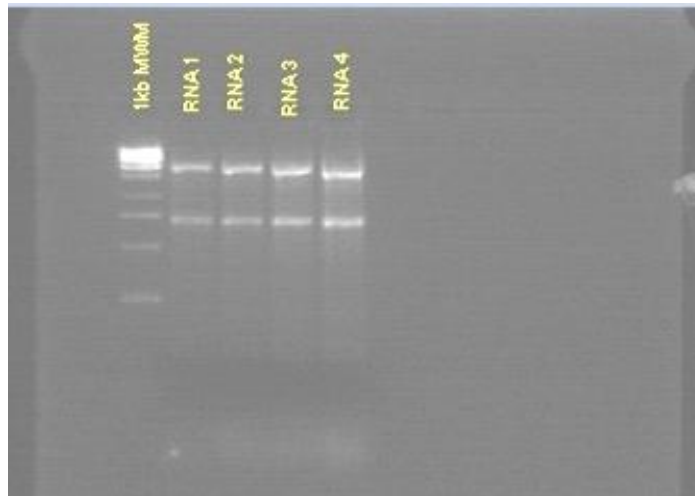
**RNA quality in HepG2 cells as determined by gel electrophoresis and the Nanodrop 1000 spectrophotometer**



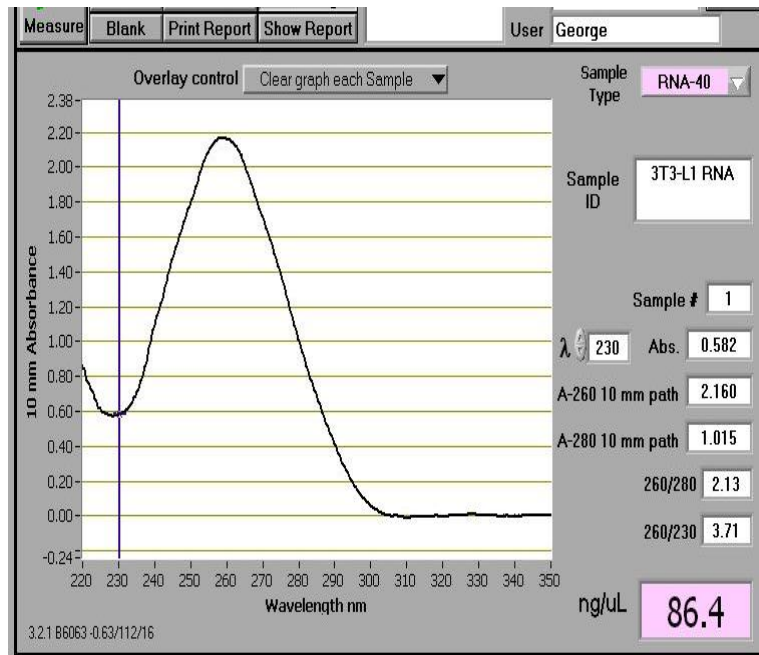
3 $\mu$ g of total RNA was added to 2 $\mu$ l of gel loading dye and separated on 1% TBE agarose gel at 98V for 40 min



**RNA quality in 3T3-L1 cells as determined by gel electrophoresis and the Nanodrop 1000 spectrophotometer**



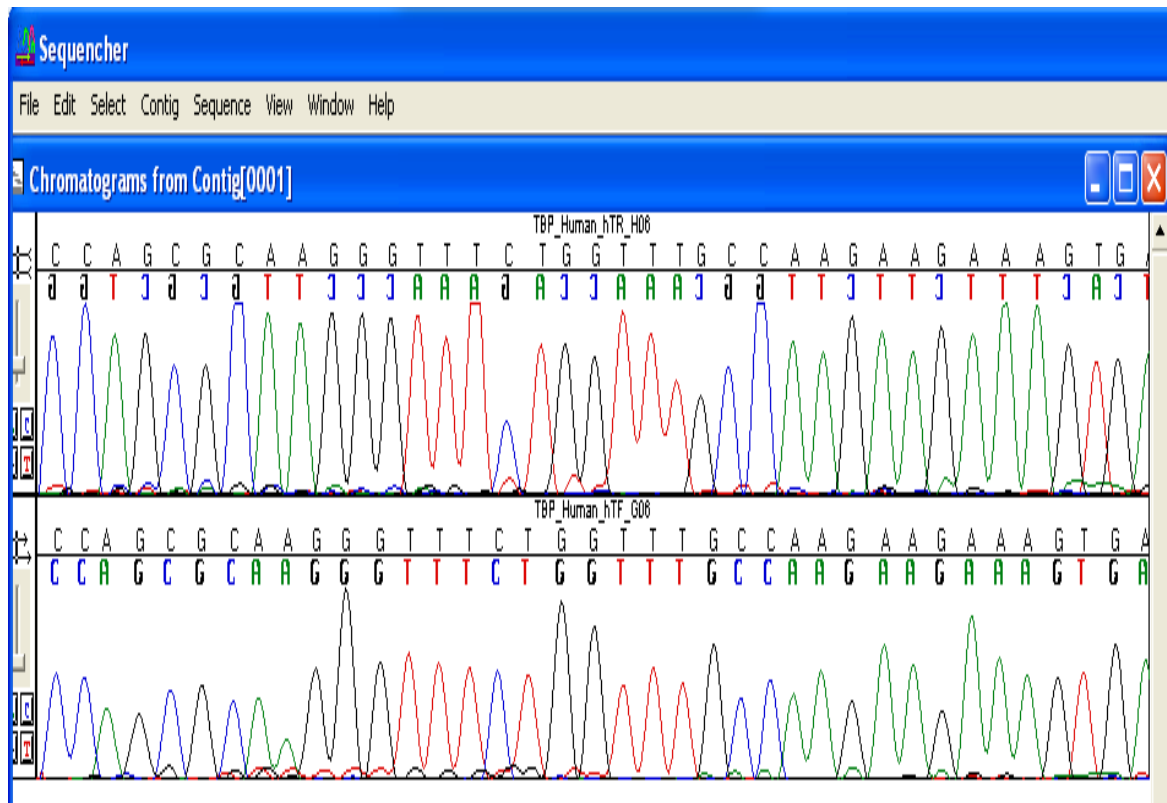
3 $\mu$ g of total RNA was added to 2 $\mu$ l of gel loading dye and separated on 1% TBE agarose gel at 98V for 40 min





**Consensus sequence of the TBP gene in HepG2 cells and a portion of its chromatogram below**

GATAACCCAAGGAATTGAGGAAGTTGCTGAGAAGAGTGTGCTGGAGATGCTCTAGGAAAAA  
ATTGAATAGTGAGACGAGTTCCAGCGCAAGGGTTTCTGGTTTGCCAAGAAGAAAGTGAACA  
TCATGGATCAGAACAACAGCCTGCCACCTTACGCTCAGGGCTTGGCCTCCCCTCAGGGTGCC  
ATGACTCCC

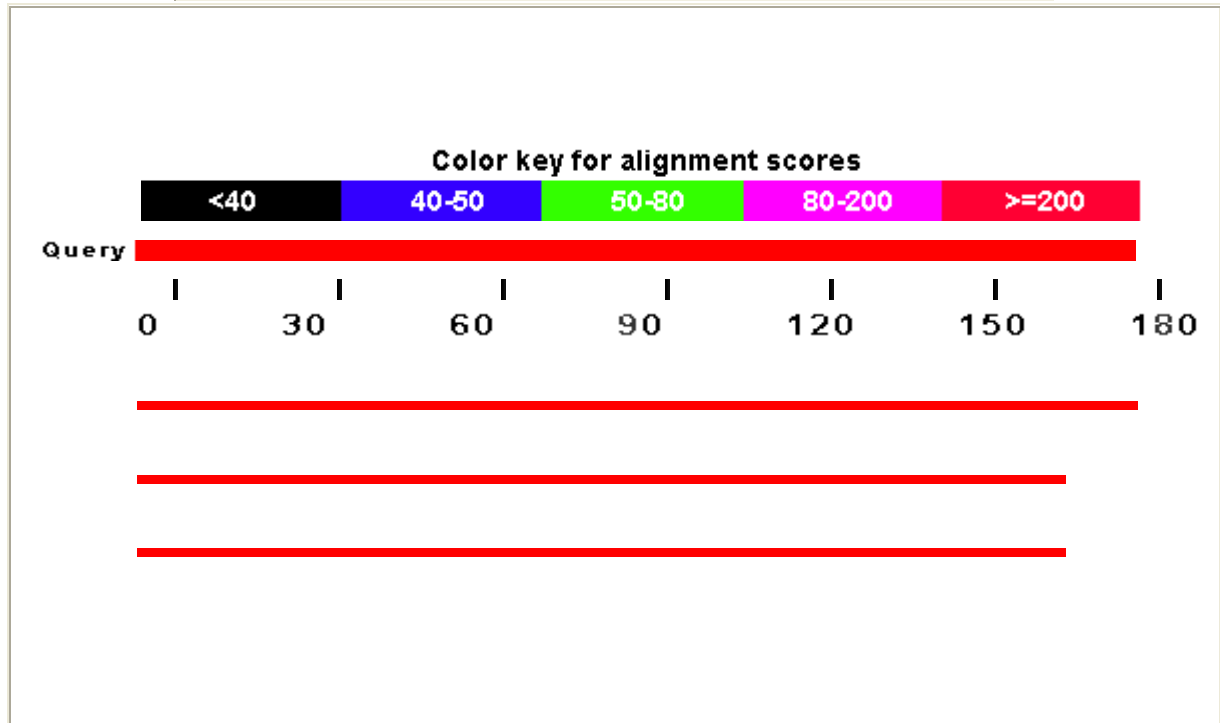


**BLAST results of sequenced PCR product of TBP gene in HepG2 cells**



BLAST

Mouse-over to show defline and scores, click to show alignments



[Descriptions](#)

Legend for links to other resources: [U](#)UniGene [E](#)GEO [G](#)Gene [S](#)Structure [M](#)Map Viewer

PubChem BioAssay

Accession transcripts	Description	Max score	Total score	Query coverage	E value	Max identity	Links
<a href="#">NM_003194.3</a>	Homo sapiens TATA box binding protein (TBP), mRNA	<a href="#">357</a>	357	100%	1e-96	100%	
Genomic sequences[ <a href="#">show first</a> ]							
<a href="#">NT_025741.15</a>	Homo sapiens chromosome 6 genomic contig, GRCh37 reference primary assembly	<a href="#">331</a>	<a href="#">331</a>	92%	7e-89	100%	
<a href="#">NW_001838996.1</a>	Homo sapiens chromosome 6 genomic contig, alternate assembly (based on HuRef),	<a href="#">331</a>	<a href="#">331</a>	92%	7e-89	100%	

> [refNM\\_003194.3](#) Homo sapiens TATA box binding protein (TBP), mRNA

Length=1867

Score = 357 bits (193), Expect = 1e-96  
 Identities = 193/193 (100%), Gaps = 0/193 (0%)  
 Strand=Plus/Plus

```

Query 1 GATAACCCAAGGAATTGAGGAAGTTGCTGAGAAGAGTGTGCTGGAGATGCTCTAGGAAA 60
      |
Sbjct 109 GATAACCCAAGGAATTGAGGAAGTTGCTGAGAAGAGTGTGCTGGAGATGCTCTAGGAAA 168

Query 61 AATTGAATAGTGAGACGAGTTCCAGCGCAAGGGTTTCTGGTTTGCCAAGAAGAAAGTGAA 120
      |
Sbjct 169 AATTGAATAGTGAGACGAGTTCCAGCGCAAGGGTTTCTGGTTTGCCAAGAAGAAAGTGAA 228

Query 121 CATCATGGATCAGAACAACAGCCTGCCACCTTACGCTCAGGGCTTGGCCTCCCCTCAGGG 180
      |
Sbjct 229 CATCATGGATCAGAACAACAGCCTGCCACCTTACGCTCAGGGCTTGGCCTCCCCTCAGGG 288

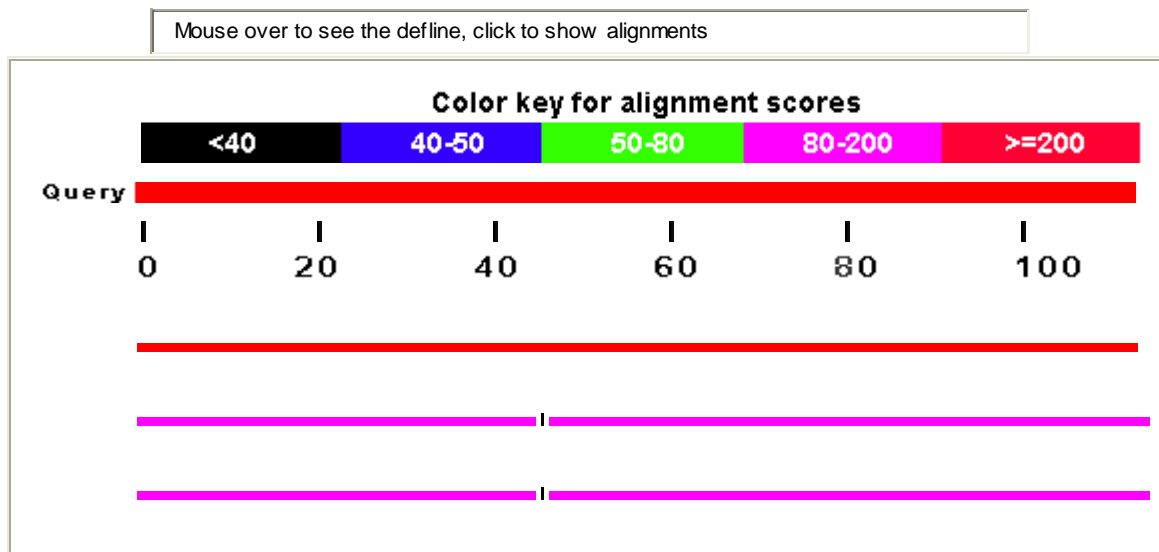
Query 181 TGCCATGACTCCC 193
      |
Sbjct 289 TGCCATGACTCCC 301
  
```

**Consensus sequence of the TBP gene in 3T3-L1 cells and a portion of its chromatogram below**

TTACCCTTCACCAATGACTCCTATGACCCCTATCACTCCTGCCACACCAGCTTCTGAGAGCTC  
 TGGAAATTGTACCGCAGCTTCAAAATATTGTATCTACCGTGAATCTTGGCTGTAAACTTGACCT  
 AAAGACCATTGCACTTCGTGCAAGAAATGCTGAATATAATCCCAAGCGATTTGCTGCAGTCA  
 TCATT



**BLAST results of sequenced PCR product of TBP gene in 3T3-L1 cells**



[Descriptions](#)

Legend for links to other resources: [U](#)UniGene [E](#)GEO [G](#)Gene [S](#)Structure [M](#)Map Viewer



PubChem BioAssay

Sequences producing significant alignments:

Accession	Description	Max score	Total score	Query coverage	E value	Max identity	Links
<a href="#">NM_013684.2</a>	Mus musculus TATA box binding protein (Tbp), mRNA	<a href="#">219</a>	219	100%	1e-56	100%	<a href="#">U</a> <a href="#">E</a> <a href="#">G</a> <a href="#">M</a>
Genomic sequences[ <a href="#">show first</a> ]							
<a href="#">NT_039649.7</a>	Mus musculus chromosome 17 genomic contig,	<a href="#">132</a>	220	100%	1e-30	100%	

strain

C57BL/6J

>  [ref|NM\\_013684.2](#)  Mus musculus TATA box binding protein (Tbp), mRNA

Length=1669

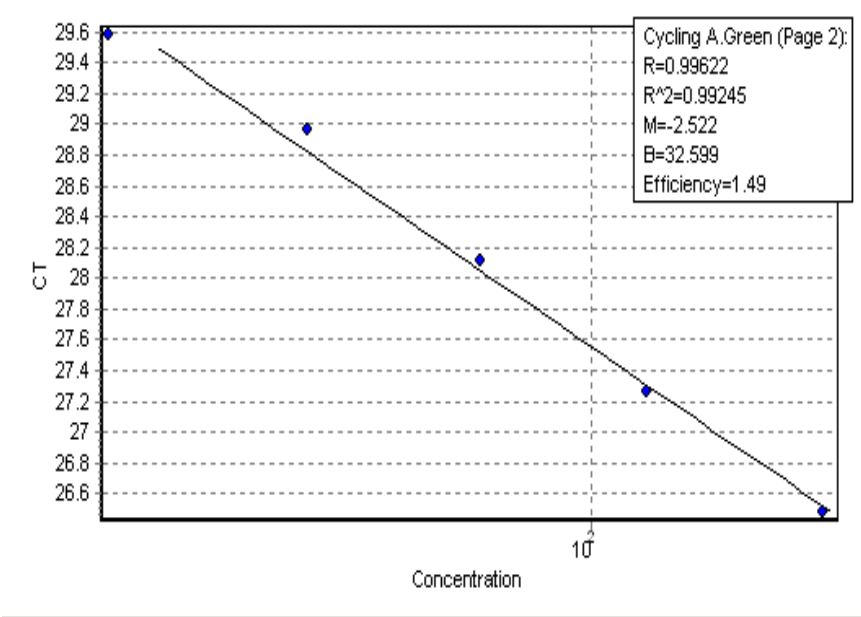
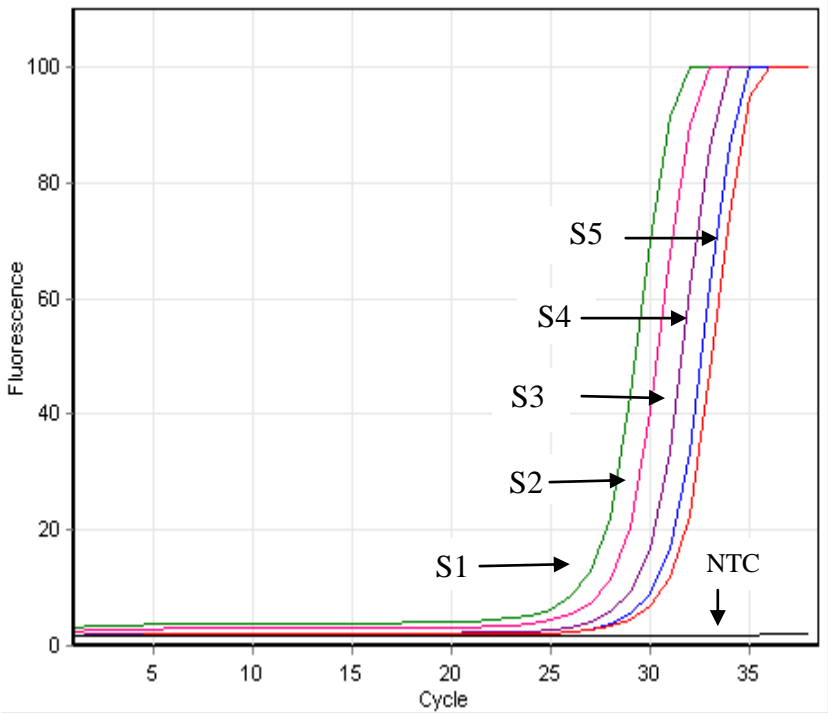
Score = 219 bits (118), Expect = 1e-56  
 Identities = 118/118 (100%), Gaps = 0/118 (0%)  
 Strand=Plus/Plus

```

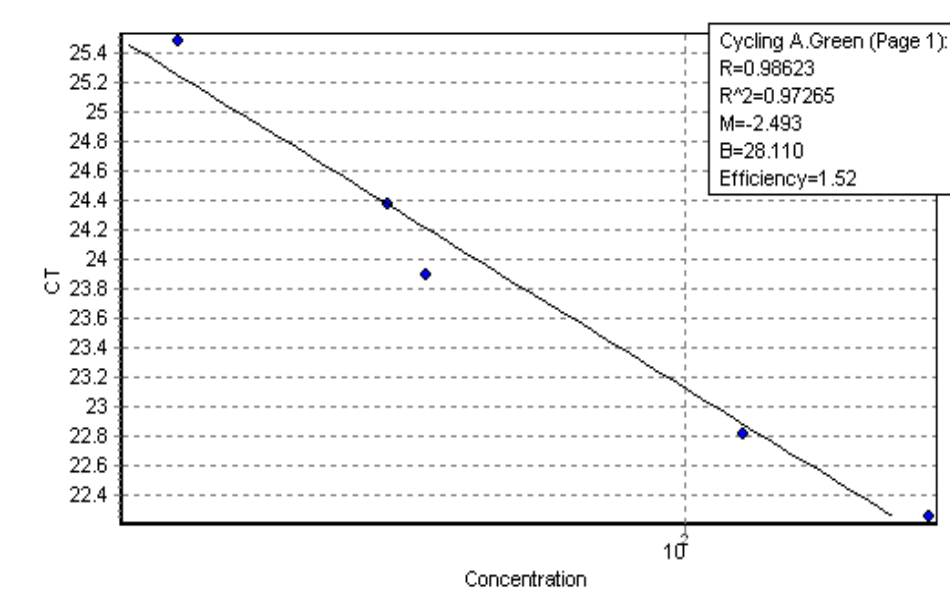
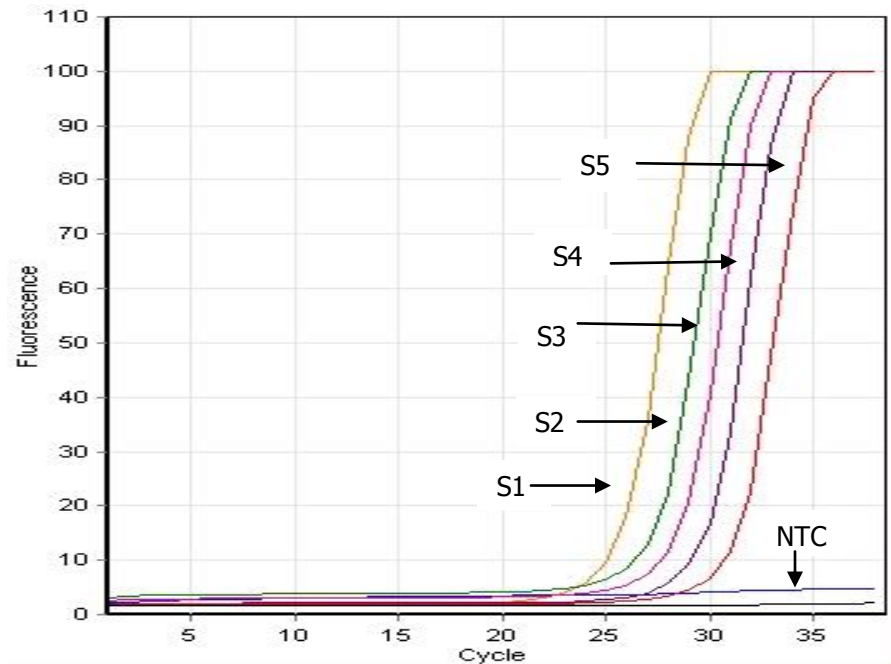
Query 1 CCTGCCACACCAGCTTCTGAGAGCTCTGGAATTGTACCGCAGCTTCAAAATATTGTATCT 60
      |||||||||||||||||||||||||||||||||||||||||||||||||||||||||||
Sbjct 607 CCTGCCACACCAGCTTCTGAGAGCTCTGGAATTGTACCGCAGCTTCAAAATATTGTATCT 666

Query 61 ACCGTGAATCTTGGCTGTAAACTTGACCTAAAGACCATTGCACTTCGTGCAAGAAATG 118
      |||||||||||||||||||||||||||||||||||||||||||||||||||||||||||
Sbjct 667 ACCGTGAATCTTGGCTGTAAACTTGACCTAAAGACCATTGCACTTCGTGCAAGAAATG 724
  
```

**Standard curve and efficiency of TBP gene amplification in HepG2 cells. S1-S5 are standards, NTC is the no template control. S1 is the standard with highest DNA concentration while S5 has the lowest concentration.**

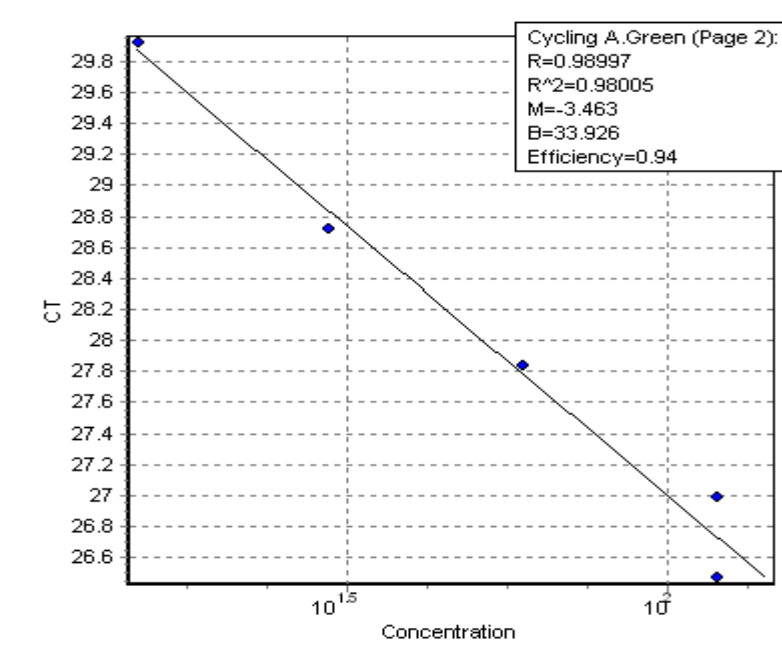
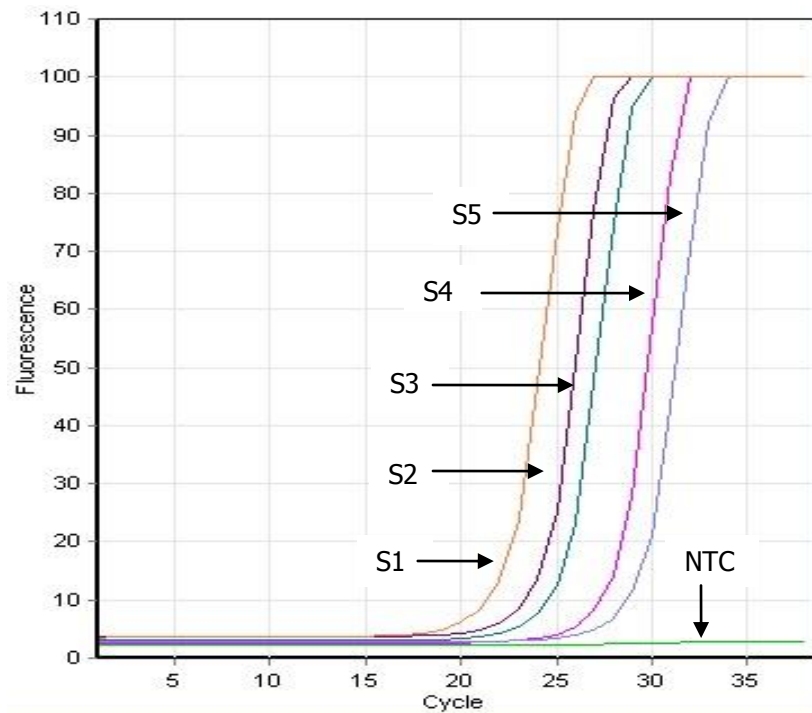


Standard curve and efficiency of PPAR $\gamma$  gene amplification in HepG2 cells. S1-S5 are standards, NTC is a non-template control. S1 is the standard with highest DNA concentration while S5 has the lowest concentration.

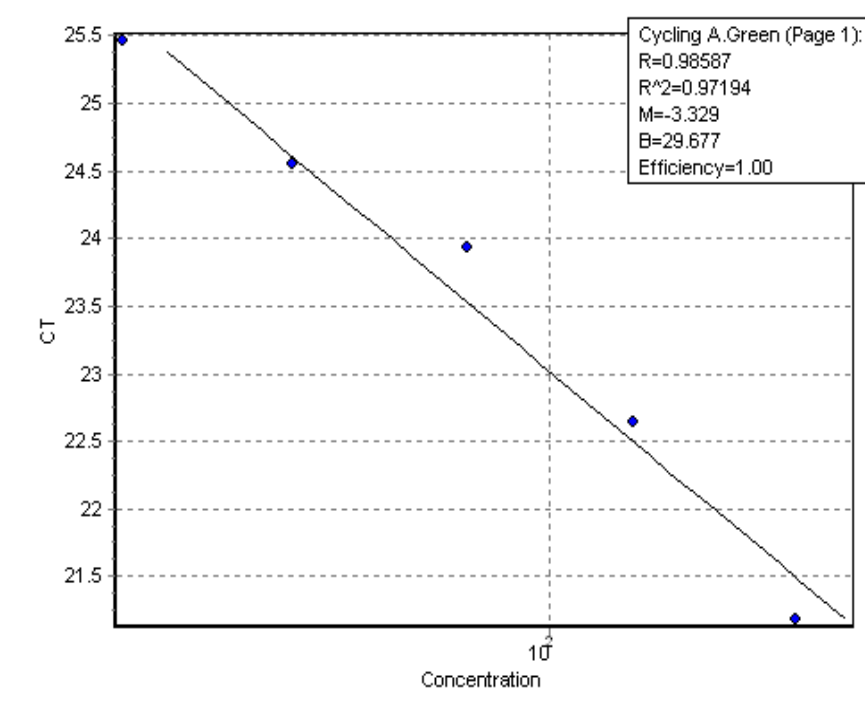
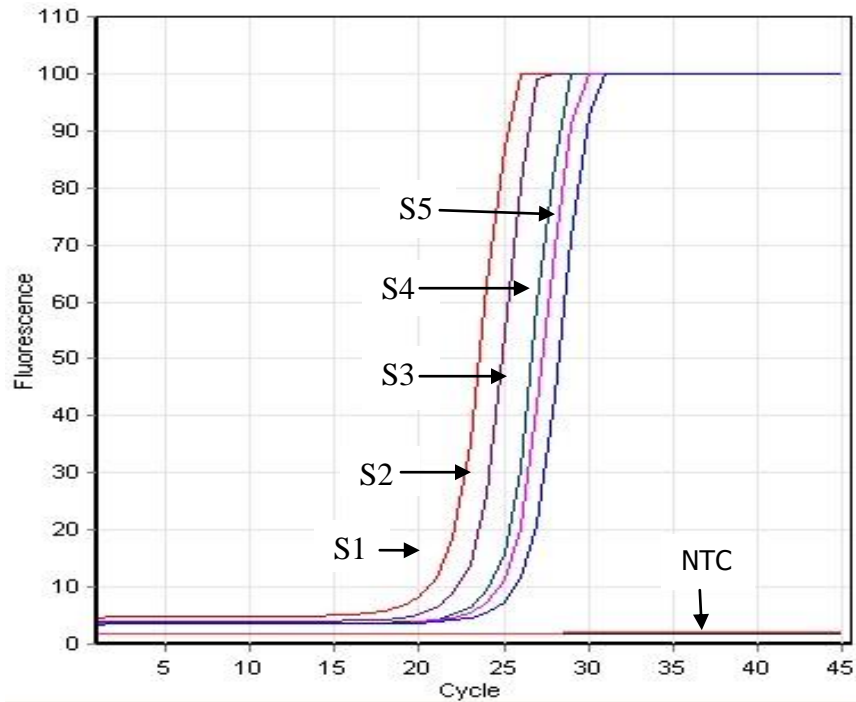




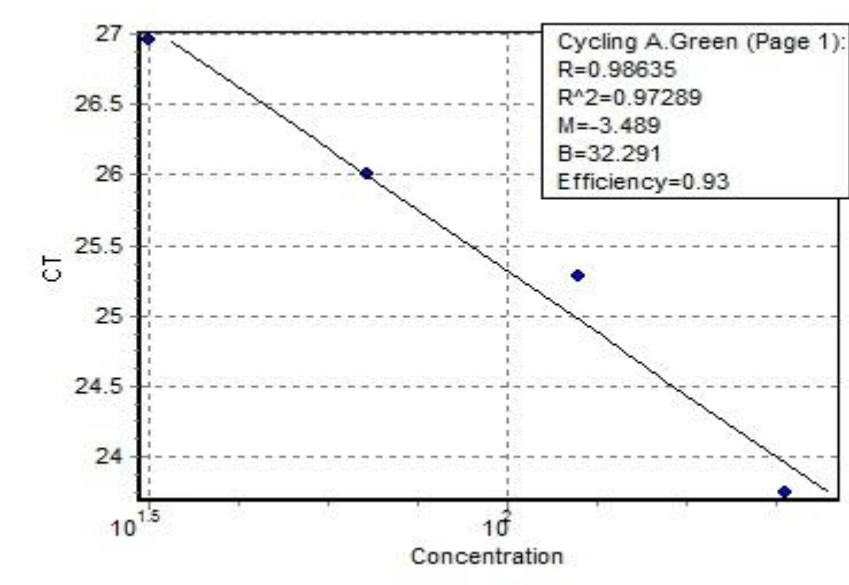
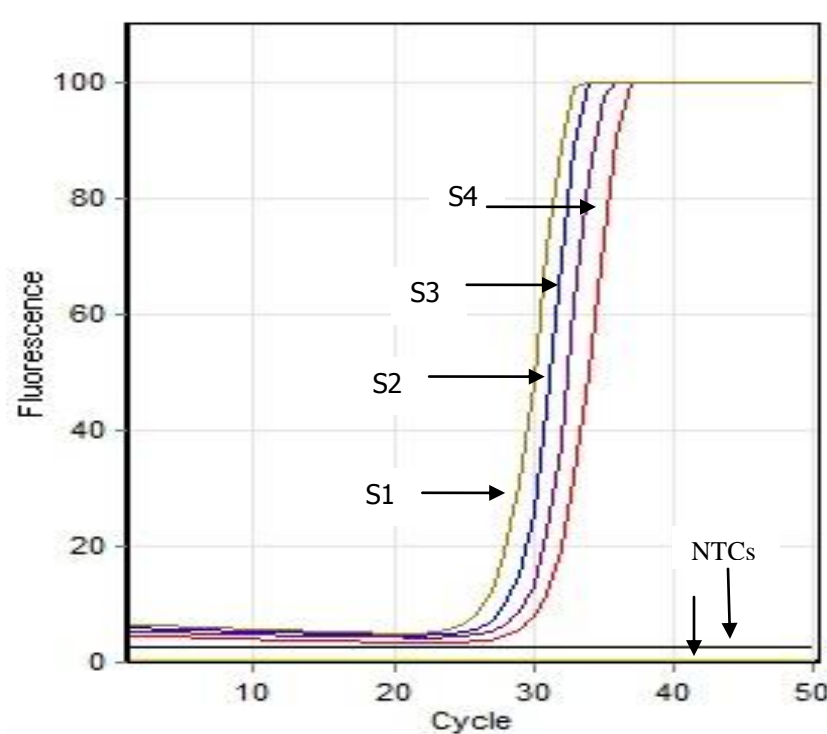
Standard curve and efficiency of TBP gene amplification in 3T3-L1 cells. S1-S5 are standards, NTC is the no template control. S1 is the standard with highest DNA concentration while S5 has the lowest concentration.



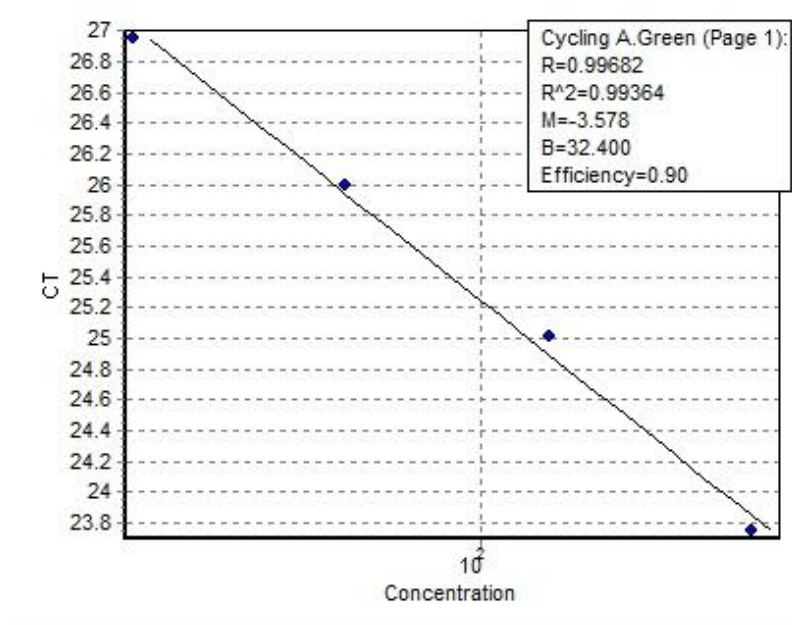
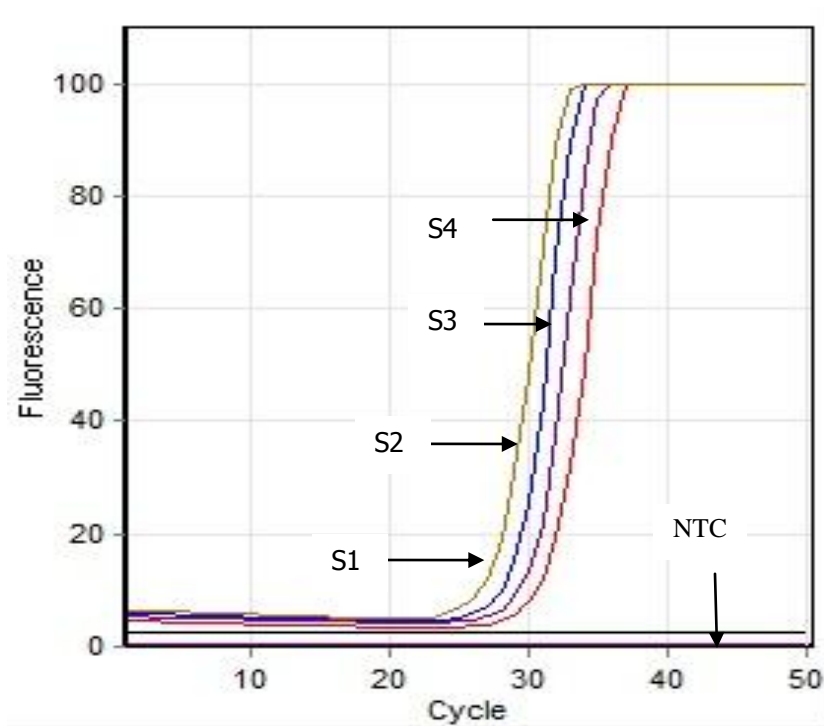
Standard curve and efficiency of PPAR $\gamma$  gene amplification in 3T3-L1 cells. S1-S5 are standards, NTC is the no template control. S1 is the standard with highest DNA concentration while S5 has the lowest concentration.



Standard curve and efficiency of ALP gene amplification in HepG2 cells (S1-S4 are standards, NTC is the no template control. S1 is the standard with highest DNA concentration while S4 has the lowest concentration).



Standard curve and efficiency of ALP gene amplification in 3T3-L1 cells. (S1-S5 are standards, NTC is the no template control. S1 is the standard with highest DNA concentration while S5 has the lowest concentration).



## **APPENDIX II**

## APPENDIX II

### Lipid accumulation (OD/20x 10<sup>4</sup> cells) in HepG2 and 3T3-L1 cells

**AII.1**

Cell line		day 0	day 4	day 7	day 11
<b>HepG2</b>	Mean (N=3)	<b>0.20</b>	<b>0.57</b>	<b>0.83</b>	<b>0.93</b>
	SD	0.01	0.15	0.15	0.33
	SEM	0.01	0.08	0.08	0.17
<b>3T3-L1</b>	Mean (N=3)	<b>0.030</b>	<b>0.061</b>	<b>0.148</b>	<b>0.202</b>
	SD	0.004	0.019	0.019	0.018
	SEM	0.002	0.010	0.009	0.009

### ALP activity (IU/μg protein) in HepG2 and 3T3-L1 cells

**AII.2**

Cell line		day 0	day 4	day 7	day 11
<b>HepG2</b>	Mean (N=4)	<b>6.32</b>	<b>9.29</b>	<b>7.68</b>	<b>3.74</b>
	SD	0.79	0.53	2.60	0.91
	SEM	0.39	0.27	1.30	0.45
<b>3T3-L1</b>	Mean (N=4)	<b>0.00</b>	<b>7.21</b>	<b>9.94</b>	<b>6.57</b>
	SD	0.00	2.58	3.60	1.48
	SEM	0.00	1.29	1.80	0.74

**Lipid content of HepG2 and 3T3-L1 cells in the presence and absence of Levamisole and Histidine (N=3). AII.3**

Cell	treatment		day 0	day 4	day 7	day 11
<b>HepG2</b>	No	<b>Mean</b>	<b>0.068</b>	<b>0.207</b>	<b>0.286</b>	<b>0.356</b>
		SD	0.007	0.059	0.085	0.104
		SEM	0.004	0.029	0.042	0.052
	Levamisole	<b>Mean</b>		<b>0.135</b>	<b>0.180</b>	<b>0.261</b>
		SD		0.043	0.035	0.072
		SEM		0.022	0.017	0.036
	Histidine	<b>Mean</b>		<b>0.128</b>	<b>0.138</b>	<b>0.137</b>
		SD		0.009	0.042	0.014
		SEM		0.005	0.021	0.021
<b>3T3-L1</b>	No	<b>Mean</b>	<b>0.040</b>	<b>0.109</b>	<b>0.266</b>	<b>0.400</b>
		SD	0.009	0.037	0.059	0.040
		SEM	0.004	0.019	0.029	0.020
	Levamisole	<b>Mean</b>		<b>0.094</b>	<b>0.129</b>	<b>0.217</b>
		SD		0.033	0.072	0.109
		SEM		0.016	0.036	0.055
	Histidine	<b>Mean</b>		<b>0.082</b>	<b>0.085</b>	<b>0.099</b>
		SD		0.042	0.057	0.053
		SEM		0.021	0.029	0.026

**ALP activity (IU/μg protein) in HepG2 and 3T3-L1 cells in the presence and absence of Levamisole and Histidine (N=3). AII.4**

Cell	treatment		day 0	day 4	day 7	day 11
<b>HepG2</b>	No	<b>Mean</b>	<b>1.17</b>	<b>6.43</b>	<b>4.13</b>	<b>1.86</b>
		SD	0.83	0.95	2.14	1.18
		SEM	0.42	0.48	1.07	0.59
	Levamisole	<b>Mean</b>		<b>4.56</b>	<b>1.52</b>	<b>1.25</b>
		SD		1.94	0.59	1.68
		SEM		0.97	0.29	0.84
	Histidine	<b>Mean</b>		<b>1.07</b>	<b>0.34</b>	<b>0.22</b>
		SD		0.77	0.15	0.06
		SEM		0.38	0.07	0.03
<b>3T3-L1</b>	No	<b>Mean</b>	<b>0.23</b>	<b>2.75</b>	<b>3.57</b>	<b>0.85</b>
		SD	0.40	1.04	1.01	0.46
		SEM	0.20	0.52	0.51	0.23
	Levamisole	<b>Mean</b>		<b>0.13</b>	<b>0.79</b>	<b>0.50</b>
		SD		0.23	0.46	0.21
		SEM		0.11	0.23	0.11
	Histidine	<b>Mean</b>		<b>0.18</b>	<b>0.14</b>	<b>0.10</b>
		SD		0.32	0.12	0.17
		SEM		0.16	0.06	0.09

**PPAR $\gamma$  gene expression in HepG2 and 3T3-L1 cells (N=3)**

**AII.5**

Cell type	Gene		day 0	day 4	day 7
<b>HepG2</b>	<i>PPAR</i>	Mean	<b>69.07</b>	<b>272.33</b>	<b>113.27</b>
		SD	42.34	74.59	10.65
		SEM	24.47	43.11	6.15
	<i>TBP</i>	Mean	<b>65.43</b>	<b>58.40</b>	<b>73.90</b>
		SD	21.19	14.72	20.96
		SEM	12.25	8.51	12.11
<b>3T3-L1</b>	<i>PPAR</i>	Mean	<b>348.73</b>	<b>835.43</b>	<b>542.6</b>
		SD	285.49	727.08	541.98
		SEM	165.02	420.28	313.28
	<i>TBP</i>	Mean	<b>72.77</b>	<b>56.9</b>	<b>71.70</b>
		SD	24.76	11.48	22.51
		SEM	14.31	6.63	13.01

**PPAR $\gamma$  gene expression in HepG2 cells in the presence of Levamisole and Histidine (N=3)**

**AII.6**

Cell	Gene	treatment		day 0	day 4	day 7
<b>HepG2</b>	<i>PPAR</i>	No Inhibitor	<b>mean</b>	<b>119.60</b>	<b>209.20</b>	<b>168.63</b>
			SD	75.35	101.63	85.42
			SEM	37.68	50.82	42.71
		Levamisole	<b>mean</b>		<b>235.60</b>	<b>179.37</b>
			SD		97.47	67.17
			SEM		48.74	33.58
		Histidine	<b>mean</b>		<b>222.47</b>	<b>167.93</b>
			SD		96.35	84.75
			SEM		48.18	42.37
	<i>TBP</i>	No Inhibitor	<b>mean</b>	<b>118.50</b>	<b>125.97</b>	<b>111.17</b>
			SD	86.22	93.28	90.17
			SEM	43.11	46.64	45.36
		Levamisole	<b>mean</b>		<b>133.30</b>	<b>96.03</b>
			SD		91.53	87.03
			SEM		45.76	43.51
		Histidine	<b>mean</b>		139.10	113.47
			SD		97.26	113.47
			SEM		48.63	56.74



**PPAR $\gamma$  gene expression in 3T3-L1 cells in the presence of Levamisole and Histidine (N=3) AII.7**

Cell	Gene	treatment		day 0	day 4	day 7
<b>3T3-</b>	<i>PPAR</i>	No Inhibitor	<b>mean</b>	<b>102.0</b>	<b>274.1</b>	<b>230.8</b>
			SD	38.67	41.65	48.75
			SEM	19.38	20.83	24.38
		Levamisole	<b>mean</b>		<b>262.0</b>	<b>156.3</b>
			SD		45.81	103.20
			SEM		22.91	51.60
		Histidine	<b>mean</b>		<b>225.5</b>	<b>184.7</b>
			SD		1.27	30.98
			SEM		0.64	15.49
	<i>TBP</i>	No Inhibitor	<b>mean</b>	<b>78.73</b>	<b>98.73</b>	<b>75.03</b>
			SD	34.56	34.93	20.81
			SEM	17.28	17.47	10.40
		Levamisole	<b>mean</b>		<b>88.57</b>	<b>65.73</b>
			SD		37.32	13.19
			SEM		18.66	6.60
		Histidine	<b>mean</b>		<b>77.85</b>	<b>67.33</b>
			SD		0.21	17.63
			SEM		0.11	8.82

**MAPK1 gene expression in 3T3-L1 cells 72 hours post-transfection(N=3) AII.8**

	treatment	Expt 1	Expt 2	Expt 3	Mean	SD	SEM
MAPK1	Anti- siRNA	9.50	6.80	18.20	<b>11.50</b>	5.96	3.44
	Control siRNA	29.00	40.80	132.10	<b>67.30</b>	56.43	32.58
	Non-transfected	31.20	38.62	134.10	<b>67.97</b>	57.39	33.13
Ref gene ( <i>TBP</i> )	Anti- siRNA	118.30	104.30	245.40	<b>156.00</b>	77.74	44.88
	Control siRNA	124.60	148.00	245.50	<b>171.70</b>	64.42	36.04
	Non-transfected	119.50	153.78	239.95	<b>171.08</b>	62.06	35.83

**MAPK1 gene expression in HepG2 cells 72 hours post-transfection(N=3) AII.9**

	treatment	Expt 1	Expt 2	Expt 3	Mean	SD	SEM
MAPK1	Anti- siRNA	10.40	5.10	4.30	<b>6.60</b>	3.30	1.90
	Control siRNA	20.50	18.10	27.70	<b>22.10</b>	5.00	2.90
	Non-transfected	22.10	15.45	30.04	<b>22.53</b>	7.30	4.22
Ref gene ( <i>TBP</i> )	Anti- siRNA	104.20	98.70	131.30	<b>111.40</b>	17.50	10.10
	Control siRNA	101.30	112.60	159.30	<b>124.40</b>	30.70	17.80
	Non-transfected	98.56	109.78	174.94	<b>127.76</b>	41.24	28.81

**Data for RNAi studies in 3T3-L1 cells**

**AII.10**

ALP activity in transfected 3T3 cells [IU/ $\mu$ g protein] (N=3)

		expt1	expt2	expt3	Mean	SEM	SD
day 0		0.001	0.001	0.000	0.001	0.000	0.001
day 7	No siRNA	0.016	0.019	0.010	0.015	0.007	0.005
	With Anti-siRNA	0.004	0.002	0.002	0.003	0.001	0.001
	With control siRNA	0.014	0.014	0.018	0.015	0.008	0.002
day 11	No siRNA	0.006	0.004	0.005	0.005	0.002	0.001
	With Anti-siRNA	0.001	0.002	0.002	0.002	0.001	0.000
	With control siRNA	0.004	0.006	0.007	0.006	0.003	0.001

Lipid accumulation in transfected

3T3 cells (OD/2x10<sup>4</sup> cells)

		expt1	expt2	expt3	Mean	SEM	SD
day 0		0.05	0.04	0.05	0.05	0.00	0.01
day 7	No siRNA	0.30	0.27	0.30	0.29	0.01	0.02
	With Anti-	0.07	0.08	0.09	0.08	0.00	0.01
	With Control siRNA	0.27	0.24	0.28	0.26	0.01	0.02
day 11	No siRNA	0.41	0.40	0.35	0.39	0.02	0.03
	With Anti-siRNA	0.11	0.12	0.16	0.13	0.01	0.03
	With Control siRNA	0.41	0.37	0.41	0.40	0.01	0.02

*TNSALP* gene expression in transfected 3T3

cells

		expt1	expt2	expt3	Mean	SEM	SD
day 0		0.00	0.00	0.00	0.00	0.00	0.00
day 7	No siRNA	4523.30	1212.30	382.15	2039.25	1095.46	2190.93
	With Anti-siRNA	1065.10	172.60	70.40	436.03	273.59	547.18
	With Control siRNA	3890.50	1303.70	391.30	1861.83	907.57	1815.14
day 11	No siRNA	1074.70	1071.80	81.20	742.57	286.38	572.76
	With Anti-siRNA	174.50	122.10	7.80	101.47	42.62	85.24
	With Control	920.40	795.70	72.60	596.23	228.87	457.75

*TBP* gene expression in transfected 3T3 cells

		expt1	expt2	expt3	Mean	SEM	SD
day 0		96.10	95.70	34.10	75.30	17.84	35.68
day 7	No siRNA	131.60	138.90	24.20	98.23	32.11	64.22
	With Anti-siRNA	126.10	111.50	34.70	90.77	24.55	49.10
	With Control siRNA	151.20	100.20	42.40	97.93	27.22	54.44
day 11	No siRNA	104.70	208.20	35.10	116.00	43.55	87.10
	With Anti-siRNA	142.70	152.20	38.00	110.97	31.68	63.37
	With Control siRNA	201.30	119.90	37.20	119.47	41.03	82.05

**Data for RNAi studies in HepG2 cells (N=3) AII.11**

ALP activity (IU/ $\mu$ g protein) in transfected HepG2 cells

		exp1	exp2	exp3	Mean	$\pm$ SD	SEM
Day 0		0.006	0.007	0.007	<b>0.007</b>	0.001	0.00
Day 4	No siRNA	0.028	0.016	0.024	<b>0.023</b>	0.006	0.00
	with Anti-siRNA	0.005	0.004	0.006	<b>0.005</b>	0.001	0.00
	with Control siRNA	0.026	0.029	0.021	<b>0.025</b>	0.004	0.00
Day 7	No siRNA	0.011	0.016	0.01	<b>0.012</b>	0.003	0.00
	with Anti-siRNA	0.002	0.007	0.001	<b>0.003</b>	0.003	0.00
	with Control siRNA	0.006	0.006	0.008	<b>0.007</b>	0.001	0.00
Day 11	No siRNA	0.006	0.006	0.007	<b>0.006</b>	0.001	0.00
	with Anti-siRNA	0.003	0.001	0.002	<b>0.002</b>	0.001	0.00
	with Control siRNA	0.006	0.009	0.002	<b>0.006</b>	0.004	0.00

***Appendix II***

Intracellular lipid accumulation(OD/2 x10<sup>4</sup> cells) in transfected HepG2 cells

		exp1	exp2	exp3	<b>Mean</b>	± SD	SEM
Day 0		0.07	0.08	0.07	<b>0.07</b>	0.01	0.00
Day 4	No siRNA	0.10	0.09	0.07	<b>0.09</b>	0.03	0.00
	with Anti-siRNA	0.09	0.11	0.10	<b>0.10</b>	0.02	0.01
	with Control siRNA	0.10	0.09	0.08	<b>0.08</b>	0.02	0.01
Day 7	No siRNA	0.25	0.22	0.20	<b>0.22</b>	0.03	0.01
	with anti-siRNA	0.17	0.16	0.17	<b>0.17</b>	0.01	0.00
	with Control siRNA	0.25	0.31	0.29	<b>0.28</b>	0.03	0.02
Day	No siRNA	0.48	0.5	0.47	<b>0.48</b>	0.02	0.01
	with Anti-siRNA	0.23	0.25	0.24	<b>0.28</b>	0.01	0.01
	with Control siRNA	0.42	0.41	0.44	<b>0.42</b>	0.02	0.01

*TNSALP* gene expression in transfected HepG2 cells (cDNA[ng/ml])

		exp1	exp2	exp3	<b>Mean</b>	± SD	SEM
Day 0		195.6	177.1	180.3	<b>184.3</b>	9.9	5.7
Day 4	No siRNA	2247.4	1052.9	489.0	<b>1263.1</b>	897.8	448.9
	with Anti-siRNA	233.3	124.0	185.1	<b>180.8</b>	54.8	27.4
	with Control siRNA	2065.2	1288.5	322.0	<b>1225.2</b>	873.3	436.7
Day 7	No siRNA	281.9	116.4	266.5	<b>221.6</b>	91.4	45.7
	with Anti-siRNA		35.9	150.4	<b>93.2</b>	81.0	40.5
	with Contro siRNA	264.7	195.6	231.9	<b>230.7</b>	34.6	17.3
Day	No siRNA	270.6	202.9	273.3	<b>248.9</b>	39.9	19.9
	with Anti-siRNA	45.3	202.9	136.2	<b>128.1</b>	79.1	39.6
	with Control siRNA	58.4	174.7	210.5	<b>147.9</b>	79.5	39.8

*TBP* gene expression in transfected HepG2 cells (cDNA[ng/ml])

		expt1	expt2	expt3	mean	± SD	SEM
Day 0		160.3	96.4	164.9	<b>140.5</b>	38.3	19.1
Day 4	No	219.5	228.2	124.3	<b>190.7</b>	57.6	28.8
	With Anti-siRNA	188.0	154.4	43.3	<b>128.6</b>	75.7	37.9
	With Control siRNA	147.0	193.5	122.8	<b>154.4</b>	35.9	18.0
Day 7	No	310.2	202.1	135.1	<b>215.8</b>	88.4	44.2
	With Anti-siRNA	220.6	153.9	176.4	<b>183.6</b>	33.9	17.0
	With Control siRNA	296.2	148.1	190.6	<b>211.6</b>	76.3	38.1
Day 11	No	56.9	109.0	214.6	<b>126.8</b>	80.3	40.2
	With Anti-siRNA	229.3	236.5	217.2	<b>227.7</b>	9.8	4.9
	With Control siRNA	254.8	141.4	201.6	<b>199.3</b>	56.7	28.4

**Anthropometric data for subjects who participated in the study on polymorphism in the promoter region of TNSALP gene. N=6, black women**

	Subject study number						Mean	SD
	1	2	3	4	5	6		
Age	48	41	58	55	52	44	<b>49.7</b>	<b>±6.3</b>
Weight	90.2	76.0	79.4	91.4	82.7	77.30		
Height	1.61	1.55	1.54	1.68	1.52	1.51		
BMI	34.8	31.6	33.5	32.4	35.8	33.9	<b>33.0</b>	<b>±4.6</b>

(N= 6, White women)

	Subject study number						Mean	SD
	21	22	233	24	25	26		
Age	27	39	22	53	45	51	<b>39.5</b>	<b>±11.9</b>
Weight	85.8	86.6	61.9	85.7	99.3	79.6		
Height	1.70	1.61	1.63	1.52	1.68	1.60		
BMI	29.7	33.4	23.3	37.1	35.2	31.1	<b>31.5</b>	<b>±4.5</b>

**UNIVERSITY OF THE WITWATERSRAND, JOHANNESBURG**

Division of the Deputy Registrar (Research)

**HUMAN RESEARCH ETHICS COMMITTEE (MEDICAL)**

R14/49 Chirambo

**CLEARANCE CERTIFICATE**

**PROTOCOL NUMBER M070214**

**PROJECT**

The Role Played by Alkaline Phosphatase in  
Different Lipid-Storing Cell Types

**INVESTIGATORS**

Dr GM Chirambo

**DEPARTMENT**

Chemical Pathology

**DATE CONSIDERED**

07.03.02

**DECISION OF THE COMMITTEE\***

Approved unconditionally

**Unless otherwise specified this ethical clearance is valid for 5 years and may be renewed upon application.**

**DATE**            07.03.05

**CHAIRPERSON** .....



(Professors PE Cleaton-Jones, A Dhai, M Vorster,  
C Feldman, A Woodiwiss)

\*Guidelines for written 'informed consent' attached where applicable

cc: Supervisor :            Dr N Crowther

---

**DECLARATION OF INVESTIGATOR(S)**

To be completed in duplicate and **ONE COPY** returned to the Secretary at Room 10005, 10th Floor, Senate House, University.

I/We fully understand the conditions under which I am/we are authorized to carry out the abovementioned research and I/we guarantee to ensure compliance with these conditions. Should any departure to be contemplated from the research procedure as approved I/we undertake to resubmit the protocol to the Committee. **I agree to a completion of a yearly progress report.**

PLEASE QUOTE THE PROTOCOL NUMBER IN ALL ENQUIRIES

## **BIBLIOGRAPHY**



## **BIBLIOGRAPHY**

Aaranson S and Todaro G (1968). Development of 3T3-like lines from Balb-c mouse embryo cultures: transformation susceptibility to SV40. *J Cell Physiol* **72**: 141-148.

Adachi H, Kurachi H, Homma H, Adachi K, Imai T and Morishige K (1994). Epidermal growth factor promotes adipogenesis of 3T3-L1 cell *in vitro*. *Endocrinology* **135**: 1824-30.

Ailhaud G, Grimaldi P and Negrel R (1992). Cellular and molecular aspects of adipose tissue development. *Ann Rev Nutr* **12**: 207-33.

Akune T, Ohba S, Kamekura S, Yamaguchi M, Chung U and Kawaguchi H (2004). PPAR $\gamma$  insufficiency enhances osteogenesis through osteoblast formation from bone marrow progenitors. *J Clin Invest* **113**: 846-855.

Albright A and Stem J (1998). 'Adipose tissue.' < <http://www.sportssci.org/encyc/adipose/adipose.html> > [accessed 13 Dec2009].

Ali A, Penny C, Paiker J, Psaras G, Ikram F and Crowther N (2006). The relationship between alkaline phosphatase activity and intracellular lipid accumulation in murine 3T3-L1 cells and human preadipocytes. *Anal Bioch* **354**: 247-54.

Ali A, Penny C, Paiker J, van Niekerk C, Smit A and Crowther N (2005). Alkaline phosphatase is involved in the control of adipogenesis in the murine preadipocyte cell line, 3T3-L1. *Clin Chim Acta* **351**: 101-109.

Ali A, Psaras G, Penny C, Paiker J, Ekram F and Crowther N (2006). Ethnic differences in adipogenesis and adipocyte alkaline phosphatase activity. *Diabet Med* **23**(Suppl 4): 121-122.

Almahbobi G, Williams L and Hall P (1992). Attachment of steroidogenic lipid droplets to intermediate filaments in adrenal cells. *J Cell Sci* **101**: 383-393.

Andracchi S and Korte G (1991). Expression of plasma membrane alkaline phosphatase in normal and regenerating choriocapillaries in the rabbit. *Acta Anat* **141**: 289-93.

Angelin B, Reihner E, Rudling M, Ewerth S, Björkhem I and Einarsson K (1987). *In vitro* studies of lipid metabolism in human liver. *Am Heart J* **113**: 482-487.

Argo C, Jezzou J, Al-Osaimi A and Caldwell S (2009). Thiazolidinediones for the treatment in NASH: sustained benefit after drug discontinuation? *J Clin Gastroenterol* **43**: 565-68.

Arulmozhi D, Kurian R, Veeranjanyulu A and Bodriarikal S (2007). Antidiabetic and antihyperlipidemic effects of *Myristica fragrans* in animal models. *Pharmaceut Biol* **45**: 64-8.

Asada-Kubota M and Kanamura S (1986). Intracellular localization of alkaline phosphatase in freshly isolated foetal rat hepatocytes. *Histochem J* **18**: 500-6.

Barroso I, Gurnel M, Crowley V, Agostin M, Schwabe J, Soos M, *et al.* (1999). Dominant negative mutations in human PPAR gamma associated with severe insulin resistance, diabetes mellitus and hypertension. *Nature* **402**: 880-83.

Basi N, George M and Pointer R (1994). Regulation of glycogen synthase activity in isolated rat adipocytes by levamisole. *Life Sci* **54**: 1027-34.

Bell R and Coleman R (1980). Enzymes of glycerolipid synthesis in eukaryotes. *Ann Rev Biochem* **49**: 459-87.

Berglund L, Björkhem I and Einarsson K (1982). Apparent phosphorylation-dephosphorylation of soluble phosphatidic acid phosphatase in rat liver. *Biochem Biophys Res Comm* **105**: 288-95.

Bergman R, Kim S, Catalano K, Hsu I, Chiu J, kabir M, *et al.* (2006). Why visceral fat is bad:mechanisms of the metabolic syndrome. *Obesity* **14**(Supp): 16S-19S.

Bernlohr D, Bolanowski M, Kelly T and Lane M (1985). Evidence for an increase in transcription of specific mRNAs during differentiation of 3T3-L1 preadipocytes. *J Biol Chem* **260**: 5563-67.

Bianco P, Costantini M, Dearden L and Bonucci E (1988). Alkaline phosphatase positiveprecursors of adipocytes in the human bone marrow. *Br J Haematol* **68**: 401-3.

Bielby J and Chin C (1987). ALP isoenzymes incompletely resolved by fast protein liquid chromatography. *Clin Chem* **33**: 2327.

Bjorntorp P (1974). Effects of age , sex and clinical conditions on adipose tissue cellularity in man. *Metabolism* **23**: 1091-1102.

Bostrom P, Magnusson B, svenson P, Wikland O, Boren J, Carlson L, *et al.* (2006). Hypoxia converts human macrophages into TAG-loaded foam cells. *Arterioscler Thromb Vasc Biol* **26**: 1871-1876.

Bounassisi V, Sato G and Cohen A (1962). Hormone producing cultures of adrenal and pituitary tumour origin. *Proc Natl Acad Sci USA* **48**: 1184-1190.

Bradford M (1976). A rapid and sensitive method for the quantitation of microgram quantities of protein utilising the principle of protein-dye binding. *Anal Biochem* **72**: 248-254.

Brasaemle D, Barber T, Wolins N, Serrero G, Mackie L and Londos C (1997). Adipose differentiation-related protein is an ubiquitously expressed lipid storage droplet-associated protein. *J Lipid Res* **38**: 2249-2263.

Bray G (2004). Obesity is a chronic, relapsing neurochemical disease. *Int J Obes* **28**: 34-38.

Brown M and Goldstein L (1983). Lipoprotein metabolism in the macrophage : implication for cholesterol deposition in atherosclerosis. *Ann Rev Biochem* **52**: 223-261.

Brun R, Tontonoz P, Forman B, Ellis R, Chen J, Evans R, *et al.* (1996). Differential activation of adipogenesis by multiple PPAR isoforms. *Genes Develop* **10**: 974-984.

Burd A, Poissonet C, Garn M, Lavelle M, Sabet M and Bridges B (1985). Adipose tissue growth patterns during human gestation: a histomeric comparison of buccal and gluteal fat depots. *Int J Obes* **9**: 247-56.

Burry R (2000). Specificity controls for immunocytochemical methods. *J Histochem Cytochem* **48**: 163-65.

Burt A, Mutton A and Day C (1998). Diagnosis and interpretation of steatosis and steatohepatitis. *Semin Diagn Pathol* **15**: 246-58.

Calhau C, Martel F, Soares-da-Silva P, Hipólito-Reis C and Azevedo I (2002). Regulation of [(3)H]MPP(+) transport by phosphorylation/dephosphorylation pathways in RBE4 cells: role of ecto-alkaline phosphatase. *Arch Pharmacol* **365**: 349-56.

Camp H, Ren D and Leff T (2002). Adipogenesis and fat-cell function in obesity and diabetes. *Trends in Molecular Medicine* **8**: 442-447.

Caplen N, Parrish S, Iman F, Fire A and Morgan R (2001). Specific inhibition of gene expression by small double-stranded RNAs in invertebrate and vertebrate systems. *Proc Natl Acad Sci USA* **98**: 9742-7.

Carlsson P and Mahlapuu M (2002). Forkhead transcription factors: key players in development and metabolism. Forkhead transcription factors: key players in development and metabolism. *Dev Biol* **250**: 1-23.

Carman G and Han G (2009). Phosphatidic Acid Phosphatase, a key enzyme in the regulation of lipid synthesis. *J Biol Chem* **284**: 2593-97.

Chisholm R (2002). 'Cytoskeleton'. <<http://www.encyclopedia.com/doc/1G2-3400700108.html> [accessed March 4, 2010].

Chitturi S, Farrell G and George J (2004). Non-alcoholic steatohepatitis in the Asia-Pacific region: future shock? *J Gastroenterol Hepatol* **19**: 368-74.

Christy R, Kaestner K, Geiman D and Lane M (1991). CCAAT/enhancer binding protein gene promoter: binding of nuclear factors during differentiation of 3T3-L1 preadipocytes. *Proc Natl Acad Sci USA* **88**: 2593-97.

Chung S, Ahn B, Kim M, Choi H, Park H, Kang S, *et al.* (2010). Control of adipogenesis by the SUMO-specific protease SENP2. *Mol Cell Biol* **30**: 2135-46.

Cinti S (2002). Adipocyte differentiation and transdifferentiation: plasticity of the the adipose organ. *J. Endocrinol Invest* **25**: 823-835.

Clarke S, Robinson C and Gimble J (1997). CCAAT/EBP directly modulate transcription from the PPAR gamma 2 promoter. *Biochem Biophys Res Commun* **240**: 99-103.

Cnop M, Hannaert J, Gruppig A and Pipeleers D (2002). Low density lipoprotein can cause death of islet  $\beta$  – cells by its cellular uptake and oxidative modification. *Endocrinology* **143**: 3449-3453.

Cnop M, Hannaert J, Hoorens A, Eizirik D and Pipeleers D (2001). Inverse relationship between cytotoxicity of free fatty acids in pancreatic islet cells and cellular TAG accumulation. *Diabetes* **50**: 1771-1777.

Cocco C, Marin M and Rizzotti P (1987). Isoelectric focussing on cellulose acetate membrane: a separation procedure for ALP isoenzymes. *Clin Biochem* **20**: 399-404.

Cornelius P, Emerback S, Bjursell G, Olivercona T and Pekala P (1988). Regulation of lipoprotein lipase mRNA content in 3T3-L1 cells by tumour necrosis factor. *Biochem J* **249**: 765-769.

Cornelius P, MacDougald O and Lane M (1994). Regulation of adipocyte development. *Ann Rev Nutr* **14**: 99-129.

Cox W and Singer V (1999). A High-resolution, Fluorescence-based Method for Localization of Endogenous Alkaline Phosphatase Activity. *J Histochem Cytochem* **47**: 1443–55.

Crofton P, Elton R and Smith A (1979). High molecular weight ALP: a clinical study. *Clin Chim Acta* **98**: 263-275.

Cypess A, Williams G, Goldfine A, Tseng Y and Kolodny G (2009). Identification and importance of brown adipose tissue in adult humans. *N Engl J Med* **360**: 1509-17.

Day C and Yeaman S (1994). The biochemistry of alcohol induced fatty liver. *Biochim Biophys Acta* **1215**: 33-48.

Decker K (1985). Eicosanoids, signal molecules of liver cells. *Semin Liver Dis* **5**: 175-90.

Detmers P, Zhou D, Powell D, Lichstein H, Kelly M and Pironkova R (1995). Endotoxin receptors (CD14) are found with CD16 (Fc gamma RIII) in an intracellular compartment of neutrophils that contains alkaline phosphatase. *J. Immunol* **155**: 2085-95.

DiDonata D and Brasaemle D (2003). Fixation methods for the study of lipid droplets by immunofluorescence microscopy. *J Histochem Cytochem* **51**: 773-80.

Downward J (2004). RNA interference. *Br Med J* **328**: 1245-1248.

Draguet C, Gillerot Y and Mornet E (2004). Childhood hypophosphatasia: a case report due to a novel mutation. *Arch Pediatre* **11**: 440-443.

Draude G and Reinhard L (2000). TGF-beta1 downregulates CD36 and scavenger receptor A but upregulates LOX -1 in human macrophages. *Am J Physiol Heart Circ Physiol* **278**: H1042-H1048.

Dreyer C, Krey G, Keller H, Givel F, Helftenbein G and Wahli W (1992). Control of the peroxisomal beta-oxidation pathway by a novel family of nuclear hormone receptors. *Cell* **68**: 879-87.

Duee P, Pegorier J, el Manoubi L, Herbin C, Kohl C and Girard J (1985). Hepatic triacylglyceride hydrolysis and development of ketogenesis in rabbits. *Am J Physiol Endocrinol Metab* **249**: E478-E484.

Dynan W and Tjian R (1985). Control of eukaryotic mRNA synthesis by sequence specific-DNA binding proteins. *Nature* **316**: 774-778.

El Achhab Y, Meyre D, Boutia-Naji N, Berraho M, Deweirder M and Vatin V (2009). Association of the ENPP1 K121Q polymorphism with type 2 diabetes and obesity in the Moroccan population. *Diabetes Metab* **35**: 37-42.

Elbashir S, Harborth J, Lendeckel W, Yalcin A, Weber K and Tuschl T (2001). Duplexes of 21-nucleotides RNAs mediate RNA interference in cultured mammalian cells. *Nature* **411**: 494-8.

Ellis M and Manganiello V (1985). A role for soluble cAMP phosphodiesterase in differentiation of 3T3-L1 preadipocytes. *J Cell Physiol* **124**: 191-8.

Escalente D, Recillas F, Hernandez D, Castro S and Terao M (1996). Retinoic acid and methylation of cis- regulatory elements control the mouse TNSALP gene expression. *Mech Dev* **57**: 21-32.

Fajas L, Debril M and Auwrex J (2001). PPAR $\gamma$  : from adipogenesis to carcinogenesis. *J Mol Endocrinol* **27**: 1-9.



Farrel G (2003). Non-alcoholic steatohepatitis: what is it, and why is it important in the Asia-Pacific region? *J Gastroenterol Hepatol* **18**: 124-38.

Feingold K, Soued M, Serio M, Moser A, Dinarello C and Grunfeld C (1989). Multiple cytokines stimulate hepatic lipid synthesis *in vivo*. *Endocrinology* **125**: 267-74.

Fernyhough M, Okine E, Hausman G, Vierck J and Dodson M (2007). PPAR gamma and Glut-4 expression as developmental regulators/markers for preadipocyte differentiation into an adipocyte. *Domest Anim Endocrinol* **33**: 367-78.

Fire A, Xu S, Montgomery M, Kostas S, Driver S and Mello C (1998). Potent and specific genetic interference by double-stranded RNA in caenorhabditis elegans. *Nature* **391**: 806-811.

Fishman W (1989). On the importance of being stereo-specific. *Clin Chim Acta* **186**: 129-132.

Fishman W (1990). Alkaline phosphatases:Recent progress. *Clin Biochem* **23**: 99-104.

Flegal K, Granbald B, Williamson D and Gail M (2005). Excess deaths associated with underweight, overweight and obesity. *JAMA* **293**: 1861-1867.

Fong D, Nehra V, Lindor K and Buchman A (2000). Metabolic and nutritional considerations in non alcoholic fatty liver. *Hepatology* **32**: 3-10.

Foretz M, Guichard C, Ferré P and Foufelle F (1999). Sterol regulatory element binding protein-1c is a major mediator of insulin action on the hepatic expression of glucokinase and lipogenesis-related genes. *Proc Natl Acad Sci USA* **96**: 12737-12742.

Forman B, Chen J and Evans R (1997). Hypolipidemic drugs, polyunsaturated fatty acids and eicosanoids are ligands for PPAR alpha and delta. *Proc Natl Acad Sci USA* **94**: 4312-17.

Forman B, Tontonoz P, Chen J, Brun R, Spiegelman B and Evans R (1995). 15-deoxy-delta<sup>12,14</sup>-postaglandin J<sub>2</sub> is a ligand for the adipocyte determination factor PPAR gamma. *Cell* **83**: 803-12.

Franke W, Hergt M and Grund C (1987). Rearrangement of the vimentin cytoskelton during adipose conversion: formation of an intermediate filament cage around lipid globules. *Cell* **49**: 131-41.

Frubeck G, Gomez A, Mumzabal F and Burrel M (2001). The adipocyte: a model for integration of endocrine and metabolic signalling in energy metabolism regulation. *Am J Physiol Endocrinol Metab* **280**: E827-E847.

Galperin M and Jedizejas M (2001). Conserved core structure and active site residues in alkaline phosphatases superfamily enzymes. *Proteins* **45**: 318-24.

Gao Z, He Q, Peng B, Chiao P and Ye J (2006). Regulation of nuclear translocation of HDAC3 by I{kappa}B{alpha} is required for tumor necrosis factor inhibition of peroxisome proliferator-activated receptor {gamma} function. *J Biol Chem* **281**: 4540-4547.

Garcia A, Subramanian V, Sekowski A, Bhattacharyya S, Love M and Brasaemle D (2004). The Amino and Carboxyl Termini of Perilipin A Facilitate the Storage of Triacylglycerols. *J Biol Chem* **279**: 8409-16.

Garlid K, Jaburek M and Jezek P (1998). The mechanism of proton transport mediated by mitochondrial uncoupling proteins. *FEBS Lett* **438**: 10-14.

Geloan A, Roy P and Bukowecki L (1989). Regression of white adipose tissue in diabetic rats. *Am J Physiol* **257**: E547-53.

Gerhold D, Liu F, Jiang G, Li Z, Xu J, Lu M, *et al.* (2002). Gene expression profile of adipocyte differentiation and its regulation by peroxisome proliferator-activated receptor-gamma agonists. *Endocrinology* **143**: 2106-18.

Gesta S, Tseng Y and Kahn C (2007). Developmental origin of fat: tracking obesity to its source. *Cell* **131**: 242-56.

Gijsbers R, Ceulemans H, Stahlman W and Billen M (2002). Structural and catalytic similarities between nucleoside pyrophosphatases/phosphodiesterases and alkaline phosphatases. *J Biol Chem* **276**: 1361-8.

Girard J, Perdereau D, Fonfelle F, Prip-Bnus C and Fere P (1994). Regulation of lipogenic enzyme gene expression by nutrients and hormones. *FASEB J* **8**: 36-42.

Gonchoroff D, Branum E and O'Brien J (1989). Alkaline phosphatase isoenzymes of liver and bone origin are incompletely resolved by wheat -germ-lectin affinity chromatography. *Clin Chem* **35**: 29-32.

Goodman J (2008). The gregarious lipid droplet. *J Biol Chem* **283**: 28005-9.

Goodpaster B and Wolf D (2004). Skeletal muscle lipid accumulation in obesity, insulin resistance and Type 2 diabetes. *Paediatr Diabetes* **5**: 219-226.

Green H and Kehinde O (1975). An established cell line and its differentiation in culture II. Factors affecting adipose conversion. *Cell* **5**: 19-27.

Greenberg A, Egan J, Wek S, Garty N, Blanchette-Mackie E and Londos C (1991). Perilipin, a major hormonally regulated adipocyte-specific phosphoprotein associated with the periphery of lipid storage droplets. *J Biol Chem* **266**: 11341-11346.

Greenberg C, Evans J, Smith S, Redekopp S, Haworth J, Mulivor R, *et al.* (1990). Infantile hypophosphatasia: localization within chromosome region 1p36.1-34 and perinatal diagnosis using linked DNA markers. *Am J Hum Genet* **46**: 286-292.

Gregoire F, Smas C and Sul H (1998). Understanding of adipocyte differentiation. *Physiol Rev* **78**: 783-809.

Griffin C, Smith M, Henthorn S, Harris H, Weiss M, Raducha M, *et al.* (1987). Human placental and intestinal ALP genes map to 2q34-q37. *Am J Hum Genet* **41**: 1025-1034.

Griffiths J and Black J (1987). Separation and identification of ALP isoenzymes and isoforms in serum of healthy persons by isoelectric focussing. *Clin Chem* **33**: 2171-2177.

Hagerstrand I and Skude G (1976). Improved electrophoretic resolution of human serum ALP isoenzymes in agarose gel by Triton X-100. *Scan J Clin Lab Invest* **36**: 127-129.

Han R and Coleman J (1995). Dependence of the phosphorylation of ALP by phosphatase monoesters on the pKa of the leaving group. *Biochemistry* **34**: 4238-45.

Harris H (1982). Multilocus enzyme systems and the evolution of gene expression. In: The Harvey Lectures: series 76. H. Harris. New York, Academic Press: 95-124.

Harris H (1990). The human alkaline phosphatases:What we know and what we don't know. *Clin Chim Acta* **186**: 133-150.

Hass P, Wada G, Herman M and Sussman H (1979). Alkaline phosphatase of mouse teratoma cells: Immunochemical and structural evidence for its identity as a somatic gene product. *Proc Natl Acad Sci USA* **76**: 1164-1168.

Hatta M, Daitoku H, Matsuzaki H, Deyam Y, Yoshimura Y and Suzuki K (2002). Regulation of ALP promoter activity by forkhead transcription factor FKHR. *Int J Mol Med* **9**: 147-152.

Hautekeete M and Geerts A (1997). The hepatic stellate (Ito) cells: Its role in human liver disease. *Virchows Arch* **430**: 195-207.

Hawrylak K and Stinson R (1988). The solubilisation of tetrameric alkaline phosphatase from human liver and its conversion into various forms by phosphoinositol phospholipase C. *J Biol Chem* **263**: 14363-14373.

Heid H, Moll R, Scwetlick I, Rackwitz H and Keeman T (1998). Adipophilin is a specific marker of lipid accumulation in diverse cell types and diseases. *Cell Tissue Res* **294**: 309-321.

Hendrix P, Hoylaerts M, Nouwen E and DeBroe M (1990). Enzyme immunoassay of human placental and germ-cell ALP in serum. *Clin Chem* **36**: 1793-1799.

Henthorn P, Raducha M, Edwards Y, Weiss M, Slaughter C, Lefferty M, *et al.* (1987). Nucleotide and amino acid sequences of human intestinal ALP: close homology to placental ALP. *Proc Natl Acad Sci USA* **84**: 1234-1238.

Henthorn P, Raducha M, Fedd K, Lafferty M and Whyte M (1992). Different missense mutations at the TNSALP gene locus in autosomal recessively inherited forms of mild and severe hypophosphatasia. *Proc Natl Acad Sci USA* **89**: 9924-9928.

Henthorn P, Raducha M, Kadesch T, Weiss M and Harris H (1988). Sequence and characterisation of the human intestinal ALP gene. *J Biol Chem* **263**: 12011-12019.

Herasse M, Spentchian M, Taillandier A and Mornet E (2002). Evidence of a founder effect for the TNSALP gene E174K mutation in hypophosphatasic patients. *Eur J Hum Genet* **10**: 666-668.

Hirsch J and Batchelor B (1976). Adipose tissue cellularity and human obesity. *Clin. Endocrinol. Metab* **5**: 299-311.

Ho P, Chuang Y, Hung C and Wei L (2011). Cytoplasmic receptor-interacting protein 140 (RIP 140) interacts with perilipin to regulate lipolysis. *Cell Signal* **23**: 1397-403.

Hsu W (1980). Toxicity and drug interactions of levamisole. *J Am Vet Med Assoc* **176**: 1166-69.

Hsu Y, Chang J, Tsai C, Chien T and Kuo P (2007). Myricetin induces human osteoblast differentiation through bone morphogenetic protein-2/p38 mitogen-activated protein kinase pathway. *Biochem Pharmacol* **73**: 504-14.

Hua J, Berger J, Pan Y, Hulmes J and Udenfriend S (1986). Partial sequencing of human adult fetal and bovine intestinal ALP: Comparison with the human placental and liver enzymes. *Proc Natl Acad Sci USA* **83**: 2368-2372.

Hyde R, Christie G, Litherand G, Hajduch E, Taylor P and Hundal H (2001). Subcellular localization and adaptive up-regulation of the system A (SAT2) amino acid transporter in skeletal muscle cells and adipocytes. *Biochem J* **355**: 563-68.

Iba K, Chiba H, Sawada N, Hirota S, Ishii S and Mori M (1995). Glucocorticoids induce mineralization coupled with bone protein expression without influence on growth of a human osteoblastic cell line. *Cell Struct Funct* **20**: 319-30.

Inoue M, Ohtake T, Motomura W, Takahashi N, Hosoki Y, Miyoshi S, *et al.* (2005). Increased expression of PPAR gamma in high fat diet-induced liver steatosis in mice. *Biochem Biophys Res Comm* **336**: 215-22.

Iqbal S, Whitaker P, Holand S, Madira W and Davies T (2000). Comparison of serum catalytic activity and immunoreactivity of bone ALP. *Clin Chim Acta* **294**: 57-66.

Ishida Y, Komaru K, Ito M, Amaya Y, Kohno S and Kimimitso O (2003). Tissue non-specific ALP with an Asp<sup>289</sup>-Val mutation fails to reach the cell surface and undergoes proteasome-mediated degradation. *J Biol Chem* **134**: 63-70.

Ismail M (2008). "Alcoholic fatty liver." <http://www.emedicine.medscape.com/article/170409-overview>. [accessed 11 Dec 2009].

Iyer V, Tran T, Foster E, Dai W, Clark R and Knoll B (2005). Differential phosphorylation and dephosphorylation of  $\beta$ 2-adrenoceptor sites Ser 262 and Ser 355, 356. *Br J Pharmacol* **147**: 249-59.

Jaenisch R and Bird A (2003). Epigenetic regulation of gene expression: how the genome integrates intrinsic and environmental signals. *Nat Genet* **33** (Suppl): 245-54.

Jemmerson R and Low M (1987). Phosphatidylinositol anchor of Hela cell alkaline phosphatase. *Biochemistry* **26**: 5703-5709.

Jennings R, Brocklehurst D and Hirst M (1970). A comparative study of ALP enzymes using starch gel electrophoresis and sephadex gel filtration with special reference to high molecular weight enzymes. *Clin Chim Acta* **30**: 509-517.

Jessen B and Stevens G (2002). Expression profiling during adipocyte differentiation of 3T3-L1 fibroblasts. *Gene* **299**: 95-100.

Jiang J, Johnson C and Zarnegar R (2001). Peroxisome proliferator activated receptor gamma-mediated transcriptional up-regulation of the hepatocyte growth factor gene promoter via a novel composite cis-acting element. *J Biol Chem* **276**: 25049-56.

Kadesch T and Kildjian M (1990). Analysis of the promoter of liver/bone/kidney ALP in *vivo* and in *vitro*. *Nucleic Acids Res* **18**: 957-961.

Kadonaga J, Jones K and Tjian R (1986). Promoter-specific activation of RNA polymerase II transcription by Sp1. *Trends Biochem Sci* **11**: 20-23.

Kaibori M, Kwon A, Oda M, Kamiyama Y, Kitamura N and Okumura T (1998). Hepatocyte growth factor stimulates synthesis of lipids and secretion of lipoproteins in rat hepatocytes. *Hepatology* **27**: 1354-61.

Kang H, Shyr C, Huang C, Tsai M, Orimo H, Lin P, *et al.* (2008). Altered TNSALP Expression and Phosphate Regulation Contribute to Reduced Mineralization in Mice Lacking Androgen Receptor. *Mol Cell Biol* **28**: 7354-67.



Kersten S, Desvergne B and Walter Wahli W (2000). Roles of PPARs in health and disease. *Nature* **405**: 421-24.

Kihn L, Rutkowski D and Stinson R (1990). Incorporation of human liver and placental alkaline phosphatase into liposomes and membranes is via phosphatidylinositol. *Biochem Cell Biol* **68**: 1112-18.

Kim J, Sarraf P, Wright M, Yao K, Mueller E, Solanes G, *et al.* (1998). Nutritional and insulin regulation of fatty acid synthetase and leptin gene expression through ADD1/SREBP1. *J Clin Invest* **101**: 1-9.

Kim J and Spiegelman B (1996). ADD1/SREBP1 promotes adipocyte differentiation and gene expression linked to fatty acid metabolism. *Genes Dev* **10**: 1096-1107.

Kim K, Song M, Yoo E, Choe S, Park S and Kim J (2004). Regulatory Role of Glycogen Synthase Kinase 3 for Transcriptional Activity of ADD1/SREBP1c. *J Biol Chem* **279**: 51999-52006.

Kim Y, Lee M, Wozney J, Cho J and Ryoo H (2004). Bone Morphogenetic Protein-2-induced Alkaline Phosphatase Expression Is Stimulated by Dlx5 and Repressed by Msx2. *J Biol Chem* **279**: 50773-80.

Kirkland J, Hollenberg C and Gillon A (1993). Aging, differentiation and gene expression in rat epididymal preadipocytes. *Biochem Cell Biol* **71**: 556-561.

Kliwer S, Lenhard J, Willson T, Patel I, Morris D and Lehmann J (1995). A postaglandin J<sub>2</sub> metabolite binds PPAR gamma and promotes adipocyte differentiation. *Cell* **83**: 813-19.

Kliwer S, Sundseth S, Jones S, Brown P and Wisely G (1997). Fatty acids and eicosanoids regulate gene expression through direct interactions with PPAR gamma and alpha. *Proc Natl Acad Sci USA* **94**: 4318-23.

Komaru K, Ishida Y, Amaya Y, Sone M and Orimo H (2005). Novel aggregate formation of a frame-shift mutant protein of TNSALP ascribed to three cysteine residues in the C-terminal extension. *FEBS J* **272**: 1704-17.

Koon R (2009). "The basics of essential fatty acids". <http://www.naturalproductsinsider.com/article> [accessed 28 Dec 2009].

Korostishevsky M, Cohen Z, Malkin I, Ermakov S, Yarenchuk O and Livshits G (2010). Morphological and biochemical features of obesity are associated with mineralization genes' polymorphisms. *Int J Obes* **34**: 1308-18.

Kubota N, Terauchi Y, Miki H, Tamemoto H, Yamauchi T, Komeda K, *et al.* (1999). PPAR $\gamma$  mediates high-fat diet induced adipocyte hypertrophy and insulin resistance. *Mol Cell* **4**: 597-609.

Kunnas T, Lahtio R, Kortelainen M, Kalela A and Nikkari S (2009). Gln27Glu variant of Beta2-adrenoceptor gene affects male type fat accumulation in women. *Lipids Health Dis* **8**: 43-7.

Lafontan M and Berlan M (1993). Fat cell adrenergic receptors and the control of white and brown fat cell function. *J Lipid Res* **34**: 1057–1091

Larigauderie G, Fuman C, Jaye M, Lasselin C, Corinne C, Fruchart J, *et al.* (2004). Adipophilin enhances lipid accumulation and prevents lipid efflux from THP-1 macrophages: potential role in atherogenesis. *Arterioscler Thromb Vasc Biol* **24**: 504-10.

Lau S, Ehrismann J, Schlereth A, Takada S, Mayer U and Jürgens G (2010). Cell-cell communication in Arabidopsis early embryogenesis. *Eur J Cell Biol* **89**: 225-30.

Lee L, Hirose H, Ohneda M, Johnson J, McGray J and Unger R (1994).  $\beta$ -cell lipotoxicity in the pathogenesis of NIDDM of obese rats: impairment of adipocyte  $\beta$ -cell relationships. *Proc Natl Acad Sci USA* **91**: 10878-10882.

Lefebvre A, Laville M, Vega N, Rion J, van Graal L and Auvrex J (1998). Depot-specific differences in adipose tissue gene expression in lean and obese subjects. *Diabetes* **47**: 98-103.

Lehman F (1980). Human ALP: Evidence of three isoenzymes (placental, intestinal and liver-bone-kidney type) by lectin binding affinity and immunological specificity. *Biochim Biophys Acta* **616**: 41-59.

Lehmann J, Moore L, Smith-Oliver T, Wilkison W, Wilson T and Kliewer S (1995). An antidiabetic thiazolidione is a high affinity ligand fo PPAR gamma. *J Biol Chem* **273**: 12953-56.

Lelliot C and Vidal-Paig A (2004). Lipotoxicity, an imbalance between lipogenesis *de novo* and fatty acid oxidation. *Int J Obesity* **28**: 522-528.

Lima A and Garces S (2006). Bringing bioinformatics tools to the class. *Biochem Mol Biol Educ* **34**: 332-37.

Liu J, Ma Y, Wang Y, Du Z, Shen J and Peng H (2011). Reduction of lipid accumulation in HepG2 cells by luteolin is associated with activation of AMPK1 and mitigation of oxidative stress. *Phytother Res* **25**: 588-96.

Liu P, Ying Y, Zhao Y, Mundy D, Zhu M and Anderson R (2004). Chinese hamster ovary K2 cell lipid droplets appear to be metabolic organelles involved in membrane traffic. *J Biol Chem* **279**: 3787–92.

Londos C, Brasaemle D, Schutz C, Segrest J and Kimmel A (1999). Perilipins, ADRP and other proteins that associate with intracellular neutral lipiddroplets in animal cells. *Semin Cell Dev Biol* **10**: 51-8.

Londos C, Gray J, Brasaemle D, Rondinone C, Takeda T, Dwyer N, *et al.* (1996). Perilipin: Possible roles in structure and metabolism of intracellular neutral lipids in adipocytes and steroidogenic cells. *Int J Obes Relat Metab Disord* **20** (Suppl 3): S97-S101.

Lossos I, Czerwinski D, Wechser M and Levy R (2003). Optimization of quantitative real-time RT-PCR parameters for the study of lymphoid malignancies. *Leukemia* **17**: 789–95.

Lu X, Gornia J, Copeland N, Gilbert D, Jenkins N, Londos C, *et al.* (2001). The murine perilipin gene: lipid droplet-associated perilipins derive from tissue specific mRNA splice variants and define a gene family of ancient origin. *Mamm Genome* **12**: 741-9.

MacDougald O and Lane M (1995). Transcriptional regulation of gene expression during adipocyte differentiation. *Ann Rev Biochem* **64**: 345-73.

MacDougald O and Mandrup S (2002). Adipogenesis: forces that tip the scales. *Trends Endocrinol Metab* **31**: 5-10.

Mackie-Branchette E, Dwyer N, Barber T, Coxey R, Takeda T, Rondinone C, *et al.* (1995). Perilipin is located on the surface layer of intracellular lipid droplets in adipocytes. *J Lipid Res* **36**: 1211-26.

Maduro M (2010). Cell fate specification in the C. Elegans embryo. *Dev Dyn* **239**: 1315–29.

Mandrup S and Lane M (1997). Regulating adipogenesis. *J Biol Chem* **272**: 5367-70.

Mangelsdorf D, Thummel C, Beato M, Herlich P, Schutz G and Umesomo K (1995). The nuclear superfamily:the second decade. *Cell* **83**: 835-9.

Martin G, Schoonjans K, Lefebvre A, Staels B and Auwrex J (1997). Coordinate regulation of the expression of the fatty acid transport protein and acyl coA synthatase genes by PPAR $\alpha$  and PPAR $\gamma$  gamma activators. *J Biol Chem* **272**: 28210-17.

Martin S and Parton R (2006). Lipid droplets: a unified view of a dynamic organelle. *Nature Rev Mol Cell Biol* **7**: 373-8.

Masuhara K, Suzuki S, Yoshikawa H, Tsuda T and Takaoka T (1992). Development of monoclonal antibody specific for human bone ALP. *Bone Miner* **17**: 182-6.

Mauriege P, Galitzky J, Berlan M and Lafontan M (1987). Heterogenous distribution of beta and alpha adrenoceptor binding sites in human fat cells from various fat depots:functional consequences. *Eur J Clin Invest* **17**: 156-65.

Mayani H (2003). A Glance into Somatic Stem Cell Biology: Basic Principles, New Concepts, and Clinical Relevance. *Arch Med Res* **34**: 3-15.

McCarthy A, Cortizo A, Gimenez G, Bruzzon L and Etcheverry S (1998). Non-enzymatic glycosylation of ALP alters its biological properties. *Mol Cell Biochem* **181**: 63-9.

McComb R, Bowers G and Posen S (1979). Alkaline phosphatases. New York, Plenum Press: 350-360.

McCurdy R, McGrath J and Sim A (2008). Validation of the comparative quantification method of real-time PCR analysis and cautionary tale of housekeeping gene selection. *Gene Ther Mol Biol* **12**: 15-24.

McDougall K, Beecroft J, Wasnidge C, King W and Hahnel A (1998). Sequences and expression patterns of alkaline phosphatase isoenzymes in preattachment bovine embryos and the adult bovine. *Mol Reprod Dev* **50**: 7-17.

McGarry J and Dobbins R (1999). Fatty acids, lipotoxicity and insulin secretion. *Diabetologia* **42**: 128-38.

McGavock J, Victor R, Unger R and Szczepanick L (2006). Adiposity of the heart, revisited. *Ann Int Med* **144**: 517-24.

McKenna M, Hamilton T and Sussman H (1979). Comparison of human ALP isoenzymes. *Biochem J* **181**: 67-73.

Meister G and Tuschli T (2004). Mechanisms of gene silencing by double-stranded RNA. *Nature* **431**: 343-9.

Michalopoulos G and DeFrances M (1997). Liver regeneration. *Science* **276**: 60-6.

Mornet E, Taillandier A, Peyamaure S, Kaper F, Muller F and Brenner R (1998). Identification of fifteen novel mutations in the TNSALP gene in European patients with severe hypophosphatasia. *Eur J Hum Genet* **6**: 308-14.

Morrison R and Farmer S (1999). Role of PPAR $\gamma$  in regulating a cascade expression of cyclin-dependent kinase inhibitors, p18 and p21, during adipogenesis. *J. Biol Chem* **272**: 21473-78.

Moss D (1982). Alkaline phosphatase isoenzymes. *Clin Chem* **28**: 2007-2016.

Moss D and Edward R (1984). Improved electrophoretic resolution of bone and liver ALP resulting from partial digestion with neuroaminidase. *Clin Chim Acta* **143**: 177-82.

Motomura W, Inoue M, Ohtake T, Takahashi N, Nagamine M, Tanno S, *et al.* (2006). Up-regulation of ADRP in fatty liver in human and liver steatosis in mice fed with high fat diet. *Biochem Biophys Res Comm* **340**: 1111-18.

Mueller H, Stinson R, Mohyuddin E and Milner J (1983). Isoenzymes of ALP in infantile hypophosphatasia. *J Lab Clin Med* **102**: 24-30.

Mulivor R, Plotkin A and Harris H (1978). Differential inhibition of the products of the human ALP loci. *Ann Hum Genet* **42**: 1-13.

Mumm S, Jonathan J, Finnegan P, Henthorn P, Podgorink M and Whyte M (2002). Denaturing gradient gel electrophoresis analysis of the TNSALP gene in hypophosphatasia. *Mol Genet Metab* **75**: 143-53.

Murphy D (2001). The biogenesis and functions of lipid bodies in animals, plants and microorganisms. *Prog Lipid Res* **40**: 325-38.

Naito J, Kaji H, Sowa H, Hendy G, Sugimo T and Chihara K (2005). Menin suppresses osteoblast differentiation by antagonizing AP-1 factor, JunD. *J Biol Chem* **280**: 4785-91.

Nardi N and da Silva Meirelles L (2006). Mesenchymal Stem Cells: Isolation, In Vitro Expansion and Characterization. Handbook of Experimental Pharmacology. A. Wobus and K. Boheler. Berlin, Springer Berlin Heidelberg. **174**: 249-82.

Narisawa S, Fröhlander N and Millán J (1997). Inactivation of two mouse alkaline phosphatase genes and establishment of a model of infantile hypophosphatasia. *Dev Dyn* **208**: 432-6.

Narisawa S, Huang L, Iwasaki A, Hasegawa H, Alpers D and Millan J (2003). Accelerated fat absorption in intestinal alkaline phosphatase knock out mice. *Mol Cell Biol* **23**: 7525-30.

Neyrinck A, Margagliotti S, Gomez C and Delzenne N (2004). Kupffer cell-derived prostaglandin E<sub>2</sub> is involved in regulation of lipid synthesis in rat liver tissue. *Cell Biochem Funct* **22**: 327-32.

Nowrouzi A and Yazdanparast R (2005). Alkaline phosphatase retained in HepG2 hepatocarcinoma cells versus alkaline phosphatase released to culture medium: Difference of aberrant glycosylation. *Biochem Biophys Res Comm* **330**: 400-49.

Ntambi J and Kim Y (2000). Adipocyte differentiation and gene expression. *J Nutr* **130**: 3122S-26S.

Ohki T, Tateishi R, Shiina S, Goto E, Sato T, Nakagawa H, *et al.* (2009). Visceral fat accumulation is an independent risk factor for hepatocellular carcinoma recurrence after curative treatment in patients with suspected NASH. *Gut* **58**: 839-44.



Ohkubo S, Kimura J and Matsuka I (2000). Ecto-alkaline phosphatase in NG108-15 cells: a key enzyme mediating P1 antagonist-sensitive ATP response. *Br J Pharmacol* **131**: 1667-72.

Ohsaki Y, Maeda T and Fujimoto T (2005). Fixation and permeabilization protocol is critical for the immunolabeling of lipid droplet proteins. *Histochem Cell Biol* **124**: 445-52.

Okazaki T, Suzuki M, Naga T and Nagai I (2004). Abnormal ALP isoenzymes detected in the serum of elderly patients. *Scan J Clin Lab Invest* **64**: 611-618.

Orimo H and Shimada T (2005). Regulation of the human tissue-nonspecific alkaline phosphatase gene expression by all-trans-retinoic acid in SaOS-2 osteosarcoma cell line. *Bone* **36**: 866-76.

Orimo H, Sone M, Inoue M, Tsubaiko Y, Sakiyama T and Shimada T (2002). Importance of deletion of T nucleotide 1559 in the TNSALP gene in Japanese patients with hypophosphatasia. *J Bone Miner Metab* **20**: 28-33.

Pfaffl M and Horgan G (2002). Relative expression software tool (REST©) for group-wise comparison and statistical analysis of relative expression results in real-time PCR. *Nucleic Acids Res.* **30**: e36.

Pighin D, Karabatas L, Rossi A, Chicco A, Basabe J and Lombardo Y (2003). Fish Oil Affects Pancreatic Fat Storage, Pyruvate Dehydrogenase Complex Activity and Insulin Secretion in Rats Fed a Sucrose-Rich Diet. *J Nutr* **133**: 4095-4101.

Pol A, Martin S, Fernandez M, Ferguson C, Carozzi A, Luetterforst R, *et al.* (2004). Dynamic and Regulated Association of Caveolin with Lipid Bodies: Modulation of Lipid Body Motility and Function by a Dominant Negative Mutant. *Mol Biol Cell* **15**: 99-110.

Posen S, Cornish C and Kleerekperk K (1977). Alkaline phosphatase and metabolic bone disease. In : Metabolic Bone Disease. A. L. S. New York, Academic Press: 141-163.

Powell E, Clooksley W, hanson R, Seale J, Halliday J and Powell L (1990). The natural history of non-alcoholic steatohepatitis: a follow-up study of forty-two patients for up to 21 years. *Hepatology* **11**: 74-80.

Price C (1993). Multiple forms of human serum alkaline phosphatase: detection and quantitation. *Ann Clin Biochem* **30**: 355-371.

Primrose B and Twyman R (2005). Principles of Gene Manipulation. . Munich, Blackwell Publishing.

Puoane T, Steyn K, Bradshaw D, Laubscher R, Fourie J, Lambert V, *et al.* (2002). Obesity in South Africa: the South African demographic and health survey. *Obesity Res* **10**: 1038-48.

Querido E and Chartranda P (2008). Using Fluorescent Proteins to Study mRNA Trafficking in Living Cells. *Methods Cell Biol* **85**: 273-92.

Rae C, Hare N and Bubb W (2003). Inhibition of glutamine transport depletes glutamate and GABA neurotransmitter pools:further evidence for metabolic compartmentation. *J Neurochem* **85**: 503-14.

Ramirez-Zacarius J, Casro-Munozledo F and Kuri-Harench W (1992). Quantitation of adipose conversion and triglycerides by staining intracytoplasmic lipids with oil red O. *Histochem* **97**: 493-7.

Reaven G, Abbasi F and McLaughlin T (2004). Obesity, insulin resistance and cardiovascular disease. *Recent Prog Horm Res* **59**: 207-23.

Reed B and Lane M (1979). Expression of insulin receptors during preadipocyte differentiation. *Adv Enzyme Reg* **18**: 97-117.

Reynaert H, Geerts A and Herrion J (2005). The treatment of non-alcoholic steatohepatitis with thiazolidinediones. *Aliment Pharmacol Ther* **22**: 897-905.

Rhoades R and Bell D (2009). Cellular physiology. Medical Physiology: Principles of Clinical Medicine. 4ed. Philadelphia, Lippincott Williams: 18-19.

Ristow M, Muller W, Pfeiffer A, Krone W and Kahn C (1998). Obesity associated with a mutation in a genetic regulator of adipocyte differentiation. *NEJM* **339**: 953-9.

Robinson S, Dinulescu D and Cone R (2000). Genetic models of obesity and energy balance in the mouse. *Ann Rev Genet* **3**: 687-745.

Rosalki S and Foo A (1984). Two new methods for separating and quantifying bone and liver ALP isoenzyme in plasma. *Clin Chem* **30**: 1182-6.

Rosen E, Sarraf P, Troy A, Bradwin G, Moore K, Milstone D, *et al.* (1999). PPAR gamma is required for the differentiation of adipose tissue *in vitro* and *in vivo*. *Mol Cell* **4**: 611-7.

Rosen E and Spiegelman B (2000). Molecular regulation of adipogenesis. *Ann Rev Cell Dev Biol* **16**: 145-171.

Rosen E, Walker C, Puigserver P and Spiegelman B (2000). Transcriptional regulation of adipogenesis. *Genes Dev* **14**: 1293-1307.

Rossetti L, Guiaccari A and DeFronzo R (1990). Glucose toxicity. *Diabetes Care* **13**: 610-20.

Ruan H, Pownall H and Lodish H (2003). Troglitazone antagonizes TNF- $\alpha$ -induced reprogramming of adipocyte gene expression by inhibiting the transcriptional regulatory functions of NF- $\kappa$ B. *J Biol Chem* **278**: 28181-92.

Ruesch J and Klem D (1994). Nutrition and fat cell differentiation. *Endocrinology* **140**: 2935-37.

Salans L, Cushman S and Weisman R (1973). Studies of human adipose tissue: adipose cell size and number in non-obese and obese patients. *J Clin Invest* **52**: 929-41.

Sandouk T, Reda D and Hoffman C (1993). Antidiabetic agent, pioglitazone enhances adipocyte differentiation by 3T3-F442A cells. *Am J Physiol Cell Physiol* **264**: C1600-C1608.

Santoro N, Cirillo G, Lepore M, Palma A, Amato A and Savarese P (2009). Effect of the rs997509 polymorphism on the association between ENPP1, metabolic syndrome and impaired glucose tolerance in childhood obesity. *J Clin Endocrinol Metab* **94**: 300-5.

Schadinger L, Bucher N, Schreiber B and Farmer S (2005). PPAR $\gamma$ 2 regulates adipogenesis and lipid accumulation in steatotic hepatocytes. *Am J Physiol Endocrinol Metab* **288**: E1195-E1205.

Schaffer J (2003). Lipotoxicity: when tissues overeat. *Curr Opin Lipidol* **14**: 281-7.

Schmitz P (2000). Signalling aspects of insulin resistance in skeletal muscle: mechanisms induced by lipid oversupply. *Cell Signal* **12**: 583-94.

Schoenau E, Herzog K and Boehies H (1986). Liquid chromatographic determination of isoenzymes of ALP in serum and tissue homogenates. *Clin Chem* **32**: 816-8.

Schoonjans K, Peinado J, Lefebvre A, Heyman R, Briggs M, Deeb S, *et al.* (1996). PPAR $\alpha/\gamma$  activators direct a tissue specific transcriptional response via a PPRE in the lipoprotein lipase gene. *EMBO J* **15**: 5336-48.

Scott R, Florine D, Willie J and Yun K (1982). Coupling of growth arrest and differentiation at a distinct state in the G1 phase of the cell cycle:G<sub>D</sub>. *Proc Natl Acad Sci USA* **79**: 845-9.

Sebastian D, Herrero L, Serra D, Asins G and Hegardt F (2007). CPTI overexpression protects L6E9 muscle cells from fatty acid induced insulin resistance. *Am J Physiol Endocrinol Metab* **292**: E677-86.

Serfling E, Jasin M and Schaffner W (1985). Enhancers and eukaryotic gene transcription. *Trends Genet* **1**: 224-30.

Serrero G, Lepak N, Hayashi J and Goodrich S (1993). Impaired epidermal growth factor production in genetically obese ob/ob mice. *Am J Physiol* **264**: E800-03.

Servetnick A, Brasaemle D, Gray J, Kimmel A, Wolf H and Londos C (1995). Perilipins are associated with cholesteryl ster droplets in steroidogenic adrenal cortical and Leydig cells. *J Biol Chem* **270**: 16970-3.

Severini G, Aliberti L and DiGovanan R (1991). Diagnostic aspects of ALP: separation of isoenzymes in normal and pathological human serum by HPLC. *J Chromatog Biomed Appl* **563**: 147-52.

Shao D and Lazaar M (1997). PPAR $\alpha$ , CCAAT/enhancer binding protein alpha and cell cycle status regulate the commitment to adipocyte differentiation. *J Biol Chem* **272**: 21473-8.

Shao Q, Arakaki N, Ohnishi T, Nakamura O and Daikuhara Y (1996). Effect of hepatocyte growth factor/scatter factor on lipogenesis in adult rat hepatocytes in primary culture. *J Biochem* **119**: 940-6.

Shinozaki T and Pritzker K (1996). Regulation of alkaline phosphatase: implications for calcium pyrophosphate dihydrate crystal dissolution and other alkaline phosphatase functions. *J Rheumatol* **4**: 677-83.

Shiota A, Yamashita Y, Fujise N, Masunaga H, Yasuda H and Higashio K (2000). A deleted form of human hepatocyte growth factor stimulates hepatic lipogenesis and lipoprotein synthesis in rats. *Pharmacol Res* **42**: 443-52.

Siede W and Steiffert V (1977). Quantitative alkaline phosphatase isoenzyme determination by electrophoresis on cellulose acetate membranes. *Clin Chem* **23**: 28-33.

Sinha A, Erickson A and Seal U (1997). Fine structure of Leydig cells in crabster, leopard and Ross seals. *J Reprod Fertil* **49**: 51-4.

Siomi H and Siomi M (2009). On the road to reading the RNA-interference code. *Nature* **457**: 396-404.

Siriha P, Bianchi B, Mayer-Sabel E and Righetti P (1986). Resolution of ALP isoenzymes in serum by isoelectric focussing in immobilized pH gradients. *Clin Chem* **32**: 1264-8.

Sivertsson L, Ek M, Darnell M, Edebert I, Ingelman-Sundberg M and Neve E (2010). CYP3A4 Catalytic Activity Is Induced in Confluent Huh7 Hepatoma Cells. *Drug Metab Dispos* **38**: 995-1002.

Slaughter C, Coseo M, Cancro M and Harris H (1981). Detection of enzyme polymorphism by using monoclonal antibodies. *Proc Natl Acad Sci USA* **78**: 1124-8.

Smas C and Sul H (1995). Control of adipocyte differentiation. *Biochem J* **309**: 697-710.

Smith M, Weiss M, Griffin C, Murray J, Buetow K, Emmanuel B, *et al.* (1988). Regional assignment of the gene for human liver/bone/kidney ALP to chromosome 1. *Genomics* **2**: 139-43.

Sobhonslidsuk A, Jongjirasiri S, Thakkestian A, Wisedopas N, Bunnag P and Puavilai G (2007). Visceral fat and insulin resistance as predictors of non-alcoholic steatohepatitis. *World J Gastroenterol* **13**: 3614-8.

Soloveva V, Graves R, Rasenick M, Spiegelman B and Ross S (1997). Transgenic Mice Overexpressing the  $\beta$ 1-Adrenergic Receptor in Adipose Tissue Are Resistant to Obesity. *Mol Endocrinol* **11**: 27-38.

Souza S, Muliro K, Liscum L, Lien P, Yamamoto M, Schaffer J, *et al.* (2002). Modulation of Hormone-sensitive Lipase and Protein Kinase A-mediated Lipolysis by Perilipin A in an Adenoviral Reconstituted System. *J Biol Chem* **277**: 8267-72.

Straub B, Stoeffel P, Heid H, Zimmermann R and Schirmacher P (2008). Differential pattern of lipid droplet-associated proteins and *de novo* perilipin expression in hepatocyte steatogenesis. *Hepatology* **47**: 1936-46.

Su T, Wang M, Oxender D and Sattiel A (1998). Triglitazone increases system A amino acid transport in 3T3-L1 cells. *Endocrinology* **139**: 832-7.

Szczepanick L, Barbcook E, Schick F, Dobbins R, Garg A, Burns D, *et al.* (1999). Measurement of intracellular TAG stores by H spectroscopy: validation *in vivo*. *Am J Physiol* **276**: E977-E989.

Sztalryd C, Xu G, Dorward H, Tansey J, Contreras J, Kimmel A, *et al.* (2003). Perilipin A is essential for the translocation of hormone-sensitive lipase during lipolytic activation. *J Cell Biol* **161**: 1093-1103.

Taghert P, Doe C and Goodman C (1984). Cell determination and regulation during development of neuroblasts and neurones in grasshopper embryo. *Nature* **307**: 163-5.

Taillandier A, Lia-Baldini AS, Mouchard M, Robin R, Muller F, Simon-Bouy B, *et al.* (2001). Twelve novel mutations in the TNSALP gene in patients with various forms of hypophosphatasia. *Hum Mutat* **18**: 83-4.

Takahashi M, Takahashi Y, Takahashi K, Zolotanjov F, Hong K, Kitazawa R, *et al.* (2008). Chemerin enhances insulin signalling and potentiates insulin-stimulated glucose uptake in 3T3-L1 adipocytes. *FEBS Lett* **528**: 573-8.

Tansey J, Huml A, Vogt R, Davis K, Jones J, Fraser K, *et al.* (2003). Functional Studies on Native and Mutated Forms of Perilipins: A role in protein kinase A-mediated lipolysis of triacylglycerols in Chinese Hamster ovary cells. *J Biol Chem* **278**: 8401-6.



Tansey J, Sztalryd C, Gruia-Gray J, Roush D, Zee J, Gavrilova O, *et al.* (2001). Perilipin ablation results in a lean mouse with aberrant adipocyte lipolysis, enhanced leptin production, and resistance to diet-induced obesity. *Proc Natl Acad Sci USA* **98**: 6494-9.

Targett-Adams P, Chambers D, Gledhills S, Hope G, Coy J, Girod A, *et al.* (2003). Live analysis and targeting of the lipid droplet-binding adipocyte differentiation-related protein. *J Biol Chem* **278**: 15998-16007.

Terao M and Mintz B (1987). Cloning and characterization of a cDNA coding region for mouse placental alkaline phosphatase. *Proc Natl Acad Sci USA* **84**: 7051-5.

Thomaskutty K, Basi N, Mckenzie M and Pointer R (1993). Regulation of pyruvate dehydrogenase activity in rat fat pads and isolated hepatocytes by levamisole. *Pharmacol Res* **27**: 263-71.

Tontonoz P, Hu E, Devine J, Beale E and Spiegelman B (1995). PPAR $\gamma$ 2 regulates adipose expression of phosphoenyl pyruvate carboxyl kinase gene. *Mol Cell Biol* **15**: 351-7.

Tontonoz P, Hu E, Graves R, Budavari A and spiegelman B (1994). mPPAR $\gamma$ 2: tissue-specific regulator of an adipocyte enhancer. *Genes Dev* **8**: 1224-34.

Tontonoz P, Hu E and Spiegelman B (1994). Stimulation of adipogenesis in fibroblasts by PPAR $\gamma$ , a lipid-activated transcriptional factor. *Cell* **79**: 1147-56.

Tontonoz P, Kim J, Graves R and Spiegelman B (1993). ADD1: A novel helix-loop-helix transcriptional factor associated with adipocyte determination and differentiation. *Mol Biol Cell* **13**: 4753-9.

Tran T, Friedman J, Baameur F, Knoll B, Moore R and Clark R (2007). Characterization of  $\beta$ 2-Adrenergic Receptor Dephosphorylation: Comparison with the Rate of Resensitization. *Mol Pharmacol* **71**: 147-60.

Tunaru S, Kero J, Schaub A, Wufka C, Blaukat A, Pfeffer K, *et al.* (2003). PUMA-G and HM74 are receptors for nicotinic acid and mediate its anti-lipolytic effect. *Nature Med* **9**: 352-5.

Tylzanowski P, Verschueren K, Huylebroeck D and Luyten F (2001). Smad-interacting protein 1 is a repressor of L/B/K ALP transcription in bone morphogenic protein-induced osteogenic differentiation of C2C12 cells. *J Biol Chem* **276**: 40001-7.

Vaananen H (2005). Mesenchymal stem cells. *Ann Med* **37**: 469-79.

Valetti C, Wetzel D, Schrader M, Hasban M, Gill S, Kreis T, *et al.* (1999). Role of dynactin in endocytic traffic: effects of dynamitin overexpression and colocalization with CLP-170. *Mol Cell Biol* **10**: 4107-20.

Vankoningsloo S, De Pauw A, Houbion A, Tejerina S, Demazy C, de Longueville F, *et al.* (2006). CREB activation induced by mitochondrial dysfunction triggers triglyceride accumulation in 3T3-L1 preadipocytes. *J Cell Sci* **119**: 1266-82.

Vosper H, Patel L, T. G, Khoudoli G, Hill A, Macphee C, *et al.* (2001). The PPAR $\delta$  promotes lipid accumulation in human macrophages. *J Biol Chem* **276**: 44258-65.

Wall N and Shi Y (2003). Small RNA: can RNA interference be exploited for therapy. *Lancet* **362**: 1401-3.

Wang H, Khaoustov V, Krishnan B, Cai W, Stoll B, Burrin D, *et al.* (2006). Total Parenteral Nutrition Induces Liver Steatosis and Apoptosis in Neonatal Piglets. *J Nutr* **136**: 2547-52.

Wang S and Fong T (1995). A lipid droplet specific capsule is present in rat adrenal cells: evidence from a monoclonal antibody. *Biochem Biophys Res Commun* **217**: 81-88.

Wang X, Goh C and Li B (2007). p38 mitogen-activated protein kinase regulates osteoblast differentiation through osterix. *Endocrinology* **148**: 1629-37.

Watanabe H, Takinami H, Sone M, Orimo H and Ishikawa I (2005). Characterization of the mutant (A115V) TNSALP gene from adult-type hypophosphatasia. *Biochem Biophys Res Commun* **327**: 124-9.

Watanabe H, Voshima H, Sone M, Orimo H and Ishikawa I (2001). A novel point mutation (C571T) in the TNSALP gene in a case of adult-type hypophosphatasia. *Oral Dis* **7**: 331-5.

Waymire K, Mahuren D, Jaje M, Guilatre T, Coburn S and Macgregor G (1995). Mice lacking tissue non-specific alkaline phosphatase die from seizures due to defective metabolism of vitamin B6. *Nature Genet* **11**: 45-51.

Weiss M, Cole D, Ray K, Whyte M, Lafferty M, Mulivor R, *et al.* (1989). A missense mutation in the human LBK ALP gene causing a lethal form of hypophosphatasia. *Proc Natl Acad Sci USA* **856**: 7666-9.

Weiss M, Ray K, Henthorn P, Lamb B, Kadesch T and Harris H (1988). Structure of the human liver/bone/kidney alkaline phosphatase gene. *J Biol Chem* **263**: 12002-10.

Weston A, Hoffman L and Underhill T (2003). Revisiting the role of retinoid signalling in skeletal development. *Birth Defects Res* **69**: 156-73.

Whitaker K and Moss D (1979). Comparison of radioactive peptides obtained from specifically labelled human renal and placental ALP. *Biochem J* **183**: 189-192.

Whittaker J (1973). Segregation during ascidian embryogenesis of egg cytoplasmic information for tissue-specific enzyme development. *Proc Natl Acad Sci USA* **70**: 2096-100.

Whyte M (1994). Hypophosphatasia and the role of alkaline phosphatase in skeletal mineralisation. *Endocrine Rev* **15**: 439-61.

Wong C, Lee J, Ching Y, Jin D and Oi-lin Ng I (2003). Genetic and Epigenetic Alterations of DLC-1 Gene in Hepatocellular Carcinoma. *Cancer Res* **63**: 7646-51.

Wu Z, Bucher N and Farmer S (1996). Induction of PPAR gamma during the conversion of 3T3 fibroblasts into adipocytes is mediated by C/EBP beta, C/EBP delta and glucocorticoids. *Mol Biol Cell* **16**: 4128-36.

Wu Z, Xie Y, Bucher N and Farmer S (1995). Conditional ectopic expression of C/EBP beta in NIH3T3 cells induces PPAR gamma and stimulates adipogenesis. *Genes Dev* **9**: 2350-63.

Wu Z, Xie Y, Morrison R, Bucher N and Farmer S (1998). PPAR $\gamma$  induces the insulin-dependent glucose transport Glut4 in the absence of C/EBP $\alpha$  during the conversion of 3T3 fibroblasts into adipocytes. *J Clin Invest* **101**: 22-32.

Xu W (2006). Resistin increase lipid accumulation and CD36 expression in human macrophages. *Biochem Biophys Research Commun* **351**: 376-82.

Yamamoto K, Awogi T, Okuyama K and Takahashi N (2003). Nuclear localization of alkaline phosphatase in cultured human cancer cells. *Med Electron Microsc* **36**: 47-51.

Yew W, Cao Z, Classon M and McKnight S (1995). Cascade regulation of terminal adipocyte differentiation by three members of the C/EBP family of leucine zipper proteins. *Genes Dev* **15**: 168-81.

Yki-Jarvinen H and Westerbacka J (2005). The fatty liver and insulin resistance. *Curr Mol Med* **5**: 287-95.

Yokoyama C, Wang X, Briggs M, Admon A, Wu J, Hua X, *et al.* (1993). SREBP-1, a basic-helix-loop-helix-leucine zipper protein that controls transcription of the low density lipoprotein receptor gene. *Cell* **75**: 187-97.

Zhang B, Berger J, Hu E, Szalkowski D, White-Carrington S, Spiegelman B, *et al.* (1996). Negative regulation of peroxisome proliferator-activated receptor-gamma gene expression contributes to the antiadipogenic effects of tumor necrosis factor-alpha. *Mol Endocrinol* **10**: 1457-66.

Zhang Y, Brown M, Peach C, Russel G and Wordsworth B (2007). Investigation of the role of ENPP1 and TNSAP genes in chondrocalcinosis. *Rheumatology (Oxford)* **46**: 586-9.

Zhang Y, Shao J, Xie Q and Alpers D (1996). Immunolocalization of alkaline phosphatase and surfactant-like particle proteins in rat duodenum during fat absorption. *Gastroenterology* **110**: 478-88

Zhao C, Jiang L, Zhuo-Jun Deng L, Liang B and Li J (2004). Peroxisome proliferator activated receptor-g in pathogenesis of experimental fatty liver disease. *World J Gastroenterol* **10**: 1329-32.

Zhu Y, Qi C, Korenberg J, Chen X, Noya D, Sambasiva R, *et al.* (1995). Structural organization of mouse peroxisome proliferator-activated receptor g gene: alternative promoter use and different splicing yield two m PPARg isoforms. *Proc Natl Acad Sci USA* **92**: 7921-5.

Zizola C, S F, Jitngarmkusol S, Kadereit B, Yan N and Vogel S (2010). Cellular retinol-binding protein type I (CRBP-I) regulates adipogenesis. *Mol Cell Biol* **30**: 3412-20.